Aus dem CharitéCentrum für Grundlagenmedizin CC2

Institut für Biochemie

Direktorin: Prof. Dr. Britta Eickholt

Habilitationsschrift

Ubiquitin modification and its perception by the MHC class I antigen processing pathway

zur Erlangung der Lehrbefähigung

für das Fach Biochemie

vorgelegt dem Fakultätsrat der Medizinischen Fakultät

Charité-Universitätsmedizin Berlin

Von

Dr. Frédéric Ebstein

geb. in Caen

Eingereicht im November 2016

Dekan: Prof. Dr. med. Axel Pries

1. Gutachter: Prof. Dr. Dirk Busch

2. Gutachter: Prof. Dr. Peter van Endert

Contents

1. Summary

It is more than forty years since it was described that MHC class I molecules bind and present peptides to CD8+ T cells, yet it is only recently that the pathway for processing and delivering peptides for MHC class I complexes has begun to be unraveled. It is now well appreciated that most of the MHC class I-restricted peptides derive from the degradation of proteins by the ubiquitin-proteasome system (UPS). In this process, proteins are tagged with a small protein called ubiquitin for subsequent degradation by 26S proteasome complexes. This allows the generation of peptides which are subsequently transported into the lumen of the endoplasmic reticulum (ER) where they bind to MHC class I molecules before being transported to the cell surface. Depending on the origin of antigens, the MHC class I processing pathway may be referred to as direct or cross-presentation. By convention, the term direct presentation (or direct priming) applies to antigens of endogenous origin, while cross-presentation (or cross-priming) is restricted to exogenous antigens. It is assumed that MHC class I cross-presentation is restricted to a subset of immune cells capable of phagocytosis including dendritic cells (DC), whereas direct MHC class I antigen presentation occurs as a consequence of protein homeostasis in almost all nucleated cells of the body.

Although the regulation of MHC class I antigen processing by proteasomes is well documented, the mechanisms controlling the selection of antigens for ubiquitin modification as well as their trafficking and recognition by proteasomes remain poorly understood. To close this gap of knowledge, our aim in this work was to unveil the events of the MHC class I processing pathway taking place upstream antigen breakdown by proteasomes. Interestingly, our data reveal that the supply of MHC class I-restricted peptides by the UPS is not restricted to antigens bearing ubiquitin modifications. Here, we identified the ubiquitin-like protein HLA-F-adjacent transcript 10 (FAT10) as an efficient and alternative signal for MHC class I antigen presentation. In this process, FAT10-marked antigens are shuttled to the 26S proteasome by the ubiquitin-binding proteins NEDD8 ultimate buster (NUB) 1 and/or NUB1 long (NUB1L) for degradation, leading to the generation of fully functional MHC class I epitopes. We also report the Rpn10 subunit of the 19S regulator particle as a universal receptor for ubiquitin- and FAT10-modified proteins, thereby allowing their recognition by proteasomes prior to

their processing into MHC class I-restricted peptides. Finally, our data support a role the ER-associated degradation machinery (ERAD) in the MHC class I antigen processing pathway whereby p97/VCP ensures the extraction of antigens from the ER in direct priming and ER-like vesicles in cross-priming into the cytoplasm for subsequent degradation by proteasomes. Altogether, our data describe the identification of a novel inducible FAT10/NUB1(L)/Rpn10 route for MHC class I presentation and report p97/VCP as an ERAD protein functioning at the interface of the direct and cross-presentation pathways. Future work will attempt to determine the precise contribution of these components to the mounting of cytotoxic T cell responses *in vivo*.

2. Introduction

The 2004 Nobel Prize in Chemistry went to three scientists for their discovery of a “heat-stable polypeptide of the ATP-dependent proteolytic system” (Ciechanover et al., 1980; Ciechanover et al., 1978; Hershko et al., 1979) which was later identified as the ubiquitin molecule (Wilkinson et al., 1980). Ubiquitin is part of the ubiquitin-proteasome system (UPS) which ensures the degradation of most of short-lived intracellular proteins in eukaryotes (Rechsteiner and Hill, 2005). In this pathway, proteins which are misfolded, oxidized, damaged and/or no longer needed are typically tagged with ubiquitin chains making them targets for destruction by the 26S proteasome. By maintaining protein homeostasis in the cell, the UPS represents a major source of peptides which can be further degraded into amino acids by various peptidases in the cytoplasm. Alternatively, such proteasomal products may be presented at the cell surface in association with major histocompatibility (MHC) class I molecules for presentation to CD8+ T cells. Therefore, the conversion of proteins into MHC class I peptide ligands for recognition by CD8+ T cells involves two fundamental steps: (i) the modification of these proteins by ubiquitin and (ii) their subsequent degradation by 26S proteasomes.

2.1. Ubiquitin and ubiquitin-conjugation

Proteins destined to be broken down by 26S proteasomes must undergo a so-called ubiquitination process (sometimes also referred as to ubiquitylation). As depicted in Fig. 1, conjugation of ubiquitin involves a sequence of reactions (Rajapurohitam et al., 2002). Ubiquitin is first activated by an ubiquitin-activating enzyme (E1) in an ATP-hydrolyzing reaction that initially results in formation of ubiquitin adenylate intermediate bound to the enzyme. E1 then transfers the activated ubiquitin to a so-called ubiquitin-conjugating enzyme (E2), which builds a thioester linkage between the active site cysteine and ubiquitin (Rajapurohitam et al., 2002). E2 enzymes then support conjugation to substrates together with ubiquitin-protein ligases (E3) that recognize specific substrates. Herein, really interesting new gene (RING) E3 ligases bind both E2 enzymes and the protein substrate to mediate ubiquitin transfer, while homologous to E6-AP carboxyl terminus (HECT) E3 ligases first accept the ubiquitin from E2 enzymes before allowing its transfer to protein substrates (Pickart and Eddins, 2004). It was long assumed that ubiquitination primarily occurs via

isopeptide bonds to lysine residues of target proteins (Breitschopf et al., 1998). However, a limited number of protein substrates has been shown to be conjugated on threonine (T), serine (S), cysteine (C) residues as well as at the N-terminus (McDowell et al., 2010; Tait et al., 2007; Vosper et al., 2009).

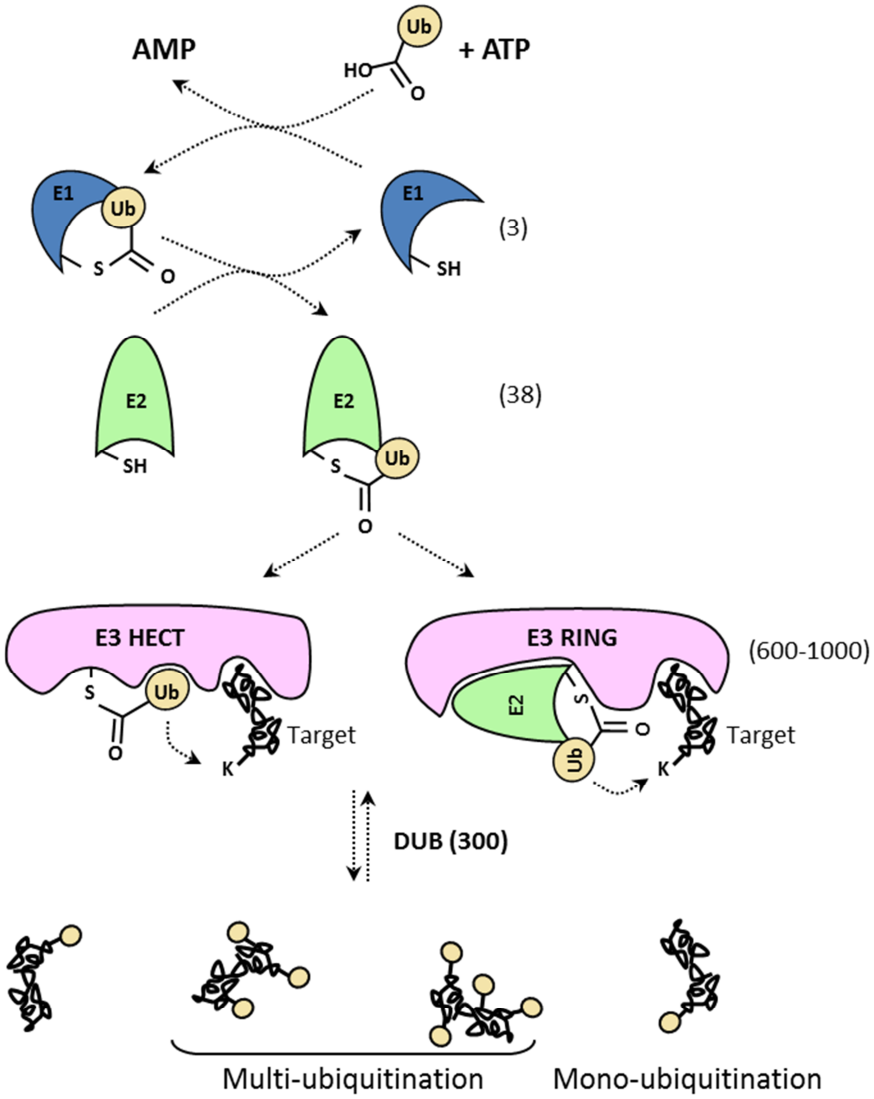

Figure 1: Ubiquitin conjugation pathway of protein substrates. Ubiquitin is first activated by a E1 ubiquitin-activating enzyme in a reaction that requires ATP hydrolysis. The activated ubiquitin is then transferred to a E2 ubiquitin-conjugating enzyme and used for the modification of protein substrates on lysine (K) residues with the help of HECT and/or RING E3 ubiquitin ligases (modified from (Hurley et al., 2006)).

Proteins may be attached to one single ubiquitin moiety on one or several acceptor sites resulting in mono- or multi-ubiquitination, respectively. Mono-ubiquitination has been reported to regulate DNA repair and/or gene expression (Passmore and Barford, 2004), while multi-ubiquitination is primarily involved in receptor endocytosis (Haglund et al., 2003). The ubiquitin molecule itself exhibits seven lysine residues (K6, K11, K27, K29, K33, K48 and K63) as well as an NH2-terminal methionine (referred as to M1) which can be used individually and/or in combination for the formation of poly-ubiquitin chains (Komander and Rape, 2012). This leads to the assembly of at least eight types of poly-ubiquitin chains with distinct biological functions (Fig. 2).

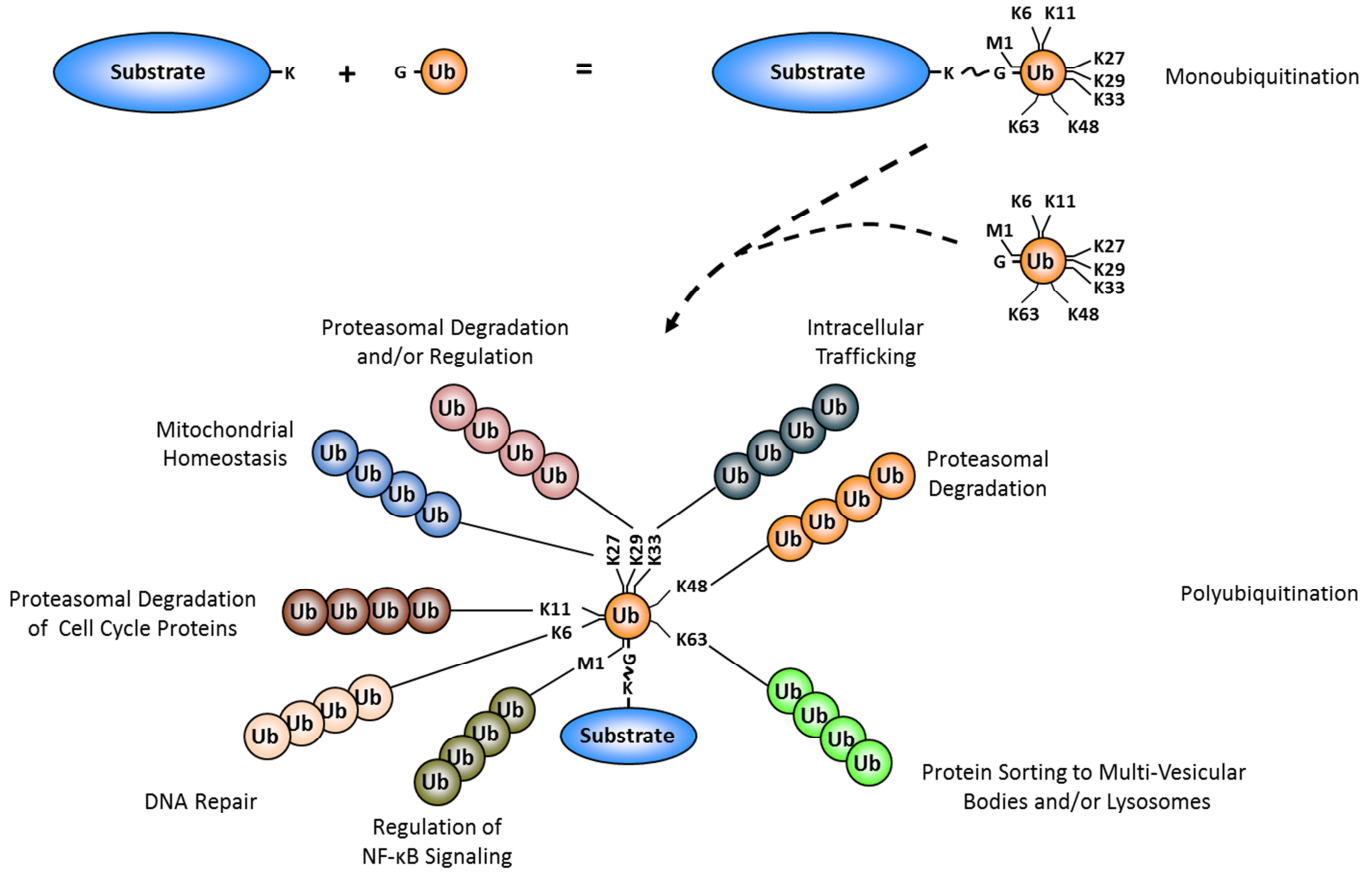

Figure 2: The type of ubiquitin chain determines the fate of the modified protein substrate. The NH2-terminal methionine (M1) as well as each of the seven lysine residues of the ubiquitin molecule is a potential acceptor site for modification with further ubiquitin moieties. This allows the formation of eight different poly-ubiquitin chains leading to various outcomes for the modified protein.

A well accepted view in this field is that K48-linked poly-ubiquitin chains target substrates for degradation by 26S proteasomes (Chau et al., 1989; Thrower et al., 2000). However, K11- and K29-linked poly-ubiquitin chains are likely to signal to proteasome-mediated degradation as well, since these chains are enriched following proteasome inhibition (Kim et al., 2011; Wagner et al., 2011; Wickliffe et al., 2011). Other ubiquitin linkages mainly perform non-proteolytic functions such as NF-κB activation by M1-linked poly-ubiquitin chains (Tokunaga and Iwai, 2012). Recent work has underlined important roles for K6-linked poly-ubiquitin chains in DNA repair (Morris and Solomon, 2004). Both K33- and K63-linked poly-ubiquitin chains have been reported to be involved in protein sorting in Golgi apparatus (Yuan et al., 2014), multi-vesicular bodies (Huang et al., 2013) and/or lysosomes (Kirkin et al., 2009). The K27-linked chains are the most enigmatic ones but an increasing body of evidence points to a potential role in mitochondrial biology (Geisler et al., 2010).

It rapidly became clear that the existence of these eight chains types was only the tip of the iceberg and that a much greater variety of ubiquitin-based signals exists, as the linkage propagated throughout the poly-ubiquitin chain is not necessarily the same. There is, indeed, increasing evidence that various linkages can be present in the same poly-ubiquitin chain allowing the assembly of heterologous “mixed chains” (Boname et al., 2010; Emmerich et al., 2013; Goto et al., 2010; Ikeda and Dikic, 2008; Kravtsova-Ivantsiv and Ciechanover, 2012). Besides, a single ubiquitin moiety embedded within a chain can be simultaneously modified at more than one site giving rise to “branched linkages” (Kim et al., 2007; Meyer and Rape, 2014; Peng et al., 2003). In addition to K48-linked poly-ubiquitin chains directing targets for proteasome-mediated degradation, mono-ubiquitin or poly-ubiquitin chains linked through a range of other lysine residues in the ubiquitin molecule can alter the localization or activity of the target protein, generally through the differential recruitment of ubiquitin-binding proteins.

Major substrates for ubiquitination include (i) fully translated mature proteins and (ii) the so-called defective ribosomal products (DRiPs). While the modification of full-length proteins with ubiquitin may have regulatory function, the ubiquitination of DRiPs is a pure quality control process that eliminates nonfunctional newly synthetized proteins during translation (Dolan et al., 2011; Yewdell and Nicchitta, 2006). Importantly, both fully

translated mature proteins and DRiPs represent good antigen sources for MHC class I presentation (Rock et al., 2014; Schubert et al., 2000).

2.1.1. Ubiquitin-like modifiers

Interestingly, in addition to ubiquitin which is constitutively expressed in all cells, a series of ubiquitin-like proteins sharing structural homology with the ubiquitin molecule may be up-regulated in response to inflammatory stimuli. These include interferon-stimulated gene 15 (ISG15) and the HLA F-adjacent transcript 10 (FAT10) as well as their inherent conjugation machineries (Fig. 3).

IFN-α/β and, to a lesser extent, IFN-γ are strong inducers of the ISG15 conjugation system (Ebstein et al., 2013). ISG15 is a ubiquitin-like modifier which can be conjugated to a vast number of cellular proteins through the sequential action of three conjugation enzymes that are also induced by IFN-α/β: E1 (UBE1L), E2 (UBE2L6) and E3 (Herc5 and TRIM25). As illustrated in Fig. 3, intersections occur between the ubiquitin and the ISG15 conjugation pathways with UBE2L6 being involved in both of these processes. However and in contrast to the ubiquitin system that uses a large number of E3 enzymes to select substrates in a specific manner, most of the IFN-induced ISG15 conjugation relies on a single E3 enzyme, namely Herc5 (Wong et al., 2006). Unlike ubiquitin, ISG15 is not a degradation signal for 26S proteasomes and the functional consequences of ISG15 modification are largely unknown. The observation that many components of the antiviral response are frequently modified with ISG15 (Yuan and Krug, 2001; Zhao et al., 2005) suggested a potential role of this modifier in innate immunity. However, the antiviral function of ISG15 remains controversial, since ISG15 null mice show an increased susceptibility to infection with coxsackievirus virus B3 (CVB3) (Rahnefeld et al., 2014), Sindbi virus, influenza virus or herpes virus (HSV) type 1 (Lenschow et al., 2007) but not with vesicular stomatitis virus (VSV) (Knobeloch et al., 2005) or lymphocytic choriomeningitis virus (LCMV) (Osiak et al., 2005).

Both TNF-α and IFN-γ lead to the activation of the FAT10 conjugation machinery within the infected cells. FAT10 is probably one of the most recent identified members of the ubiquitin-like family and, its biological significance remains obscure. Interestingly, like ubiquitin, FAT10 targets its modified substrates to the 26S proteasome for degradation (Hipp et al., 2005; Raasi et al., 2001). FAT10 is frequently constitutively expressed in tumors such

as hepatocellular carcinoma as well as gastric and gynecological cancers (Ji et al., 2009; Lee et al., 2003). In spite of an increased susceptibility of lymphocytes to apoptosis, the overall phenotype of the FAT10 knockout mice does not substantially vary from that of their wild-type littermates (Canaan et al., 2006), suggesting that this ubiquitin-like modifier is not essential.

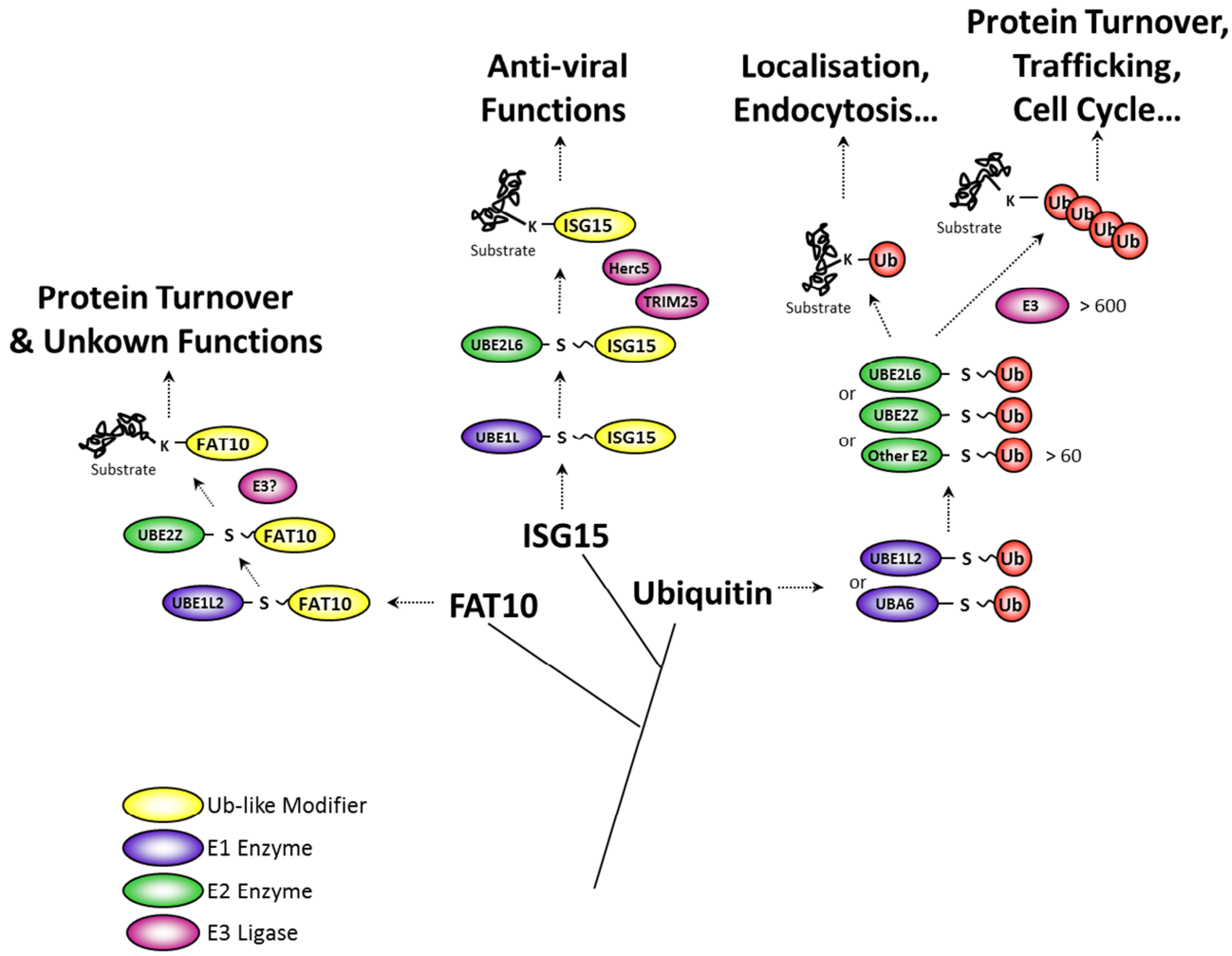

Figure 3: Conjugation pathways of ubiquitin and ubiquitin-like proteins. Like ubiquitin, the ubiquitin-like modifiers ISG15 and FAT10 use a conjugation system that relies on E1 and E2 enzymes as well as on E3 ligases. These pathways partially overlap with UBE2L6 being the E2 ubiquitin-conjugation enzyme for both ISG15 and ubiquitin. Likewise, Both FAT10 and ubiquitin require UBE1L2 and UBE2Z as E1 and E2 enzyme, respectively (modified from (Schulman and Harper, 2009)).

In a similar manner to ubiquitin and ISG15, the conjugation of FAT10 to cellular proteins relies on a E1-E2-E3 enzyme cascade which is not fully characterized. Herein, UBE1L2 has been recently described an E1 enzyme for FAT10 (Chiu et al., 2007) and, apparently, the UBE2Z ubiquitin E2 enzyme could also be used for FAT10 conjugation (Aichem et al., 2010). However and up to now, no FAT10-specific E3 enzymes have been experimentally verified. Our current knowledge about potential FAT10 substrates is also extremely limited with LRRFIP2, LULL1 and UBE1 being so far identified (Bialas et al., 2015; Buchsbaum et al., 2012).

2.2. The proteasome as peptide supplier for MHC class I antigen presentation

The 26S proteasome is composed of one 20S proteolytic complex and two axially positioned 19S regulatory complexes (Puttaparthi et al., 2007) which contain ATPase activity and are responsible for the recognition of the ubiquitinated proteins (Lam et al., 2002; Tanaka and Tsurumi, 1997). The 20S proteasome is itself defined as the latent and free form of proteasomes which is composed of 2 copies each of 7 α and β type subunits, each encoded by a distinct gene (Coux et al., 1996).

2.2.1. Standard and immunoproteasomes

Certain β subunits of the 20S core such as LMP2 ($i\beta_1$), MECL1 ($i\beta_2$) or LMP7 ($i\beta_5$) subunits are inducible and can replace the standard (S-Proteasome) β_1, β_2 and β_5 subunits, conveying differing proteolytic functions to the so-called immunoproteasome (I-Proteasome) (Kloetzel and Ossendorp, 2004). While S-Proteasomes are constitutively expressed in all cells, I-Proteasomes are present in immune cells including dendritic cells (DC) or can be formed in other cell types by interferon (IFN)-α/β or IFN-γ (Ebstein et al., 2009; Strehl et al., 2005; Tanaka, 1994). Complexity to this system has been recently added through the discovery of intermediate-type proteasomes bearing one or two out of the three inducible subunits (Guillaume et al., 2010; Guillaume et al., 2012; Klare et al., 2007). Importantly, the ability of 20S proteasomes to produce peptides suited for presentation by MHC class I molecules can be enhanced by the proteasome activator PA28 (Liu et al., 2007). The PA28 regulator is a ring shaped complex composed of a heterohexamer of two types of

subunits α and β having similar molecular masses of approximately 28 kDa (Zhang et al., 1998). PA28 binds to the 20S proteasome and the resulting PA28-20S-PA28 complex degrades proteins independently of ubiquitination (Baumeister et al., 1998). Alternatively, both PA28 and 19S regulators can simultaneously bind the 20S core particle to form a PA28-20S-19S hybrid proteasome complex, whose precise function remains to be fully determined (Liu et al., 2007). Under physiological conditions, the majority of proteasomes exists in form of 26S complexes which are the configuration responsible for ATP- and ubiquitin-dependent degradation (Livnat-Levanon et al., 2014).

The intrinsic subunit composition of proteasomes critically determines their capacity of generating peptides that are relevant and suitable for MHC class I presentation. Over the past two decades, several experimental approaches have been used to explore the role of the inducible subunits LMP7, LMP2 and MECL1 in MHC class I antigen processing as well as in other cellular processes including protein homeostasis (Seifert et al., 2010), cell signaling and/or proliferation (Basler et al., 2013; Ebstein et al., 2012a; Kruger and Kloetzel, 2012). One common method for evaluating I-Proteasome function *in vivo* is undoubtedly represented by the use of knock-out mice with an individual or combined deficiency of the inducible subunits. However and despite the massive efforts undertaken in these models, no general consensus has been reached as to how I-Proteasomes exactly affect the generation of MHC class I-restricted peptides, since both beneficial and detrimental effects have been reported. A substantial number of studies originally suggested that the incorporation of at least one of the three inducible subunits was critically required for the initiation of CTL responses directed against viral antigens (de Graaf et al., 2011; Hutchinson et al., 2011; Kincaid et al., 2012; Sijts et al., 2000; Van Kaer et al., 1994). Similar observations have been made in mice deficient for LMP7 or LMP2 and infected with parasites (Chou et al., 2010; Chou et al., 2008; Ishii et al., 2006; Tu et al., 2009). On the other hand, I-Proteasomes have also been reported to abrogate the presentation of self- (Zaiss et al., 2011), tumor (Chapiro et al., 2006; Dannull et al., 2007; Morel et al., 2000) and viral epitopes (Basler et al., 2004). Finally, a substantial body of evidence indicates that the switch from S-Proteasome to I-Proteasome has no detectable effect of the efficiency of the CTL response (Brosch et al., 2012; Frausto et al., 2007; Nussbaum et al., 2005). Recent work suggest that intermediated-type proteasomes bearing standard and inducible subunits may be the best equipped

proteasome complexes for the generation of the majority of tumor epitopes (Guillaume et al., 2010; Guillaume et al., 2012; Vigneron and Van den Eynde, 2012).

2.3. The MHC class I antigen processing pathway

The MHC class I antigen presentation pathway is an orchestrated pathway referring to the conversion of protein antigens into MHC class I-restricted peptides. It involves: (i) the generation of peptides by proteasomes, (ii) the transport into the lumen of the endoplasmic reticulum (ER), (iii) the binding to nascent MHC class I molecules and (iv) the trafficking of such MHC class I/peptide complexes via the secretory pathway to the cell surface for presentation to CD8+ T cells. Depending on the endogenous or exogenous origin of antigens, one can distinguish between direct and cross-presentation, respectively.

2.3.1. Direct presentation

MHC class I direct presentation (Fig. 4) occurs as a consequence of protein homeostasis in almost all nucleated cells of the body. Remarkably, most of the generated proteasomal products are too long and need to be further cleaved or trimmed from the N- and/or C-termini until the correct size (8-10 amino acids) is attained for optimal binding to MHC class I molecules in the ER (Lazaro et al., 2015). Such post-proteasomal processing may take place in various cellular compartments including the cytoplasm, the ER or the Golgi apparatus. Major cytosolic peptidases participating in the generation of MHC class I-restricted peptides are mostly aminopeptidases and include puromycin-sensitive aminopeptidase (PSA), bleomycin hydrolase (BH) (Stoltze et al., 2000), thimet oligopeptidase (TOP) (York et al., 2003), leucine aminopeptidase (LAP) (Beninga et al., 1998), aminopeptidase-B (AP-B) and prolyl-oligopeptidase (POP) (Urban et al., 2012). Proteolytic trimming in the ER typically involves the IFN-γ-inducible ER-associated aminopeptidases (ERAP) 1 and 2 (Saveanu et al., 2005) and/or the angiotensin-converting enzyme (ACE) (Shen et al., 2011). Eventually, MHC class I ligands may be subjected to a final processing step during their transport to the cell surface in the trans-Golgi network by the pro-protein convertase furin (Gil-Torregrosa et al., 1998; Medina et al., 2009; Tiwari et al., 2007).

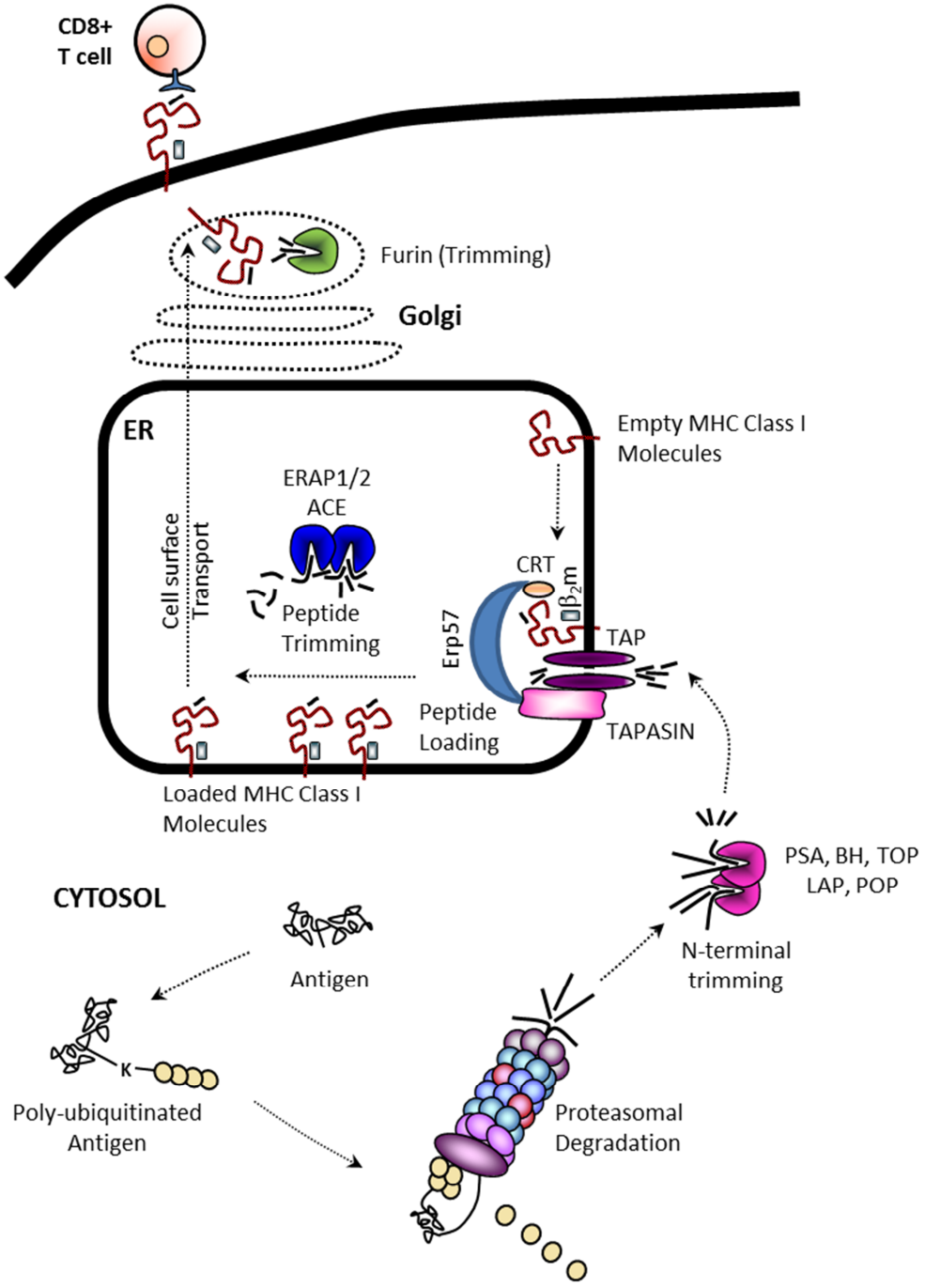

Figure 4: MHC class I antigen presentation pathway. MHC class I direct presentation starts with the modification of antigens with ubiquitin. Ubiquitin-modified antigens are then degraded in the cytosol by the 26S proteasome, thereby leading to the generation of peptides which after N-terminal trimming from are exported into the ER via TAP. Once in the ER, these peptides are loaded onto MHC class I molecules prior to their subsequent transport to the cell surface for recognition through CD8+ T cells.

The translocation of proteasomal degradation products from the cytosol into the lumen of the ER is ensured by the transporters with antigen processing (TAP) 1 and 2. Both TAP1 and TAP2 are associated in the ER with MHC class I heavy chain/β2-microglobulin (β2-m) dimers via the TAP-associated molecule Tapasin (Tsn) (Ortmann et al., 1997; Sadasivan et al., 1996). The binding of TAP to Tsn and MHC class I molecules in the ER is believed to be stabilized by the protein disulphide isomerase ERp57 which, in turn, binds to Tsn and the lectin chaperone calreticulin which, itself, recognizes a glycosylated part of the MHC class I molecule. These interactions allow the formation of a protein complex called peptide loading complex (PLC) in which empty MHC class I molecules are loaded by high-affinity peptides (Peaper et al., 2005). Newly formed peptide-MHC class I complexes dissociate from the PLC prior to transportation to the cell surface via the Golgi apparatus for recognition by CD8+ T cells.

2.3.2. Cross-presentation

Antigen cross-presentation describes the unique capacity of DC to acquire exogenous antigens and present them onto MHC class I molecules. DC represent a heterogeneous group of professional antigen-presenting cells (APC) found in the blood, lymph nodes and in a small amount in non-lymphoid tissues throughout the body. DC are considered as the major professional APC of the immune system presenting processed antigens to the effector T cells. At least two pathways in which peptides from exogenous antigens could be made and bound to MHC class I molecules have been described (Fig. 5). The first one involves the transfer of exogenous antigens from endosomes into the cytosol for subsequent degradation by proteasomes (Arnold et al., 1995; Fonteneau et al., 2003; Kovacsovics-Bankowski and Rock, 1995; Li et al., 2001; Norbury et al., 1995). The second one implies the production of MHC class I ligands inside the endosomes by non-proteasome proteases (Shen et al., 2004). It is assumed that the contribution of the endosome-to-cytosol pathway to cross-presentation is more important under physiological conditions than the endosomal one (Rock and Shen, 2005). In 2003, a flurry of studies reported the existence of a cellular process whereby endosomes may fuse with ER-derived vesicles in DC to promote cross-presentation (Ackerman et al., 2003; Guermonprez et al., 2003; Houde et al., 2003). Interestingly, the resulting endosome-ER mixed compartments possess newly synthesized MHC class I molecules as well as many ER-derived elements such as TAP, tapasin, calreticulin

and ERp57 making them potentially fully competent organelles for MHC class I antigen presentation (Cresswell et al., 1999). Besides, they appear capable of recruiting further proteins with antigen processing properties such as the insulin-regulated aminopeptidase (IRAP) which ensures amino-terminal peptide trimming of internalized antigens (Saveanu et al., 2009; Weimershaus et al., 2012).

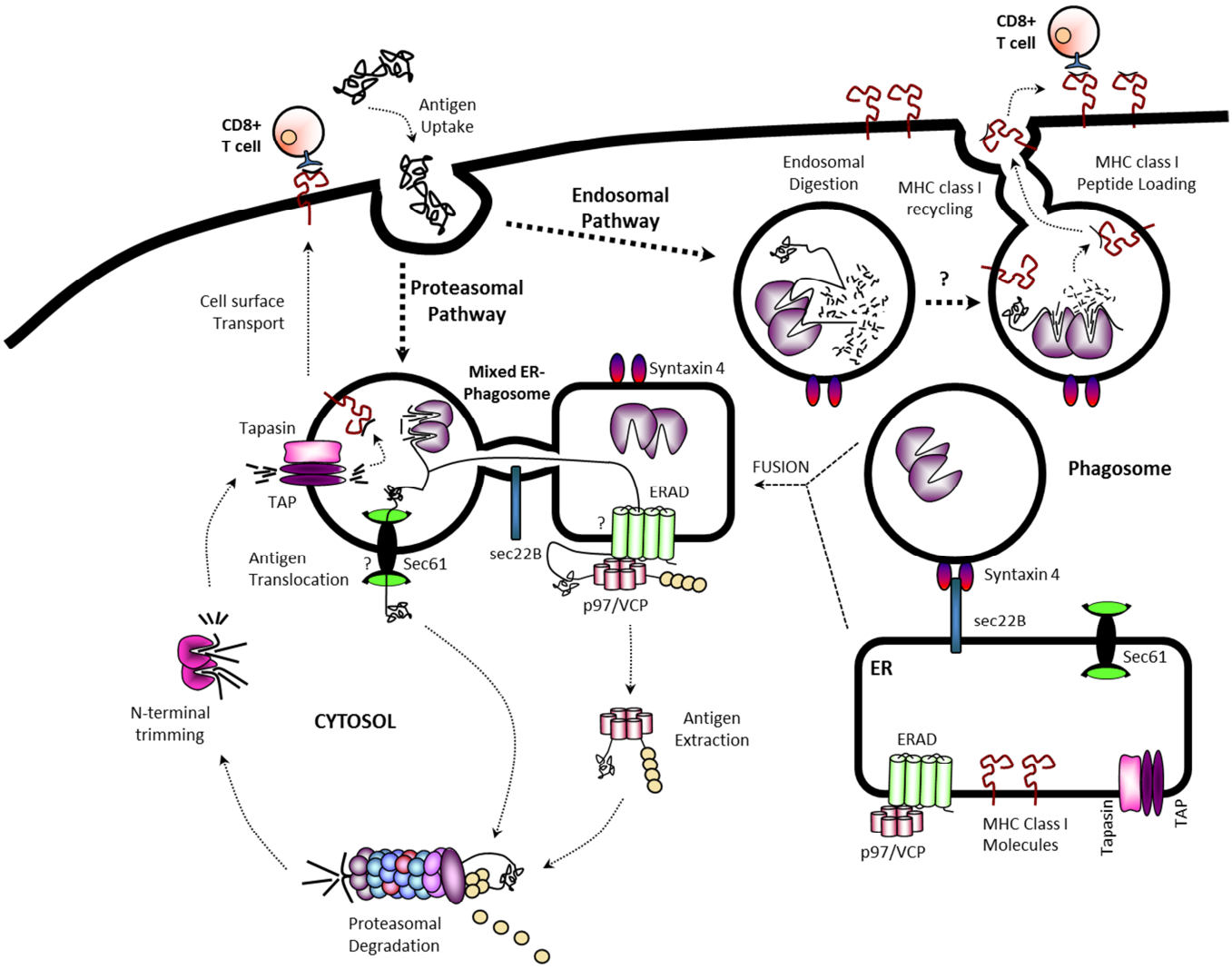

Figure 5: Potential MHC class I cross-presentation pathways. MHC class I cross-presentation begins with the uptake of exogenous proteins by DC. The proteasomal pathway implies the transport of internalized antigens from ER-endosome mixed compartments into the cytosol for degradation by 26S proteasomes. Whether such export occurs through the sec61 translocation channel and/or ERAD remains controversial. The endosomal route describes the generation of MHC class I-restricted epitopes in endosomes by non-proteasome enzymes.

Given their positive staining for Rab5, EEA1 (Burgdorf et al., 2007), Rab14 (Saveanu et al., 2009) and RAB3b/3c (Zou et al., 2009), it is assumed that such compartments partially originate from early endosomes. The trafficking of ER-vesicles into endosomes is thought to rely on the SNARE sec22b (Cebrian et al., 2011). Controversy exists in the field as to how antigens gain access to the cytosol for proteasome degradation. It has been reported that the transfer of antigens from endosome-ER mixed compartments into the cytosol could be mediated by the ER translocation channel sec61 (Zehner et al., 2015). However, other studies have shown a possible role for the ER-associated degradation (ERAD) machinery in this process. ERAD is a quality control system responsible for the degradation of aberrant proteins in the ER which allows the transport of substrates across the ER membrane from the lumen into the cytosol through a channel called the retro-translocation channel (as opposed to the translocation channel sec61 which allows the trafficking of proteins from the cytosol into the ER lumen). Importantly, the retro-translocation of polypeptides across the ER membrane requires their poly-ubiquitination and subsequent extraction from the membrane by the p97 ATPase [also called valosin-containing protein (VCP)] (Ye et al., 2005). The p97/VCP protein itself is associated to the ER membrane via specific interaction with a membrane protein complex containing Derlin-1 and the VCP-interacting membrane protein (VIMP). Once in the cytoplasm, the “pulled” substrate is degraded by the 26S proteasome (Meusser et al., 2005). The observation that antigen cross-presentation is blocked by over-expression of a dominant-negative form of p97 supports the implication of ERAD may in the endosome-to-cytosol pathway (Ackerman et al., 2006). The precise nature of such retro-translocation channel for cross-presentation, however, remains to be fully defined.

3. Objectives

Although the role of proteasomes in the supply of MHC class I-restricted is well documented, our current knowledge on how ubiquitin regulates MHC class I antigen processing and presentation is still limited and partially conflicting. Pioneering work of Townsend and colleagues originally suggested that ubiquitin modification allows antigens to enter the MHC class I antigen processing pathway, as evidenced by the increased MHC class I presentation of antigens fused with one ubiquitin moiety (Townsend et al., 1988). The notion that ubiquitin modification is a prerequisite for the processing of endogenous antigens was further supported by later studies showing that MHC class I antigen presentation is compromised in cells defective in ubiquitin conjugation and/or for antigens devoid of ubiquitin acceptor sites (Grant et al., 1995; Michalek et al., 1993). However, it was later suggested that MHC class I antigen presentation, although relying on proteasomes, may occur in a ubiquitin-independent manner (Cox et al., 1995; Yellen-Shaw and Eisenlohr, 1997). In these works, it is implied but nor formally demonstrated that 20S rather 26S proteasome complexes are responsible for the supply of MHC class I-restricted peptides. It is also argued that the ubiquitin-dependency for MHC class I processing may vary according to the folded state and/or localization of antigens (Huang et al., 2011; Michalek et al., 1996; Park et al., 2010).

Therefore, to broaden our understanding in this field, our aim in this work is to dissect the MHC class I antigen processing pathway upstream protein degradation by proteasomes at the level of ubiquitin conjugation, trafficking and recognition. We expect from the use of dendritic cells and tumor cells as antigen-presenting cell models to gain new insights into the MHC class I direct and cross-presentation pathways.

4. Results and Discussion

4.1. Transcriptome analysis of dendritic cells reveals the activation of the ISG15 and FAT10 conjugation machineries in response to maturation stimuli (this chapter is based on Ebstein and coworkers (Ebstein et al., 2009))

Dendritic cells (DC) are professional antigen-presenting cells which are capable of cross-presentation and reside in the periphery at an immature stage. Upon maturation, they migrate into the lymph nodes where they present MHC/peptide complexes to T cells and stimulate them to initiate primary immune responses. To further understand the maturation process at the level of the ubiquitin-proteasome system (UPS), we used the human U133 2.0 Plus-Array (Affimetrix) to assess the transcriptional program in DC in response to various stimuli including a cytokine cocktail of TNF-α, IL-6, IL-1-β and PGE2 as well as LPS, Poly(I:C) or CD40L. Interestingly, the core response common to the four maturation regimens comprised a total of 33 up-regulated genes. Many of these genes encode proteins belonging to the FAT10-conjugation machinery such as the FAT10 ubiquitin-like protein itself as well as the UBE1L2 E1 enzyme and the NUB1 ubiquitin-binding protein. Noteworthy, both LPS and Poly(I:C) induced the transcription of signature of genes from the interferon (IFN) pathway including the ubiquitin-like modifier ISG15 as well as enzymes linked to the ISG15 conjugation system (i.e. HERC5, TRIM25, UBE2L6, USP18). Interestingly, we further demonstrate that the increased expression of the E2 enzyme UBE2L6 is required for efficient antigen cross-presentation by DC in response to LPS. In summary, our data underline the importance of remodeling the UPS for DC function.

The International Journal of Biochemistry & Cell Biology 41 (2009) 1205–1215

Contents lists available at ScienceDirect

The International Journal of Biochemistry & Cell Biology

journal homepage: www.elsevier.com/locate/biocel

Maturation of human dendritic cells is accompanied by functional remodelling of the ubiquitin-proteasome system

Frédéric Ebstein, Nicole Lange, Sabrina Urban, Ulrike Seifert, Elke Krüger, Peter-Michael Kloetzel*

Charité-Universitätsmedizin Berlin, CCM, Institut für Biochemie, Monbijoustr. 2, D-10117 Berlin, Germany

ARTICLE INFO

Article history:
Received 7 August 2008
Received in revised form 28 October 2008
Accepted 29 October 2008
Available online 5 November 2008

Keywords:
Dendritic cells
Ubiquitin-proteasome system
ISG15
FAT10
UBE2L6
Cross-presentation

ABSTRACT

Dendritic cell maturation is the process by which immature dendritic cells differentiate into fully competent antigen-presenting cells that initiate T cell responses. Although some mechanistic aspects of DC maturation have begun to be characterised, very little is known about the genetic events regulating the ubiquitin-proteasome system which plays a key role at various levels of the immune response. Therefore, we here investigated the expression of more than 1000 genes related to the ubiquitin-proteasome system in maturing dendritic cells following various stimuli and identified a specific set of transcripts induced by lipopolysaccharide and/or Poly(I:C) which is largely distinct from that induced by CD40 ligand or pro-inflammatory cytokines. This group of genes was dependent on a type I interferon autocrine loop and included E1 and E2 enzymes, E3-ligases, de-ubiquitylating enzymes, proteasome components as well as the ubiquitin-like modifiers ISG15 and FAT10. We further demonstrate that the increased expression of the E2 enzyme UBE2L6 (UbcH8) is required for efficient antigen cross-presentation by dendritic cells. In summary, our data underline the importance of remodelling the ubiquitin-proteasome system for dendritic cell function.

1. Introduction

Dendritic cells (DCs) are considered the "sentinels" of the immune system specialized in antigen capture, processing and presentation of antigens to initiate T cell responses (Banchereau et al., 2001; Steinman and Banchereau, 2007). DC maturation can be induced by various stimuli such as cytokines (Jonuleit et al., 1997), T cells (Caux et al., 1994) or pathogens (Cella et al., 1999; De Smedt et al., 1996) and is accompanied by a major switch from antigen capture to antigen processing and presentation capacities. This process is associated with DC migration towards T cell rich areas of peripheral lymphatic tissues where they present MHC-bound antigenic peptides to both CD4+ T cells and CD8+ cytotoxic T cells (CTLs). Importantly, protective immunity requires antigen presentation by fully matured DCs (mDC) (Menges et al., 2002).

To recognise pathogens, immature DCs (imDCs) are equipped with a battery of surface and intracellular receptors like that of the toll-like receptor (TLR) family. Ligand binding to TLRs triggers a signalling cascade that ultimately ends up in the activation of the transcription factor NF-κB, or in a parallel pathway of IFN regulatory factors (IRFs). Thereby, the production of cytokines like TNFα or type I IFN (IFNα, IFNβ) is induced (Kanzler et al., 2007).

Protein modification by ubiquitin (Ub) or ubiquitin-like (Ubls) proteins represents an important regulatory mechanism in the modulation of immune responses (Liu et al., 2005; Wong et al., 2003). Classically, conjugation of multiple Ub moieties to proteins serves as signal for their selective degradation by the proteasome (Glickman and Ciechanover, 2002). Depending on the kind of ubiquitylation, such modifications can also function in signalling and endocytosis (Mukhopadhyay and Riezman, 2007).

Conjugation of Ub or Ubls is mediated in a three-step process by a machinery of conserved enzymes. One of the 15 human Ub-activating enzymes (E1) can bind and activate Ub or Ubls in an ATP-dependent manner and transfer the Ub-moiety to one of the 70 corresponding family members of the Ub-conjugating enzymes (E2) (Wong et al., 2003). Finally, Ub is conjugated to substrates by one of the more than 600 specific E3 ligases (Wong et al., 2003) that physically interact with the substrate. Importantly, ubiquitylation is a reversible process, since Ub can be removed by multiple de-ubiquitinating enzymes (DUB).

Abbreviations: CTL, cytotoxic T cells; DCs, dendritic cells; DUB, de-ubiquitylating enzyme; FAT10, F-adjacent transcript 10; HCMV, human cytomegalovirus; ISG15, interferon stimulated gene 15; IRF, interferon response factor; NUB1, Nedd8-ultimate buster-1; PAMP, pathogen-associated molecular patterns; PGE2, prostaglandin E2; Poly(I:C), copolymer of polyinosinic and polycytidylic acids; pp65, phosphoprotein 65; TLR, toll-like receptor; Ub, ubiquitin; Ubl, ubiquitin-like modifier; UPS, ubiquitin proteasome system.

* Corresponding author. Tel.: +49 30 450 528 071; fax: +49 30 450 528 921.
E-mail address: p-m.kloetzel@charite.de (P.-M. Kloetzel).

1357-2725/$ – see front matter © 2008 Elsevier Ltd. All rights reserved.
doi:10.1016/j.biocel.2008.10.023

It is well established that antigen presentation requires the generation of antigenic peptides by the UPS (Kloetzel and Ossendorp, 2004; Rock et al., 2002). Therein, activity of the multi-subunit proteasome complex can be controlled by different modes of regulation, such as subunit expression, subunit incorporation and interaction of the 20S core with different regulators. One of these compositionally distinct proteasomes is the so-called immunoproteasome, containing specialized immunosubunits and favouring the generation of peptides that are suitable for MHC class I molecules (Kloetzel and Ossendorp, 2004; Strehl et al., 2005).

Until today, our understanding of the regulation of the UPS during DC maturation is very limited. Except for expression studies of 20S immunoproteasomes (Li and Hassel, 2001; Macagno et al., 1999; Whiteside et al., 2004) hardly anything is known about the primary events during DC maturation involving and affecting the UPS, including the expression of UPS genes in response to specific maturation stimuli. Due to the limited number of UPS genes that were included in the various studies so far, gain of detailed knowledge of UPS gene expression in human DCs has been slow.

To obtain a better and first comprehensive insight into the mechanisms underlying the conversion of immature to mature DCs in terms of the expression of UPS-related genes, we performed comparative expression profiling of approximately 1200 UPS-related genes during DC maturation in response to four different prototypic maturation stimuli. These include a cytokine cocktail (IL-1-β + IL-6 + TNF-α + PGE2) (Jonuleit et al., 1997) and CD40 ligand (CD40L) mimicking inflammation or T cell interaction, respectively. In addition, maturation was induced by LPS via toll-like receptor 4 (TLR4) or Poly(I:C) via TLR3 signalling pathways (Kanzler et al., 2007). These pathogen associated molecular patterns (PAMPs) simulate bacterial or viral infection, respectively. Depending on the maturation stimulus, specific sets of UPS genes were differentially expressed, both at the RNA and protein level. Our data demonstrate that the coordinated expression of a number of UPS genes during maturation of human DCs is regulated by autocrine mechanisms involving type I IFNs and TNF-α. Using RNA interference directed against the major up-regulated Ub-conjugating E2 enzyme UBE2L6 (UbcH8), we further show that the remodelling of the UPS in response to PAMPs is required for the presentation of cell-associated antigens to MHC class I molecules (a processed referred as cross-presentation). Taken together, these results describe for the first time the numerous changes of the UPS during DC maturation and underscore the importance of these changes for DC function.

2. Materials and methods

2.1. Generation of immature DC

DCs were cultured in RPMI1640 supplemented with 10% FCS plus 1% penicillin/streptomycin (Biochrom). Immature DCs were generated from Buffy coats of healthy donors obtained from the German Red Cross after informed consent. Peripheral blood mononuclear cells (PBMCs) were separated by Ficoll-Paque (Biochrom) gradient centrifugation and DCs were generated from purified CD14+ cells by using antibody-coated microbeads and magnetic separation (Milteny Biotech). Selected CD14+ cells were cultured for 5 days in the presence of GM-CSF (500 U/ml) and IL-4 (100 U/ml) (Strathmann Biotec).

2.2. Induction of DC maturation

Day 5-im DCs were seeded on 24-well plates at 1×10^6 cells/ml and maturation was induced by addition of either a cocktail of pro-inflammatory cytokines and prostaglandins (Jonuleit et al., 1997) including TNF-α (10 ng/ml) + IL-1-β (10 ng/ml) + IL-6 (1000 U/ml) + PGE2 (1 μg/ml) (Strathmann Biotec), LPS (1 μg/ml) (Sigma), Poly(I:C) (50 μg/ml) (Invivogen) or flagged CD40L (500 ng/ml), anti-Flag mAb (1 μg/ml) (Alexis Biochemicals) for various period of times. In some experiments, 1 μM of the proteasome inhibitor MG132 (Calbiochem) was added for the last 2 h of stimulation. Mouse anti-human IFNAR2 antibodies (CD118) and mouse anti-human TNFR1 (R&D Systems) were used at the concentration of 10 μg/ml. IFN-β and TNF-α productions were assessed by ELISA (TFB, Inc. and BD Biosciences, respectively). FITC- or PE-conjugated monoclonal antibodies against CD11c, CD80, CD83, CD86, HLA-ABC and HLA-DR (BD Biosciences) were used for phenotypic analysis.

2.3. Preparation of RNA, microarray hybridization, and data analysis

Total RNA was extracted from frozen cell pellets using the High Pure RNA Isolation kit (Roche Diagnostics). For microarray analysis total RNA was amplified and labelled (Message AmpII-Biotin enhanced Kit, Ambion). The Human U133 2.0 Plus-Array (Affymetrix) was custom hybridized and evaluated by standard procedures (Signature Diagnostics). Subgenome analysis for UPS-related genes is based on conserved motif bioinformatics custom-provided by Milteny Biotech (Bergisch Gladbach, Germany). The data discussed in this publication have been deposited in NCBIs Gene Expression Omnibus (GEO, http://www.ncbi.nlm.nih.gov/geo/) and are accessible through GEO Series accession number GSE10316.

2.4. cDNA synthesis and Taqman® real-time PCR

For real-time PCR, 1 μg total RNA was reverse transcribed using the First Strand cDNA synthesis kit (Roche Diagnostics). Real-time PCR was performed in duplicates to determine the mRNA levels of each gene using primers and probes of TaqMan® Gene Expression Assays (Applied Biosystems) with a Rotor Gene 3000 (Corbett Research). The relative amounts of each gene were acquired and calculated with the comparative cycle threshold values using the Rotor Gene Monitor Software (version 4.6) and normalised to an endogenous reference (HPRT1). For each target gene analysed, cDNA was amplified and then sub-cloned into the pCR2.1-TOPO TA-cloning vector (Invitrogen GmbH, Karlsruhe, Germany). The resulting plasmids were then linearized and used to prepare an eight-fold dilution series of amplification standards from 5×10^5 to 328 copies per μl.

2.5. Immunoblotting analysis

Cells were lysed in a Tris buffer (0.15 M NaCl, 0.05 M Tris, 5 mM EDTA, 10 mM MG132, 100 mM NEM and 1% NP40, pH 7.5). Thirty micrograms of protein from each cell extract was separated by SDS-PAGE and immunoblotted with anti-ISG15 (gift from K.P. Knobeloch), anti-FAT10 (Biomol) and anti-Ub (Dako), antibodies. POD-coupled goat anti-rabbit (1:5000) secondary antibodies were used. Detection was performed by enhanced chemiluminescence.

2.6. HCMV-pp65$_{495-503}$-specific CD8+ T cell clone

An HLA*A0201-restriced HCMV pp65-specific CD8+ T cell clone was prepared following the procedure of Fonteneau et al. (2001). Briefly, cultures containing pp65-specific CD8+ T cells were obtained from stimulations with DCs with the synthetic peptide NLVPMVATV and were cloned by limiting dilution in the presence of irradiated feeder cells, phytohemagglutinin (PHA and Sigma) and

IL-2 (Chiron Therapeutics, Emeryville, CA, USA) to yield clone16. The clone was used at least 10 days, after restimulation in vitro, when it was at a resting state.

2.7. UBE2L6 siRNA mediated gene silencing

Chemically synthesised siRNA oligonucleotides targeting UBE2L6 (Catalogue no. L-008569-00-0020) and control siRNA (Catalogue no. D-001210-0X) were obtained from Dharmacon Inc., USA. siRNA duplexes were dissolved in siRNA suspension buffer (Dharmacon) to a final concentration of 20 μM, incubated at room temperature for 30 min and stored in aliquots at −80 °C.

2.8. siRNA transfer to DC via electroporation

siRNA were delivered in DCs by electroporation following the procedure of Schaft et al. (2005). Briefly, cells were harvested and washed once with RPMI medium and re-suspended with Opti-MEM without phenol red (Invitrogen) at a concentration of 4×10^7 cells/ml. Respective amounts of siRNA duplexes (2000 nM) were transferred to a 4-mm cuvette (BioRad Laboratories GmbH, Munich, Germany). Two hundred microliters of cell suspension (containing 8×10^6 cells) was added and pulsed in a GenePulser 2 apparatus (BioRad). Pulse conditions were square-wave pulse 500 V and 0.5 ms. After electroporation, cells were transferred to pre-warmed RPMI medium supplemented with 10% FCS in the presence of GM-CSF and IL-4 for 48 h.

2.9. Assay for cross-presentation of pp65+ necrotic cells

HeLa cells stably transfected with pp65 cDNA were used as a source of pp65 antigen. Necrosis of pp65+ HeLa cells was induced by 4–5 repetitive freeze and thaw cycles. Following 48 h of incubation with siRNA, immature DCs were plated in a 96-well plates (3×10^4 cells/well) and co-cultured with necrotic cells (at a ratio 1:2) or 1 μM peptide in the presence of the anti-pp65 T cell clone16 at the ratio 1:1 in a final volume of 150 μl for 4–12 h. The maturation stimulus LPS (1 μg/ml) was added to the wells. Activation of pp65-CTL was assessed through quantitation of secreted IFN-γ by ELISA as described below.

2.10. ELISA for IFN-γ secretion

ELISA for IFN-γ was performed following the manufacturer's instructions (BD Biosciences). Ninety-six-well plates were coated overnight with primary anti-IFN-γ mAb, washed and blocked for 1 h with PBS-10% FCS. Diluted (1:10) supernatants from CTL experiments were added to pre-coated wells in duplicates and supplemented with secondary antibodies and stretptavidin-bound POD for 1 h. Plates were washed and incubate for 30 min with TMB substrate (BD Biosciences). Optical density was counted at 450 nm on an ELISA apparatus.

3. Results

3.1. Phenotype changes of matured DC in response to Poly(I:C), LPS, CD40L and the cytokine cocktail

To assess DC activation and maturation patterns, we first compared the phenotypic modifications elicited by four prototypic stimuli including a cytokine cocktail, Poly(I:C), LPS and CD40L. Expression of maturation-related cell surface molecules on DCs was determined by flow cytometry 24 and 48 h after culture of imDCs in the absence or in the presence of the maturation stimuli. As

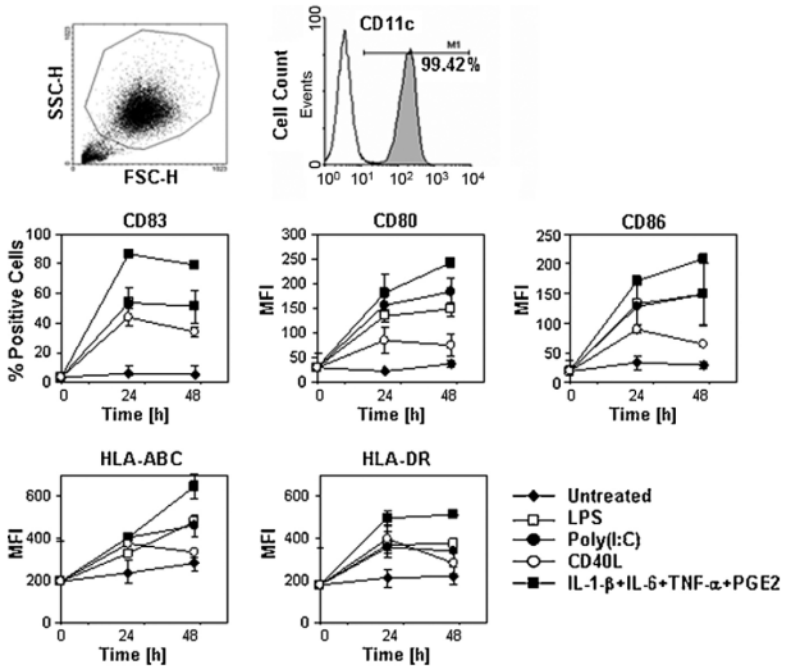

Fig. 1. Kinetics of changes in the expression patterns of different surface molecules of DCs during maturation. Day 5-immature DCs were cultured in the presence of a cytokine cocktail, Poly(I:C), LPS, CD40L or left untreated. DCs were gated according to their morphological properties and only viable cells (propidium iodide negative) were included in the final analysis. Labelled cells were analysed at the indicated time points by flow cytometry and the values represent either mean fluorescence intensity (MFI) for CD80, CD86, HLA-ABC and HLA-DR or the percentage of positive cells for CD83.

Table 1
Summary of the number of regulated UPS-related genes from the Human U133 2.0 Plus-Array (Affymetrix).

	Genes induced > 3			Genes repressed < 3		
	4 h	8 h	16 h	4 h	8 h	16 h
Poly(I:C)	74	109	105	98	109	113
LPS	89	107	111	156	121	87
CD40L	66	97	98	108	89	94
IL1β + IL6 + TNFα + PGE2	55	56	47	88	48	25

shown in Fig. 1, a 5-day culture of monocytes in the presence of GM-CSF and IL-4 yielded typical CD14-immature DCs, 99% of which expressing the DC-lineage marker CD11c. Importantly, cell populations contained no CD3-, CD19-, CD20- or CD56-positive cells (data not shown). All four maturation strategies increased the fraction of cells expressing the maturation marker CD83 as well as the median expression levels of CD80, CD86, HLA-ABC and HLA-DR as phenotype features of activated DCs, but to different extents. In agreement with previous reports (Jonuleit et al., 1997), the highest median fluorescence intensity of the analysed surface molecules was attained with the cytokine cocktail (90% CD83+ cells). Stimulation of DCs with either Poly(I:C) or LPS led to 60% CD83+ cells, with lower expression of CD80, CD86, HLA-ABC and HLA-DR relative to their cytokine cocktail-stimulated counterparts. As expected, CD40L had little effect on DC maturation, as flow cytometric measurements of CD40L-treated cells showed a bimodal distribution of CD83, indicating that only a fraction of the cells acquired an activated phenotype. However, up-regulation of other maturation markers became apparent at 24 h with intermediate levels expression of CD80, CD86, HLA-ABC and HLA-DR. Thus, our data show that all four maturation procedures induce the expected outcome of downstream-cellular responses of mDCs resulting in the increased surface expression of MHC class I and class II molecules required for T cell activation.

3.2. Identification of differentially expressed UPS-related genes

To elucidate the transcriptional regulation of UPS-related genes during the maturation of human DCs, mRNA expression profiles were generated by treatment of imDCs with LPS, Poly(I:C), the cytokine cocktail or CD40L in time course experiments. Using Affymetrix microarrays, we focused our analysis on approximately 1200 UPS-related genes which have been selected due to their previous functional description as part of the UPS or based on conserved motif searches using bioinformatics. Only genes that exhibited at least a 3-fold increased hybridization signal after 4, 8, or 16 h of induction of maturation were considered for analysis. Importantly, depending on the donor the relative induction rates of the identified UPS genes can vary without that the quality of the induced genes was strongly affected. The highest number of differentially expressed UPS-related genes was observed after LPS treatment with 142 up-regulated and 206 down-regulated mRNAs. Similarly, Poly(I:C) and the cytokine cocktail induced also more than 100 differentially expressed UPS-genes, while the number of genes induced by CD40L was smaller (Table 1). Regardless of the stimulus, among the induced UPS-components were E1 enzymes, E2 enzymes, identified or putative E3-ligases or components of multi-subunit E3-ligases, DUBs, proteasome components, proteins containing UBA-domains that bind Ub or Ubl-, Ub-like modifiers (Supporting information, SI Tables 1–4; Fig. 2) and others (data not shown). Interestingly, DC maturation induces the Ubl modifiers ISG15 and FAT10, whose functions seem to be connected with the immune response, while other Ubl modifiers such as Sumo or Nedd8 seemed to be less affected.

3.3. Only a subset of UPS genes is commonly induced by LPS, Poly(I:C) CD40L and the cytokine cocktail during DC maturation

To study whether different DC maturation regimens exert different effects on the transcriptional regulation of the UPS genes we next analysed overlapping UPS gene expression during DC maturation in response to Poly(I:C), LPS, CD40L and the cytokine cocktail (SI Tables 1–4; Fig. 2). The genes commonly affected by the four different maturation regimens were visualized by a Venn diagram (Fig. 2). Only 33 mRNAs were found to be up-regulated under all applied maturation regimens. These included the genes encoding the Ubl FAT10 as well as its specific E1 enzyme UBE1L2 (Chiu et al., 2007), PA28-β, the Fat10 binding adapter molecule NUB1 (Hipp et al., 2004, 2005), the E2 enzyme UBE2J1, 21 known or putative E3-ligase components and 5 DUBs. Moreover, up-regulation of SQSTM1 which is involved in escorting ubiquitylated proteins to proteasomes and/or autophagosomes has been observed (Fig. 2). Comparison of the expression profiles revealed a set of genes that were specifically affected by LPS and Poly(I:C) but not by CD40L or the combined treatment of pro-inflammatory cytokines (Fig. 2). These infection simulating stimuli induced a strongly overlapping set of 25 UPS-genes (Fig. 2). Most strikingly, the induced set included all known components of the ISG15-modification system (ISG15, the E1 enzyme UBE1L, the E2 enzyme UBE2L6, the E3 ligases HERC5 and TRIM25, and the DUB USP18 (Dastur et al., 2006; Malakhov et al., 2002; Pitha-Rowe et al., 2004; Wong et al., 2006; Zhao et al., 2004; Zou and Zhang, 2006)) supporting the idea that ISG15 protein modification plays an important role in the innate immune response. In contrast, there existed considerably less overlap in the expressed genes comparing stimulation with the cytokine cocktail and CD40L which seem to induce a more stimulus-specific gene expression program. In summary, the data suggest a DCs specific differential regulation of a relatively distinct set of UPS-related genes in response to a specific stimulus that mimic either infection, T cell stimulation or inflammation (Banchereau et al., 2001; Steinman and Banchereau, 2007) (Fig. 2).

3.4. Poly-Ub and ISG15 conjugates were increased in DC following treatment with LPS or Poly(I:C)

Poly(I:C) or LPS induced maturation of human DCs resulted in the significant up-regulation of several E1, E2 and E3 enzymes. To test whether this up-regulation of the Ub-conjugation machinery is also reflected at the protein level we studied the state of poly-ubiquitylation throughout DC maturation. Both Poly(I:C) and LPS treatment of imDCs resulted in a strong up-regulation of high molecular weight poly-Ub-conjugates starting very early at 4 h after stimulation. Short treatment of DCs with MG132 resulted in an additional accumulation of Ub-conjugates showing that these proteins are degraded by proteasomes (Fig. 3A). In contrast, maturation by the cytokine cocktail or CD40L revealed only negligible effects on the levels of Ub-conjugates (data not shown). Thus, Ub conjugate formation may not contribute to antigen generation under these conditions.

To further substantiate our microarray expression analyses, we selected a group of target genes to be confirmed by real-time RT-PCR and at the protein expression level. In the first set of experiments we focused on the genes of the ISG15-conjugation system (Fig. 3B). Consistent with the array data real-time PCR revealed a strong up-regulation of all tested genes of the ISG15 machinery in response to LPS and/or Poly(I:C). In contrast, no induction of these genes was observed after the treatment with the cytokine cocktail or after CD40L stimulation. Remarkably, Poly(I:C) induced the ISG15 machinery to a much greater extent than LPS. Furthermore, the up-regulation of these genes followed a distinct expression

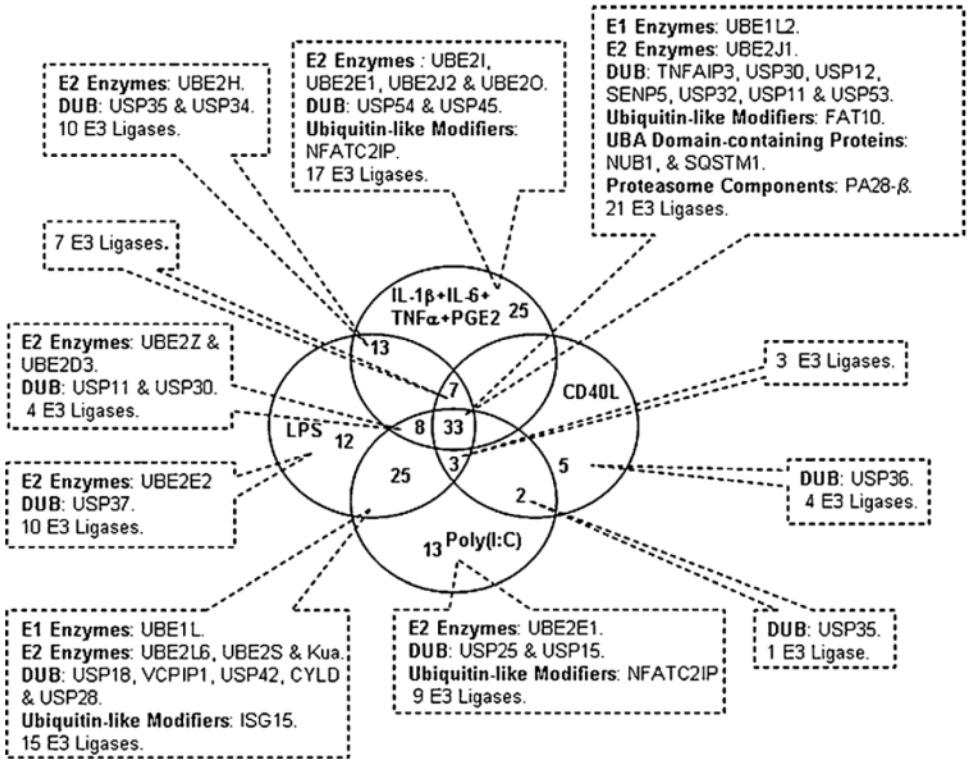

Fig. 2. Classification of the genes up-regulated by the treatment with Poly(I:C), LPS, CD40L and the cytokine cocktail. Selected genes and gene groups are listed in boxes in each area. In total, there were 32 genes induced by the treatment with cytokine cocktail, 50 LPS-induced genes, 45 Poly(I:C)-induced genes and 13 genes up-regulated following CD40L treatment. There was an almost perfect overlap of increased expression by LPS and Poly(I:C).

kinetics during DC maturation peaking at 8 h after Poly(I:C) or LPS stimulation for all members of the ISG15 machinery. The LPS or Poly(I:C) induced up-regulation of ISG15 mRNA was followed by a significant increase in the amount of free ISG15 protein. In addition, high molecular weight ISG15 conjugates were detectable approximately 12 h post-treatment and increased throughout DC maturation (Fig. 3C). The formation of ISG15 conjugates was particularly high following Poly(I:C) stimulation, as reflected by low levels of free ISG15 and the concomitant sharp increase of ISG15 conjugates. Importantly, detectable ISG15 modification occurred later than Ub modification (Fig. 3C). Proteasome inhibition by MG132 did not result in further increase of conjugates which is in agreement with previous studies (Li and Hassel, 2001) indicating that ISG15 modification during DC maturation is not directly connected with proteasome dependent protein degradation.

3.5. DC activation is associated with FAT10 conjugate formation

Since FAT10 belonged to the small group of UPS genes that was induced by all four applied maturation strategies we tested FAT10-expression, that of its reported E1 enzyme UBE1L2, and that of the FAT10-binding adapter NUB1 in time course experiments by real-time PCR. Treating imDCs with either LPS, Poly(I:C), the cytokine cocktail or CD40L resulted in the up-regulation of FAT10 during the course of DC maturation. In contrast to ISG15, significant up-regulation of FAT10 mRNA levels was only observed in the later stages of DC maturation (SI Tables 1–4; Fig. 4A). In agreement and as illustrated in Fig. 3B, DCs treated with the cytokine cocktail or LPS or any of the two other stimuli (data not shown) resulted in an increase of free FAT10 protein and concomitantly in an accumulation of high molecular weight FAT10 conjugates. Interestingly, reliable detection of high molecular weight FAT10 conjugates required the presence of proteasome inhibitors indicating that modification of proteins by FAT10 is a signal for their proteasomal degradation. This appears to be in agreement with previous reports that studied FAT10 as part of proteasome dependent but Ub-independent degradation mechanism (Hipp et al., 2004, 2005).

3.6. UPS genes are induced by an autocrine mechanism upon DC maturation

The coordinate up-regulation of a larger set of UPS genes following induction of DC maturation by different stimuli raised the question concerning the underlying regulatory mechanisms. Since ISG15 expression is known to be induced by type I IFNs, we first determined the expression of IFN-α and IFN-β mRNAs in DCs under the four different maturation regimens. Only Poly(I:C)- and to much lesser extent LPS-treatment of imDCs induced the expression and secretion of IFN-β (Fig. 5A and B). Very rapidly (after 4 h) levels of IFN-β mRNA massively increased and then declined gradually, whereas expression of IFN-α mRNA exhibited delayed induction kinetics (after 12 h). Supernatants from Poly(I:C)-treated DCs exhibited high levels of secreted IFN-β (up to 75 IU/ml), a concentration reported to improve cross-presentation (Longman et al., 2007). The concentration of IFN-β in LPS-treated

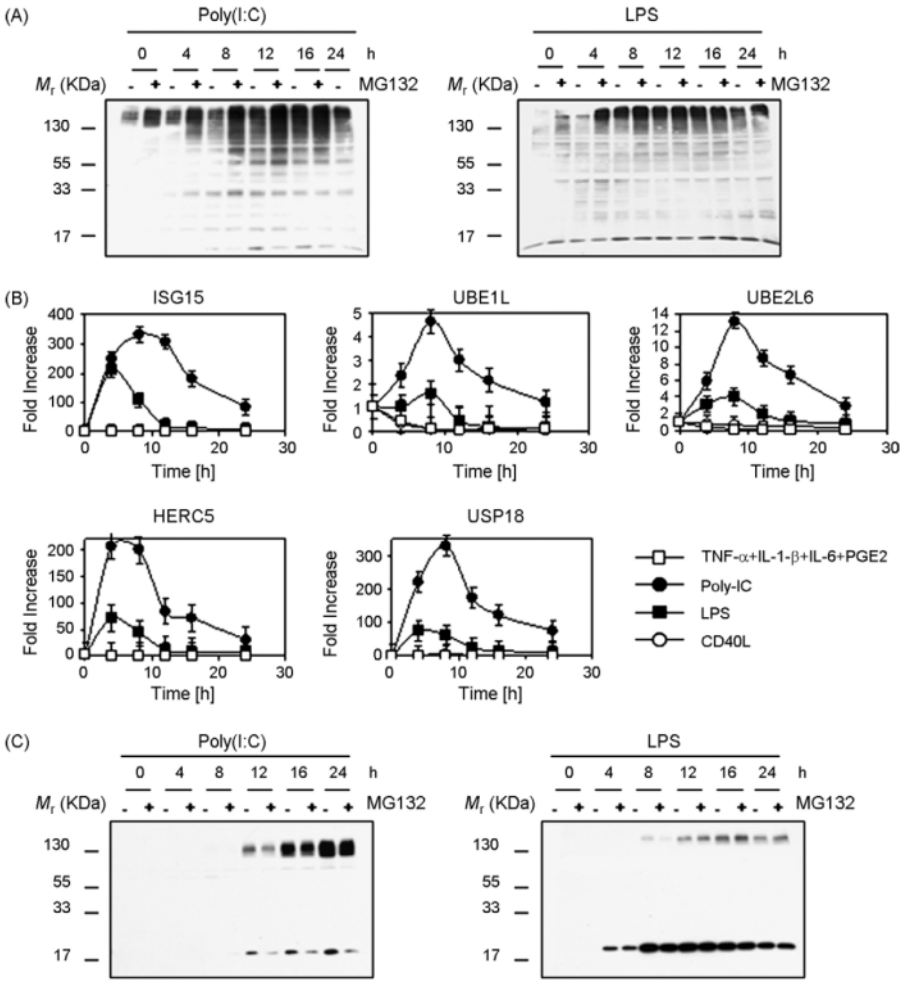

Fig. 3. Verification of array analyses by real-time PCR and protein expression analysis. (A) Accumulation of high molecular eight Ub-conjugates in maturing DCs following LPS and/or Poly(I:C) treatment. Equal amounts of proteins were immuno-blotted using an anti-Ub antibody. MG132 (1 μM) was added for the last 2 h of stimulation. (B) Quantitative real-time PCR analysis of the expression of ISG15, UBE1L, UBE2L6, HERC5 and USP18 following cytokine cocktail, LPS, Poly(I:C) or CD40L, as indicated. Results are expressed as average fold change from immature DCs. Values were normalised with HPRT1 a reference mRNA species. Deviations are indicated as bars. (C) Accumulation of high molecular weight ISG15-conjugated proteins in maturing DCs following LPS and/or Poly(I:C) treatment. Equal amounts of proteins immuno-blotted using an anti-ISG15 antibody. In some experiments, MG132 (1 μM) was added for the last 2 h of stimulation.

DCs was low (5 IU/ml) but detectable (Fig. 5B). In contrast, all maturation stimuli applied induced the secretion of TNF-α, most prominently by CD40L (Fig. 5C). To determine whether the coordinate up-regulation of the UPS genes during DC maturation is due to autocrine stimulation of DCs by type I IFNs cytokine signalling was abrogated by an IFN I-receptor antibody. Blocking of the IFN I-receptor strongly impaired the expression of genes related to the ISG15-conjugation system in response to Poly(I:C) (Fig. 6A). This is in agreement with published microarray data on maturing dendritic cells treated directly with type I IFNs (Longman et al., 2007). Interestingly, impaired induction was not restricted to the genes of the ISG15 machinery (as might have been expected) but was also observed for the cytokine-inducible genes of the 20S proteasome (Fig. 6B). These experiments thus demonstrate that IFN-α/β produced by DCs following Poly(I:C) stimulation controls the coordinate up-regulation of different sets of UPS genes via an autocrine loop. Surprisingly, our experiments also showed that FAT10 expression and even more pronounced that of the β-subunit of the proteasomes activator PA28 was also impaired in the presence of IFN I-receptor antibodies. Supporting the notion that both FAT10 and PA28-β are type I IFN-responsive, treating DCs with either IFN-α or IFN-β resulted in a more than 10-fold increase in FAT10 mRNA expression and over 5-fold increase in PA28-β mRNA expression, as determined by real-time PCR (data not shown). Since these genes are also induced by CD40L and the combined treatment of cytokines which do not produce IFN-α/β, this suggests the existence of different regulatory pathways for these genes.

3.7. *TNF-α produced by Poly(I:C)-treated DC regulates FAT10 in an autocrine fashion*

It has been shown that FAT10 expression can be stimulated by combined treatment of cells with TNF-α and IFN-γ (Bates et al., 1997; Liu et al., 1999; Raasi et al., 1999). Similarly also the

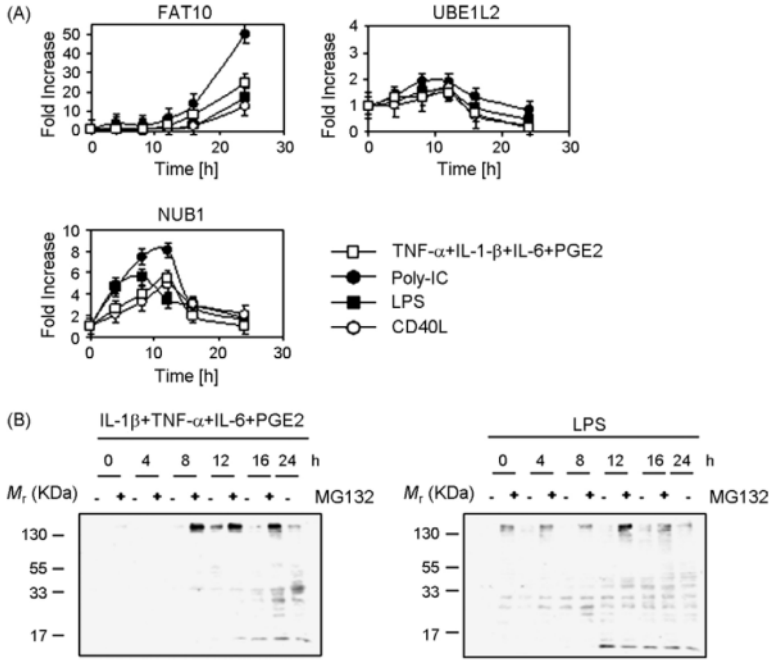

Fig. 4. Analysis of FAT10 and FAT10 modification. (A) Quantitative real-time PCR analysis of *FAT10* and *UBE1L2* following treatment with cytokine cocktail, LPS, Poly(I:C) or CD40L, as indicated. (B) Endogenous *FAT10* conjugates in DCs subjected to treatment with the cytokine cocktail or LPS. The free FAT10 and endogenous FAT10 conjugates were detected by immuno-blotting using a FAT10 antibody. MG132 (1 μM) was added during the last 2 h of stimulation.

induction of several proteasome genes has been correlated with TNF-α. In agreement with previous studies, mature DCs are an abundant source of TNF-α, regardless of the maturation-inducing agents used (Fig. 5C). This suggested that the expression of FAT10 and the inducible proteasome genes may also be regulated by a TNF-α mediated autocrine feedback loop. To test this hypothesis, TNFα-signalling was blocked by a TNF-receptor antibody in Poly(I:C)-stimulated imDCs. Indeed, the blockade of TNF-receptor

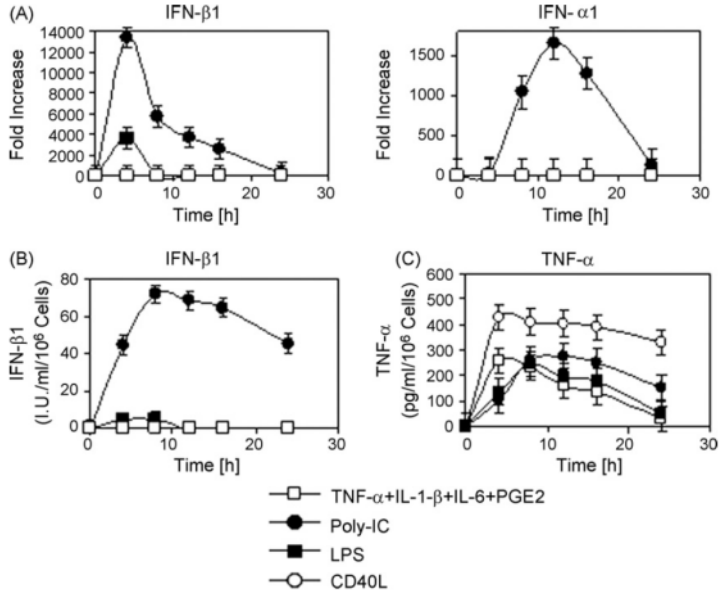

Fig. 5. Analysis of Type I IFN and TNF-α synthesis. (A) Quantitative real-time PCR analysis of IFN-β and IFN-α in response to cytokine cocktail, LPS, Poly(I:C) or CD40L, as indicated. (B) After exposure of DCs to the maturation-inducing agents, conditioned media were collected and analysed for the presence of IFN-β by ELISA. (C) After exposure of DCs to the maturation-inducing agents, conditioned media were collected and analysed for the presence of TNF-α by ELISA.

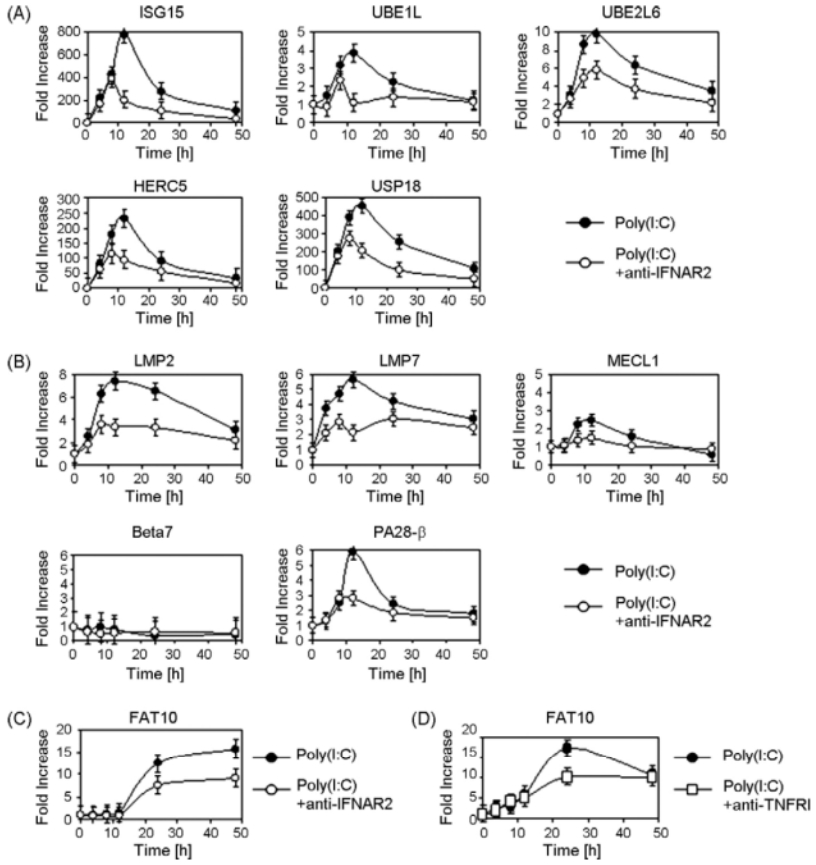

Fig. 6. Type I IFN is required for optimal induction of UPS-related genes and TNF-α for FAT10. DCs were activated with Poly(I:C) for different time periods in the presence or the absence of 10 μg/ml neutralising anti-IFNAR2 antibodies (CD118). Transcription of genes related to the ISG15-conjugation system (A), to proteasomes (B) or to the FAT10-modification machinery (C) was quantified by real-time PCR. (D) DCs were activated with Poly(I:C) for various time periods in the presence or the absence of 10 μg/ml neutralising anti-TNFR1 antibodies. Transcription of FAT10 gene was quantified by quantitative real-time PCR. Data are expressed as means ± SD and are representative of two experiments with different donors.

resulted in decreased expression of FAT10 mRNA indicating that efficient FAT10 expression during DC maturation requires the combined action of type I IFNs and TNF-α (Fig. 6D). In contrast, blockage of TNF-receptor had no effect on the Poly(I:C) induced expression of any of the proteasome subunits or on the expression of the ISG15 conjugation machinery (data not shown).

3.8. Gene silencing of the E2 Ub-conjugating enzyme UBE2L6 results in impaired cross-presentation of the HCMV-pp65$_{495–503}$ epitope

In view of our observation that the UPS is profoundly affected by PAMPs, we asked whether this remodelling had an impact on DC function. Therefore, we evaluated its role in cross-presentation in DCs by silencing the expression of the E2 Ub-conjugating enzyme UBE2L6, which functions at the intersection of the Ub- and ISG15-modification systems (Zhao et al., 2004). Gene silencing was performed by electroporating day 5 immature DCs using small inhibitory RNA oligonucleotides (siRNA) specific for UBE2L6. After 2 days of incubation with siRNA, DCs were induced to maturation by stimulation with LPS. As shown in Fig. 7A, electroporation of DCs with enhanced green fluorescent protein (EGFP) mRNA yielded 90% of EGFP+ cells, indicating high transfection efficiency, as determined by flow cytometry (Fig. 7A). Treatment of DCs with UBE2L6 siRNA resulted in potent inhibition of UBE2L6 expression, as shown by substantial decreased of mRNA levels (15 copies/μl) (Fig. 7B). Importantly, electroporation of DCs with siRNA did not alter the viability or ability to respond to maturation stimuli (data not shown). We next examined the requirement of UBE2L6 for antigen cross-presentation of the human cytomegalovirus (HCMV)-phosphoprotein (pp65)$_{495–503}$ antigenic peptide. To this aim, DCs were pulsed with necrotic pp65-expressing HeLa cells and antigen cross-presentation was monitored using a CD8+ T cell clone which recognises the NLVPMVATV epitope of pp65 in the context of HLA*A0201. In these experiments, we co-cultured two dead cells per DC in the presence of LPS, as it is assumed that this culture condition allows efficient cross-presentation of cell-derived antigens (Fonteneau et al., 2003). As shown in Fig. 7C, DCs with inhibited UBE2L6 expression were far less able to cross-present pp65 epitopes, as shown by less IFN-γ production (44% and 30% at 8 and 12 h, respectively) compared with that from T cells that were exposed to untreated DCs and DCs treated with control siRNA. It is unlikely that the failure of UBE2L6-silenced DCs to optimally stimulate pp65 CTL was attributed to decreased stimulatory capacities, as peptide-

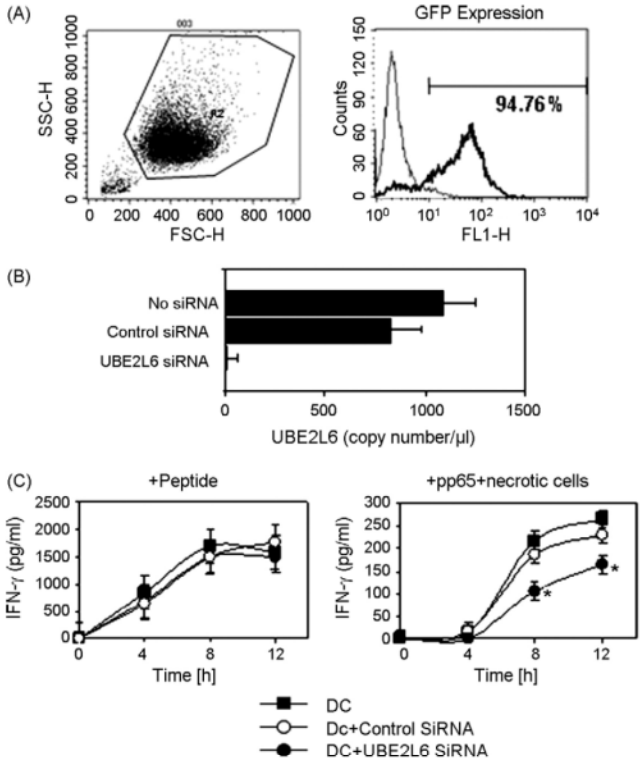

Fig. 7. Cross-presentation of a pp65 HLA-A2-restricted epitope is impaired in UBE2L6-silenced DCs (A) DCs were electroporated with EGFP mRNA, and EGFP expression in these cells was determined by FACS analysis (thick line). DCs electroporated without RNA served as negative control (thin line). (B) Knockdown of UBE2L6 was evaluated by quantitative real-time PCR, as described in Section 2. (C) Necrotic pp65-expressing HeLa cells were fed to DCs at a ratio 2:1 and co-cultured with a pp65-specific CD8+ clone in the presence of LPS (1 μg). Additional control consisted in DCs pulsed with pp65 synthetic peptide at 1 μM. Stimulation of CTL was analysed by secretion of IFN-γ using ELISA (*$p < 0.1$, Student's *t*-test). One representative experiment is shown.

loaded DCs treated with UBE2L6 siRNA activate pp65 CTL to a similar extent as seen with untreated DCs or DCs transfected with control siRNA (Fig. 7C). Since UPS dependent cross-presentation of epitopes has been shown to account for approximately 50% of cross presented MHC class I epitopes in DC (Shen et al., 2004), this experiment also demonstrates that the up-regulated UBE2L6 is the major E2 enzyme involved in UPS dependent cross-presentation during the early phase of DC maturation. This experiment also indicates that the remodelling of the UPS during following TLR agonist engagement is a prerequisite for efficient UPS dependent antigen cross-presentation by DC.

4. Discussion

The UPS plays an important role at various levels of the immune response (Elliott and Neefjes, 2006; Liu et al., 2005; Yewdell, 2005). Best studied is its role in MHC class I antigen processing in connection with the IFN induced immunoproteasomes and PA28 in infected target cells (Kloetzel and Ossendorp, 2004). However, little is known about the UPS and the expression and regulation of its genes during maturation of human DCs.

In a comprehensive approach we have here identified defined sets of UPS genes that are expressed in DCs following different maturation stimuli. Furthermore, our data reveal that the differential and coordinate expression of subsets of UPS genes is regulated by autocrine mechanisms involving type I IFNs and TNF-α. Interestingly, the number of up-regulated genes as well as the extent of gene activation strongly depends on the type of maturation stimulus. Thus, there exist clear differences in UPS gene regulation during DC maturation depending on whether DCs respond to an infectious stimulus or whether they are induced under T cells stimulatory or inflammatory conditions (Figs. 2 and 3).

Our data further demonstrate that remodelling of UPS-related gene expression resulted in increased protein modification with Ub, ISG15 or FAT10 probably as a reflection of enhanced protein modification activity. Therein both infection simulating PAMPs, but not the two other stimuli, significantly induce the enhanced formation of poly-Ub-conjugates already very early during DC maturation in a transient manner (Fig. 3A). This fact is in agreement with the hypothesis that most MHC class I ligands in response to infection are derived from freshly translated proteins, which are ubiquitylated for degradation (Yewdell, 2005).

The most notable induced subset of LPS- and Poly(I:C)-regulated genes comprises the ISG15 modification machinery. Consequently, we also detected a significant increase in ISG15 protein and in ISG15 conjugated target proteins (Fig. 3B and C). The connection of proteasomal degradation and ISG15-modification is still a matter of discussion (Liu et al., 2003). Although it is now appreciated that ISG15 is a critical host antiviral molecule (Li and Hassel, 2001), we could not detect a connection of ISG15 modification during the maturation of human DCs and proteasome dependent protein degradation (Fig. 3C). Thus, the mechanisms by which ISG15 exert its antiviral activity and in particular its role during DC maturation still remain open.

While ISG15 and its enzymes are only up-regulated in response to Poly(I:C) and LPS the Ubl modifier FAT10, is induced by all stimuli examined. Thus FAT10, the FAT10-binding adapter molecule Nub1 and its recently reported E1 enzyme UBE1L2 that also activates Ub belong to the few genes found to be induced under all four stimulation strategies used in this study (Figs. 2 and 4). In agreement with studies reporting the rapid proteasome dependent degradation of FAT10 conjugates in target cells (Chiu et al., 2007), accumulated FAT10-conjugates were stabilized by proteasome inhibition (Fig. 4). No obvious histological differences were found in FAT10 deficient mice (Hipp et al., 2004, 2005). However, the lymphocytes of FAT10 knockout mice were, on average, more prone to spontaneous apoptotic death, indicating that FAT10 may function as a survival factor (Canaan et al., 2006). Whether FAT10 is also involved in the regulation of the apoptotic death of mature DCs remains to be shown.

The enhanced formation of FAT10-modified proteins during DC maturation implies the presence of so far unknown E2 and E3 enzymes involved in FAT10 conjugation. Interestingly, only one of all (putative) E2 enzymes and 21 potential E3 ligases (out of approximately 500) are significantly induced under all four maturation strategies, raising the possibility that UBE2J1 and one of the three E3-ligases (Fig. 2) may be among the enzymes involved in FAT10 modification.

Efficient function of the UPS requires sophisticated mechanisms that control the coordinate expression of UPS genes. However, the mechanisms of coordinate or differential regulation of UPS genes in mammalian cells are still to a large extent an enigma. Well established is the role of IFN-γ or type I IFNs as inducer of immunoproteasome components in target cells upon infection (Wong et al., 2003). The PAMPs Poly(I:C) and LPS signal infection via the TLR3 and TRL4 pathways and induce the production type I IFNs in DCs (Shin et al., 2006; Strehl et al., 2005). Here we show that blocking of type I IFN signalling strongly impaired the concerted induction of the ISG15 modification machinery and immunoproteasome subunits including PA28β. Since Poly(I:C) strongly induced the synthesis and secretion of type I IFNs our experiments have important implications in linking TLR3-signalling to the coordinate and induced expression of UPS genes in maturing DCs in an autocrine regulation loop involving predominantly IFN-β. In comparison with ISG15, onset of FAT10 gene transcription during DC maturation was delayed indicating the existence of different regulatory pathways controlling ISG15 and FAT10 activity. Indeed, only a partial impairment of FAT10 transcription was observed by IFN I receptor blocking. In the experiments reported here we never detected secretion of IFN-γ during DC maturation. However, blocking the TNF-α receptor suggested that FAT10 transcription in maturing DCs is predominantly regulated by an autocrine loop involving TNF-α (Fig. 6D). We hypothesised that the up-regulation of the UPS following PAMPs engagement plays a key role in DC biology including antigen processing and presentation to CTL. To make this determination, we silenced the Ub-conjugating E2 enzyme UBE2L6 (UbcH8) and measured the effect of this down regulation on cross-presentation by DCs to a pp65-specific CD8+ T cell clone using necrotic pp65-expressing HeLa cells as a source of antigens. Our results revealed a substantial impairment of the cross presenting capacities of UBE2L6-silenced DCs. The observed effect of a 44% down-regulation appears to be even more pronounced considering that UPS-dependent cross-presentation only accounts for approximately 50% of the total cross presented MHC class I epitopes. The fact that down-regulation of cross-presentation is not complete also indicates that internalised pp65 antigens can be processed through different cellular routes. This is in agreement with a previous report showing that cross-presentation might follow two distinct pathways: (i) one cytosolic proteasome- and TAP-dependent pathway and (ii) one endosomal proteasome-independent pathway involving the protease cathepsin S (Shen et al., 2004). It is therefore conceivable that the amount of CTL pp65 response which was not affected by UBE2L6 siRNA probably reflects the portion of pp65 antigens that gained access to the endosomal degradation pathway which does not depend on the UPS. The observed slightly reduced inhibition at later time points may be explained by an increasing importance of the endosomal/lysosomal function in later stages of DC maturation or by a gradual shift towards this pathway due to the almost complete inhibition of the UPS pathway.

In conclusion, our results provide evidence that exposure of imDCs to PAMPs, but not to cytokines or CD40L, signals infection and triggers numerous changes in the UPS. This in turn results very rapidly in enhanced modification of substrates with Ub at time points when DCs undergo a molecular switch from antigen capture to antigen processing and presentation later on. Thus, the enhanced Ub modification basically contributes to enhanced antigen processing, presentation and cross presentation. On the other hand, the changes of the UPS gene expression program by inflammation or T cell interaction may rather function in signalling or endocytosis processes.

Acknowledgements

This work was supported by a grant of the Deutsche Forschungsgemeinschaft to PMK as part of the Sonderforschungsbereich 421. We would like to thank K.P. Knobeloch (FMP Berlin) for providing us an anti ISG15 antibody. Kay Hofmann and Hartmut Scheel (Milteny Biotech, Bergisch Gladbach, Germany) are acknowledged for assistance in identification of UPS-related genes. We are also grateful to Drs N. Schaft and J. Dörrie (Hautklinik Universitätsklinikum, Erlangen, Germany) for valuable help and advice with electoporation.

Appendix A. Supplementary data

Supplementary data associated with this article can be found, in the online version, at doi:10.1016/j.biocel.2008.10.023.

References

Banchereau J, Schuler-Thurner B, Palucka AK, Schuler G. Dendritic cells as vectors for therapy. Cell 2001;106:271–4.
Bates EE, Ravel O, Dieu MC, Ho S, Guret C, Bridon JM, et al. Identification and analysis of a novel member of the ubiquitin family expressed in dendritic cells and mature B cells. Eur J Immunol 1997;27:2471–7.
Canaan A, Yu X, Booth CJ, Lian J, Lazar I, Gamfi SL, et al. FAT10/diubiquitin-like protein-deficient mice exhibit minimal phenotypic differences. Mol Cell Biol 2006;26:5180–9.
Caux C, Massacrier C, Vanbervliet B, Dubois B, Van Kooten C, Durand I, et al. Activation of human dendritic cells through CD40 cross-linking. J Exp Med 1994;180:1263–72.
Cella M, Salio M, Sakakibara Y, Langen H, Julkunen I, Lanzavecchia A. Maturation, activation, and protection of dendritic cells induced by double-stranded RNA. J Exp Med 1999;189:821–9.
Chiu YH, Sun Q, Chen ZJ. E1-L2 activates both ubiquitin and FAT10. Mol Cell 2007;27:1014–23.
Dastur A, Beaudenon S, Kelley M, Krug RM, Huibregtse JM. Herc5, an interferon-induced HECT E3 enzyme, is required for conjugation of ISG15 in human cells. J Biol Chem 2006;281:4334–8.
De Smedt T, Pajak B, Muraille E, Lespagnard L, Heinen E, De Baetselier P, et al. Regulation of dendritic cell numbers and maturation by lipopolysaccharide in vivo. J Exp Med 1996;184:1413–24.
Elliott T, Neefjes J. The complex route to MHC class I-peptide complexes. Cell 2006;127:249–51.
Fonteneau JF, Kavanagh DG, Lirvall M, Sanders C, Cover TL, Bhardwaj N, et al. Characterization of the MHC class I cross-presentation pathway for cell-associated antigens by human dendritic cells. Blood 2003;102:4448–55.
Fonteneau JF, Larsson M, Somersan S, Sanders C, Munz C, Kwok WW, et al. Generation of high quantities of viral and tumor-specific human CD4+ and CD8+ T-cell clones using peptide pulsed mature dendritic cells. J Immunol Methods 2001;258:111–26.

Glickman MH, Ciechanover A. The ubiquitin-proteasome proteolytic pathway: destruction for the sake of construction. Physiol Rev 2002;82:373–428.
Hipp MS, Kalveram B, Raasi S, Groettrup M, Schmidtke G. FAT10, a ubiquitin-independent signal for proteasomal degradation. Mol Cell Biol 2005;25:3483–91.
Hipp MS, Raasi S, Groettrup M, Schmidtke G. NEDD8 ultimate buster-1L interacts with the ubiquitin-like protein FAT10 and accelerates its degradation. J Biol Chem 2004;279:16503–10.
Jonuleit H, Kuhn U, Muller G, Steinbrink K, Paragnik L, Schmitt E, et al. Pro-inflammatory cytokines and prostaglandins induce maturation of potent immunostimulatory dendritic cells under fetal calf serum-free conditions. Eur J Immunol 1997;27:3135–42.
Kanzler H, Barrat FJ, Hessel EM, Coffman RL. Therapeutic targeting of innate immunity with Toll-like receptor agonists and antagonists. Nat Med 2007;13:552–9.
Kloetzel PM, Ossendorp F. Proteasome and peptidase function in MHC-class-I-mediated antigen presentation. Curr Opin Immunol 2004;16:76–81.
Li XL, Hassel BA. Involvement of proteasomes in gene induction by interferon and double-stranded RNA. Cytokine 2001;14:247–52.
Liu M, Li XL, Hassel BA. Proteasomes modulate conjugation to the ubiquitin-like protein, ISG15. J Biol Chem 2003;278:1594–602.
Liu YC, Pan J, Zhang C, Fan W, Collinge M, Bender JR, et al. A MHC-encoded ubiquitin-like protein (FAT10) binds noncovalently to the spindle assembly checkpoint protein MAD2. Proc Natl Acad Sci U S A 1999;96:4313–8.
Liu YC, Penninger J, Karin M. Immunity by ubiquitylation: a reversible process of modification. Nat Rev Immunol 2005;5:941–52.
Longman RS, Braun D, Pellegrini S, Rice CM, Darnell RB, Albert ML. Dendritic-cell maturation alters intracellular signaling networks, enabling differential effects of IFN-alpha/beta on antigen cross-presentation. Blood 2007;109:1113–22.
Macagno A, Gilliet M, Sallusto F, Lanzavecchia A, Nestle FO, Groettrup M. Dendritic cells up-regulate immunoproteasomes and the proteasome regulator PA28 during maturation. Eur J Immunol 1999;29:4037–42.
Malakhov MP, Malakhova OA, Kim KI, Ritchie KJ, Zhang DE. UBP43 (USP18) specifically removes ISG15 from conjugated proteins. J Biol Chem 2002;277:9976–81.
Menges M, Rossner S, Voigtlander C, Schindler H, Kukutsch NA, Bogdan C, et al. Repetitive injections of dendritic cells matured with tumor necrosis factor alpha induce antigen-specific protection of mice from autoimmunity. J Exp Med 2002;195:15–21.
Mukhopadhyay D, Riezman H. Proteasome-independent functions of ubiquitin in endocytosis and signaling. Science 2007;315:201–5.
Pitha-Rowe I, Hassel BA, Dmitrovsky E. Involvement of UBE1L in ISG15 conjugation during retinoid-induced differentiation of acute promyelocytic leukemia. J Biol Chem 2004;279:18178–87.
Raasi S, Schmidtke G, de Giuli R, Groettrup M. A ubiquitin-like protein which is synergistically inducible by interferon-gamma and tumor necrosis factor-alpha. Eur J Immunol 1999;29:4030–6.
Rock KL, York IA, Saric T, Goldberg AL. Protein degradation and the generation of MHC class I-presented peptides. Adv Immunol 2002;80:1–70.
Schaft N, Dorrie J, Thumann P, Beck VE, Muller I, Schultz ES, et al. Generation of an optimized polyvalent monocyte-derived dendritic cell vaccine by transfecting defined RNAs after rather than before maturation. J Immunol 2005;174:3087–97.
Shen L, Sigal LJ, Boes M, Rock KL. Important role of cathepsin S in generating peptides for TAP-independent MHC class I crosspresentation in vivo. Immunity 2004;21:155–65.
Shin EC, Seifert U, Kato T, Rice CM, Feinstone SM, Kloetzel PM, et al. Virus-induced type I IFN stimulates generation of immunoproteasomes at the site of infection. J Clin Invest 2006;116:3006–14.
Steinman RM, Banchereau J. Taking dendritic cells into medicine. Nature 2007;449:419–26.
Strehl B, Seifert U, Kruger E, Heink S, Kuckelkorn U, Kloetzel PM. Interferon-gamma, the functional plasticity of the ubiquitin-proteasome system, and MHC class I antigen processing. Immunol Rev 2005;207:19–30.
Whiteside TL, Stanson J, Shurin MR, Ferrone S. Antigen-processing machinery in human dendritic cells: up-regulation by maturation and down-regulation by tumor cells. J Immunol 2004;173:1526–34.
Wong BR, Parlati F, Qu K, Demo S, Pray T, Huang J, et al. Drug discovery in the ubiquitin regulatory pathway. Drug Discov Today 2003;8:746–54.
Wong JJ, Pung YF, Sze NS, Chin KC. HERC5 is an IFN-induced HECT-type E3 protein ligase that mediates type I IFN-induced ISGylation of protein targets. Proc Natl Acad Sci U S A 2006;103:10735–40.
Yewdell JW. The seven dirty little secrets of major histocompatibility complex class I antigen processing. Immunol Rev 2005;207:8–18.
Zhao C, Beaudenon SL, Kelley ML, Waddell MB, Yuan W, Schulman BA, et al. The UbcH8 ubiquitin E2 enzyme is also the E2 enzyme for ISG15, an IFN-alpha/beta-induced ubiquitin-like protein. Proc Natl Acad Sci U S A 2004;101:7578–82.
Zou W, Zhang DE. The interferon-inducible ubiquitin-protein isopeptide ligase (E3) EFP also functions as an ISG15 E3 ligase. J Biol Chem 2006;281:3989–94.

4.2. The ubiquitin-like modifier FAT10 efficiently targets antigens to MHC class I presentation (this chapter is based on the work of Ebstein and coworkers (Ebstein et al., 2012b))

The HLA-F adjacent transcript 10 (FAT10) is a member of the growing family of ubiquitin-like proteins and is strongly up-regulated following inflammatory and/or immunological stimuli including TNFα- and IFN-γ. Like ubiquitin, FAT10 serves as a signal for protein degradation by proteasomes. However, it remains unclear whether the breakdown of FAT10-modified substrates leads to the production of peptides potentially suitable for MHC class I antigen presentation. In this work, investigations were undertaken to address this issue using a model substrate consisting of the human cytomegalovirus (HCMV)-derived pp65 antigen which is fused to FAT10 at its NH2-terminus. The impact of FAT10 modification on pp65 processing and presentation was assessed by measuring the activation of a CD8+ T cell clone recognizing the HLA-A2-restricted $pp65_{495-503}$ antigenic peptide. Interestingly and in contrast to ubiquitin, we show that covalent attachment of FAT10 to pp65 resulted in substantial improvement of pp65 antigen presentation which is not influenced by immunoproteasomes or PA28. Taken together, these data highlight the importance of the FAT10 conjugation system as a new and alternative pathway for MCH class I presentation.

Cell. Mol. Life Sci. (2012) 69:2443–2454
DOI 10.1007/s00018-012-0933-5

Cellular and Molecular Life Sciences

RESEARCH ARTICLE

The FAT10- and ubiquitin-dependent degradation machineries exhibit common and distinct requirements for MHC class I antigen presentation

Frédéric Ebstein · Andrea Lehmann · Peter-Michael Kloetzel

Received: 5 September 2011 / Revised: 16 January 2012 / Accepted: 26 January 2012 / Published online: 19 February 2012

Abstract Like ubiquitin (Ub), the ubiquitin-like protein FAT10 can serve as a signal for proteasome-dependent protein degradation. Here, we investigated the contribution of FAT10 substrate modification to MHC class I antigen presentation. We show that N-terminal modification of the human cytomegalovirus-derived pp65 antigen to FAT10 facilitates direct presentation and dendritic cell-mediated cross-presentation of the HLA-A2 restricted $pp65_{495–503}$ epitope. Interestingly, our data indicate that the pp65 presentation initiated by either FAT10 or Ub partially relied on the 19S proteasome subunit Rpn10 (S5a). However, FAT10 distinguished itself from Ub in that it promoted a pp65 response which was not influenced by immunoproteasomes or PA28. Further divergence occurred at the level of Ub-binding proteins with NUB1 supporting the pp65 presentation arising from FAT10, while it exerted no effect on that initiated by Ub. Collectively, our data establish FAT10 modification as a distinct and alternative signal for facilitated MHC class I antigen presentation.

Keywords FAT10 · Ubiquitin · Immunoproteasomes · PA28 · NUB1 · Antigen presentation

Abbreviations

DUB	De-ubiquitylating enzyme
FAT10	HLA-F adjacent transcript 10
NUB1	NEDD8 ultimate buster 1
PA28	Proteasome activator 28
pp65	Phosphoprotein 65
Ub	Ubiquitin
UBL	Ubiquitin-like modifier
UPS	Ubiquitin–proteasome system

Electronic supplementary material The online version of this article (doi:10.1007/s00018-012-0933-5) contains supplementary material, which is available to authorized users.

F. Ebstein · A. Lehmann · P.-M. Kloetzel (✉)
Institut für Biochemie, Charité-Universitätsmedizin Berlin, Campus CVK, Oudenaderstr.16, 13347 Berlin, Germany
e-mail: p-m.kloetzel@charite.de

Introduction

The production of minimal CD8+ T cell antigenic peptides mostly depends on the degradation of target proteins by the ubiquitin–proteasome system (UPS). In this pathway, covalently attached ubiquitin (Ub) typically marks a substrate protein for degradation by the 26S proteasome, and it has been shown that increased susceptibility to ubiquitylation can facilitate MHC class I antigen presentation in vivo [1–3]. Conjugation of Ub to lysine (K) side chains of target proteins uses the concerted actions of a succession of specific enzymes (E1, E2 and E3) that sequentially transfer the activated Ub to a protein substrate. K48-linked chains are the most abundant forms of poly-Ub chains within the cells and target substrates for 26S proteasome-mediated degradation. The 26S proteasome complex consists of two sub-complexes: the 19S regulatory particle and the 20S particle containing the three catalytic subunits β_1, β_2 and β_5. In mammalian cells, upon induction by type I and/or II interferon (IFN), these constitutive catalytic subunits are replaced by the inducible subunits iβ_1/LMP2, iβ_2/MECL1 and iβ_5/LMP7, forming the immunoproteasome (i-proteasome) [4–6]. Studies of i-proteasome function have revealed that, in most instances, it generates MHC class I-binding peptides more efficiently than standard proteasomes (s-proteasomes) [7–9]. IFN-γ stimulation is also accompanied by increased expression of the proteasome activator PA28, which associates with the 20S proteasome, thereby forming

so-called hybrid proteasomes complexes (i.e. 19S-20S-PA28) that enhance the production of antigenic peptides [10, 11].

Over the past decade, a growing number of Ub-like proteins (UBL) sharing structural homology with Ub have been identified, such as NEDD8, SUMO, ISG15 and FAT10 [12, 13]. Like Ub, they exhibit the capacity to be conjugated to K residues in a substrate protein, and are involved in the regulation of diverse cellular processes, including nuclear transport, transcription, stress response, and DNA damage. FAT10 (HLA-F-adjacent transcript 10) is the most recently identified member of the UBL family and, up to now, very little is known about its biological function. FAT10 gene expression has been reported to be under the influence of cytokines, including TNF-α and IFN-γ, and is timely induced during the later phase of dendritic cell (DC) maturation and during apoptosis [14–16]. Increased levels of both free FAT10 and FAT10-protein conjugates have also been reported in various tumours including hepatocellular carcinoma as well as gastric and gynaecological cancers [17, 18]. Although the lymphocytes from FAT10$^{-/-}$ mice were, on average, more prone to spontaneous apoptotic death, no histological differences were found between wild-type and FAT10$^{-/-}$ mice [19]. Within cells, FAT10 is covalently conjugated to cellular proteins in a pathway involving an E1-E2-E3 enzyme cascade, which is only partially characterised. Recently, UBE1L2 and UBE2Z have been reported to function as E1 and E2 enzymes for FAT10, respectively [20, 21], whereas no FAT10-specific E3 enzymes have so far been experimentally verified.

Interestingly, FAT10 shares with Ub the unique ability of targeting substrates for proteasomal degradation [15, 22]. However, there exists no information whether FAT10 modification of a substrate protein may contribute to the peptide supply for MHC class I-restricted antigen presentation. Here, we show that an N-terminal fusion of the human cytomegalovirus (HCMV)-derived pp65 antigen with FAT10 accelerates the proteasomal degradation of pp65 and results in improved presentation of the HLA-A2-restricted pp65$_{495–503}$ epitope. Importantly, the antigen processing pathway used by this FAT10-pp65 fusion protein differs considerably from that used by an Ub-pp65 chimera in terms of i-proteasomes, PA28 and Ub-binding proteins. In summary, our data underscore the importance of the FAT10 conjugation system as an alternative and distinct pathway for MHC class I antigen processing.

Materials and methods

Reagents and antibodies

Anti-pp65 (CH12), anti-FAT10 (FL-165) and anti-β-actin (C4) antibodies were purchased from Santa Cruz Biotechnology. Monoclonal anti-LMP2 (LMP2-13), anti-Ub (FK2), anti-Rpn10 (S5a-18) and polyclonal anti-NUB1 antibodies were obtained from Biomol. The polyclonal anti-PA28-β was purchased from Cell Signaling. Anti-HA monoclonal antibody (16B12) was obtained from Covance. Antibodies against PA28-α, MECL1 (K65/4) and LMP7 (K63/5) were from the laboratory stock and used as previously described [23]. MG132 (benzyloxycarbonyl-Leu-Leu-Leu-CHO), *N*-ethylmaleimide (NEM) and phytohaemagglutinin (PHA-L) were all purchased from Sigma. Lipopolysaccharide (LPS) was obtained from Invivogen. Unless specified, all recombinant cytokines used in this study (IL-2, TNF-α, IFN-γ) were purchased from Miltenyi Biotec. The peptide pp65$_{495–503}$ (NLVPMVATV) was custom-synthesised by our peptide synthesis facility (Institute of Biochemistry, Charité, Berlin).

Cell culture

The stable cell line HeLa A2+ (clone 33) was established in our laboratory and cultivated in Iscove Medium supplemented with 10% FCS in the presence of 2 µg/ml puromycin. The expression of HLA-A2 molecules on the cell surface was determined using flow cytometry, using the BB7.2 mAb (kindly provided by Dr. A. Paschen, Essen, Germany). The clone 33/2 (HeLa A2+/IP) is a derivative of the clone 33 that stably expresses the three inducible subunits LMP2, MECL1 and MECL1 and was maintained in the presence of 2 µg/ml puromycin and 300 µg/ml hygromycin. HEK293 cells were grown in DMEM medium (Biochrom, Berlin, Germany) containing 10% FCS, 2 mM L-glutamine and 100 U/ml penicillin and streptomycin (purchased from PAA Laboratories), as previously described [24]. DC were generated from enriched CD14+ monocytes cultured in the presence of GM-CSF (500 U/ml) and IL-4 (100 U/ml) for 5 days. The pp65 CTL clone 61, specific for pp65$_{495–509}$, was generated from sensitisations of naïve CD8+ T cells with peptide-pulsed DC, as previously described [14]. It was regularly expanded at 37°C (5% CO2) in RPMI 1640 medium supplemented with 8% human serum (Promocell) and recombinant IL-2 (150 U/ml) in the presence of irradiated BLCL cells and allogeneic peripheral blood mononuclear cells (PBMC) and PHA-L (1 µg/ml).

Plasmids

The full-length sequence of the HCMV-derived pp65 was PCR amplified from the pcDNA6-pp65.35 plasmid (kind gift of B. Plachter, Johannes Gutenberg-University, Mainz, Germany) and cloned into the eukaryotic expression vector pcDNA3.1/*myc*-HIS (version B). To generate Ub-pp65 and FAT10-pp65 fusion proteins, the sequences encoding Ub

and FAT10 were PCR amplified from LPS-treated DC cDNA and cloned in frame into the pcDNA3.1/pp65-*myc*-HIS construct. A DNA fragment corresponding to the FAT10 coding sequence was amplified from LPS-treated DC cDNA by PCR using a forward primer encoding the FLAG tag sequence. The PCR-amplified DNA was then cloned into the pcDNA3.1/Zeo(+) expression vector (Invitrogen) to generate a N-terminal FLAG-tagged version of the FAT10 protein. Likewise, the sequence encoding the amino acids 1–76 of human Ub was amplified by PCR using forward primer encoding the epitope tag derived from the influenza HA protein (YPYDVPDY) and cloned into the pEGFPN3 plasmid (BD Clontech), so that a HA-Ub-GFP fusion product can be synthesised following transfection of mammalian cells. The full-length cDNA for NUB1 and NUB1L was amplified by PCR from LPS-treated DC using specific primers containing sequences derived from the 5′ and 3′ portions, including their stop codons and restriction enzyme sites compatible with cloning into pcDNA3.1/myc-HIS expression vector.

In vitro transfection and western blotting

HeLa, HeLa A2+, HeLa A2+/IP and HEK293 cells were transfected with 4 μg of each plasmid using Lipofectamine 2000 (Invitrogen). Sixteen hours after transfection, cells were rapidly washed in ice-cold PBS and solubilised with a NP40-based lysis buffer (50 mM Tris, 50 mM NaCl, 5 mM $MgCl_2$, 100 mM NEM, 10 μM MG132 and 0.1% NP40) for 15 min on ice. The cell lysates were clarified by centrifugation (14,000*g* for 15 min). Protein concentration of supernatants was determined using a BCA™ protein assay kit (Thermo Scientific), and 30 μg proteins were resolved on SDS-PAGE and transfer to PVDF membranes (MilliQ). Membranes were blocked for 30 min in PBS containing 5% milk followed by overnight incubation with primary antibodies. After subsequent washings and incubation with horseradish peroxidase-coupled secondary antibodies, immunoblots were developed with the use of enhanced chemoluminescence (ECL) (Amersham).

Immunoprecipitation

HeLa cells were transfected with an expression vector encoding a HA-tagged Ub-GFP fusion protein (HA-Ub-GFP) alone or in combination with plasmids encoding *myc*-tagged versions of the pp65, Ub-pp65 or FAT10-pp65 constructs. After a 16-h transfection, whole-cell lysates were made in lysis buffer (150 mM NaCl, 50 mM Tris, 1% Triton® X-100, 10 μM MG132, 100 mM NEM, pH 8.0) and pre-cleared by centrifugation at >14,000*g* for 15 min at 4°C. The protein concentration in each cleared supernatant was quantified using the BCA™ protein assay kit. Each sample was diluted in additional lysis buffer to adjust each sample so that it has an equal concentration of protein in 1 ml of total lysis buffer (typically 1 mg/ml). Forty microlitre of *myc*-coated magnetic beads (μMACS myc Kit; Miltenyi Biotec) were added to the supernatants, incubated 1 h at 4°C with rotation and loaded onto μMACS columns (Miltenyi Biotec). Immunoprecipitates were washed twice and eluted in loading buffer according to the manufacturer's instructions prior to SDS-PAGE and western blotting with pp65 and HA antibodies.

RNA interference

RNA interference (RNAi) oligonucleotides specific for PA28-α (L-012254-00), PA28-β (L-011370-01), LMP2 (L-006023-00), MECL1 (L-006019-00), LMP7 (L-006022-00), Rpn10 (L-011365-00) and NUB1/NUB1L (L-019158-00) were all purchased from Dharmacon. Non-targeting control siRNA (D-001810-10) were also used in each experiment and also obtained from Dharmacon. Briefly, HeLa A2+ and/or HEK293 cells were seeded in six-well plates and transiently transfected with non-targeting or targeting siRNA at a final concentration of 100 nM by using the Xtremgene kit (Roche), according to the manufacturer's protocol. The knockdown of the specified protein was determined by western blotting using the appropriate antibody. For DC transfection, 4×10^7 cells were resuspended in 100 μl Opti-MEM without red phenol (Invitrogen) and transferred into a 4-mm electroporation cuvette (Biorad) with 1,000 nmol siRNA duplex. The electroporator (Genepulser; Biorad) used a square-wave pulse of 500 V for 1 ms. Cells were then immediately transferred into 4 ml of RPMI 1640 with 10% FCS, containing GM-SCF and IL-4.

Antigen presentation assay

HeLa A2+ or HeLa A2+/IP were transiently transfected with pp65, FAT10-pp65 and Ub-pp65 and used as targets cells for their potential to activate the production of IFN-γ by the pp65 CD8+ T cell clone 61. Following 4 h of transfection, target cells were serially diluted and then co-cultured with a fixed amount of T cells, resulting in graded effector-to-target (E:T) ratio in a final volume of 100 μl of RPMI 1640 supplemented with 10% FCS on U-bottom 96-well plates. After 16 h of incubation, the supernatants were collected and the IFN-γ content was determined using a commercially available human ELISA kit according to the manufacturer's instructions. The data in the figures refer to the mean of two replicates. The SD was below 5% of the mean.

Cross-presentation assay

Whole cell lysates were used as pp65 antigen sources for cross-presentation and prepared by four cycles of rapid freeze/thaw lysis of HeLa cells transiently transfected with pp65, Ub-pp65 or FAT10-pp65. Immature DC from HLA-A2+ donors were plated in duplicate on a 96-well plate at 50,000 cells per well and incubated for various periods of time with the various whole cell lysates in the presence of the pp65 CD8+ T cell clone 61 at different responder-to-stimulator ratio in a final volume of 200 µl. Alternatively, DC were used as unloaded or after being pulsed with 1 µM of the $pp65_{495–503}$ synthetic peptide NLVPMVATV in the presence of LPS (1 µg/ml).

Statistical analysis

Student's *t* test (one-tailed) was used for data analysis when appropriate.

Results

FAT10 modification of pp65 improves the presentation of the HCMV $pp65_{495–503}$ epitope

Because both Ub and FAT10 serve as signals for proteasome-dependent degradation, we compared their impact on MHC class I presentation. To this end, fusion proteins consisting of the HCMV-derived pp65 antigen N-terminally tagged with either Ub or FAT10 were expressed in HeLa A2+ cells. Monitoring the steady-state levels of the different pp65 constructs revealed that the expression level of FAT10-pp65 was strongly reduced when compared to that of the untagged pp65 (Fig. 1a). Importantly, the transcriptional activity of these two plasmids was identical (Fig. S1A). Furthermore, the expression level of pp65 and FAT10-pp65 in the detergent-insoluble fraction showed no significant differences (Fig. S1B), indicating that the cellular distribution of both of these constructs was similar. Taken together, these data strongly suggest that reduced signal for the FAT10-pp65 fusion protein observed in the detergent-soluble fraction reflects higher protein turnover. Detection of the Ub-pp65 fusion protein revealed the expected efficient initiation of poly-Ub chain formation in vivo, as shown by a typical 8-kDa ladder of high molecular weight bands detected with the pp65 antibody. Of the three bands detected, the lower one had the same molecular size as the untagged pp65, indicating that the Ub is partially removed by de-ubiquitylating enzymes (DUB). Of note, double conversion of glycine 75 and 76 to alanine and valine at the isopeptidase site (UbAV-pp65) did not efficiently block the Ub cleavage from the fusion protein, as determined by western blotting (Fig. S2A).

To analyze the ubiquitylation state of our different pp65 constructs, HeLa cells were transfected with HA-Ub-GFP alone or in combination with pp65-*myc*, Ub-pp65-*myc* or FAT10-pp65-*myc* for 16 h and were subsequently subjected to a 6-h treatment with 10 µM MG-132. Following incubation, the pp65 constructs were immunoprecipitated using *myc* magnetic beads and analysed by immunoblotting with anti-HA (against Ub) and anti-pp65 antibodies. As shown in Fig. 1b, N-terminal tagging of pp65 with Ub results in a strong poly-ubiquitylation of the Ub-pp65 fusion protein. A prolonged exposure of the western blot with the anti-pp65 antibody reveals that at least four Ub moieties are attached to the Ub-pp65 construct in these cells (Fig. S3). In contrast, the untagged pp65 and the FAT10-pp65 constructs were only slightly and similarly ubiquitylated.

To test the impact of pp65, Ub-pp65 and FAT10-pp65 on the presentation of the $pp65_{495–503}$ epitope in HeLa A2+ cells, pp65 epitope presentation was monitored using a CD8+ T cell clone (CTL clone 61) that specifically recognises the immunodominant $pp65_{495–503}$ epitope. To prevent saturation levels of MHC class I/peptide complexes, HeLa A2+ cells were transfected with each construct for only 4 h. As shown in Fig. 1c, in comparison to the untagged pp65, the FAT10-pp65 fusion protein enhanced antigen presentation approximately twofold and activated the CTL clone 61 to a similar extent as that seen with the Ub-pp65 fusion protein. Importantly, the improved $pp65_{495–503}$ presentation obtained with either Ub-pp65 or UbAV-pp65 was substantially reduced when all the seven lysine residues of the fused Ub moiety were changed into arginine residues (UbK0-pp65) (Fig. S2B and S2C). These data formally show that the enhanced pp65 CTL response initiated by Ub-pp65 relies on the poly-ubiquitylation of its N-terminal Ub.

The $pp65_{495–509}$ epitope presentation derived from FAT10-pp65 is less dependent on Rpn10 than that derived from Ub-pp65

The observation that the FAT10- and Ub-pp65 fusion proteins similarly supported $pp65_{495–503}$ epitope presentation raised the question concerning a putative receptor for 26S proteasome targeting. A major 26S proteasome receptor for poly-ubiquitylated substrates is the Rpn10 subunit of the 19S regulatory particle, originally called S5a [25, 26].

To determine whether Rpn10 may also serve as a receptor for FAT10-modified substrates, we determined the steady-state level of pp65, Ub-pp65 and FAT10-pp65 in Rpn10-siRNA-silenced HeLa A2+ cells. As illustrated in Fig. 2a, RNAi treatment against Rpn10 for 96 h resulted in an almost complete depletion of the Rpn10 subunit. The

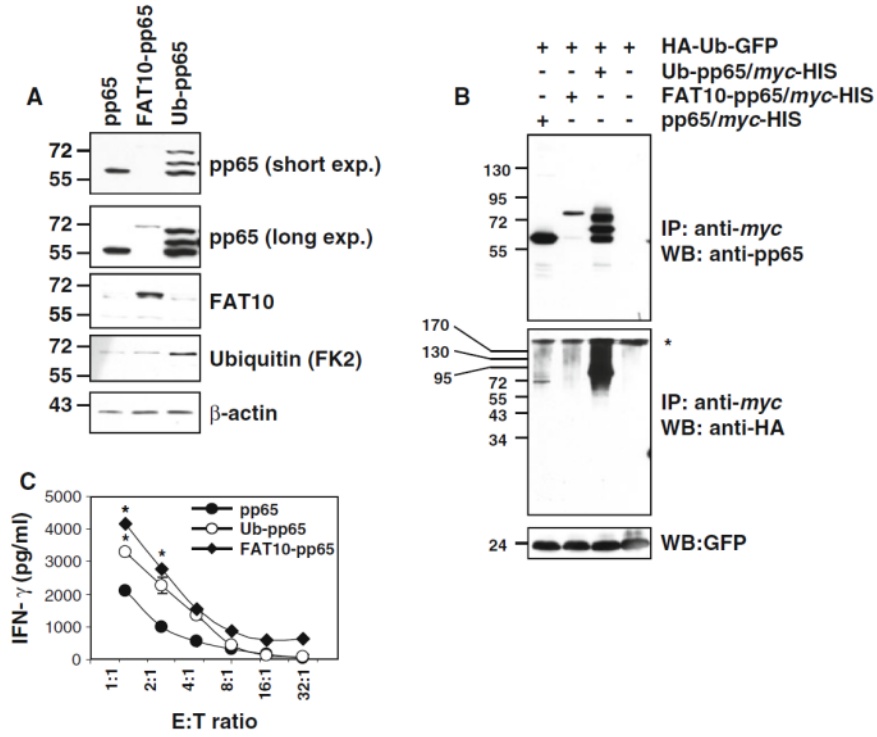

Fig. 1 Increased reactivity of the $pp65_{495–503}$-specific CTL clone 61 by HeLa A2+ cells transiently expressing either Ub-pp65 or FAT10-pp65. **a** HeLa A2+ cells were transfected with the various plasmids for 24 h and whole cell extracts were mixed with sample buffer, followed by SDS-PAGE separation and western blotting with *pp65*, *Ubiquitin* (*FK2*) and *FAT10* antibodies. Loading control was ensured by probing the membrane with the anti-*β*-actin mAb. **b** HeLa cells were transfected with *HA-Ub-GFP* alone or in combination with *pp65-myc*, *Ub-pp65-myc* or *FAT10-pp65-myc* for 16 h after which they were subjected to a 6-h treatment with 10 μM MG-132. Following incubation, cells were harvested and subjected to immunoprecipitation with *myc*-coated magnetic beads and western blot analysis with anti-HA (against Ub) and anti-pp65 mAb, as indicated. Loading control in this experiment was ensured by monitoring the expression levels of the GFP protein, which is immediately cleaved from the HA-Ub-GFP fusion product by hydrolases shortly after synthesis. **c** Following a 4-h transfection, HeLa A2+ cells expressing pp65, Ub-pp65 or FAT10-pp65 were washed and added to the pp65 CTL clone 61 recognising the HLA-A2-restricted $pp65_{495–503}$ epitope at various E:T ratio for 16 h. The activation of the CTL clone 61 was assessed by measuring IFNγ content in the supernatant by ELISA ($^*p < 0.01$, compared with untagged pp65, $n = 3$)

Rpn10 knockdown was associated with a substantial stabilisation of Ub-pp65 and FAT10-pp65 indicating that both of these fusion proteins are targeted to Rpn10 for proteasomal degradation. The steady-state level of the untagged pp65 in Rpn10-depeleted cells was also significantly affected which is in line with the observation that wild-type pp65 undergoes poly-ubiquitylation in vivo. Nevertheless, the stabilisation of FAT10-pp65 observed in the absence of Rpn10 was less pronounced than that observed for the two other pp65 constructs, suggesting a reduced affinity of FAT10-pp65 for Rpn10 or that Rpn10 is not the only FAT10 interacting 26S proteasome subunit.

Next, we tested whether Rpn10 silencing may exert any effect on the presentation of the $pp65_{495–503}$ epitope arising from our various pp65 constructs. As shown in Fig. 2b, Rpn10 down-regulation resulted in a significant impairment of $pp65_{495–503}$ epitope presentation deriving from the untagged pp65 protein and the Ub-pp65 fusion protein. Impairment of Rpn10 expression also affected the efficiency of pp65 epitope presentation exerted by the FAT10-pp65 fusion protein. However, the observed decrease of pp65 epitope presentation was less pronounced, which appears to be in concordance with the reduced stabilization of FAT10-pp65 upon Rpn10 deficiency demonstrated in Fig. 2a. These data not only reveal that Rpn10 is involved in the proteasomal degradation of pp65 and Ub-pp65 but also suggest that Rpn10 can act as receptor for FAT10-modified substrates.

FAT10-pp65 processing is not controlled by i-proteasomes and/or PA28

In many cases, i-proteasomes or the proteasome activator PA28 positively influence presentation of epitopes arising

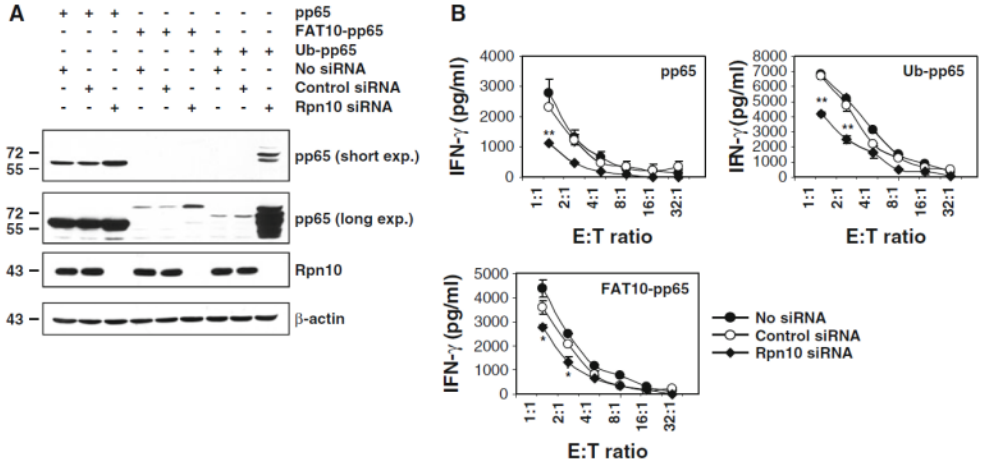

Fig. 2 Rpn10 knockdown in HeLa A2+ cells leads to impaired presentation of the $pp65_{495–503}$ epitope generated from pp65, Ub-pp65 or FAT10-pp65 proteins. **a** The role of Rpn10 in the turn-over of the *pp65*, *Ub-pp65* or *FAT10-pp65* substrates was examined by treating HeLa A2+ cells with either *control* or *Rpn10 siRNA* for 4 days followed by a subsequent transfection with the pp65, Ub-pp65 or FAT10-pp65 plasmids for 24 h, as indicated. The gene silencing efficiency for Rpn10 was determined by western blotting using a monoclonal antibody against Rpn10. The influence of Rpn10 depletion on the steady-state level of pp65, Ub-pp65 and FAT10-pp65 was examined by western blotting using the anti-pp65 antibody. **b** Rpn10-depleted HeLa A2+ cells were transfected with the pp65, Ub-pp65 or FAT10-pp65 plasmids for 4 h and used as target cells in a 16-h co-culture against the CTL clone 61. Controls in this CTL assay consist in the use of HeLa A2+ cells expressing pp65, Ub-pp65 or FAT10-pp65 which have been treated with non-targeting siRNA (*control siRNA*) or left untreated (*no siRNA*). The activation of the CTL clone 61 was assessed by measuring the IFN-γ content in the supernatant by ELISA. ($^*p < 0.01$ and $^{**}p < 0.005$, compared to untreated cells or cells treated with control siRNA, $n = 2$)

from poly-ubiquitylated antigens [27, 28]. Therefore, we next studied the role of i-proteasomes in the processing of FAT10-pp65 in HeLa A2+/IP cells that predominantly express i-proteasomes [24]. As shown in Fig. 3a, expression of either pp65 or Ub-pp65 in HeLa A2+/IP resulted in improved antigen presentation of the $pp65_{495–503}$ epitope, when compared to HeLa A2+ control target cells that predominantly express s-proteasomes. In striking contrast, the presence of i-proteasomes exerted no effect on the efficiency of the FAT10-mediated pp65 epitope presentation, indicating that the molecular prerequisites for FAT10-dependent antigen processing differ from those of the Ub-dependent pathway.

We next studied the effects of PA28 on the presentation of the $pp65_{495–503}$ epitope derived from the FAT10-pp65 fusion protein. To deprive the target cells of PA28, both PA28-α and PA28-β were silenced by siRNA. Cells transfected without siRNA or non-targeting siRNA oligonucleotides (control siRNA) were used as controls. Following successful down-regulation of PA28 (Fig. 3c), HeLa A2+ cells were transfected with pp65, Ub-pp65 or FAT10-pp65 and the $pp65_{495–503}$ CTL response was monitored by IFN-γ release assays. As shown in Fig. 3b, the presentation of the $pp65_{495–503}$ epitope liberated from untagged pp65 or the FAT10-pp65 fusion remained largely unaffected in PA28-depeleted HeLa A2+ cells. In contrast, the presentation of the $pp65_{495–503}$ epitope derived from the Ub-pp65 fusion protein was considerably reduced following down-regulation of PA28 expression in HeLa A2+ cells. Taken together, these data demonstrate that neither i-proteasomes nor PA28 significantly influence the processing of FAT10-modified substrates for MHC class I presentation. This conclusion finds further support by the observation that the accumulation of FAT10-modified proteins following a combined treatment of TNF-α and IFN-γ is not altered in i-proteasome- or PA28-depleted HEK293 cells (Fig. 4).

NUB1 and its splicing variant NUB1L specifically regulate the $pp65_{495–503}$ presentation arising from FAT10-pp65

Both the Ub-binding proteins NUB1 and its splicing variant NUB1L have been shown to accelerate the degradation of FAT10 [29] and thus appear to be important regulators of both poly-Ub- and FAT10-dependent protein degradation. We therefore next investigated the effects of NUB1 and NUB1L on the steady-state levels of pp65, Ub-pp65 and FAT10-pp65. Untagged versions of NUB1 or NUB1L were co-expressed in HeLa A2+ cells together with pp65, Ub-pp65 or FAT10-pp65 and their relative expression levels were monitored by western blotting using a monoclonal

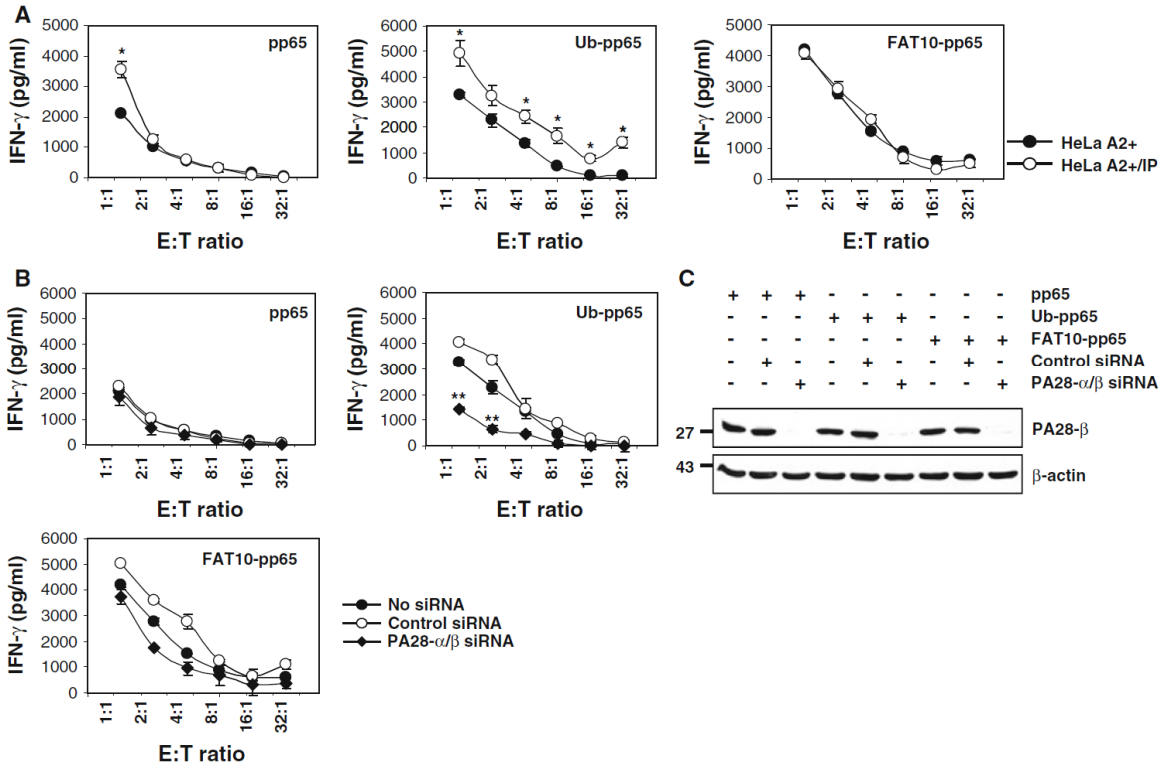

Fig. 3 The presentation of the $pp65_{495–503}$ antigenic peptide arising from the FAT10-pp65 fusion protein is not influenced by i-proteasomes and/or PA28. **a** The role of i-proteasomes in the presentation of the $pp65_{495–503}$ antigenic peptide arising from the *pp65*, *Ub-pp65* and *FAT10-pp65* fusion proteins was assessed in a 16-h CTL assay using targets cells consisting of HeLa A2+ cells having dominantly s-proteasomes or HeLa A2+/IP cells over-expressing the three inducible subunits LMP2, MECL1 and LMP7, as indicated ($*p < 0.01$, compared with HeLa A2+ having predominantly a s-proteasome, $n = 3$). **b** HeLa A2+ cells were left untreated (*no siRNA*) or treated with non-targeting siRNA (*control siRNA*) or a combination of siRNA specific for PA28-α and PA28-*β*. After 48 h, these cells were subjected to a short 4-h transfection with the *pp65*, *Ub-pp65* and *FAT10-pp65* plasmids and used as target cells in a CTL assay for monitoring the presentation of the $pp65_{495–503}$ peptide, as described in **a** ($**p < 0.005$, compared with untreated cells or cells treated with control siRNA, $n = 3$). **c** The content of HeLa A2+ for PA28 was analysed by western blotting using an antibody specific for *PA28-β*. Anti-*β*-actin antibody was used to ensure equal protein loading

anti-pp65 antibody. In accordance with previous studies [30], both NUB1 and NUB1L significantly enhanced the degradation rate of the FAT10-pp65 fusion protein (Fig. 5a). However, only NUB1L significantly accelerated the turnover of the Ub-pp65 fusion protein, suggesting that NUB1 and NUB1L differ in their ability to shuttle Ub substrates for proteasomal degradation. Coincidently, over-expression of either NUB1 or NUB1L resulted in substantially improved presentation of the FAT10 derived $pp65_{495–503}$ antigenic peptide (Fig. 5b). Likewise, over-expression of NUB1L together with Ub-pp65 was accompanied by an increased activation of the $pp65_{495–503}$ CD8+ T-cell clone. By contrast, the over-expression of either NUB1 or NUB1L had no substantial effect on the $pp65_{495–503}$ antigen presentation arising from the untagged pp65 (Fig. 5b).

To test and compare the impact of pp65, Ub-pp65 and FAT10-pp65 on cross-presentation, monocyte-derived DC were loaded with whole cell lysates containing pp65, Ub-pp65 or FAT10-pp65, co-cultured with the pp65 CTL clone 61 in the presence of LPS, and IFN-γ release was assayed, as previously described [14, 31]. As shown in Fig. 6a, DC fed with either FAT10-pp65 or Ub-pp65 proteins elicited significant responses following 12 h of co-culture which almost equalled those measured with the synthetic 9-mer pp65 peptide, but which were nearly twofold greater than those observed with the untagged pp65 protein. Interestingly, the enhancement of pp65 cross-presentation elicited by the Ub-pp65 was already visible after 4 h, while enhancement of the immune response elicited by the FAT10-pp65 fusion protein became detectable after 12 h of co-culture. Importantly, the early pp65 CTL response observed with Ub-pp65 was abrogated when using prefixed DC (Fig. S4), indicating that the pp65 cross-presentation initiated in the first 4 h of

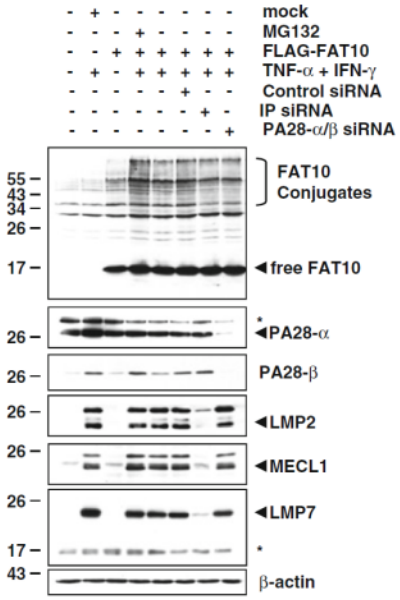

Fig. 4 The expression pattern of FAT10-protein conjugates in response to TNF-α and IFN-γ is not altered by depletion of either i-proteasomes or PA28. The role of PA28 and the i-proteasome in the steady-state level of the accumulated FAT10-modified substrates was assessed by treating HEK293 cells with siRNA specific for PA28-α/β or for the three inducible proteasomal subunits LMP2/MECL1/LMP7 (IP), respectively. After 24 h, cells were treated with a combined treatment of TNF-α and IFN-γ or left untreated prior to a subsequent 24-h transfection with the flag-tagged FAT10 plasmid. The membrane shown was subjected to western blot analysis using antibodies against *FAT10*, *PA28-α*, *PA28-β*, *LMP2*, *MECL1* and *LMP7*, as indicated. Equal loading was determined by using anti-β-actin mAb

co-culture requires processing and is not due to peptide transfer from the antigen-donor cells to the DC cell surface HLA-A2+ molecules.

Because of the observation that both NUB1 and NUB1L accelerate the degradation of FAT10-pp65, we next aimed to estimate the transcription level of both of these proteins in maturing DC following LPS stimulation using RT-PCR. As shown in Fig. 6b, NUB1 and, to a much lesser extent, NUB1L were induced in LPS-treated DC from 4 h of stimulation. However, we were unable to determine whether both abundant splice variants of the two NUB1 isoforms were translated because they were indistinguishable in western blot analyses (Fig. 6c). To address the role of the increased expression of NUB1 and NUB1L in cross-presentation, day-5 immature DC were electoporated with siRNA specific for NUB1/NUB1L for 24 h prior to a subsequent stimulation with LPS, which resulted in a strong impairment of NUB1/NUB1L up-regulation (Fig. 6d). Strikingly, the $pp65_{495–503}$ cross-presentation arising from DC fed with pp65, Ub-pp65 or FAT10-pp65 was reduced by about 20% in NUB1/NUB1L-depleted DC (Fig. 6e), demonstrating the contribution of NUB1/NUB1L to proteasome-dependent cross-presentation of the $pp65_{495–503}$ epitope.

Discussion

FAT10 is the only UBL so far known that shares with Ub the capacity of targeting substrates for proteasomal breakdown. However, very little is known about its function and nothing is known about its ability to support the generation of peptides suitable for MHC class I presentation. Here, we demonstrate that FAT10 modification of the HCMV-derived antigen pp65 (FAT10-pp65) enhances the presentation of the HLA-A2-restricted $pp65_{495–509}$ antigenic peptide (Fig. 1c) and provide evidence that FAT10-pp65 differs from Ub-modified pp65 in using the proteasome machinery. The $pp65_{495–503}$ presentation obtained with Ub-pp65 is improved by approximately 50%. This is less than originally observed by Townsend and colleagues with the $NP_{365–370}$ peptide using a Ub-Arg-NP fusion protein (N-end rule) [1]. However, this discrepancy can be explained by the fact that, in contrast to the $pp65_{495–503}$ presentation, the $NP_{365–370}$ presentation is defective and, as such, increases much more dramatically following N-terminal Ub fusion.

While this paper was under revision, an interesting study of Buchsbaum and co-workers reported that the increased degradation rate of a FAT10-GFP fusion protein is facilitated by poly-ubiquitylation [32]. Our data show that our FAT10-pp65 fusion protein is not more poly-ubiquitylated than the untagged pp65 (Fig. 1c; Fig. S3), suggesting that the accelerated degradation of this construct cannot be attributed to its enhanced poly-ubiquitylation state. Our results do not formally exclude a possible involvement of the Ub-conjugation system in the regulation of the breakdown of FAT10-pp65. Nevertheless, our results would still imply that the processing of a substrate bearing simultaneously FAT10 and Ub differs from that of Ub-tagged or posttranslationally Ub-modified proteins.

Also, the FAT10-pp65 fusion protein expressed in HeLa cells improved cross-presentation of the pp65 epitope by LPS-stimulated DC demonstrating that FAT10 modification provides an alternative signal for efficient antigen processing and subsequent MHC class I presentation.

Induction of FAT10 synthesis requires IFN-γ and TNF-α [22], which also trigger the synthesis of i-proteasomes and the proteasome activator PA28. Despite this, and in striking contrast to poly-ubiquitylated pp65, the FAT10-dependent pp65 epitope presentation was already most efficient in the presence of s-proteasomes and was not further enhanced by i-proteasomes or PA28 (Fig. 3a, b). These data suggest that

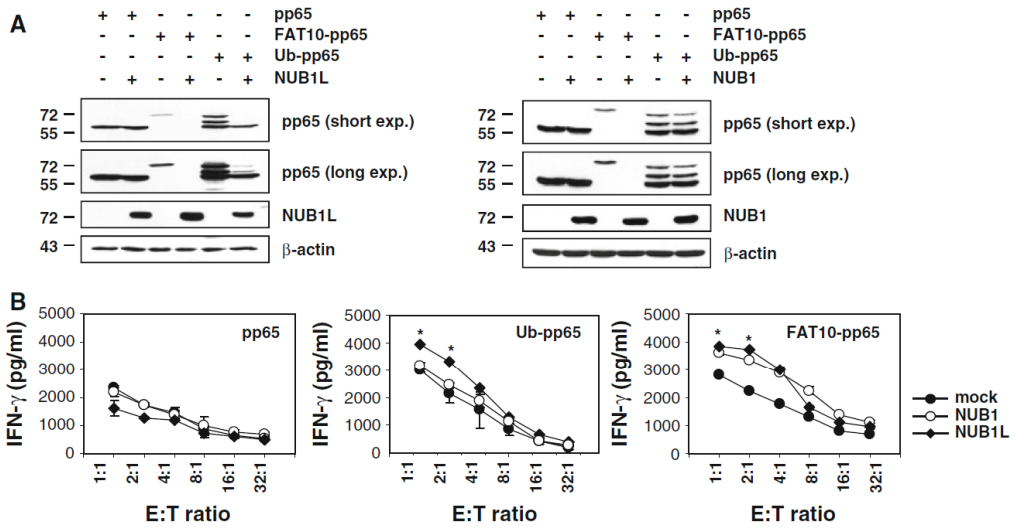

Fig. 5 NUB1 and NUB1L accelerate the protein turnover of FAT10-pp65 which results in improved presentation of the $pp65_{495–509}$ antigenic peptide in HeLa A2+ cells. **a** Untagged versions of *NUB1* and *NUB1L* were co-expressed together with *pp65*, *Ub-pp65* or *FAT10-pp65* in HeLa A2+ cells and their respective influence on the steady-state level of each pp65 antigenic variant was determined by western-blot using an anti-pp65 monoclonal antibody. The over-expression of NUB1 and NUB1L was checked by probing the membrane with a polyclonal antibody recognising both NUB1 and NUB1L (equal protein loading was ensured by using the anti-β-actin mAb). **b** The effects of NUB1 and NUB1L over-expression were also tested for the presentation of the $pp65_{495–503}$ peptide emerging from *pp65*, *Ub-pp65* or *FAT10-pp65*. HeLa A2+ cells were transfected with either the pcDNA3.1 empty vector (*mock*), *NUB1* or *NUB1L* for 24 h prior to a subsequent transient transfection with the pp65, Ub-pp65 or FAT10-pp65 constructs for 4 h. Cells co-expressing NUB1 or NUB1L and the various pp65 antigenic forms were subsequently tested for their capacity to present the $pp65_{495–503}$ antigenic peptide using the CTL clone 61 in a 16-h IFN-γ release assay ($^*p < 0.01$, compared to HeLa A2+ cells transfected with the pcDNA3.1 empty vector, $n = 2$)

the degradation of the FAT10- and Ub-protein conjugates are governed by different molecular mechanisms. One possible explanation for this surprising result may be that FAT-10- and Ub-modified proteins interact with the 26S proteasome in different ways. Interestingly, our experiments show that both FAT10-pp65 and Ub-pp65 share the 19S regulator subunit Rpn10 (Fig. 2a), known to bind poly-Ub-chains as interaction partner [25, 26]. However, siRNA experiments also revealed that, while Rpn10 deficiency exerts profound negative effects on the presentation of the pp65 epitope derived from Ub-pp65, the effect on the FAT10-pp65-derived epitope is considerably less pronounced (Fig. 2b). In light of the extremely efficient proteasome-dependent turnover of FAT10-pp65, this may indicate that FAT10 binds Rpn10 less efficiently and/or that Rpn10 is not the only and not the decisive interaction partner of FAT10 modified proteins within the 26S proteasome complex.

So far, NUB1L and its natural splicing variant NUB1 (which has a deletion of 14 amino acids) had been the only proteins identified to ferry FAT10 for proteasome-dependent degradation [22, 30]. Our data further support a role for both NUB1 and NUB1L in facilitating the breakdown of FAT10-modified substrates, as evidenced by decreased steady-state levels of the FAT10-pp65 fusion protein in cells over-expressing NUB1 or NUB1L (Fig. 5a). Importantly, the accelerated degradation of FAT10-pp65 by NUB1 or NUB1L was accompanied by a marked increase of the $pp65_{495–503}$ CTL response (Fig. 5b). However, our experiments rule out an entirely overlapping function of NUB1 and NUB1L because only NUB1L was found to enhance the turnover of the Ub-pp65 fusion (Fig. 5a). Thus, unlike NUB1 (which appears FAT10-specific), NUB1L seems to be positioned at the intersection of the Ub and FAT10 pathways, suggesting a model in which the accelerated disposal of Ub-modified proteins by NUB1L is connected to an increased supply of antigenic peptides for MHC class I presentation.

The optimal form of the antigenic source for effective cross-priming is still a matter of debate, ranging from stable antigens as being a favourable source for cross-presentation [33–35] to unstable proteins, including defective ribosomal products (DriPs), being more effective than mature proteins for stimulating cross-priming [36, 37]. Our data show that both Ub and FAT10 fusion proteins serving as vehicles for pp65 delivery into DC were by far superior in activating CTL to the untagged pp65 (Fig. 6a). This data would support the notion that short-lived proteins

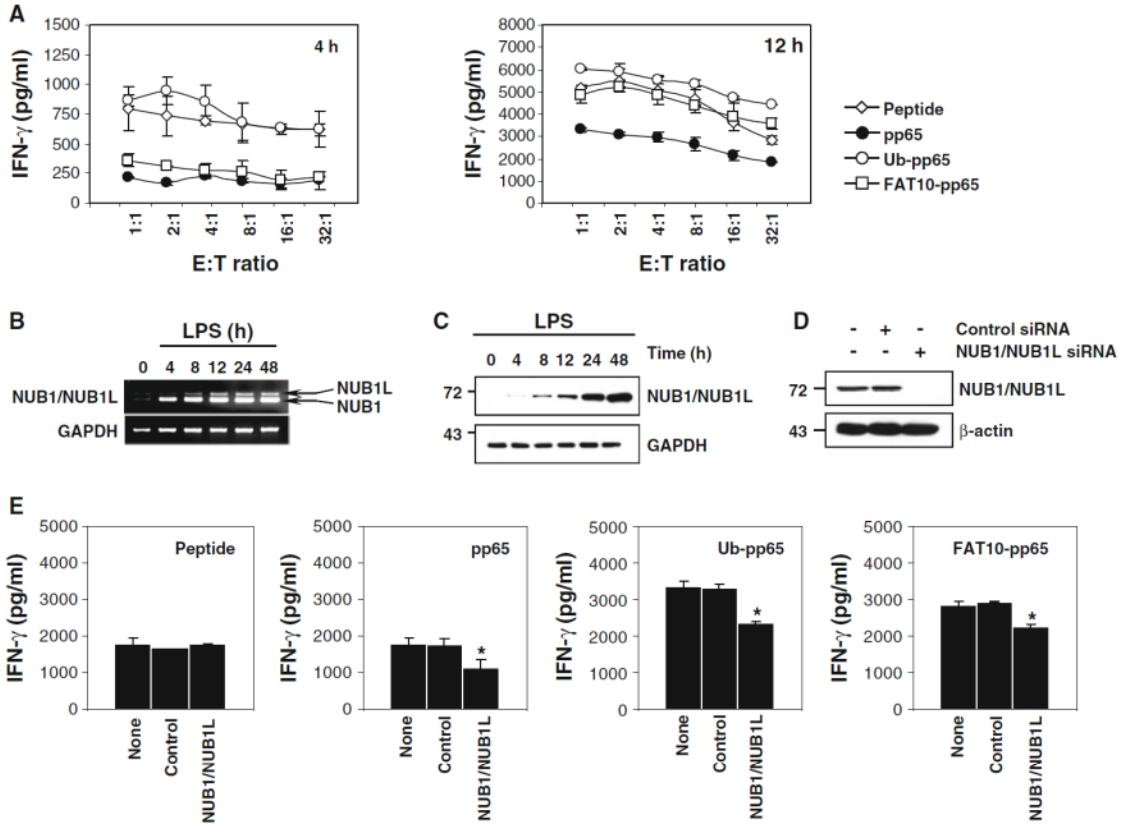

Fig. 6 Both FAT10 and Ub facilitate cross-presentation of the $pp65_{495–503}$ epitope by DC when fused to the N-terminus of the HCMV-derived pp65 protein. **a** Immature HLA-A2+ DC were fed with *pp65*, *Ub-pp65* or *FAT10-pp65* necrotic HeLa cells at a ratio at 2 per DC and simultaneously exposed to LPS (1 μg/ml) to induce maturation. The ability of pp65-, Ub-pp65- and FAT10-pp65-pulsed DC to stimulate the CTL clone 61 was tested in a 4- or 12-h IFN-γ release assay, as indicated. Internal controls consist in DC loaded with 1 μm of the 9-mer synthetic $pp65_{495–503}$ peptide ($^*p < 0.01$, compared to DC loaded with untagged pp65, $n = 2$). **b** RT-PCR analysis of NUB1 and NUB1L transcripts in LPS-treated DC following various periods of time. The amplified RT-PCR products NUB1 and NUB1L were separated on 2% agarose gels and visualised by ethidium bromide. Electrophoresis of the PCR products showed *NUB1* (222 bp) band and a larger band corresponding to *NUB1L* (256 bp). PCR using *GAPDH* showed similar amplification levels among the samples tested. **c** Time-course induction of NUB1 and NUB1L in DC following LPS stimulation as assessed by western-blotting. Day 5-immature DC were treated with 1 μg/ml LPS for various periods of time, as indicated. Thirty micrograms of total cellular proteins were loaded in each lane and resolved 12% SDS-PAGE gel followed by western blotting with a polyclonal antibody specific for both *NUB1* and *NUB1L*. Equal amounts of proteins was ensured using *GAPDH* antibody. **d** Western blot analysis for NUB1/NUB1L in untreated DC or DC treated with *control siRNA* or *NUB1/NUB1L*-specific *siRNA*, as indicated. **e** HLA-A2+ DC with a knockdown of NUB1/NUB1L were loaded with 1 μM of the $pp65_{495–503}$ synthetic *peptide* or cell-associated *pp65*, *Ub-pp65* and *FAT10-pp65* and subsequently cultured with the CTL clone 61 at a E:T ratio of 1:1 in the presence of LPS (1 μg/ml). Cross-presentation of the $pp65_{495–503}$ peptide was assessed by measuring the IFN-γ content in the supernatant following 12 h of co-culture ($^*p < 0.01$, compared to DC treated with control siRNA, $n = 2$)

are better cross-presented than the stable ones. Interestingly, there exist kinetic differences in enhancing cross-presentation, with cross-presentation from the FAT10-pp65 fusion being considerably lower during the first 4 h of the assay than that observed with Ub-pp65. However, Ub-pp65 and FAT10-pp65 exerted almost identical cross-presentation efficiency after 12 h of co-culture.

Interestingly, NUB1 and, to a lesser extent, NUB1L are induced during the course of LPS-induced DC maturation. The fact that at the transcriptional level the NUB1/NUB1L ratio was close to 10 (Fig. 6b, c), seems to suggest that NUB1 is the major isoform in mature DC silencing of NUB1/NUB1L expression and was accompanied by a slight but significant decrease of the pp65 cross-presentation levels

by DC (Fig. 6e). Surprisingly, however, impairment was not restricted to DC loaded with FAT10-pp65 but was also observed to a similar extent with DC loaded with either untagged pp65 or Ub-pp65. This appears to contrast with the observation that NUB1 and/or NUB1L can only enhance MHC class I presentation of FAT10 substrates. However, given the sensitivity of the assay, the low amounts of NUB1L expressed during DC maturation are probably sufficient to influence processing of the pp65 epitope derived from untagged pp65 and Ub-pp65. Alternatively, the sensibility of pp65 and Ub-pp65 to NUB1/NUB1L down-regulation may indicate that both forms of the pp65 antigen undergo FAT10 modification within DC prior to proteasomal degradation for cross-presentation. Proteasome-dependent cross-presentation was previously estimated to only contribute to total cross-presentation to approximately 30% [38]. Keeping this in mind, the observed inhibitory effect on cross-presentation of about 20% exerted through the knockdown of NUB1/NUB1L support the central role of the two proteasomal adapter proteins in antigen cross-presentation.

Collectively, our findings outline the FAT10-NUB1/NUB1L-Rpn10 axis as a novel route for MHC class I antigen direct presentation and DC-based cross-presentation. Considering the strongly delayed expression of FAT10 upon cytokine stimulation, the existence of this new route may allow presentation of antigenic peptides that would not be generated in adequate amounts by the classical Ub-conjugation pathway. Nevertheless, the contribution of each pathway to antigen presentation is difficult to assess. The moderate or absent phenotype exhibited by FAT10-deficient mice [19] suggests that the FAT10-conjugation pathway may not be a privileged and/or the predominantly used pathway for MHC class I presentation. This hypothesis is further supported by the observation that FAT10 is not expressed in cells under normal conditions. It is instead conceivable that the FAT10-conjugation machinery represents a complementary pathway which is used when Ub availability becomes a rate-limiting factor. Interestingly, FAT10 is up-regulated at the transcriptional level by cytokines (i.e., TNF-α and/or IFN-γ), which are also thought to deplete the pool of free Ub by increasing the formation of Ub-protein conjugates in immune cells [14, 39] as well as in non-immune cells [24]. Therefore, the role of the FAT10-dependent degradation machinery may be to support an overloaded Ub pathway in the removal of damaged proteins in later phases of stimulation. For the same reason, this route may be up-regulated in some pathological conditions such as viral infections and/or tumours, and may explain the observation that FAT10 is over-expressed in tumours exhibiting an alteration of the Ub-conjugation system such as in gastric cancer [17, 40]. Taken together, these data highlight the FAT10-dependent degradation machinery as a distinct MHC class I antigen processing pathway and suggest new avenues for FAT10-based immunotherapy in viral infections as well as in anti-tumour vaccinations.

Acknowledgments This work was supported by grants of the Deutsche Forschungsgemeinschaft (DFG) to P.M.K. as parts of the SPP 1365 "The regulatory and functional network of ubiquitin family protein" and of the KL427/15-1 "The function of the ubiquitin–proteasome system (UPS) in MHC class I antigen processing in target cells and maturing human dendritic cells (hDCs)". We are grateful to Dr. U. Seifert for providing us the HeLa-derived stable transfectants 33 and 33/2.

References

1. Townsend A, Bastin J, Gould K, Brownlee G, Andrew M, Coupar B, Boyle D, Chan S, Smith G (1988) Defective presentation to class I-restricted cytotoxic T lymphocytes in vaccinia-infected cells is overcome by enhanced degradation of antigen. J Exp Med 168(4):1211–1224
2. Grant EP, Michalek MT, Goldberg AL, Rock KL (1995) Rate of antigen degradation by the ubiquitin-proteasome pathway influences MHC class I presentation. J Immunol 155(8):3750–3758
3. Tobery TW, Siliciano RF (1997) Targeting of HIV-1 antigens for rapid intracellular degradation enhances cytotoxic T lymphocyte (CTL) recognition and the induction of de novo CTL responses in vivo after immunization. J Exp Med 185(5):909–920
4. Goldberg AL, Cascio P, Saric T, Rock KL (2002) The importance of the proteasome and subsequent proteolytic steps in the generation of antigenic peptides. Mol Immunol 39(3–4):147–164
5. Tanaka K, Kasahara M (1998) The MHC class I ligand-generating system: roles of immunoproteasomes and the interferon-gamma-inducible proteasome activator PA28. Immunol Rev 163:161–176
6. Fruh K, Yang Y (1999) Antigen presentation by MHC class I and its regulation by interferon gamma. Curr Opin Immunol 11(1):76–81
7. Chen W, Norbury CC, Cho Y, Yewdell JW, Bennink JR (2001) Immunoproteasomes shape immunodominance hierarchies of antiviral CD8(+) T cells at the levels of T cell repertoire and presentation of viral antigens. J Exp Med 193(11):1319–1326
8. Gileadi U, Moins-Teisserenc HT, Correa I, Booth BL Jr, Dunbar PR, Sewell AK, Trowsdale J, Phillips RE, Cerundolo V (1999) Generation of an immunodominant CTL epitope is affected by proteasome subunit composition and stability of the antigenic protein. J Immunol 163(11):6045–6052
9. Cerundolo V, Kelly A, Elliott T, Trowsdale J, Townsend A (1995) Genes encoded in the major histocompatibility complex affecting the generation of peptides for TAP transport. Eur J Immunol 25(2):554–562
10. Schwarz K, Eggers M, Soza A, Koszinowski UH, Kloetzel PM, Groettrup M (2000) The proteasome regulator PA28alpha/beta can enhance antigen presentation without affecting 20S proteasome subunit composition. Eur J Immunol 30(12):3672–3679
11. Kruger E, Kuckelkorn U, Sijts A, Kloetzel PM (2003) The components of the proteasome system and their role in MHC

class I antigen processing. Rev Physiol Biochem Pharmacol 148:81–104
12. Kerscher O, Felberbaum R, Hochstrasser M (2006) Modification of proteins by ubiquitin and ubiquitin-like proteins. Annu Rev Cell Dev Biol 22:159–180
13. Herrmann J, Lerman LO, Lerman A (2007) Ubiquitin and ubiquitin-like proteins in protein regulation. Circ Res 100(9):1276–1291
14. Ebstein F, Lange N, Urban S, Seifert U, Kruger E, Kloetzel PM (2009) Maturation of human dendritic cells is accompanied by functional remodelling of the ubiquitin-proteasome system. Int J Biochem Cell Biol 41(5):1205–1215
15. Raasi S, Schmidtke G, Groettrup M (2001) The ubiquitin-like protein FAT10 forms covalent conjugates and induces apoptosis. J Biol Chem 276(38):35334–35343
16. Ross MJ, Wosnitzer MS, Ross MD, Granelli B, Gusella GL, Husain M, Kaufman L, Vasievich M, D'Agati VD, Wilson PD, Klotman ME, Klotman PE (2006) Role of ubiquitin-like protein FAT10 in epithelial apoptosis in renal disease. J Am Soc Nephrol 17(4):996–1004
17. Lee CG, Ren J, Cheong IS, Ban KH, Ooi LL, Yong Tan S, Kan A, Nuchprayoon I, Jin R, Lee KH, Choti M, Lee LA (2003) Expression of the FAT10 gene is highly upregulated in hepatocellular carcinoma and other gastrointestinal and gynecological cancers. Oncogene 22(17):2592–2603
18. Ji F, Jin X, Jiao CH, Xu QW, Wang ZW, Chen YL (2009) FAT10 level in human gastric cancer and its relation with mutant p53 level, lymph node metastasis and TNM staging. World J Gastroenterol 15(18):2228–2233
19. Canaan A, Yu X, Booth CJ, Lian J, Lazar I, Gamfi SL, Castille K, Kohya N, Nakayama Y, Liu YC, Eynon E, Flavell R, Weissman SM (2006) FAT10/diubiquitin-like protein-deficient mice exhibit minimal phenotypic differences. Mol Cell Biol 26(13):5180–5189
20. Chiu YH, Sun Q, Chen ZJ (2007) E1–L2 activates both ubiquitin and FAT10. Mol Cell 27(6):1014–1023
21. Aichem A, Pelzer C, Lukasiak S, Kalveram B, Sheppard PW, Rani N, Schmidtke G, Groettrup M (2010) USE1 is a bispecific conjugating enzyme for ubiquitin and FAT10, which FAT10ylates itself in cis. Nat Commun 1:13
22. Hipp MS, Kalveram B, Raasi S, Groettrup M, Schmidtke G (2005) FAT10, a ubiquitin-independent signal for proteasomal degradation. Mol Cell Biol 25(9):3483–3491
23. Kuckelkorn U, Ferreira EA, Drung I, Liewer U, Kloetzel PM, Theobald M (2002) The effect of the interferon-gamma-inducible processing machinery on the generation of a naturally tumor-associated human cytotoxic T lymphocyte epitope within a wild-type and mutant p53 sequence context. Eur J Immunol 32(5):1368–1375
24. Seifert U, Bialy LP, Ebstein F, Bech-Otschir D, Voigt A, Schroter F, Prozorovski T, Lange N, Steffen J, Rieger M, Kuckelkorn U, Aktas O, Kloetzel PM, Kruger E (2010) Immunoproteasomes preserve protein homeostasis upon interferon-induced oxidative stress. Cell 142(4):613–624
25. Deveraux Q, Ustrell V, Pickart C, Rechsteiner M (1994) A 26 S protease subunit that binds ubiquitin conjugates. J Biol Chem 269(10):7059–7061
26. Thrower JS, Hoffman L, Rechsteiner M, Pickart CM (2000) Recognition of the polyubiquitin proteolytic signal. EMBO J 19(1):94–102
27. Schultz ES, Chapiro J, Lurquin C, Claverol S, Burlet-Schiltz O, Warnier G, Russo V, Morel S, Levy F, Boon T, Van den Eynde BJ, van der Bruggen P (2002) The production of a new MAGE-3 peptide presented to cytolytic T lymphocytes by HLA-B40 requires the immunoproteasome. J Exp Med 195(4):391–399
28. Sun Y, Sijts AJ, Song M, Janek K, Nussbaum AK, Kral S, Schirle M, Stevanovic S, Paschen A, Schild H, Kloetzel PM, Schadendorf D (2002) Expression of the proteasome activator PA28 rescues the presentation of a cytotoxic T lymphocyte epitope on melanoma cells. Cancer Res 62(10):2875–2882
29. Schmidtke G, Kalveram B, Weber E, Bochtler P, Lukasiak S, Hipp MS, Groettrup M (2006) The UBA domains of NUB1L are required for binding but not for accelerated degradation of the ubiquitin-like modifier FAT10. J Biol Chem 281(29):20045–20054
30. Hipp MS, Raasi S, Groettrup M, Schmidtke G (2004) NEDD8 ultimate buster-1L interacts with the ubiquitin-like protein FAT10 and accelerates its degradation. J Biol Chem 279(16):16503–16510
31. Bachem A, Guttler S, Hartung E, Ebstein F, Schaefer M, Tannert A, Salama A, Movassaghi K, Opitz C, Mages HW, Henn V, Kloetzel PM, Gurka S, Kroczek RA (2010) Superior antigen cross-presentation and XCR1 expression define human CD11c + CD141 + cells as homologues of mouse CD8+ dendritic cells. J Exp Med 207(6):1273–1281
32. Buchsbaum S, Bercovich B, Ciechanover A (2012) FAT10 is a proteasomal degradation signal that is itself regulated by ubiquitination. Mol Biol Cell 23(1):225–232
33. Norbury CC, Basta S, Donohue KB, Tscharke DC, Princiotta MF, Berglund P, Gibbs J, Bennink JR, Yewdell JW (2004) CD8 +T cell cross-priming via transfer of proteasome substrates. Science 304(5675):1318–1321
34. Wolkers MC, Brouwenstijn N, Bakker AH, Toebes M, Schumacher TN (2004) Antigen bias in T cell cross-priming. Science 304(5675):1314–1317
35. Basta S, Stoessel R, Basler M, van den Broek M, Groettrup M (2005) Cross-presentation of the long-lived lymphocytic choriomeningitis virus nucleoprotein does not require neosynthesis and is enhanced via heat shock proteins. J Immunol 175(2):796–805
36. Blachere NE, Darnell RB, Albert ML (2005) Apoptotic cells deliver processed antigen to dendritic cells for cross-presentation. PLoS Biol 3(6):e185
37. Janda J, Schoneberger P, Skoberne M, Messerle M, Russmann H, Geginat G (2004) Cross-presentation of Listeria-derived CD8 T cell epitopes requires unstable bacterial translation products. J Immunol 173(9):5644–5651
38. Shen L, Sigal LJ, Boes M, Rock KL (2004) Important role of cathepsin S in generating peptides for TAP-independent MHC class I crosspresentation in vivo. Immunity 21(2):155–165
39. Seifert U, Kruger E (2008) Remodelling of the ubiquitin-proteasome system in response to interferons. Biochem Soc Trans 36(Pt 5):879–884
40. Sugiura T (2011) The cellular level of TRIM31, an RBCC protein overexpressed in gastric cancer, is regulated by multiple mechanisms including the ubiquitin-proteasome system. Cell Biol Int 35(7):657–661

4.3. MHC class I cross-presentation of the Melan-A/MART-1_{26-35} tumor epitope by dendritic cells relies on the ERAD protein p97/VCP (this chapter is based on the work of Ménager and coworkers (Menager et al., 2014))

Synthetic long peptides (SLP) represent an additional and promising therapeutic strategy for antitumor vaccination. Such approach consists in the internalization of SLP by professional antigen-presenting cells (APC) such as DC and their subsequent processing and presentation onto MHC class I molecules. Up to now, the intracellular mechanisms involved in cross-presentation of SLP are unclear. In this work, we have characterized the cross-presentation pathway of the Melan-A/MART-1_{16-40} SLP containing the HLA-A2-restricted tumor epitope$_{26-35}$ (A27L) in human DC. Using confocal microscopy and specific inhibitors, we show that SLP_{16-40} is rapidly taken up by DC and follows a conventional TAP- and proteasome-dependent cross-presentation pathway. Our data support a role for the ERAD-related ubiquitin-binding protein p97/VCP in the transfer of SLP_{16-40} from early endosomes to the cytoplasm and rule Derlin-1 out as a possible retro-translocation channel for cross-presentation. Our findings propose a model for cross-presentation of SLP which is in line with the hypothesis that internalized antigens undergo a ubiquitination process for their extraction from the early endosomes by p97/VCP.

OPEN ACCESS Freely available online

PLOS ONE

Cross-Presentation of Synthetic Long Peptides by Human Dendritic Cells: A Process Dependent on ERAD Component p97/VCP but Not sec61 and/or Derlin-1

Jérémie Ménager[1,2,3], Frédéric Ebstein[4], Romain Oger[1,2,3], Philippe Hulin[1,3], Steven Nedellec[1,3], Eric Duverger[5], Andrea Lehmann[4], Peter-Michael Kloetzel[4], Francine Jotereau[1,2,3], Yannick Guilloux[1,2,3]*

1 INSERM U892, Nantes, France, **2** Université de Nantes, Nantes, France, **3** CNRS, UMR 6299, Nantes, France, **4** Institut of Biochemistry, Charité University Hospital, Humboldt University, Berlin, Germany, **5** Glycobiochimie, ICOA, Université d'Orléans, Orléans, France

Abstract

Antitumor vaccination using synthetic long peptides (SLP) is an additional therapeutic strategy currently under development. It aims to activate tumor-specific $CD8^+$ CTL by professional APCs such as DCs. DCs can activate T lymphocytes by MHC class I presentation of exogenous antigens - a process referred to as "cross-presentation". Until recently, the intracellular mechanisms involved in cross-presentation of soluble antigens have been unclear. Here, we characterize the cross-presentation pathway of SLP Melan-$A_{16–40}$ containing the HLA-A2-restricted epitope$_{26–35}$ (A27L) in human DCs. Using confocal microscopy and specific inhibitors, we show that $SLP_{16–40}$ is rapidly taken up by DC and follows a classical TAP- and proteasome-dependent cross-presentation pathway. Our data support a role for the ER-associated degradation machinery (ERAD)-related protein p97/VCP in the transport of $SLP_{16–40}$ from early endosomes to the cytoplasm but formally exclude both sec61 and Derlin-1 as possible retro-translocation channels for cross-presentation. In addition, we show that generation of the Melan-$A_{26–35}$ peptide from the $SLP_{16–40}$ was absolutely not influenced by the proteasome subunit composition in DC. Altogether, our findings propose a model for cross-presentation of SLP which tends to enlarge the repertoire of potential candidates for retro-translocation of exogenous antigens to the cytosol.

Citation: Ménager J, Ebstein F, Oger R, Hulin P, Nedellec S, et al. (2014) Cross-Presentation of Synthetic Long Peptides by Human Dendritic Cells: A Process Dependent on ERAD Component p97/VCP but Not sec61 and/or Derlin-1. PLoS ONE 9(2): e89897. doi:10.1371/journal.pone.0089897

Editor: Jean Kanellopoulos, University Paris Sud, France

Received October 21, 2013; **Accepted** January 25, 2014; **Published** February 27, 2014

Funding: This work was supported by grants from the Ligue Nationale contre le Cancer and Comite 44, Institut National de la Santé et de la Recherche Médical, Institut National du Cancer (PL074), and the European Network for the Identification and Validation of Antigens and Biomarkers in Cancer and their Application in Clinical Tumor Immunology Network (503306). JM was supported by a doctoral fellowship from the Ministère de l'Ensiegnement Supérieur et de la Recherche. The funders had no role in study design, data collection and analysis, decision to publish, or preparation of the manuscript.

Competing Interests: The authors have declared that no competing interests exist.

* E-mail: Yannick.guilloux@univ-nantes.fr

Introduction

The notion that the immune system can recognize and mount a response against tumors was initially postulated by Coley [1]. The development of immune responses against tumors *in vivo* involves the presentation of target structures on the cell surface of cancer cells, namely, tumor-associated antigens (TAA). These molecules must be presented effectively to effector cells of the immune system (NK, LT $CD8^+$, $CD4^+$,…) for the establishment of a lasting and beneficial immune response. Although anti-tumor immunity requires both innate and adaptive immune responses, it is generally accepted that $CD8^+$ CTL are the most effective antitumor effector cells [2,3].

The adaptive immune response depending on CTL involves TAA expression by tumor cells and requires TAA presentation by professional APCs. Among professional APC, DCs possess the unique ability, via co-stimulatory signals, to activate naive T lymphocytes in secondary lymphoid organs [4,5]. Indeed, DCs take up extracellular TAA, process them intracellularly into antigenic peptides and load them onto major histocompatibility class I and class II molecules (MHC). The process whereby an exogenous antigen is acquired, processed and presented as peptide bound on MHC class I is known as "cross-presentation" [6,7,8]. Many compartments are involved in cross-presentation of soluble antigens [9] that critically depend on the nature of the antigen. Early endosomes internalize soluble antigens [10], the ER and Golgi apparatus are involved in presentation of endogenous antigens but can participate in the processing of antigens internalized by DCs [7,11]. Furthermore, lysosomes have been recently reported to participate in cross-presentation of some antigens [12].

Current immunotherapy strategies are designed to provide either passive or active immunity against malignancies by harnessing the immune system to target tumors [13]. Among the various therapies, one common approach is therapeutic vaccination consisting in the injection of antigen from cancer cells in order to stimulate specific anti-tumor immunity. Many immunotherapy strategies, in particular those involving DCs, are under development [4,14]. However, all of these strategies of therapeutic vaccination have so far exhibited low clinical benefit for patients [15].

A new immunotherapy strategy has emerged based on synthetic long peptides (SLP). SLP are usually 25–50 amino acids long and contain antigenic epitopes that require endocytosis and processing by professional APC such as DCs [15,16]. Indeed, SLPs cannot be

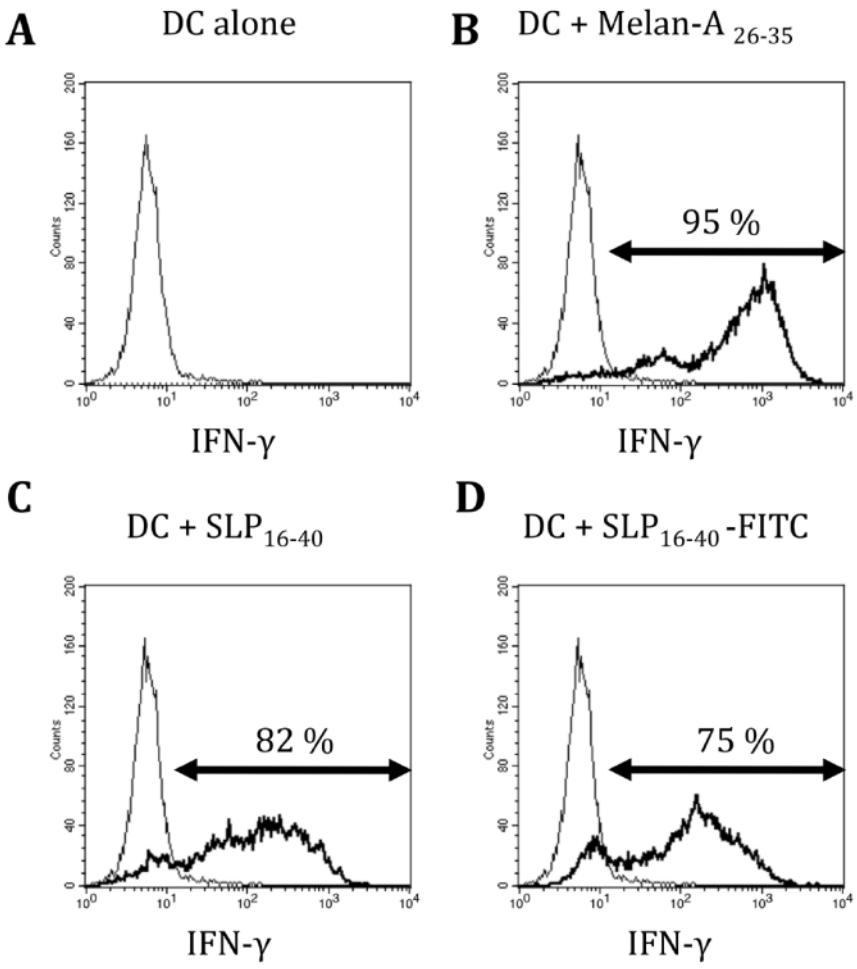

Figure 1. $SLP_{16–40}$-FITC is cross-presented efficiently by the DC. Flow cytometry of DC activation of the 10C10 CD8+ T-cell clone 10C10. DC were pulsed for 3 h in the presence of short peptide $MelanA_{26–35}$, $SLP_{16–40}$, or $SLP_{16–40}$-FITC before co-culture with the 10C10 clone at a 1:1 cell ratio. The histogram represents the fluorescence emitted by the 10C10 clone stained with anti-IFN-γ.
doi:10.1371/journal.pone.0089897.g001

loaded exogenously on MHC-I and their processing requires a cross-presentation mechanism restricted to DCs for induction of a CTL response, thereby inducing anti-tumor immunity rather than tolerance [4,17]. Several studies and clinical trials have been performed using SLP as vaccines with promising results against vulvar intraepithelial neoplasia lesions, cervical cancer and ovarian cancer [18,19,20,21].

In this study, we designed a SLP from the Melan-A/MART-1 TAA. This SLP of 25 amino acids covers positions 16 to 40 of Melan-A/MART-1 ($SLP_{16–40}$) and includes the A27L modification which allows a better anchoring of the immunodominant Melan-A/MART-1 26–35 epitope to the HLA-A*0201 molecule [22]. This $SLP_{16–40}$ includes epitopes recognized by HLA class I restricted T-cell clones [23,24]. A previous study, published by our group had shown that this $SLP_{16–40}$ and its natural homologue are efficiently and durably cross-presented by DCs [25]. In addition our group has shown that cross-presentation of modified $SLP_{16–40}$ results in efficient priming of a CD8 tumor reactive T cell repertoire. Nonetheless, to the best of our knowledge, the cellular mechanism involved in this cross-presentation by human DCs remains to be elucidated. Here, we characterize the cross-presentation pathway of $SLP_{16–40}$. We show that it is dependent on early endosomes, followed by the ERAD pathway: retro-translocation into the cytosol and poly-ubiquitinylation of the SLP for proteasome degradation. Altogether, our results define the processing mechanism of $SLP_{16–40}$ by DCs.

Materials and Methods

Culture Medium

Culture medium RPMI 1640 (Gibco BLR, Gaithersburg, MD) was supplemented with penicillin-streptomycin (100 U/ml and 100 µg/ml respectively; Life Technologies) and L-Glutamine (2 mM) (Life Technologies, Cergy-Pontoise, France) and either with 1% human plasma, 8% pooled human serum (pHS) or 10% fetal calf serum (FCS, Eurobio, Les Ulis, France).

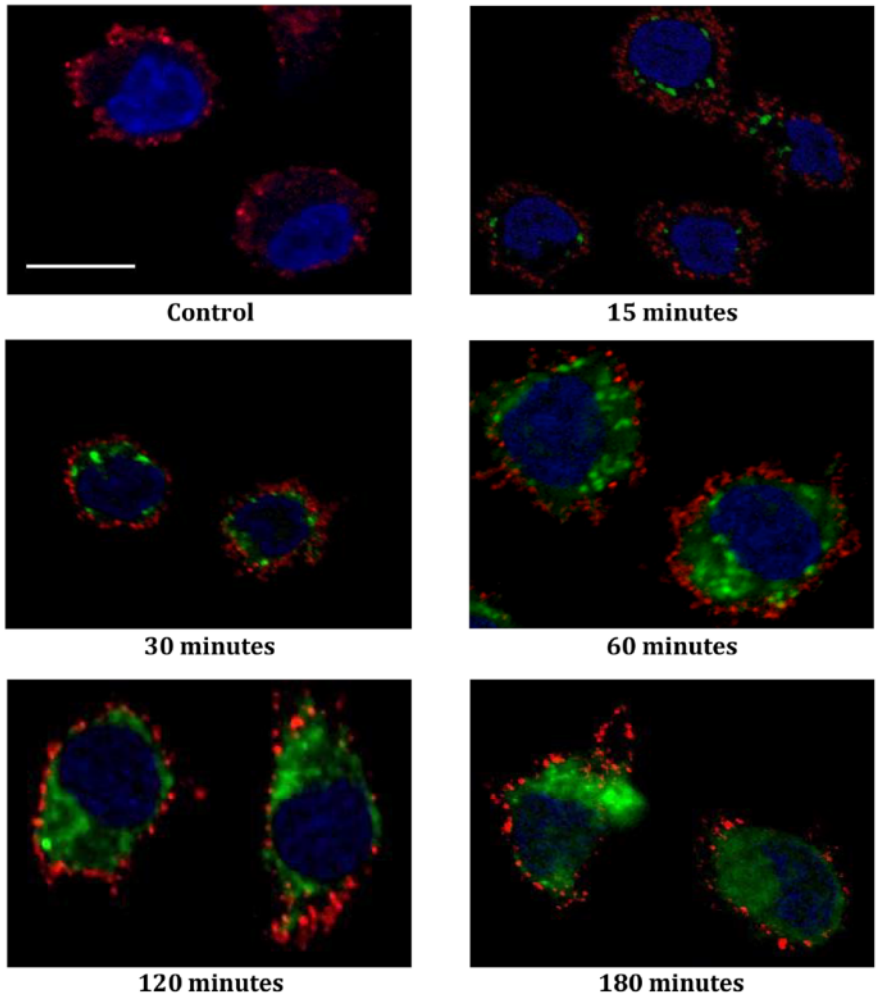

Figure 2. $SLP_{16–40}$-FITC fluorescence monitored by confocal microscopy. Immunofluorescence microscopy. Kinetics of internalization of $SLP_{16–40}$-FITC (green) by DCs. DCs were stained at the cell membrane with antibody w6–32 (red) and nuclei were counterstained with DRAQ 5 (blue). All image represent one single optical section. Step size of 0,5 µm thick. Original magnification, X60. Data are representative of two independent experiments. Scale bar represent a distance of 5 µm.
doi:10.1371/journal.pone.0089897.g002

Cell Culture

HLA-A2 Monocytes were purified using centrifugal counter-flow elutriation (Clinical Transfer Facility CICBT0503, Dr. M. Grégoire, Nantes) and cultured for 4.5 days in RPMI 1640 2% human albumin in the presence of 1000 U/mL GM-CSF (Cellgenix) and 200 U/mL IL-4 (Cellgenix): MoDCs medium [26].

Maturation of Mo-DCs was induce by addition of 1000 U/mL TNFα (Cellgenix) and 50 µg/mL poly I:C (Sigma) to the culture (Maturation MoDCs medium). Each preparation of DC was checked for purity and differentiation by flow cytometry using the markers indicated below.

Human DC phenotype was determined by the expression of CD14, CD40, CD80, CD83 and HLA-DR (data not shown).

In cross presentation assays 10^6 DCs were plated per well in 24 - well plates- pretreated with 3% polyHema (Sigma) for 16 hr to facilitate the harvest of DCs after the antigenic pulse.

The 10C10 clone was amplified as previously described [27].

Synthetic Peptides

Synthetic long peptide Melan-A/MART-$1_{16–40}$ (GHGHSYT-TAEELAGIGILTVILGVL) ($SLP_{16–40}$) and synthetic short peptide Melan-A/MART-$1_{26–35}$ with the A27L modification (ELA-GIGILTV), were synthesized with purity greater than 95% and purchased from Millegen (Labege, France). Synthetic fluorescent long peptides Melan-A/MART-$1_{16–40}$-FITC (GHGHSYTTAEE-LAGIGILTVILGVLK-FITC) ($SLP_{16–40}$-FITC) and FITC-Melan-A/MART-$1_{16–40}$ (FITC-GHGHSYTTAEELAGIGILT-VILGVL) (FITC-$SLP_{16–40}$), were produced with purity greater than 95%. All the peptides were reconstituted at 10 mM in DMSO.

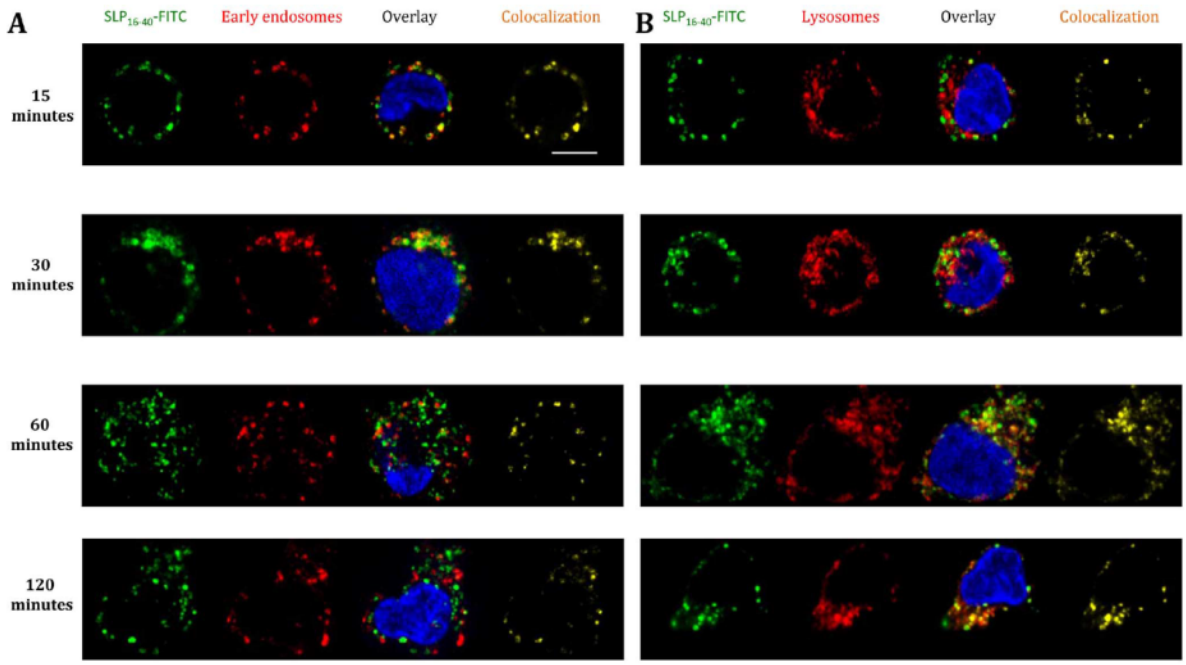

Figure 3. Study of $SLP_{16–40}$-FITC colocalization in DCs : colocalization in early endosomes and lysosomes. (A) Immunofluorescence microscopy. Kinetics of internalization of DCs incubated with $SLP_{16–40}$-FITC (green), 15, 30, 60 or 120 minutes after pulse. DCs are stained at the early endosomes with antibody anti-EEA-1 (red) and the nuclei are counterstained with DRAQ 5 (blue). All image represent one single optical section. Step size of 0,5 µm thick. Original magnification, X60. Single scans are representative for multiple cells analysed in at least 2 experiments. (B) Immunofluorescence microscopy. Kinetics of internalization of DCs incubated with $SLP_{16–40}$-FITC (green), 15, 30, 60 or 120 minutes after pulse. DCs are stained at the lysosomes with antibody LAMP-1 (red) and the nuclei are counterstained with DRAQ 5 (blue). All image represent one single optical section. Step size of 0,5 µm thick. Original magnification, X60. Single scans are representative for multiple cells analysed in at least 2 experiments. Scale bar represent a distance of 5 µm.
doi:10.1371/journal.pone.0089897.g003

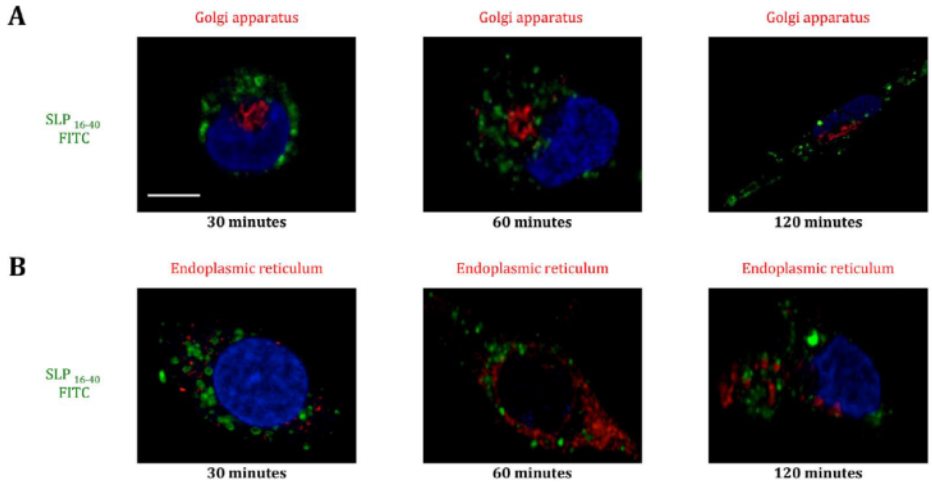

Figure 4. Study of $SLP_{16–40}$-FITC colocalization in DCs: no colocalization in Golgi and ER. (A) Immunofluorescence microscopy. Kinetics of internalization of DCs incubated with $SLP_{16–40}$-FITC (green), 30, 60 or 120 minutes after pulse. DCs are stained at the Golgi with antibody anti-GM130 (red) and the nuclei are counterstained with DRAQ 5 (blue). All image represent one single optical section. Step size of 0,5 µm thick. Original magnification, X60. Data are representative of two independent experiments. (B) Immunofluorescence microscopy. Kinetics of internalization of DCs incubated with $SLP_{16–40}$-FITC (green), 30, 60 or 120 minutes after pulse. DCs are stained at the ER with antibody anti-calreticulin (red) and the nuclei are counterstained with DRAQ 5 (blue). All image represent one single optical section. Step size of 0,5 µm thick. Original magnification, X60. Data are representative of two independent experiments. Scale bar represent a distance of 5 µm.
doi:10.1371/journal.pone.0089897.g004

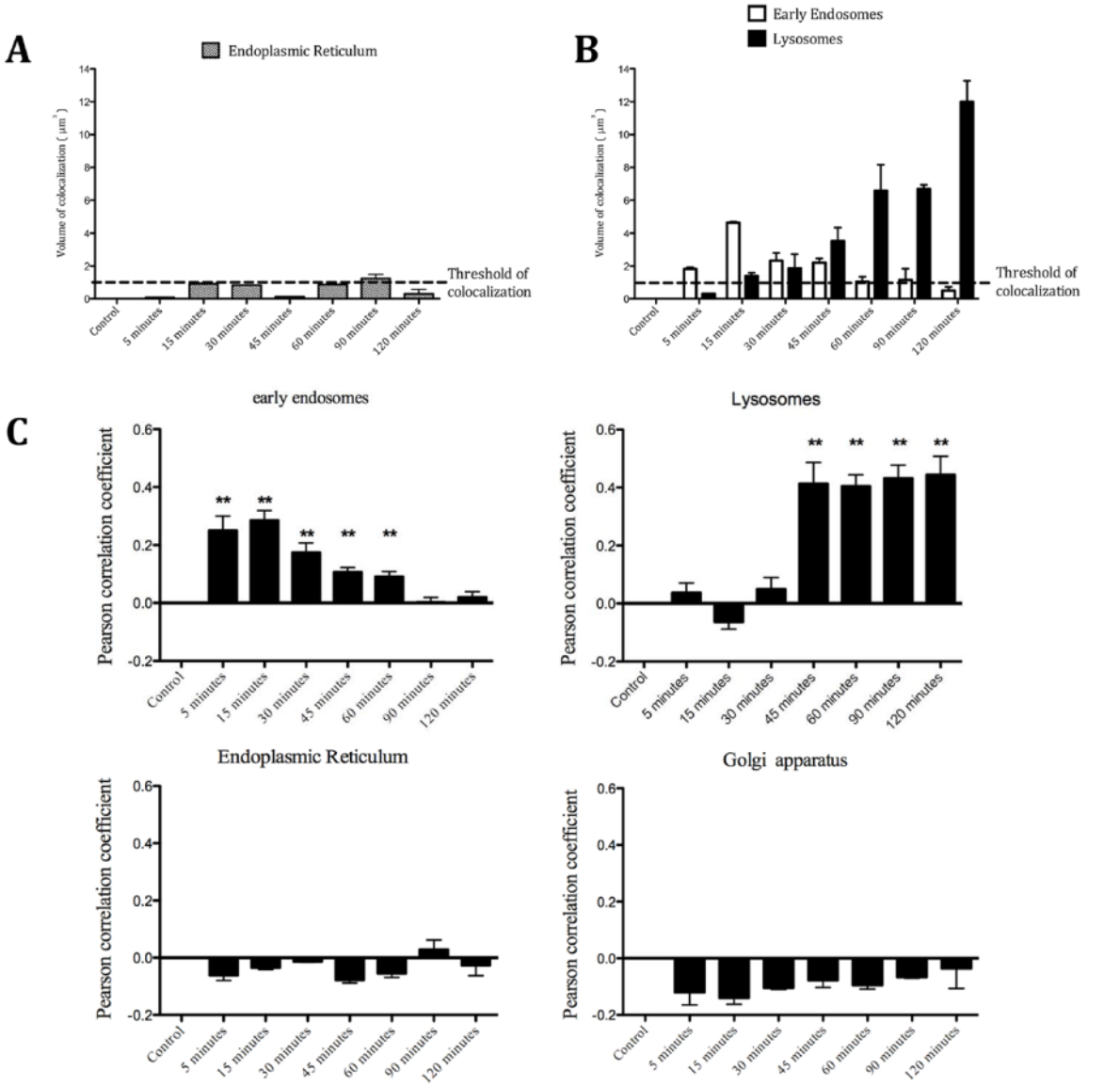

Figure 5. Kinetics of internalization of $SLP_{16–40}$ in DCs. (A) Volume measurement of green fluorescence ($SLP_{16–40}$-FITC) with red fluorescence (ER) colocalization at each time point. For each point, average volume was determined on five different cells of two independent experiments. (B) Volume measurement of green fluorescence ($SLP_{16–40}$-FITC) with red fluorescence colocalization (early endosomes or lysosomes) at each time point. Representations of colocalization in early endosomes are in white bars and colocalization in lysosomes are in black bars. For each point and each compartiment, average volume was determined in five different cells from two independent experiments. (C) The colocalization of $SLP_{16–40}$-FITC immunofluorescence with intracellular compartments (early endosomes, lysosomes, ER and Golgi apparatus) was quantified by measuring the Pearson correlation coefficient (Rr) with Velocity software. A Pearson correlation of 1 indicates complete colocalization, a value of 0 indicates no specific colocalization and a value of −1 indicates a perfect but inverse correlation (exclusion). Measurements of the Pearson correlation coefficient indicate a reasonable degree of partial colocalization of $SLP_{16–40}$ with early endosomes between 5 and 60 minutes and with lysosomes between 45 and 120 minutes. The Pearson correlation coefficient of $SLP_{16–40}$ with ER and Golgi apparatus lysosomes indicates no specific colocalization. The Pearson correlation coefficient was measured with n = 5 cells. Statistical significance of colocalization was compared to the null hypothesis of no specific colocalization (Pearson correlation coefficient value of 0).
doi:10.1371/journal.pone.0089897.g005

Immunofluorescent Staining, Flow Cytometry Analysis and Elisa Assay

CD8 T cell activation by DCs loaded in vitro with $SLP_{16–40}$ or $SP_{26–35}$ peptides was determined by using APC-labeled anti-$CD8^+$mAb and PE-labeled anti-IFNγ. Mo-DCs were stained by PKH-67 according to the manufacturer's recommendations (Sigma) in order to exclude them from the T cell gate.

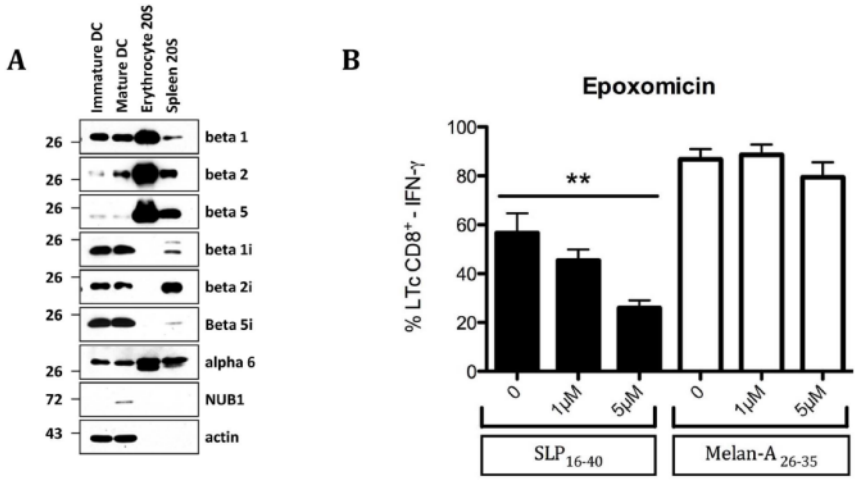

Figure 6. Immature and mature DC express mixed-type proteasomes. (A) Untreated day 5-immature DC and DC treated with LPS (1 μg/ml) for 24 hours were analysed for their proteasome content by western-blotting using antibodies against β1, β2, β5, β1i, β2i, β5i, as indicated. Purified 26 proteasomes (250 ng) from erythrocytes (standard proteasome) and spleen (mixture of standard and immunoproteasome) were used as sources to ensure antibody specificity. To control for equal loading, proteins were subjected to western blotting using the anti-β-actin antibody. (B) Flow cytometry of DC recognition by $CD8^+$ T-cell clone 10C10. DCs were treated with Epoxomicin (1 and 5 μM) for 30 min, then DCs were pulsed for 3 h in the presence of short peptide $MelanA_{26–35}$, or $SLP_{16–40}$, and inhibitor before co-culture with the 10C10 clone at a 1:1 cell ratio. Data are representative of at least three independent experiments. Statistical analysis was performed using non-parametric Mann-Whitney test and values in the presence of inhibitor were significantly different ($p<0,04$).
doi:10.1371/journal.pone.0089897.g006

For intracytoplasmic IFNγ staining, cells were stained at 4°C for 20 minutes, with anti-$CD8^+$ Ab. Then cells were fixed 10 minutes at room temperature in PBS 4% paraformaldehyde (Sigma). Anti-IFNγ was added to fixed cells and incubated for 30 minutes at room temperature. Reagent dilutions and washes were done with PBS containing 0.1% BSA and 0.1% saponin (Sigma). After staining, immunofluorescence was analyzed on a FACS calibur (BD Biosciences).

Alternatively, activation of the 10C10 CTL clone was evaluated by determining the IFNγ content in the supernatant in duplicates in a 16-hr CTL assay using a commercially available ELISA kit (BD Biosciences).

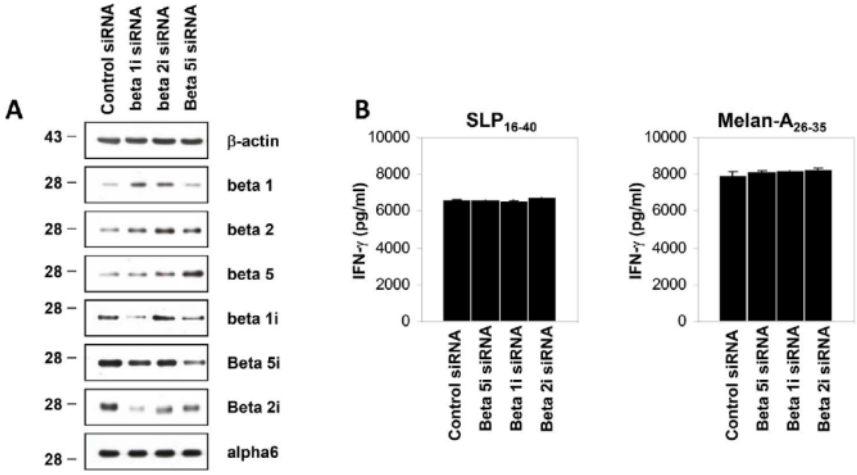

Figure 7. Effect of siRNA depletion of each of the inducible proteasome subunit β1i, β2i, β5i on the DC-mediated cross-presentation of the SLP 16–40. (A) DC were transfected with 1 μM of control siRNA or β1i, β2i, β5i -targeting siRNA for 72 hours. The knockdown of the above-stated inducible subunits as well as its impact on the steady-state level of each of the standard proteasome subunits (β1, β2, β5) was analysed by western-blotting using specific antibodies, as indicated. Antibody against b-actin was used to ensure an equal protein loading. (B) IFN-g production of the LT $CD8^+$10C10 responded to β1i, β2i, β5i -depleted DC pulsed with either SLP16–40 or Melan- A26–35. All data are shown as means +/− SD and are representative of three independent experiments.
doi:10.1371/journal.pone.0089897.g007

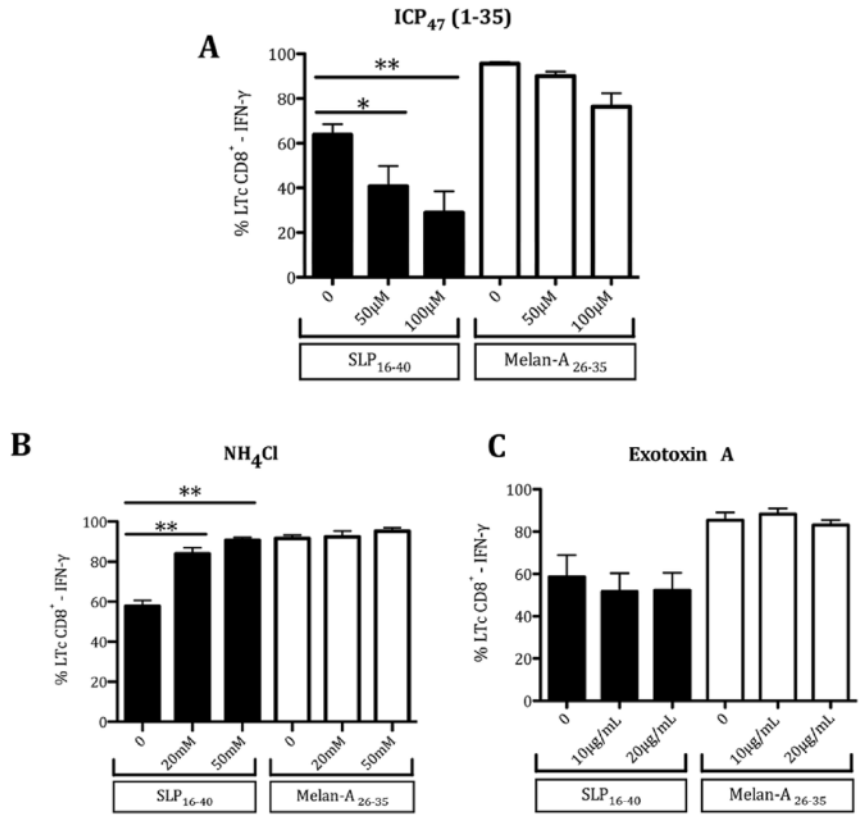

Figure 8. Effects of different inhibitors on $SLP_{16–40}$ cross-presentation. (A) TAP transport: Flow cytometry of DC recognition by LT $CD8^+$10C10. DCs were treated with inhibitor, ICP47 (50 and 100 μM) for 30 min, then DCs were pulsed for 3 h with the short peptide Melan-$A_{26–35}$, or $SLP_{16–40}$, and in the presence of the inhibitor before co-culture with the LT $CD8^+$10C10 at a 1:1 cell ratio. Data are representative of at least three independent experiments. Statistical analysis was performed using non-parametric Mann-Whitney's test and values in the presence of inhibitor were significantly different ($p<0.04$). The molecular mechanisms involved in cross-presentation of $SLP_{16–40}$. Flow cytometry of DC recognition by LT $CD8^+$10C10. DCs were treated with inhibitor, (B) NH_4Cl (20 mM and 50 mM) or (C) ExoA (10 and 20 μg/mL) for 30 min, then DCs were pulsed for 3 h in the presence of short peptide Melan-$A_{26–35}$, or $SLP_{16–40}$, and inhibitor before co-culture with the LT $CD8^+$10C10 at a 1:1 cell ratio. Data are representative of at least three independent experiments. Statistical analysis was performed using non-parametric Mann-Whitney's test and values in the presence of inhibitor were significantly different ($p<0,04$).
doi:10.1371/journal.pone.0089897.g008

SDS-PAGE and Western Blotting

For the preparation of whole cell lysates, cells were lysed in a buffer containing 50 mM NaCl, 50 mM Tris, 5 mM MgCl2, 1 mM DTT, 10% glycerol and 0.1% NP40. Protein concentrations in lysates were determined using a bicinchoninic acid assay (BCA). Five to twenty μg of whole-cell lysates were separated on a 15% SDS-polyacrylamide gel and transferred onto a PVDF membrane. In some experiments 200 ng of purified 20S proteasome from erythrocytes (Standard Proteasome) or spleen (Standard Proteasome and ImmunoProteasome) were loaded as internal controls. The blots were probed with antibodies to β1i, β5i, Beta1, Beta2, Beta5, Alpha6 (all purchased from Enzo life sciences), β2i (K65/4, laboratory stock), p97/VCP (MA3-004, Dianova), Derlin-1, sec61-a and to β-actin (Santa Cruz Biotechnology) to confirm that equal amounts were present in every lane. Bound antibodies were visualized with ECL chemiluminescence (Roche).

Antigenic Pulse and Chase, Drug Treatment of DC or $SLP_{16–40}$ Cross-presentation Assays

$SLP_{16–40}$ was pulsed at 10 μM, 37°C for 3 h on DCs in RPMI supplemented with 2% human albumin, 1000 U/mL GM-CSF, 200 U/mL recombinant human IL-4, 1000 U/mL TNFα and 50 μg/mL poly I:C. Following the pulse, 1.10^5 DC were plated per well in 96-well round-bottom plates, fixed with 0,01% glutaraldehyde containing PBS for 1 min then washed three times in RPMI. DCs were co-cultured with T-cells in the presence of 10 μg/mL Brefeldin A (BFA).

In some assays, DCs were incubated for 30 minutes before and throughout the antigen pulse period with Cytochalasine D (Sigma), ICP_{47} (1–35) (Millegen (Labege, France), *Pseudomonas aeruginosa* Exotoxin A (Sigma), NH_4Cl (Sigma), or Epoxomicin (Sigma).

1.10^5 pulsed-DCs were co-cultured for 6 h with the 10C10 clone using 1.10^5 T-cells per well, in a final volume of 100 μL of RPMI containing 8% human serum and 10 μg/ml brefeldin A (Sigma, St Louis MO, USA). The DC/T cell ratio was 1:1.

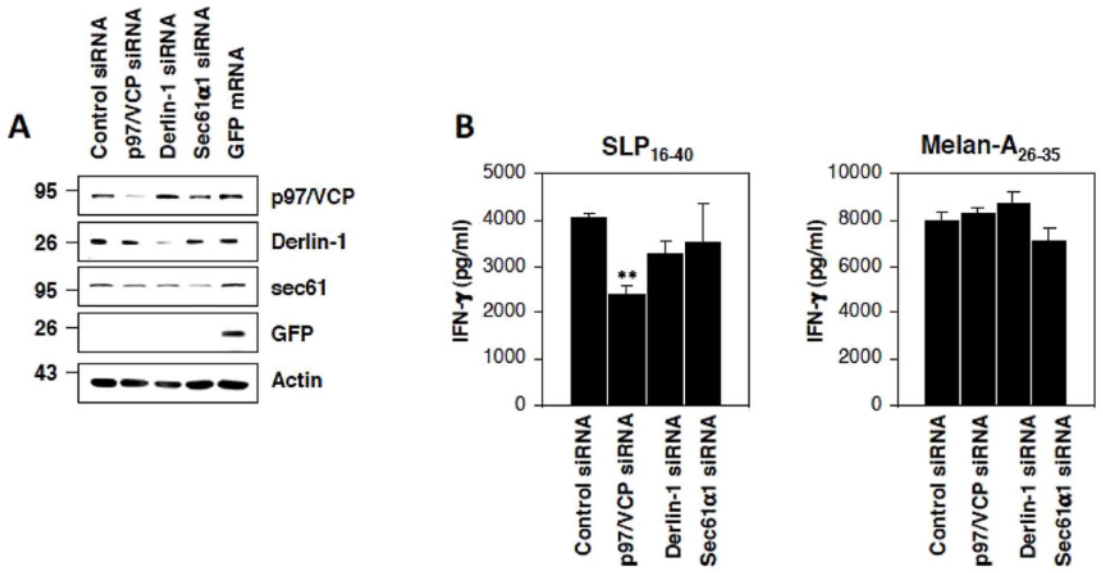

Figure 9. Gene silencing of the ERAD-related component p97/VCP substantially impairs cross-presentation of the SLP16–40. (A) Day5-immature HLA-A2+ DC were electroporated with 1 μM of either control siRNA or siRNA against p97/VCP, Derlin-1 or Sec61a1, as indicated. The steady-state protein level of each of the targeted gene was determined by western-blot analysis 72 hours later. To control for equal loading, samples were subjected to western blotting using the anti-b-actin antibody. (B) The Melan-A26–35 CTL response against siRNAtreated DC loaded with either 10 μM of SLP16–40 or 1 μM of Melan-A26–35 (as a positive control) was examined using an IFN-γ ELISA. All data are shown as means +/− SD and are representative of three independent experiments. **p<0.01 (t-Test).
doi:10.1371/journal.pone.0089897.g009

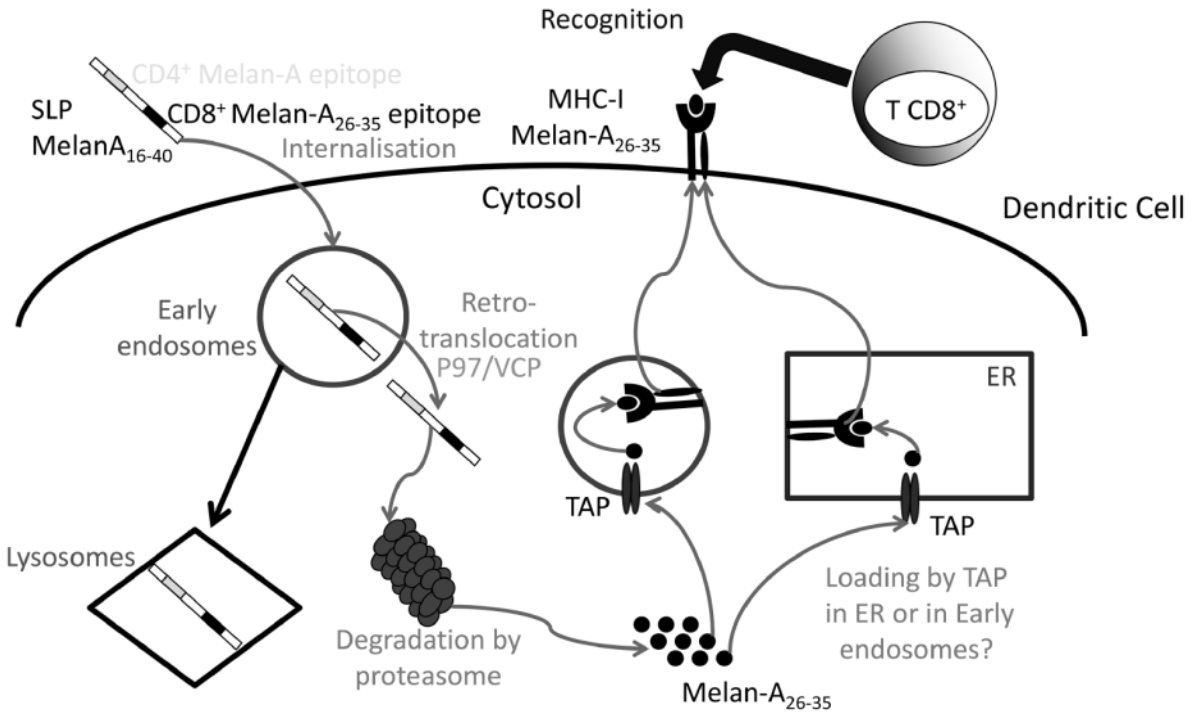

Figure 10. Putative cross-presentation mechanisms of SLP Melan-A$_{16–40}$.
doi:10.1371/journal.pone.0089897.g010

siRNA Transfection of DC

ON-TARGET plus SMART pool of interfering RNA (Dharmacon) were used to knock down p97/VCP (L-008727-00), sec61A1 (L-021503-00), Derlin-1 (E-010733-00), β1i (L-006023-00), β2i (L-006019-00) and β5i (L-006022-00). ON-TARGET plus nontargeting pool of siRNA with random nucleotides (D-001810-10) was used in each experiment as a negative control. For siRNA transfection, 4.10^7 cells were resuspended in 100 µl Opti-MEM without phenol red (Invitrogen) and transferred into a 4-mm electroporation cuvette (Biorad) with 1000 nmol siRNA duplex. The electroporator (Genepulser, Biorad) used a square-wave pulse of 500 V for 1 ms. Cells were then immediately transferred into 4 ml of MoDCs medium.

Confocal Microscopy

The mouse IgG1-mAb used in confocal microscopy were anti-HLA class-I (W6–32, produced in our laboratory), anti-GM130, anti-EEA-1, anti-LAMP-1 and anti-calreticulin (Becton Dickinson), that target respectively HLA-A,B,C and the following subcellular compartments - Golgi apparatus, early endosomes, lysosomes and ER.

DCs were pulsed for 0–48 h with SLP Melan-$A_{16–40}$ FITC (10 µM) in MoDCs maturation medium. Following the pulse, DCs were fixed in a solution of 2% formaldehyde (Sigma) and stained at room temperature for 2 h either by anti-HLA or, after permeabilization in a solution of PBS containing 0.05% triton X100 and 0.05% Tween, by the mouse IgG1-mAb, anti-GM130, anti-EEA-1, anti-LAMP-1 or anti-calreticulin. Cells were washed 3 times in PBS and secondary Alexa-568 anti-mouse IgG1 (Invitrogen) was used as detection reagent. Cells were washed and nuclei were visualized with DRAQ 5 (AXXORA). Isotype control antibodies were used in all confocal microscopy experiments to confirm specificity of antibody staining. Coverslips were mount in prolong gold antifade reagent (Invitrogen) and examined with confocal microscopy. Z-series of multiple images were acquired from DCs representative of most cells in each culture.

Cell fluorescence was visualized by confocal microscopy using a NIKON A1, R, SI instrument with APO VC, X60 NA: 1,4 oil immersion objective. An argon laser at 488 nm and diode laser at 561 nm excited the fluorescence of FITC and Alexa 568 respectively; fluorescence emission was collected respectively at 525/15 for FITC and 590/15 for Alexa-568. All images were acquired at a size of 1024 pixel by 1024 pixel and had a lateral resolution of 0.21 µm by pixel. Z-step numbers and rank were chosen according to Nyquist theorem where Z = 1/3 FWHM (Full Width at Half Maximum): typically 0.25 µm for Z-range.

For analysis, Image J software was used. Colocalization volumes were calculated with the 3D object counter plugin [28].

Quantitation of the colocalization of $SLP_{16–40}$ with the different subcellular compartments (Golgi apparatus, early endosomes, lysosomes or ER) was performed by calculating the Pearson correlation coefficient, Rr, using Volocity software (Version 6.1.1 from PerkinElmer Life Sciences). An Rr value of 1 indicates complete colocalization, an Rr value of 0 indicates no specific colocalization, and an Rr value of −1 indicates a perfect but inverse correlation (exclusion). The green and red fluorescence have been determined by performing thresholding using the 3D object counter plugin default threshold method.

Statistical Analysis

For the analysis of experimental data, quantitative data was compared by the Mann-Whitney U test (Graph Pad Prism 5).

Results

Efficient Cross-presentation of SLP Melan-$A_{16–40}$ FITC Peptides by DC

In previous studies, others and we showed that the $SLP_{15–40}$ or $SLP_{16–40}$ are cross-presented by DC [25,29]. To study the cellular mechanisms involved in cross-presentation of the analog long peptide Melan-$A_{16–40}$ A27L, a SLP, which includes the 10-mer Melan-A/Mart-$1_{26–35}$ epitope, was synthesized and coupled with FITC either to the N-terminus (FITC-$SLP_{16–40}$) or to the C-terminus ($SLP_{16–40}$-FITC). Previous results showed that fixed DC pulsed with $SLP_{16–40}$ were unable to stimulate a CTL clone specific for Melan-A/MART-$1_{26–35}$. In order to investigate the impact of FITC addition on cross-presentation, HLA-A2 DCs were incubated with different SLP ($SLP_{16–40}$, FITC-$SLP_{16–40}$, $SLP_{16–40}$-FITC) for 3 hours. Then the 10C10 CTL clone was added for 5 hours. Cross-presentation by DC of $SLP_{16–40}$ was evaluated by the IFNγ response of the T-cell clone. As shown in Figure 1, $SLP_{16–40}$-FITC was cross-presented by DCs as efficiently as its non-labeled analogue. In contrast, FITC-$SLP_{16–40}$ did not induce a response in the 10C10 clone and therefore was not cross-presented (data not shown). We thus used $SLP_{16–40}$-FITC to study the intracellular pathway involved in SLP cross-presentation.

Visualization of $SLP_{16–40}$-FITC Internalization by DCs

In order to visualize the routing of $SLP_{16–40}$, DCs were pulsed with $SLP_{16–40}$-FITC for different times, then fixed and stained with mAbs specific for MHC class-I molecules (W6–32) and a DNA dye specific for the nucleus (Draq5). As shown in Figure 2, $SLP_{16–40}$-FITC internalization was detectable in DC as early as 15 minutes after the pulse by monitoring the FITC tag. Using Immunofluorescence confocal microscopy, we observed that DCs exhibit morphology typical of intermediate-stage DCs, with most cells having a rounded shape (Fig. 2). Thereafter, we visualized a progressive internalization and accumulation of $SLP_{16–40}$-FITC in DCs between 15 min and 180 min of pulse-chase. These results demonstrate that $SLP_{16–40}$ labeled with FITC is efficiently detectable in DCs by confocal microscopy and the signal persists during its intracellular routing.

Specific Routing of $SLP_{16–40}$ toward Early Endosomes and Lysosomes

To define the intracellular routing, we incubated DCs for different periods of times (0 to 120 minutes) with $SLP_{16–40}$-FITC and then stained DCs intracellularly with antibody to early endosomes (anti-EEA-1, Fig. 3A) or lysosomes (anti-LAMP-1, Fig. 3B). Between 15 and 60 minutes after $SLP_{16–40}$-FITC incubation, DCs showed strong colocalization between $SLP_{16–40}$ and early endosomes (Fig. 3A). After this period, no colocalization could be observed with this compartment (Fig. 3A). Concerning lysosomes, colocalization started at 30 minutes until 120 minutes (Fig. 3B), thus, we propose that $SLP_{16–40}$ could be redirected from endosomes to lysosomes. No colocalization was detectable between $SLP_{16–40}$-FITC and the Golgi apparatus (anti-GM130) or the ER (anti-calreticulin) (Fig. 4). Altogether, our results indicate that $SLP_{16–40}$ was internalized by DCs in early endosomes and later reached the lysosomes.

Kinetics of Internalization of $SLP_{16–40}$ in DCs

To address more precisely the localization of $SLP_{16–40}$ in DCs, we analyzed confocal microscopy images of each cell with the Image J 3D cell counter plugin. This application allows the measurement of the colocalization volume defined by the overlap

of the green fluorescent object ($SLP_{16–40}$) with the red fluorescent object (intracellular compartment) in the whole cell. To this end, we defined a threshold of no colocalization with the endoplamic reticulum staining (Fig. 5A).

We evaluated the colocalization volume for early endosome and lysosome (Fig. 5B). Between 5 and 30 minutes, SLP-$FITC_{16–40}$ colocalization was high in early endosomes and weak in lysosomes. Between 30 and 120 minutes, the trend reversed and the colocalization seemed to increase in lysosomes. Moreover, we observed that $SLP_{16–40}$-FITC accumulated in lysosomes from 30 to 120 minutes post-pulse.

Quantitation of $SLP_{16–40}$-FITC colocalized with early endosomes, lysosomes, ER and Golgi apparatus was measured by the Pearson correlation coefficient (Rr value). Rr values indicate specific partial colocalization of $SLP_{16–40}$ with early endosomes between 5 and 60 minutes and with lysosomes between 45 and 120 minutes (Figure 5C). This demonstrates that the volumes of detected colocalization represent the specific colocalization between the $SLP_{16–40}$ and this two subcellular compartments rather then a juxtaposition of fluorescence. On the other hand, Rr values indicate no specific colocalization of $SLP_{16–40}$ with the ER or Golgi apparatus, in accordance with microscopy images displayed.

Overall, these data suggest that $SLP_{16–40}$ is rapidly internalized by DCs in early endosomes, and then redirected to the lysosomes where it accumulates.

Proteasomal Processing of $SLP_{16–40}$

Various proteases may be involved in the processing of $SLP_{16–40}$. In DCs, the proteasome is involved in generation of many MHC-I epitopes from endogenous proteins (endogenous pathway) but also from exogenous proteins during cross-presentation [30]. The standard proteasome and the immunoproteasome are multimeric complexes characterized by the catalytic subunits (β1, β2, β5) and (β1i, β2i, β5i) respectively. Apart from the standard proteasome, there are at least three subtypes of immunoproteasome: two intermediate proteasomes (β5i and β1i, β5i) and the classical immunoproteasome [31]. We found that DCs used in the present study essentially expressed the immunoproteasome or intermediate proteasomes because few subunits of standard proteasome were detectable (Fig. 6A).

To assess whether early cross presentation of $SLP_{16–40}$ by DCs requires proteasome degradation for presentation, we used epoxomicin. This drug is a highly specific, and irreversible inhibitor of the chymotrypsin-like (CT-L), trypsin-like (T-L), and peptidyl-glutamyl peptide hydrolyzing (PGPH) activities of the proteasome which modifies the proteasomal catalytic subunits β5i, β2i, β5 and β2 [32] DCs were preincubated with different doses of epoxomicin (1 and 5 μM) then incubated with $SLP_{16–40}$. Epoxomicin strongly inhibits the DC cross-presentation capacity in a dose dependent manner (Fig. 6B) but had no effect on the exogenous presentation of synthetic 10-mer epitope Melan-A/Mart-$1_{26–35}$.

To better understand the role of immunoproteasomes in this process, DC with a knockdown of any one of the three inducible subunits β1i, β2i or β5i were fed with $SLP_{16–40}$ for 3 h prior to a 16-hour CTL assay in the presence of the 10C10 clone. As shown in Fig. 7A, gene silencing via specific siRNA was efficiently achieved at the protein level for each of the inducible subunits within 72 h of transfection. Of note, β1i depletion was accompanied by a slight but significant decreased expression of both β1i and β2i. This result is in agreement with previous studies showing that β5i incorporation is a prerequisite for β1i incorporation which, itself, is required for maintaining normal levels of β2i [33]. In addition, knockdown of β5i resulted in increased expression of its standard subunit counterpart β5 but also, albeit to a smaller extent, of β2. Similarly, targeted disruption of either β1i or β2i caused an up-regulation of both of the standard subunits β1 and β2.

However, and in spite of the up-regulation of at least any of two out of three standard subunits in DC treated with a knockdown of anyone of the three inducible subunits, no major change in $SLP_{16–40}$ cross-presentation could be observed (Fig. 7B). These results indicate that the generation of the Melan-$A_{26–35}$ peptide from $SLP_{16–40}$ in DC for cross-presentation occurs independently of the proteasomal subunit composition.

Cross-presentation of $SLP_{16–40}$ is Dependent on Functional TAP Transport

In the cytosol, the antigens degraded into peptides are transported into the ER or ER phagosome-like compartments via the transporter associated with antigen processing (TAP) for loading onto MHC class I molecules. To investigate whether TAP was involved in the cross-presentation of $SLP_{16–40}$, we used a synthetic peptide corresponding to the N-terminal 35 amino acid residues (ICP_{47} (1–35)), that can reach the cytosol and block TAP only in cells of DC lineage [34]. DCs were preincubated with ICP_{47} (1–35) and cocultured for 3 hours with $SLP_{16–40}$. We showed that ICP_{47} (1–35) decreased cross-presentation of $SLP_{16–40}$ by DCs (Fig. 8A) with a slight but no statistically significant, inhibitory effect on the exogenous presentation of synthetic 9-mer epitope Melan-A/Mart-$1_{26–35}$. These findings suggest that TAP play a role in cross-presentation of peptide from $SLP_{16–40}$ in cytosol.

$SLP_{16–40}$ Cross-presentation Depends on Early Endosomes and Retrotranslocation Machinery

To define more precisely the compartments involved in $SLP_{16–40}$ cross-presentation by DCs, we incubated DCs for 3 hours with $SLP_{16–40}$ in the presence or absence of various inhibitors. First, to elucidate the potential lysosomal involvement in cross-presentation, we used NH_4Cl, an inhibitor of lysosome acidification and maturation of early endosomes into lysosomes [35]. As shown in Fig. 8B, NH_4Cl treatment increased antigen cross-presentation of $SLP_{16–40}$ without modifying the exogenous presentation of synthetic 10-mer epitope Melan-A/Mart-$1_{26–35}$. The increased cross-presentation is likely due to an accumulation of $SLP_{16–40}$ in early endosomes due to the inhibition by NH_4Cl. These results suggest that lysosomes do not participate in $SLP_{16–40}$ cross presentation and points out a role for early endosomes in cross-presentation.

Following its internalization in early endosomes, translocation of $SLP_{16–40}$ to the cytosol is required for subsequent degradation by cytosolic proteases and/or the proteasome [8]. It has been shown that such transport across the endosomal membrane can be achieved via the ER-associated degradation pathway (ERAD) [34,36]. Indeed, the ERAD machinery normally and usually allows the retro-translocation of misfolded proteins from the ER back to the cytosol, a process that is thought to be mediated by the channels sec61 and/or Derlin-1 as well as the AAA-ATPase p97/VCP [37,38]. Because sec61 is expressed on early endosomes [39] and might play a role in antigen translocation [40,41], we next sought to determine the contribution of this protein to $SLP_{16–40}$ cross-presentation using the sec61 inhibitor Exotoxin A (Exo A). As shown in Fig. 8C, the use of this inhibitor tended to decrease slightly the cross-presentation of $SLP_{16–40}$ but this decrease was not significant.

In an attempt to generate a more specific and reliable blockade of the ERAD pathway in DC, we generated knockdown DC for each of the three above-mentioned ERAD factors (i.e., p97/VCP, Derlin-1 and sec61a1). To this end, DC were treated with siRNA targeting p97/VCP, Derlin-1 or sec61a1 for three days followed by a 3-hour pulse of either $SLP_{16–40}$ or Melan-$A_{26–35}$ prior to a 16-hour CTL recognition assay in the presence of the 10C10 clone. As shown in Fig. 9A, treatment of DC with any of the above-mentioned siRNA resulted in significant diminished expression of the corresponding protein within 72 h of transfection. Interestingly, from the three ERAD components tested, only p97/VCP was found to significantly impair $SLP_{16–40}$ cross-presentation (Fig. 9B). Taken together, these data show that the $SLP_{16–40}$ is internalized in early endosomes where it is translocated into the cytoplasm by a retro-translocation complex involving p97/VCP.

Discussion

The aim of this study was to characterize the SLP cross-presentation pathway in DCs. We selected for the present *in vitro* study a 25-mer sequence of the Melan-A/MART-1 melanoma associated antigen bearing an anchor optimized analog of the immunodominant $CD8^+$ epitope (epitope of Melan-A: Melan-$A_{26–35}$ A27L on HLA-A2) [22].

Our principal results concerning $SLP_{16–40}$ cross-presentation are summarized in Figure 10: $SLP_{16–40}$ is internalized by DCs into early endosomes. Part of it is directed into the lysosomal compartment. The remainder is exported into the cytoplasm by a retrotranslocation complex involving p97/VCP. In the cytoplasm, $SLP_{16–40}$ is processed by the proteasome and the resulting Melan-A peptide fragment is reimported by TAP into the endosomal or ER compartment for loading onto MHC class I molecules. Inhibition of lysosome acidification increased Melan-$A_{26–35}$ epitope generation, in contrast to the effect previously documented by Fonteneau et al., for a different antigen: influenza matrix protein [42]. This pathway is a mix between the "endocytic" and "cytosolic" tracks proposed by Segura and Villadongos [30] and confirm the processing of SLP-OVA_{24aa} recently published for murine DCs [43].

Here, we demonstrated, by using inhibitors and confocal microscopy that $SLP_{16–40}$ is endocytosed by DCs and routed to early endosomes. The results showed that $SLP_{16–40}$ was internalized very quickly after DC contact (15 to 30 minutes). Later on, specific colocalization of peptide with endosomes decreased and then disappeared from 60 minutes onwards, together with the appearance of $SLP_{16–40}$ colocalization with lysosomes. The decreasing colocalization between early endosomes and $SLP_{16–40}$ over time suggests an arrest of the endocytic process. One hypothesis is that DCs rapidly internalized a large quantity of SLP reaching a maximum and perhaps preventing supplemental endocytosis during the 3 h incubation with this 25-mer.

We observed a temporal correlation of colocalization between early endosomes and lysosomes (Fig. 4). This suggests that, after internalization, SLP is routed into early endosomes then redirected to and accumulated in lysosomes. This routing could be explained by maturation of DCs: early endosomes becomes late endosomes then lysosomes [44]. The colocalization and accumulation of $SLP_{16–40}$ in lysosomes after 60 minutes may represent an antigen storage compartment that could facilitate long-lasting cross-presentation of $SLP_{16–40}$ by DCs – the "lysosome-like organelles" proposed by other groups. [12]. Indeed, Amigorena's group has showed that DCs pulsed for 3 hours with the SLP Melan-$A_{15–40}$ allows efficient, long-lasting, cross-presentation of Melan-A/MART-1 tumor antigen on MHC class I molecules from an intracellular antigen storage compartment [29]. Furthermore, similar long-lasting cross-presentation by DCs was also observed for IgG-OVA complexes. In this case, lysosome like organelles were shown to be the intracellular storage compartment allowing long-term presentation of MHC class I/peptide complexes [12]. Otherwise, lysosomes are involved in generation of $CD4^+$ T-cell epitopes to produce the MHC-II/peptide complex at the cell surface for activation of $CD4^+$ T lymphocytes. Activated $CD4^+$ T cells can promote inflammation, cooperate in the induction of $CD8^+$ T effectors and memory cells, and provide help for B cells to produce anti-tumor antibodies. As the $SLP_{16–40}$ contains potential $CD4^+$ T-cell epitopes, SLP storage in lysosomes could also permit the activation of $CD4^+$ T cell responses.

By using cytochalasin D that inhibits actin polymerization, we prevented cross-presentation, suggesting that internalization and possibly processing of $SLP_{16–40}$ require cytoskeletal actin rearrangement (data not shown). Receptor mediated endocytosis and macropinocytosis are efficient mechanisms that can guide exogenous antigens into the MHC class I and II presentation pathway in DCs [9] but this remains to be elucidated. As proposed by Quakkelaar and Melief, it could be interesting to experiment the coupling of SLP to adjuvants like TLR ligands or receptor specific ligands in order to reinforce internalization, cross-presentation and the induction of specific T cell responses by SLP [45].

Although various mechanisms have been proposed to explain cross-presentation, the route used by internalized antigens to gain access to the cytosol for proteasomal degradation remains elusive. Over the past few years, an increasing number of a studies point to a critical role of the ER-associated degradation pathway (ERAD) in this process [34,41,46]. The ERAD pathway is a conserved multistep process that normally ensures the transfer of misfolded proteins from the ER back to the cytoplasm for subsequent destruction by the 26S proteasome (an event also termed "retro-translocation"). To date, there is disagreement in the field with respect to identity and/or nature of the retro-translocation channel with two different protein complexes being put forward as possible candidates to fulfill this task, namely sec61 and Derlin-1 [47]. Irrespective of this concern, it now well established that all ERAD pathways converge downstream of the retro-translocation channel at p97/VCP, an AAA-ATPase responsible for "pulling" the proteins that have successfully crossed the ER membrane. Our data fully support a role for ERAD in the transport of the $SLP_{16–40}$ into the cytosol, as shown by the decreased $SLP_{16–40}$ cross-presentation observed in p97/VCP-depleted DCs (Fig. 6E).

However, in our hands, neither sec61 nor Derlin-1 gene silencing could significantly alter the $SLP_{16–40}$ cross-presentation by DC. These findings are interesting and raise the possibility of the existence of another yet unidentified channel implicated in this process. Yet, we cannot rule out a participation of Derlin-1 and/or sec61 in other DC-based cross-presentation systems when other antigen sources are applied such as full-length proteins or cell-associated antigens including apoptotic or necrotic cells. Of note, the extraction of proteins from the ER by p97/VCP requires substrate poly-ubiquitylation. Since our $SLP_{16–40}$ is a lysine-free peptide, it is conceivable that the exclusive acceptor site for poly-ubiquitylation may be represented by its N-terminus. Importantly, this implies that any blockade of the N-terminus of the $SLP_{16–40}$ would prevent its cross-presentation by DC. This assumption is supported by the observation that the N-terminally FITC-modified $SLP_{16–40}$ does not lead to the generation of the Melan-$A_{26–35}$ peptide in DC (data not shown).

In DCs, two proteasomes exist: the standard proteasome that contains the active subunits β1, β2 and β5; and the immunoproteasome, which differs only in three active subunits (the

immunosubunits β1i, β2i and β5i). Recently, the existence of additional forms of proteasomes, bearing a mixed assortment of standard and inducible catalytic subunits has been identified, which contains only one (β5i) or two (β1i and β5i) of the three inducible catalytic subunits of the immunoproteasome [31]. We were able to confirm the role of proteasomes in $SLP_{16–40}$ cross-presentation by DCs, as shown by the reduced CTL recognition observed with DC treated with epoxomicin (Fig. 5B). This mechanism is likely to involve the participation of the immunoproteasome or intermediate proteasomes, since the standard proteasome is thought to represent less than 8% of total proteasome content in mature or immature DCs [31]. This notion is further reinforced by the fact that siRNA-mediated depletion of anyone of the three inducible subunits in DC failed to influence the $SLP_{16–40}$ cross-presentation (Fig. 5D). Indeed, because the down-regulation of any of the three inducible subunits is accompanied by the reciprocal up-regulation of at least two standard subunits (Fig. 5C), our data tend to imply that standard, mixed-type and immunoproteasomes are equivalent in the generation of the Melan-$A_{26–35}$ peptide from the $SLP_{16–40}$.

This result seems to contradict previous results in which the antigenic peptide Melan-$A_{26–35}$ was generated by the standard proteasome but not by the immunoproteasome [48,49]. This discrepancy could be explained by the fact that we used a cellular model with DCs, which could represent a more complex system than purified proteasome or immunoproteasome. Many cytosolic proteases are present in DCs and using a cellular model, Melief's group has recently described the role of a cytosolic peptidase (thimet oligopeptidase) in the generation of the Melan-A/MART-1 epitope [50]. Also we could not exclude the role of cytokines in the modulation of proteasome activity in DCs [51]. Finally in the present work we evaluated the processing of Melan-A epitope via the cross-presentation pathway. Others and we have already described the cross-presentation of Melan-A peptide by DCs [25,29,51]. This result may reflect that cross-presentation process could have some differences in the generation of the Melan-A peptide in comparison with the endogenous pathway.

We have demonstrated the necessity of TAP for the cross-presentation of $SLP_{16–40}$. The TAP transporter is expressed both in early endosomes and the ER. The use of US6 or US6 chemically linked to transferrin [10] could help to discriminate between these two potential locations.

Altogether, many vaccination strategies have been used to enhance antitumor responses by exploiting the cross-presentation capacities of DCs. Recently a very encouraging clinical trial for patients with SLP vaccination was published [18]. This work underlines the therapeutic potential of SLP vaccination, which is characterized by the following advantages: easy manufacturing and easy immune monitoring as SLP contain few T cell epitope. Understanding SLP cross-presentation by DCs should contribute to the development and optimization of this immunotherapy technology.

Acknowledgments

The authors thank D. McIlroy, Dr E. Segura, and Dr. J-F. Fonteneau for carefully reading the manuscript.

Author Contributions

Conceived and designed the experiments: JM FE PH YG. Performed the experiments: JM FE RO AL YG. Analyzed the data: JM FE PH SN FJ YG. Contributed reagents/materials/analysis tools: PH ED PMK. Wrote the paper: JM FE PH PMK FJ YG.

References

1. Coley WB (1928) End Results in Hodgkin's Disease and Lymphosarcoma Treated by the Mixed Toxins of Erysipelas and Bacillus Prodigiosus, Alone or Combined with Radiation. Ann Surg 88: 641–667.
2. Restifo NP, Dudley ME, Rosenberg SA (2012) Adoptive immunotherapy for cancer: harnessing the T cell response. Nat Rev Immunol 12: 269–281.
3. Boon T, Cerottini JC, Van den Eynde B, van der Bruggen P, Van Pel A (1994) Tumor antigens recognized by T lymphocytes. Annu Rev Immunol 12: 337–365.
4. Melief CJ (2008) Cancer immunotherapy by dendritic cells. Immunity 29: 372–383.
5. Steinman RM, Banchereau J (2007) Taking dendritic cells into medicine. Nature 449: 419–426.
6. Bevan MJ (2006) Cross-priming. Nat Immunol 7: 363–365.
7. Ackerman AL, Cresswell P (2004) Cellular mechanisms governing cross-presentation of exogenous antigens. Nat Immunol 5: 678–684.
8. Joffre OP, Segura E, Savina A, Amigorena S (2012) Cross-presentation by dendritic cells. Nature reviews Immunology 12: 557–569.
9. Burgdorf S, Kurts C (2008) Endocytosis mechanisms and the cell biology of antigen presentation. Curr Opin Immunol 20: 89–95.
10. Burgdorf S, Scholz C, Kautz A, Tampe R, Kurts C (2008) Spatial and mechanistic separation of cross-presentation and endogenous antigen presentation. Nat Immunol 9: 558–566.
11. Guermonprez P, Saveanu L, Kleijmeer M, Davoust J, Van Endert P, et al. (2003) ER-phagosome fusion defines an MHC class I cross-presentation compartment in dendritic cells. Nature 425: 397–402.
12. van Montfoort N, Camps MG, Khan S, Filippov DV, Weterings JJ, et al. (2009) Antigen storage compartments in mature dendritic cells facilitate prolonged cytotoxic T lymphocyte cross-priming capacity. Proc Natl Acad Sci U S A 106: 6730–6735.
13. Baxevanis CN, Perez SA, Papamichail M (2009) Cancer immunotherapy. Crit Rev Clin Lab Sci 46: 167–189.
14. Steinman RM, Pope M (2002) Exploiting dendritic cells to improve vaccine efficacy. J Clin Invest 109: 1519–1526.
15. Melief CJ, van der Burg SH (2008) Immunotherapy of established (pre)malignant disease by synthetic long peptide vaccines. Nat Rev Cancer 8: 351–360.
16. Bijker MS, van den Eeden SJ, Franken KL, Melief CJ, van der Burg SH, et al. (2008) Superior induction of anti-tumor CTL immunity by extended peptide vaccines involves prolonged, DC-focused antigen presentation. Eur J Immunol 38: 1033–1042.
17. Bijker MS, van den Eeden SJ, Franken KL, Melief CJ, Offringa R, et al. (2007) CD8+ CTL priming by exact peptide epitopes in incomplete Freund's adjuvant induces a vanishing CTL response, whereas long peptides induce sustained CTL reactivity. J Immunol 179: 5033–5040.
18. Kenter GG, Welters MJ, Valentijn AR, Lowik MJ, Berends-van der Meer DM, et al. (2009) Vaccination against HPV-16 oncoproteins for vulvar intraepithelial neoplasia. N Engl J Med 361: 1838–1847.
19. Leffers N, Lambeck AJ, Gooden MJ, Hoogeboom BN, Wolf R, et al. (2009) Immunization with a P53 synthetic long peptide vaccine induces P53-specific immune responses in ovarian cancer patients, a phase II trial. Int J Cancer 125: 2104–2113.
20. Speetjens FM, Kuppen PJ, Welters MJ, Essahsah F, Voet van den Brink AM, et al. (2009) Induction of p53-specific immunity by a p53 synthetic long peptide vaccine in patients treated for metastatic colorectal cancer. Clin Cancer Res 15: 1086–1095.
21. Welters MJ, Kenter GG, Piersma SJ, Vloon AP, Lowik MJ, et al. (2008) Induction of tumor-specific CD4+ and CD8+ T-cell immunity in cervical cancer patients by a human papillomavirus type 16 E6 and E7 long peptides vaccine. Clin Cancer Res 14: 178–187.
22. Valmori D, Fonteneau JF, Lizana CM, Gervois N, Liénard D, et al. (1998) Enhanced generation of specific tumor-reactive CTL in vitro by selected Melan-A/MART-1 immunodominant peptide analogues. J Immunol 160: 1750–1758.
23. Kawakami Y, Eliyahu S, Sakaguchi K, Robbins PF, Rivoltini L, et al. (1994) Identification of the immunodominant peptides of the MART-1 human melanoma antigen recognized by the majority of HLA-A2-restricted tumor infiltrating lymphocytes. J Exp Med 180: 347–352.
24. Castelli C, Storkus WJ, Maeurer MJ, Martin DM, Huang EC, et al. (1995) Mass spectrometric identification of a naturally processed melanoma peptide recognized by CD8+ cytotoxic T lymphocytes. The Journal of experimental medicine 181: 363–368.
25. Chauvin JM, Larrieu P, Sarrabayrouse G, Prevost-Blondel A, Lengagne R, et al. (2012) HLA anchor optimization of the melan-A-HLA-A2 epitope within a long peptide is required for efficient cross-priming of human tumor-reactive T cells. J Immunol 188: 2102–2110.
26. Coulais D, Panterne C, Fonteneau JF, Gregoire M (2012) Purification of circulating plasmacytoid dendritic cells using counterflow centrifugal elutriation and immunomagnetic beads. Cytotherapy 14: 887–896.
27. Vignard V, Lemercier B, Lim A, Pandolfino MC, Guilloux Y, et al. (2005) Adoptive transfer of tumor-reactive Melan-A-specific CTL clones in melanoma

patients is followed by increased frequencies of additional Melan-A-specific T cells. J Immunol 175: 4797–4805.
28. Bolte S, Cordelieres FP (2006) A guided tour into subcellular colocalization analysis in light microscopy. J Microsc 224: 213–232.
29. Faure F, Mantegazza A, Sadaka C, Sedlik C, Jotereau F, et al. (2009) Long-lasting cross-presentation of tumor antigen in human DC. Eur J Immunol 39: 380–390.
30. Segura E, Villadangos JA (2011) A modular and combinatorial view of the antigen cross-presentation pathway in dendritic cells. Traffic 12: 1677–1685.
31. Guillaume B, Chapiro J, Stroobant V, Colau D, Van Holle B, et al. (2010) Two abundant proteasome subtypes that uniquely process some antigens presented by HLA class I molecules. Proc Natl Acad Sci U S A 107: 18599–18604.
32. Meng L, Mohan R, Kwok BH, Elofsson M, Sin N, et al. (1999) Epoxomicin, a potent and selective proteasome inhibitor, exhibits in vivo antiinflammatory activity. Proceedings of the National Academy of Sciences of the United States of America 96: 10403–10408.
33. Groettrup M, Standera S, Stohwasser R, Kloetzel PM (1997) The subunits MECL-1 and LMP2 are mutually required for incorporation into the 20S proteasome. Proceedings of the National Academy of Sciences of the United States of America 94: 8970–8975.
34. Ackerman AL, Giodini A, Cresswell P (2006) A role for the endoplasmic reticulum protein retrotranslocation machinery during crosspresentation by dendritic cells. Immunity 25: 607–617.
35. Hotta C, Fujimaki H, Yoshinari M, Nakazawa M, Minami M (2006) The delivery of an antigen from the endocytic compartment into the cytosol for cross-presentation is restricted to early immature dendritic cells. Immunology 117: 97–107.
36. Zehner M, Chasan AI, Schuette V, Embgenbroich M, Quast T, et al. (2011) Mannose receptor polyubiquitination regulates endosomal recruitment of p97 and cytosolic antigen translocation for cross-presentation. Proc Natl Acad Sci U S A 108: 9933–9938.
37. Claessen JH, Kundrat L, Ploegh HL (2012) Protein quality control in the ER: balancing the ubiquitin checkbook. Trends in cell biology 22: 22–32.
38. Liu Y, Ye Y (2011) Proteostasis regulation at the endoplasmic reticulum: a new perturbation site for targeted cancer therapy. Cell research 21: 867–883.
39. Ramanathan HN, Ye Y (2012) The p97 ATPase associates with EEA1 to regulate the size of early endosomes. Cell Res 22: 346–359.
40. Crespo MI, Zacca ER, Nunez NG, Ranocchia RP, Maccioni M, et al. (2013) TLR7 triggering with polyuridylic acid promotes cross-presentation in CD8alpha+ conventional dendritic cells by enhancing antigen preservation and MHC class I antigen permanence on the dendritic cell surface. Journal of immunology 190: 948–960.
41. Imai J, Hasegawa H, Maruya M, Koyasu S, Yahara I (2005) Exogenous antigens are processed through the endoplasmic reticulum-associated degradation (ERAD) in cross-presentation by dendritic cells. International immunology 17: 45–53.
42. Fonteneau JF, Kavanagh DG, Lirvall M, Sanders C, Cover TL, et al. (2003) Characterization of the MHC class I cross-presentation pathway for cell-associated antigens by human dendritic cells. Blood 102: 4448–4455.
43. Rosalia RA, Quakkelaar ED, Redeker A, Khan S, Camps M, et al. (2013) Dendritic cells process synthetic long peptides better than whole protein, improving antigen presentation and T-cell activation. European journal of immunology 43: 2554–2565.
44. Pillay CS, Elliott E, Dennison C (2002) Endolysosomal proteolysis and its regulation. Biochem J 363: 417–429.
45. Quakkelaar ED, Melief CJ (2012) Experience with synthetic vaccines for cancer and persistent virus infections in nonhuman primates and patients. Adv Immunol 114: 77–106.
46. Giodini A, Rahner C, Cresswell P (2009) Receptor-mediated phagocytosis elicits cross-presentation in nonprofessional antigen-presenting cells. Proceedings of the National Academy of Sciences of the United States of America 106: 3324–3329.
47. Needham PG, Brodsky JL (2013) How early studies on secreted and membrane protein quality control gave rise to the ER associated degradation (ERAD) pathway: The early history of ERAD. Biochimica et biophysica acta.
48. Morel S, Levy F, Burlet-Schiltz O, Brasseur F, Probst-Kepper M, et al. (2000) Processing of some antigens by the standard proteasome but not by the immunoproteasome results in poor presentation by dendritic cells. Immunity 12: 107–117.
49. Chapatte L, Ayyoub M, Morel S, Peitrequin AL, Levy N, et al. (2006) Processing of tumor-associated antigen by the proteasomes of dendritic cells controls in vivo T-cell responses. Cancer Res 66: 5461–5468.
50. Kessler JH, Khan S, Seifert U, Le Gall S, Chow KM, et al. (2011) Antigen processing by nardilysin and thimet oligopeptidase generates cytotoxic T cell epitopes. Nat Immunol 12: 45–53.
51. Lattanzi L, Rozera C, Marescotti D, D'Agostino G, Santodonato L, et al. (2011) IFN-alpha boosts epitope cross-presentation by dendritic cells via modulation of proteasome activity. Immunobiology 216: 537–547.

4.4. Critical role of the ERAD protein p97/VCP in MHC class I presentation of epitopes arising from membrane-spanning tumor antigens (this chapter is based on the works of Ebstein and coworkers (Ebstein et al., 2016a; Ebstein et al., 2016b))

Antitumor T-cell therapies rely on the ability of tumor cells to efficiently process target antigens by the UPS. As such, any impairment of the MHC class I antigen presentation machinery may potentially lead to failure of such therapies. Accordingly, the capacity of tumor cells to escape the immune system may serve as a basis for the identification of so far unknown critical components of the MHC class I antigen presentation pathway. The Melan-A/MART-1 protein is a well-known membrane-bound antigen mostly found in melanosomes of melanoma cells which gives rise to the Melan-A/MART-1_{26-35} epitope. In this work, we generated and isolated melanoma cell clones resistant to Melan-A/MART-1_{26-35} cytotoxic T cell (CTL)-mediated cytolysis by exposing melanoma cells repeatedly to Melan-A/MART-1_{26-35} CTL. Analysis of these resistant melanoma cell clones revealed a defect in the expression of the ERAD-related ubiquitin-binding protein p97/VCP. Re-expression of p97/VCP in such resistant melanoma cell clones completely restored immune recognition by CTL, confirming that p97/VCP is a critical component of the Melan-A/MART-1_{26-35} MHC class I antigen processing pathway. Interestingly, a p97/VCP-dependency was also observed for the presentation of a spliced $gp100_{47-52/40-42}$ epitope emerging from the gp100 melanoma antigen which shares the same topology of melanosome localization. In conclusion, our data highlight a critical for the p97/VCP in the supply of MHC class I-restricted peptides arising from membrane-spanning tumor antigens.

SCIENTIFIC REPORTS

OPEN

Exposure to Melan-A/MART-1_{26-35} tumor epitope specific $CD8^{+}$T cells reveals immune escape by affecting the ubiquitin-proteasome system (UPS)

Received: 18 December 2015
Accepted: 12 April 2016
Published: 04 May 2016

Frédéric Ebstein[1,*], Martin Keller[1,*], Annette Paschen[2], Peter Walden[3], Michael Seeger[1], Elke Bürger[1], Elke Krüger[1], Dirk Schadendorf[2], Peter- M. Kloetzel[1,5] & Ulrike Seifert[1,4]

Efficient processing of target antigens by the ubiquitin-proteasome-system (UPS) is essential for treatment of cancers by T cell therapies. However, immune escape due to altered expression of IFN-γ-inducible components of the antigen presentation machinery and consequent inefficient processing of HLA-dependent tumor epitopes can be one important reason for failure of such therapies. Here, we show that short-term co-culture of Melan-A/MART-1 tumor antigen-expressing melanoma cells with Melan-A/MART-1_{26-35}-specific cytotoxic T lymphocytes (CTL) led to resistance against CTL-induced lysis because of impaired Melan-A/MART-1_{26-35} epitope processing. Interestingly, deregulation of p97/VCP expression, which is an IFN-γ-independent component of the UPS and part of the ER-dependent protein degradation pathway (ERAD), was found to be essentially involved in the observed immune escape. In support, our data demonstrate that re-expression of p97/VCP in Melan-A/MART-1_{26-35} CTL-resistant melanoma cells completely restored immune recognition by Melan-A/MART-1_{26-35} CTL. In conclusion, our experiments show that impaired expression of IFN-γ-independent components of the UPS can exert rapid immune evasion of tumor cells and suggest that tumor antigens processed by distinct UPS degradation pathways should be simultaneously targeted in T cell therapies to restrict the likelihood of immune evasion due to impaired antigen processing.

The generation of antitumor cytotoxic T cell (CTL) response involves the processing and presentation of tumor antigens onto MHC class I molecules[1,2]. These specialized T cells can detect target cells that endogenously express protein molecules (i.e. mutated, over-expressed and/or tissue differentiation antigens) and subsequently remove these cells from the body[3,4]. The vast majority of peptides presented by MHC class I molecules at the cell surface for recognition by specific cytotoxic T-cells (CTL) is generated by the ubiquitin-proteasome system (UPS) with its central multicatalytic proteinase complex, the proteasome[5,6]. Peptides generated by the proteasome system are transported by TAP proteins (transporter associated with antigen presentation) into the ER where peptides of appropriate length and affinity will bind to MHC class I proteins to be presented at the cell surface for immune recognition by CTL[7–9].

The standard 20S proteasome (s-20S proteasome) with its active site β-subunits β1, β2 and β5 represents the central catalytic unit of the UPS and the catalytic core of the 30S proteasome which is built by the association of two 19S regulator complexes with the 20S core complex. IFN-γ induces the synthesis of alternative catalytic

[1]Charité-Universitätsmedizin Berlin, Institut für Biochemie, Charité-Platz 1/ Virchowweg 6, 10117 Berlin, Germany. [2]Department of Dermatology, University Hospital, University Duisburg-Essen and German Cancer Consortium (DKTK), Hufelandstr. 55, 45122 Essen, Germany. [3]Charité-Universitätsmedizin Berlin, Klinik für Dermatologie, Venerologie und Allergologie, Charité Platz 1, 10117 Berlin, Germany. [4]Institut für Molekulare und Klinische Immunologie, Medizinische Fakultät der Otto-von-Guericke-Universität Magdeburg, Leipzigerstr. 44, 39120 Magdeburg, Germany. [5]Berlin Institute of Health Kapelle-Ufer 2 10117 Berlin, Germany. *These authors contributed equally to this work. Correspondence and requests for materials should be addressed to P.M.K. (email: p-m.kloetzel@charite.de)

immunosubunits (i-subunits), i.e. β1i/LMP2, β2i/MECL1 and β5i/LMP7 and the concomitant formation of immunoproteasome (i-proteasome) subtypes[8–10]. The 30S proteasome complexes are responsible for the degradation of proteins in the nucleus and the cytosol, which are marked for degradation by a poly-ubiquitin chain and consequently recognized by specific subunits of the 19S regulator complex. A special problem arises for the degradation and processing of membrane proteins, which are co-translationally transported into the endoplasmic reticulum (ER). These proteins, if misfolded or mutated, are re-translocated to the cytosolic side of the ER to be degraded by the 30S proteasome complex in an ubiquitin-dependent manner[11–13]. This process is called ER associated degradation pathway (ERAD) and essentially requires the so-called ERAD-complex within the ER-membrane. This complex is composed of a number of different proteins including Derlin, VIMP, Herp and the E3-ligase HRD1[14,15]. Functionally associated with the ERAD pathway on the cytosolic site of the ER is the p97/VCP ATPase complex. The p97/VCP complex binds and extracts poly-ubiquitinated proteins from the membrane making them available for proteasomal degradation at the cytosolic site of the ER[16,17].

Efficient processing and generation of the target antigenic peptides by the UPS is essential for treatment of cancers by T-cell therapy. However, immune escape due to inefficient processing of HLA dependent tumor epitopes can be one important reason for failure of such therapies. It is known that tumors can down-regulate or completely lose expression of tumor antigens and HLA class I molecules, thereby escaping from T cell recognition[18,19]. Modulation of the UPS has also been observed and, in particular, the expression of the IFN-γ inducible components of the UPS such as PA28α/β and the i-subunits β1i/LMP2 and β5i/LMP7 were found to be altered in tumor cells, affecting both the quantity and in certain cases also the quality of the generated epitopes[20–22]. In some cases, a deficient expression of proteasome components could be reverted in the presence of IFN-γ, thereby also reconstituting MHC class I surface expression[23]. However, due to the complexity of the UPS and its associated pathways, only a few immune escape mechanisms have been characterized so far, although knowledge of these mechanisms is a prerequisite for the improvement of cancer immunotherapy.

To identify novel mechanisms by which tumors can become refractory to immune elimination, human melanoma cells expressing the transmembrane Melan-A/MART-1 tumor antigen were exposed to two rounds of brief co-culture with Melan-A/MART-1_{26-35}-specific CTL. Immune selected melanoma cell clones, being resistant to lysis by Melan-A/MART-1_{26-35} CTL were investigated for the underlying mechanism focusing on the role of the proteasomal antigen processing machinery. We detected a deregulated ERAD pathway as a so far unknown mechanism for immune escape of melanoma cells. In particular, the essential non-inducible ERAD component p97/VCP has been found to be down regulated in CTL-resistant melanoma cells. Rescue experiments reconstituting p97/VCP expression in melanoma cells resulted in enhanced Melan-A/MART-1_{26-35} epitope recognition, underlining the *in vivo* functional relevance of our results.

Results

Selection of melanoma cell clones resistant to CTL-mediated lysis by Melan-A/MART-1_{26-35}-specific CTL. To identify unknown immune evasion mechanisms allowing melanoma cells to circumvent recognition by specific CTL, the human HLA-A*0201-positive melanoma cell line UKRV-Mel-15a expressing the transmembrane tumor antigen Melan-A/MART-1[20,24,25] was co-incubated with an HLA-A*0201-restricted Melan-A/MART-1_{26-35}-specific CTL clone. Surviving UKRV-Mel-15a cells were exposed to two or three rounds of CTL co-culture selecting for resistant tumor cell clones. To exclude resistance due to HLA or antigen down-regulation, UKRV-Mel-15a cells were analyzed for HLA-A*0201 and Melan-A/MART-1 expression by flow cytometry. As shown in Fig. 1A, three rounds of co-culture resulted in considerable HLA-A*0201 down-regulation. We therefore decided to apply only two rounds of CTL co-culture for the selection of resistant melanoma clones, because under these conditions the HLA-A*0201 and Melan-A/MART-1 expressions of the surviving clones was similar or even higher than those of the parental UKRV-Mel-15a cell line (Fig. 1A).

We next tested the ability of the UKRV-Mel-15a derived clones to present the Melan-A/MART-1_{26-35} epitope by exposing them to Melan-A/MART-1_{26-35}-specific CTL in a 6-h antigen presentation TNF-α assay. Exposing Melan-A/MART-1_{26-35} CTL to peptide-pulsed T2 cells but not unloaded T2 cells resulted in increased production of TNF-α, thereby confirming the specificity of our read-out system (Fig. 1B, right panel). Of more than 30 UKRV-Mel-15a clones, only the clones 6, 18 and 30 exhibited significantly impaired recognition by Melan-A/MART-1_{26-35}-specific CTL and therefore were chosen for further analysis (Fig. 1B). Importantly, both TNF-α release and cytolysis by Melan-A/MART-1_{26-35}-specific CTL could be restored upon exogenous loading of UKRV-Mel-15a clones with synthetic Melan-A/MART-1_{26-35} peptide (Fig. 1C,D). This demonstrates that the HLA-A*0201 expression level on these clones was not rate limiting for immune recognition and that the observed immune escape was not due to resistance of the three selected melanoma cell clones against CTL-induced cytolysis.

Down-regulation of constituents of the antigen processing machinery in tumor cells and concomitant impaired epitope generation and presentation is a well-known evasion mechanism described for a variety of different human tumors[22,23,26,27]. However, as mentioned above, the expression of these components can be restored following IFN-γ treatment. Importantly, the expression levels of TAP1 and TAP2 as well as of the three proteasome immunosubunits in UKRV-Mel-15a clones were comparable to those of the non-selected parental UKRV-Mel-15a cells (Fig. S1). Only the clone 30 exhibited some impairment in the inducible expression of the i-subunits, as evidenced by its incapacity to up-regulate β1i/LMP2, β2i/MECL and β5i/LMP7 in response to IFN-γ. This suggests that the observed resistance of the selected UKRV-Mel-15a clones to CTL-mediated lysis was not due to an altered IFN-γ signaling pathway. This notion is supported by the observation that IFN-γ exposure failed to modify the phenotype of the UKRV-Mel-15a clones 6, 18 and 30 (Fig. 1E).

Deregulation of ERAD components in resistant melanoma cell clones. To determine which of the UPS components and its associated pathways was responsible for the down-regulation of Melan-A/MART-1_{26-35}

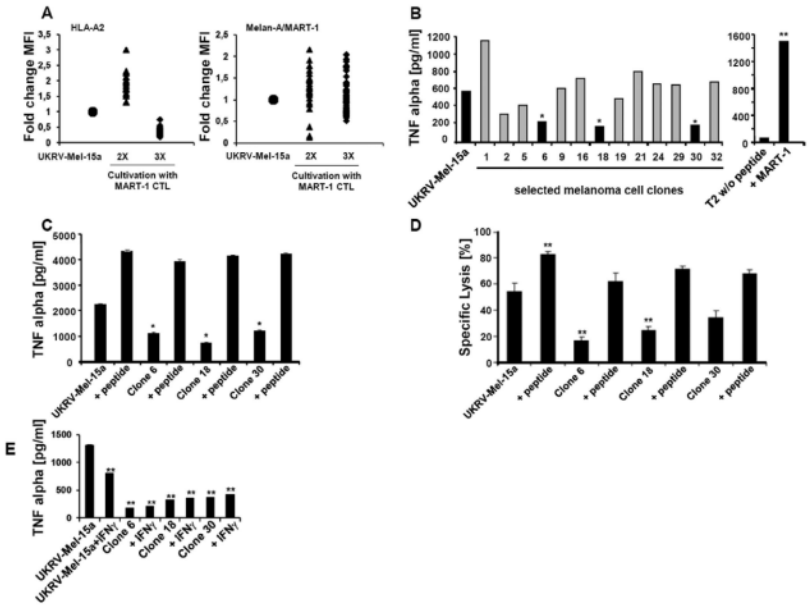

Figure 1. Analysis of melanoma cell clones resistant to MART-1_{26-35}-specific CTL lysis. (**A**) Immune selected melanoma cell clones derived from co-cultivation of UKRV-Mel-15a cells (Mel 15) with Melan-A/MART-1_{26-35} specific CTL were analyzed for HLA-A*0201 and MART-1 expression by flow cytometry after two (triangle) and three (rhomb) selection cycles. Data are presented as fold changes compared to the parental UKRV-Mel-15a cell line (circle) whose HLA-A*0201 and Melan-A/MART-1 expression levels were set to 1. (**B**) UKRV-Mel-15a clones obtained after two rounds of immune selection, were tested for their ability to present the Melan-A/MART-1_{26-35} epitope. UKRV-Mel-15a clones were co-cultured for 6 h with Melan-A/MART-1_{26-35} specific CTL, whose activation was determined by measuring the TNF-α-content in the supernatants by ELISA. The UKRV-Mel-15a clones 6, 18 and 30 (black columns) exhibited a strongly reduced capacity of presenting Melan-A/MART-1_{26-35} ($^*p < 0.05$, Student's *t* test) and were therefore selected for further analysis. T2 cells loaded with 5 μM of the Melan-A/MART-1_{26-35} synthetic peptide were included as positive control (right panel). $^{**}p < 0.01$ *vs* unloaded T2 cells (Student's *t* test). (**C**) The comparability of the HLA-A*0201 expression level across the three immune selected UKRV-Mel-15a clones was further verified by analyzing their capacity to stimulate Melan-A/MART-1_{26-35} specific CTL when loaded with 5 μM of the Melan-A/MART-1_{26-35} peptide. CTL activation was determined in a 6-h TNF-α release assay. Error bars represent standard deviation (n = 2). $^*p < 0.05$ *vs* UKRV-Mel-15a parental cells (Student's *t* test). (**D**) The sensitivity of the three UKRV-Mel-15a clones to lysis by Melan-A/MART-1_{26-35}-specific CTL was tested in a ^{51}Cr release assay (E:T 10:1). Positive control consisted in UKRV-Mel-15a clones 6, 18 and 30 exogenously pulsed with 5 μM of the Melan-A/MART-1_{26-35} peptide. $^{**}p < 0.01$ *vs* the UKRV-Mel-15a parental cell line (Student's *t* test). (**E**) The effect of IFN-γ on the presentation of Melan-A/MART-1_{26-35} by the UKRV-Mel-15a clones 6, 18 and 30 was evaluated in a 6-h TNF-α CTL assay. To this end, cells were treated with IFN-γ at 200 U/ml for 48 h prior to an exposure to Melan-A/MART-1_{26-35} CTL and measurement of the released TNF-α by ELISA. Error bars represent standard deviation (n = 2). $^{**}p < 0.01$ *vs* UKRV-Mel-15a parental cells (Student's *t* test). The experiments shown are representative of at least two.

epitope presentation; UKRV-Mel-15a clones were subjected to microarray gene expression analysis focusing on more than 1000 components of the antigen processing machinery. Interestingly, all three selected UKRV-Mel-15a clones displayed considerable alterations in the expression levels of a set of mRNAs encoding p97/VCP, VIMP, HERP and Derlin-1 (Table 1) and thus proteins whose functions are related to or directly connected with the ER-dependent degradation (ERAD) pathway[28]. Because cellular protein levels strongly depend on the rate of synthesis and their half-lives, expression levels of mRNAs and corresponding detectable protein levels do not necessarily correlate. Therefore, we next analyzed the expression levels of the affected ERAD-associated proteins by Western blot. As shown in Fig. 2A,B, all three resistant UKRV-Mel-15a clones revealed a strong down-regulation of the ERAD components p97/VCP, which is essential for the extraction of poly-ubiquitinated substrates from the ER[29], and VIMP, which is a seleno-protein associated with p97/VCP as well as with the membrane protein Derlin-1[17]. In contrast, slightly increased expression levels were found for HERP and Derlin-1 (Fig. 2A,B). Importantly, there was no substantial loss of the Melan-A/MART-1 antigen expression in the UKRV-Mel-15a

Gene	Clone 6	Clone 18	Clone 30
p97/VCP	0.622	0.513	0.451
VIMP	0.768	0.656	0.779
HERP	0.852	0.742	1.675
Derlin-1	1.971	1.954	1.991

Table 1. The immune challenge of the UKRV-Mel-15a melanoma cell line with Melan-A/MART-1_{26-35}-specific CTL results in altered expression of ERAD-related genes. Following two rounds of exposure with Melan-A/MART-1_{26-35}-specific CTL, the UKRV-Mel-15a melanoma cells resistant to cell lysis were further cultivated and cloned by limiting dilution. The transcription profile of the clones 6, 18 and 30 was analyzed by microarrays and compared to that of the untreated UKRV-Mel-15a parental cell line (shown is the expression ratio of the mRNA expression levels relative to that of the UKRV-Mel-15a parental cell line). Four genes belonging to the ERAD pathway (i.e. p97/VCP, VIMP, HERP and Derlin-1) were identified as being strongly altered in the UKRV-Mel-15a clones 6, 18 and 30.

clones 6, 18 and 30. These data therefore suggested that deregulated expression of ERAD components might be causative for the impaired Melan-A/MART-1_{26-35} epitope generation and presentation by the three UKRV-Mel-15a clones.

p97/VCP is a prerequisite for Melan-A/MART-1_{26-35} epitope generation. Apart from the first N-terminal amino acid residue which is directed to the luminal compartment, the entire Melan-A/MART-1_{26-35} 10-mer epitope is embedded within the Melan-A/MART-1 transmembrane domain[30] (Fig. 3A). Therefore, for proteasome-dependent antigen processing, the Melan-A/MART-1 protein must be retro-translocated into the cytosol. We next aimed to evaluate the impact of VIMP and HERP on Melan-A/MART-1_{26-35} epitope generation independently of the Melan-A/MART-1 endogenous expression level. To this end, both of these ERAD components were knocked down by siRNA in the Ma-Mel-91-melanoma cell line (Melan-A/MART-1^{-}/HLA-A*0201^{+}) which was subsequently engineered to express the Melan-A/MART-1 antigen. Strikingly and as illustrated in Fig. 3B, gene silencing of either VIMP or HERP resulted in a substantial reduced presentation of the Melan-A/MART-1_{26-35} epitope. Because p97/VCP expression was also found to be significantly reduced in our selected UKRV-Mel-15a clones 6, 18 and 30, we next tested its involvement in Melan-A/MART-1_{26-35} epitope generation by expressing a dominant negative mutant of p97/VCP (p97QQ), which abrogates cellular p97/VCP function[16]. Interestingly, although the expression of p97QQ had virtually no effect on cell viability (data not shown), it almost completely abrogated Melan-A/MART-1_{26-35} epitope generation, whose levels, under these conditions, were quite similar to those observed when proteasomes were inhibited with epoxomicin (Fig. 3C). Accordingly, CHX-based chase experiments show that p97/VCP silencing resulted in a significant stabilization of the Melan-A/MART-1 protein (Fig. 3D). It is to note, that neither the down-regulation of VIMP or HERP by siRNA nor the plasmid-mediated transfection of p97/VCP or p97QQ substantially affected the expression level of the Melan-A/MART-1 full-length protein (Fig. S2).

Melan-A/MART-1_{26-35} epitope recognition is rescued by overexpression p97/VCP. The observation, that the inhibition and/or gene silencing of VIMP and p97/VCP almost completely abrogated Melan-A/MART-1_{26-35} epitope presentation and that both proteins were found to be down-regulated in CTL-resistant UKRV-Mel-15a clones suggests that both or one of them may be causative for the observed immune evasion. Therefore, we next sought to determine whether the immune escape of the UKRV-Mel-15a clones was reversible by restoring p97/VCP or VIMP expression.

To this end, we performed MHC class I presentation rescue experiments by transfecting the UKRV-Mel-15a clone 18 with expression vectors encoding full-length p97/VCP or VIMP proteins. As shown in Fig. 4A,B, re-expression of p97/VCP restored stimulation of Melan-A/MART-1_{26-35}-specific T cells to levels comparable to those detected upon exposure to the parental UKVR-Mel-15a cell line, demonstrating that the observed down-regulated expression of p97/VPC was indeed responsible for the observed immune escape of the UKRV-Mel-15a Mel-15 clones. Accordingly, RNAi-mediated down-regulation of p97/VCP in the parental UKVR-Mel-15a cell line was accompanied by severe impairment of Melan-A/MART-1_{26-35} presentation (Fig. S3), further confirming that p97/VCP ensures the supply of Melan-A/MART-1_{26-35} antigenic peptides under normal conditions. This also suggests that the observed emergence of resistant clones following Melan-A/MART-1_{26-35} CTL exposure is most likely driven by the spontaneous loss of p97/VCP expression in the heterogeneous UKRV-Mel-15a parental melanoma cell population or a selective enrichment of cells expressing low levels of p97/VCP. In contrast, over-expression of the p97/VCP recruiting membrane protein VIMP failed to rescue the Melan-A/MART-1_{26-35} epitope presentation (Fig. 5A,B). This, however, is in agreement with a previous report showing that the over-expression of VIMP in COS cells alters ER morphology which may cause dysfunction of the ERAD pathway[17].

Down-regulation of p97/VCP is also an immune escape mechanism in Ma-Mel-63a cells. The data obtained so far provide strong evidence that impaired expression of p97/VCP and subsequent dysfunction of the ERAD pathway was causative for the observed immune escape of CTL challenged UKVR-Mel-15a cells. Nevertheless, the possibility remained that this may represent an isolated case due to unknown specific features of the UKVR-Mel-15a cells. Therefore, we performed a second independent experimental analysis using the Melan-A/MART-1^{+}, HLA-A*0201 melanoma cell line Ma-Mel-63a. As shown in Fig. 6A, Ma-Mel-63a cells

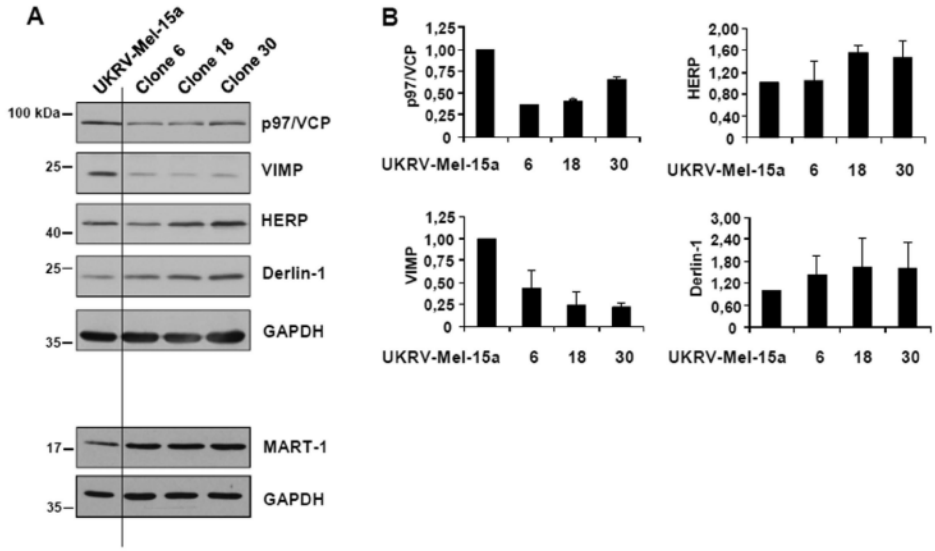

Figure 2. The expression levels of components of the ERAD pathway are altered in immune selected UKRV-Mel-15a cell clones. (**A**) The UKRV-Mel-15a clones 6, 18 and 30 as well as the UKRV-Mel-15a parental cell line were subjected to protein extraction. Whole cell extracts were resolved by SDS-PAGE followed by Western blotting using antibodies specific for p97/VCP, VIMP, HERP, Melan-A/MART-1 and Derlin-1, as indicated. Equal protein loading was ensured by probing the membrane with anti-GAPDH antibody. (**B**) Fold changes of the expression levels of p97/VCP, HERP, VIMP and Derlin-1 between the UKRV-Mel-15a parental cell line and the UKRV-Mel-15a clones 6, 18 and 30, as visualized by densitometric analysis. The band intensity of each protein was normalized to that of GAPDH and subsequently expressed as fold-changes compared to the UKRV-Mel-15a parental cell line which was set at 1.

expressed and efficiently presented the Melan-A/MART-1_{26-35} tumor epitope, as revealed by TNF-α-release assays. Importantly, overexpression of p97/VCP did not further improve the Melan-A/MART-1_{26-35} epitope presentation, suggesting that the ERAD pathway was fully functional in these cells. This notion was also supported by immunoblotting experiments revealing normal expression levels of the ERAD associated components (data not shown).

Following the same experimental conditions, Ma-Mel-63a cells were challenged twice in short-term co-culture with Melan-A/MART-1_{26-35}-specific CTL. The Ma-Mel-63a clones resistant to CTL mediated lysis were further cultivated and assessed for their capacity of presenting the Melan-A/MART-1_{26-35} epitope. Of the 33 Ma-Mel-63a clones, 3 clones (i.e. clones 9, 15 and 26) exhibited substantial impaired recognition by Melan-A/MART-1_{26-35} CTL when compared with the unchallenged parental Ma-Mel-63a cell line (Fig. 6B). Strikingly, all three clones also displayed reduced p97/VCP expression (Fig. 6C). Of these, clone 26 could not be further analyzed because it lost its endogenous Melan-A/MART-1 expression (data not shown). The Ma-Mel-63a clone 15 was finally selected for p97/VCP rescue experiments, because it revealed an almost unaltered expression level of the ERAD components VIMP, HERP or Derlin-1 as well as a normal expression of the IFN-inducible i-subunits and TAP1/2 (Figs 7A and S4). As shown in Fig. 7B,C, overexpression of p97/VCP almost completely restored Melan-A/MART-1_{26-35} epitope presentation. These data show that impaired expression of the ERAD component p97/VCP upon immune challenge with Melan-A/MART-1_{26-35}-specific T-cells is an universal event that allows melanoma cells to escape CTL-mediated cell death.

Discussion

There is mounting clinical evidence that T-lymphocytes play a central role in the regression of melanoma *in vivo* and that adoptive transfer of cultured T cells from tumor infiltrating lymphocytes may result in tumor regression[31]. However, loss of MHC class I expression has been reported to render tumors resistant to adoptive T-cell therapy[32]. In fact, analysis of tumor cells also revealed a down-regulation of the IFN-γ-inducible antigen processing machinery[33–37]. It is not clear how frequent immune escape of tumors upon T cell pressure results in the irreversible loss of IFN-γ sensitivity. Studies of tumor cell lines showed that, in most cases, the expression of down-regulated components involved in MHC class I antigen presentation was restored by IFN-γ treatment. Nevertheless, immune evasion of tumor cells upon T cell pressure still remains a problem and very little is known about escape mechanism connected with antigen processing. Our experiments show that co-cultivation of the

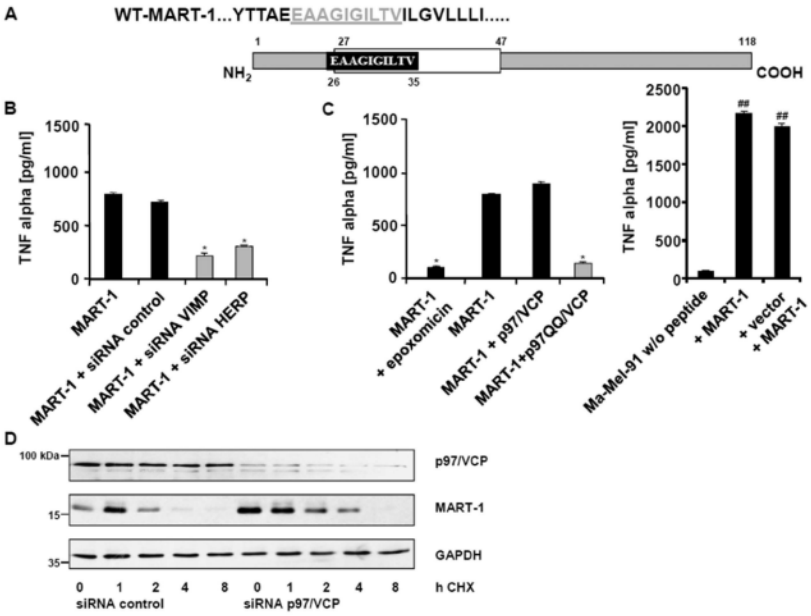

Figure 3. Melan-A/MART-1_{26-35} epitope presentation is ERAD-dependent. (**A**) Schematic representation of the Melan-A/MART-1_{26-35} epitope which is entirely localized within the transmembrane domain, except for the first amino acid residue. (**B**) The melanoma cell line Ma-Mel-91 (Melan-A/MART-1$^-$, HLA-A*0201) was exposed to non-targeting (control) siRNA or siRNA directed against VIMP or HERP1 prior to a subsequent transfection with an expression vector encoding the wild-type full-length Melan-A/MART-1 tumor antigen. The ability of these cells to present the Melan-A/MART-1_{26-35} epitope was evaluated in a 6 h TNF-α release assay upon exposure to Melan-A/MART-1_{26-35} CTL. The content of TNF-α in the supernatants was measured by ELISA. *$p < 0.05$ *vs* Ma-Mel-91 cells expressing Melan-A/MART-1 and exposed to control siRNA (Student's *t* test) (**C**) The impact of p97/VCP on Melan-A/MART-1_{26-35} presentation was evaluated by transfecting Ma-Mel-91 cells with Melan-A/MART-1 in combination with either wild-type p97/VCP or a dominant negative mutant of p97/VCP (p97QQ). After 24 h of transfection, the cells were tested for their capacity to present the Melan-A/MART-1_{26-35} antigenic peptide by cultivating them in the presence of Melan-A/MART-1_{26-35} CTL and followed by subsequent measurement of TNF-α by ELISA. In addition, proteasome dependency of Melan-A/MART-1_{26-35} epitope generation was demonstrated by treating the Ma-Mel-91 cells transfected with the Melan-A/MART-1 expression plasmid with 1 μM of the proteasome inhibitor epoxomicin for 4 h. As control, Ma-Mel-91 cells were loaded with the Melan-A/MART-1_{26-35} synthetic peptide or were transfected with the pcDNA3.1 plasmid and loaded with the Melan-A/MART-1 peptide. *$p < 0.05$ *vs* Melan-A/MART-1-expressing Ma-Mel-91 cells and **$p < 0.01$ *vs* unloaded Ma-Mel-91 cells (Student's *t* test) (**D**) Silencing of p97/VCP by siRNA results in stabilization of the Melan-A/MART-1 protein expression. HeLa cells were exposed to either non-targeting (control) or p97/VCP siRNA for 24 h prior to a subsequent 24 h transfection with an expression plasmid encoding wild-type Melan-A/MART-1 and subjected to CHX-based chase assay. Cells were collected after 1, 2, 4 and 8 h and Western blot analysis was performed for each time point using antibodies specific for Melan-A/MART-1, p97/VCP and GAPDH (loading control).

melanoma UKRV-Mel-15a and Ma-Mel-63a cells with Melan-A/MART-1_{26-35} CTL led in both instances to the isolation of several melanoma cell clones, which revealed impaired presentation of the Melan-A/MART-1_{26-35} antigenic peptide (Figs 1 and 6). However, immunoblot analyses failed to provide evidence that the expression of any of the known IFN-γ inducible components of the antigen processing and presentation machinery was significantly modified (Figs S1 and S4) and therefore did not explain the observed immune escape of the resistant UKRV-Mel-15a and Ma-Mel-63a clones.

The UPS with its more than 1000 protein components plays a central role in the generation of tumor epitopes presented by MHC class I molecules. Many of these may be directly or indirectly involved in the regulated proteasome dependent degradation of the Melan-A/MART-1 protein. Because of this complexity, we focused our analysis in particular on components of the ER associated degradation (ERAD) pathway known to be involved in the degradation of membrane-associated tumor antigens such as tyrosinase[38]. Indeed, our cDNA array analyses of melanoma cells resistant to cytolysis by Melan-A/MART-1_{26-35}-specific CTL revealed several of the known

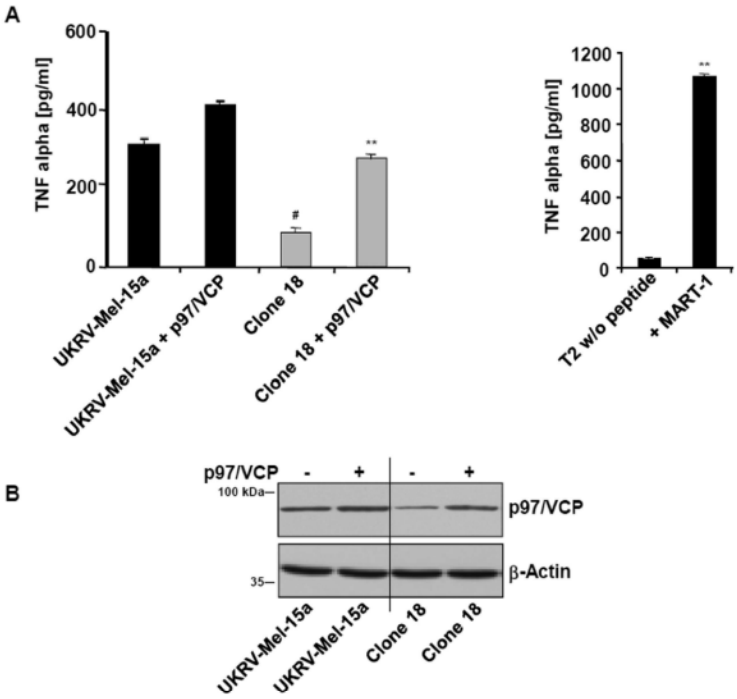

Figure 4. Re-expression of p97/VCP reconstitutes Melan-A/MART-1_{26-35} epitope presentation. (**A**) The UKRV-Mel-15a clone 18 as well as the UKRV-Mel-15a parental cells were transfected with an expression vector encoding the p97/VCP full-length protein, as indicated. After 24 h of transfection, cells were exposed to Melan-A/MART-1_{26-35} CTL to evaluate their capacity to present the Melan-A/MART-1_{26-35} epitope. Following a 6 h co-culture, the supernatants were harvested and tested for their TNF-α content by ELISA. Controls in this experiment consisted of unloaded T2 and T2 cells loaded with 5 μM of the Melan-A/MART-1_{26-35} synthetic peptide (right panel). Shown is one representative experiment out of three. $^{**}p < 0.01$ *vs* UKRV-Mel-15a clone 18 (left graph) or unloaded T2 cells (right graph) and $^{\#}p < 0.05$ *vs* UKRV-Mel-15a cells (Student's *t* test). (**B**) Melanoma cells were subjected to protein extraction and whole cell extracts were resolved on SDS-PAGE followed by Western blotting using antibodies specific for p97/VCP and β-actin (loading control), as indicated.

ERAD components to be down regulated in these cells. Interestingly, the most reproducible down-regulation was observed for the AAA ATPase p97/VCP (Table 1). Importantly, the down-regulation of p97/VCP was observed in two independent melanoma cell lines, indicating that such effect was not cell line-specific but rather a more general phenomenon in response to CTL exposure (Figs 2A and 6C). The essential and critical role of ERAD in the ubiquitin-dependent degradation of membrane proteins and, as such, in the generation of antigenic peptide derived from membrane proteins is well documented[39,40]. Given the high number of membrane-bound proteins among melanoma-associated antigens, an active contribution of ERAD in tumor surveillance is very likely. For example, a functional ERAD pathway has been reported to be a prerequisite for the breakdown of the tyrosinase antigen[38,41]. This is also true for secretory proteins such as the pro-insulin auto-antigen[42]. Interestingly, the ERAD-mediated degradation of tyrosinase occurs in an EDEM1-dependent fashion, while that of pro-insulin mainly relies on Derlin-2, HRD1 and p97/VCP. The observation that ERAD substrates do not necessarily rely on the same components implies a strong heterogeneity and plasticity of the ERAD pathway. This point is of considerable importance, as it suggests that the loss of one particular ERAD-associated protein in tumors might not necessarily cause immune escape. An exception, however, is p97/VCP which is essentially required for the extraction of substrates from the ER to the cytoplasm, regardless of the composition of the ERAD complexes and/or pathways employed. Thus, any down-regulation of p97/VCP will be accompanied by a decreased MHC class I presentation of all ERAD-dependent antigens. Importantly, the involvement of ERAD in the supply of MHC class I-restricted peptides is not exclusively restricted to hydrophobic antigens. Hence, a major role for ERAD has also been described in the cross-presentation of soluble antigens by dendritic cells (DC)[43–46], although the precise mechanisms by which internalized antigens use ERAD to gain access to the cytoplasm remain unclear. Interestingly, cross-presentation is not restricted to DC and may be also used by melanoma cells to

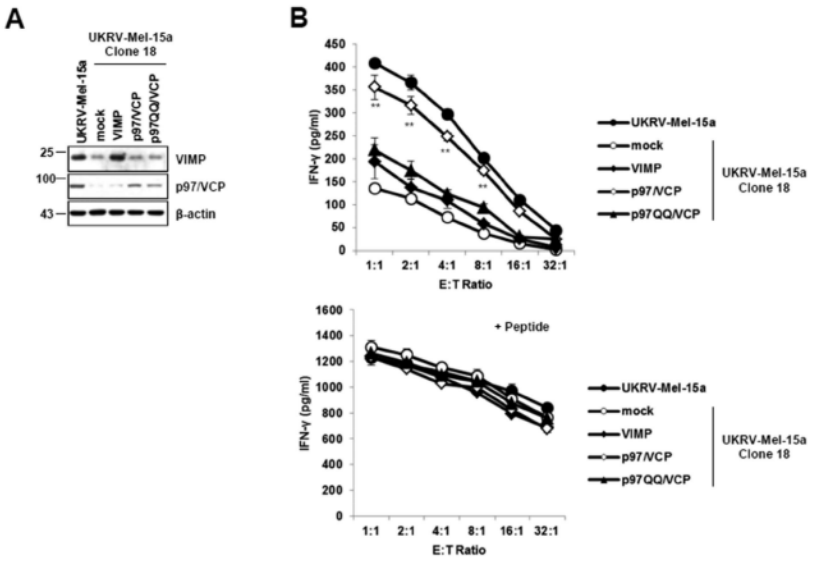

Figure 5. Melan-A/MART-1_{26-35} epitope presentation in the immune challenged UKRV-Mel-15a clone 18 is not rescued by VIMP over-expression. (**A**) The UKRV-Mel-15a clone 18 was subjected to a 24-h transfection with an empty vector (mock) or expression vectors encoding VIMP, p97/VCP or p97QQ/VCP, as indicated. Whole cell-extracts were resolved on 15% SDS-PAGE and analysed by western-blotting using antibodies against VIMP, p97/VCP and β-actin (loading control). (**B**) The ability of the UKRV-Mel-15a clone 18 over-expressing VIMP, p97/VCP or p97QQ/VCP to present the Melan-A/MART-1_{26-35} antigenic peptide was evaluated by exposing them to Melan-A/MART-1_{26-35}-specific CTL followed by IFN-γ measurement in the supernatants by ELISA. In addition, cells were pulsed with 1 μM of the Melan-A/MART-1_{26-35} synthetic peptide, as a positive control. Shown is one representative experiment out of two. $^{**}p < 0.01$ *vs* UKRV-Mel-15a clone 18 (mock) (Student's *t* test).

present antigens derived from secretory proteins such as the matrix metalloproteinase-2 (MMP2)$_{560-568}$ epitope[47]. As expected, a role for ERAD has been suggested in the processing of this antigenic peptide[48], although the implication of p97/VCP remains to be formally addressed. Our experiments demonstrate that re-expression of p97/VCP in CTL-resistant UKRV-Mel-15a clone 18 and Ma-Mel-63a clone 15 to normal levels was able to almost completely recover Melan-A/MART-1_{26-35} epitope presentation. The expression of p97/VCP is not induced by cytokines and it is not clear at the moment why its expression may be so influenced by exposure of melanoma cells to Melan-A/MART-1_{26-35} CTL. In any case, the down-regulation of ERAD is of general importance, as it will affect not only the presentation of the Melan-A/MART-1_{26-35} epitope but also the presentation of all other membrane protein-derived tumor epitopes generated by the ERAD pathway. Our data suggest that, in order to minimize or circumvent rapid immune evasion upon T-cell therapy, those tumor epitopes should be chosen and simultaneously targeted by T cells that are derived from separate antigens, which are degraded and processed by distinct degradation pathways. In this context, the option to target antigens whose degradation does not primarily rely on the UPS appears indeed particularly attractive. In view of the UPS, and *a fortiori*, p97/VCP as a major target whose deregulation might facilitate tumor escape, future research efforts may also address the functional relevance of proteasome-independent MHC class I tumor peptides in immunotherapy.

Material and Methods

Cell culture and immune selection of melanoma cells. The T2 lymphoblastoid cell line as well as the human melanoma cell lines Ma-Mel-91 cells (Melan-A/MART-1$^-$, HLA-A*0201), UKRV-Mel-15a (Melan-A/MART-1$^+$, HLA-A*0201), Ma-Mel-63a (Melan-A/MART-1$^+$, HLA-A*0201) and immune selected cell clones derived from UKRV-Mel-15a or Ma-Mel-63a were cultivated in RPMI supplemented with 10% fetal bovine serum (Biochrom AG, Germany). Authentication of these cell lines was ensured by genetic profiling on genomic DNA at the Institute for Forensic Medicine (University Hospital Essen) using the AmpFLSTR-Profiler Plus kit (Applied Biosystems)[49]. To obtain UKRV-Mel-15a or Ma-Mel-63a clones resistant to lysis by HLA-A*0201-restricted Melan-A/MART-1_{26-35}-specific CTL, melanoma cells were co-cultured for 5 h with a Melan-A/MART-1_{26-35}-specific CTL clone raised against the ELAGIGILTV mutant peptide at a ratio of 1:50. Resistant melanoma cells were kept in culture for two weeks, followed by one or two additional rounds of co-incubation with Melan-A/

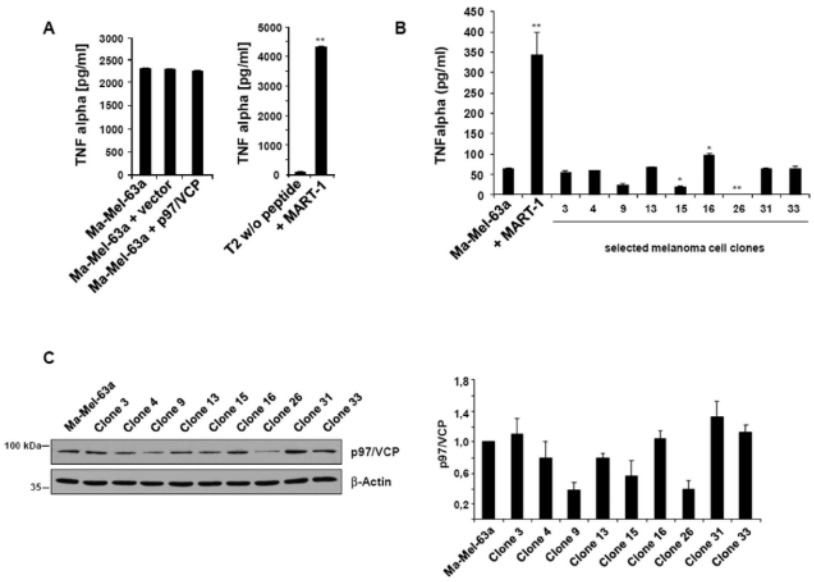

Figure 6. Analysis of Ma-Mel-63a melanoma cell clones resistant to Melan-A/MART-1_{26-35}-specific CTL lysis. (**A**) The Ma-Mel-63a cells (Melan-A/MART-1^+, HLA-A*0201^+) were tested for their ability to endogenously process and present the Melan-A/MART-1_{26-35} antigenic peptide by cultivating them with Melan-A/MART-1_{26-35} CTL. Additionally, Ma-Mel-63a cells were either transfected with pcDNA3.1 plasmid or an expression vector encoding the p97/VCP full-length protein. After 6 h, supernatants were harvested and their content for TNF-α was determined by ELISA. Controls in this assay consisted in non-pulsed T2 cells (negative) and T2 cells pulsed with 5 μM of the 10-mer synthetic peptide (right panel). $^{**}p < 0.01$ *vs* unloaded T2 cells (Student's *t* test) (**B**) The Ma-Mel-63a clones 3,4,9,13,15,16,26,31 and 33 were tested for their ability to present the Melan-A/MART-1_{26-35} epitope by culturing them with Melan-A/MART-1_{26-35}-specific CTL. Activation of CTL was assessed by measuring the TNF-α-content in the supernatants by ELISA after 6 h of co-culture. $^{*}p < 0.05$ and $^{**}p < 0.01$ *vs* the Ma-Mel-63a parental cell line (Student's *t* test). (**C**) The parental Ma-Mel-63a cell line as well as the Ma-Mel-63a clones were subjected to protein extraction and subsequent western blotting using anti-p97/VCP and anti-β-actin (loading control) antibodies. The steady-state expression levels of p97/VCP in the parental Ma-Mel-63a cell line and the Ma-Mel-63a clones were visualized by densitometric analysis. The band intensity of p97/VCP was normalized to that of β-actin and subsequently expressed as fold-changes compared to the Ma-Mel-63a parental cell line which was set as 1.

MART-1-specific CTL. UKRV-Mel-15a and Ma-Mel-63a cells were then cloned by limiting dilution at 0,3 cells/well in 96 well plates and single clones were expanded for further analysis.

Preparation of RNA, microarray hybridization, and data analysis. Microarrays hybridizations were conducted, as previously described[50]. Briefly, total RNA was extracted, amplified and labelled with biotin (Message AmpII-Biotin enhanced Kit, Ambion). The Human U133 2.0 Plus-Array (Affymetrix) was custom hybridized and evaluated by standard procedures (Signature Diagnostics). Raw data files were deposited on NCBIs Gene Expression Omnibus (GEO, http://www.ncbi.nlm.nih.gov/geo/) under the accession number GSE75929.

Transfection of melanoma cells for antigen presentation analysis. Melanoma cells were transfected with expression plasmids encoding pMART-1 wild-type, p97 wild-type, p97QQ, a dominant negative p97QQ mutant (both provided by T. Rapoport, Department of Cell Biology, Harvard Medical School, Boston, MA) (all cloned into pcDNA3.1 vector, Invitrogen)[16] or control plasmid pcDNA3.1. Transfection was performed using Lipofectamine 2000 (Invitrogen) following manufacturer's instructions. After 24–48 h of transfection, cells were harvested for further studies. For siRNA transfection, HighPerFect Reagent (Roche) was used. Cells were incubated for 72 h with ON-TARGET-plus SMART pools siRNA duplexes targeting HERP (human HERPUD1), p97/VCP or non-targeting (control) siRNA (all purchased from Dharmacon Inc.). VIMP-siRNA (5′-CTGGCGGATGAGGCTAAGAAT-3′) was purchased from Qiagen.

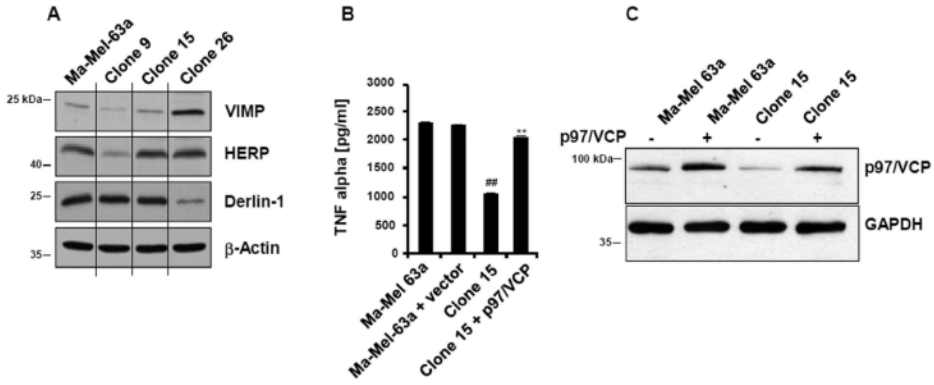

Figure 7. Melan-A/MART-1_{26-35} epitope presentation in the immune challenged Ma-Mel-63a clone 15 is rescued by p97/VCP over-expression. (**A**) The protein content of VIMP, HERP and Derlin-1 in the Ma-Mel-63a parental cell line and the Ma-Mel-63a clones 9, 15 and 26 was assessed by western-blotting, as indicated. Equal protein loading was ensured by probing the membrane with an anti-β-actin antibody. (**B**) The Ma-Mel-63a clone 15 was transfected with pcDNA3.1/p97/VCP for 24 h, as indicated and subsequently co-cultured with Melan-A/MART-1_{26-35} CTL for further 6 h. The ability of these cells to present the Melan-A/MART-1_{26-35} antigenic peptide was evaluated by measuring the content of TNF-α in the supernatants by ELISA. Control in this experiment consisted in the Ma-Mel-63a parental melanoma cell line transfected with the empty pcDNA3.1 plasmid or not. Shown is one representative experiment out of two. $^{**}p < 0.01$ *vs* Ma-Mel-63a clone 15 and $^{\#\#}p < 0.01$ *vs* Ma-Mel-63a cells (Student's *t* test). (**C**) The Ma-Mel-63a clone 15 transfected or not with p97/VCP as well as the Ma-Mel-63a parental cell line were analyzed for their p97/VCP content by western-blotting, as indicated. GAPDH was used as loading control.

Generation of Melan-A/MART-1_{26-35}-specific $CD8^+$T cell clone. A HLA-A*0201-restricted Melan-A/MART- 1-specific $CD8^+$T cell clone was generated against the ELAGIGILTV mutant peptide as described previously[51,52]. For antigen presentation analysis, melanoma cells were incubated with Melan-A/MART-1-specific T cells for 6 h at an E:T ratio of 1:1 or 8:1, as previously described[53]. As positive control, target cells were loaded with 5 μM of the Melan-A/MART-1_{26-35} ELAGIGILTV peptide for 1 or 2 h. Activation of Melan-A/MART-1-specific CTL was assessed by quantification of secreted TNF-α or IFN-γ by ELISA as described below.

ELISA. ELISA for TNF-α or IFN-γ was performed following the manufacturer's instructions (BD Biosciences). Diluted (1:5) supernatants from CTL-experiments were added to 96 wells pre-coated with anti-TNF-α or anti-IFN-γ antibodies in duplicates and supplemented with secondary antibodies and streptavidin-bound POD for 1 h. Plates were washed and incubated for 30 min with TMB substrate (BD Biosciences). Optical density was determined at 450 nm.

Immunoblot analysis. Cells were lysed in Mammalian Protein Extraction Reagent (Pierce) containing Complete Protease Inhibitors (Roche). Proteins were separated on SDS-PAGE and immunoblotted with antibodies specific for p97/VCP (provided by R. Hartmann-Petersen), VIMP, Derlin-1 (both provided by T. Rapoport), HERP (laboratory stock)[14], GAPDH (Santa Cruz), Melan-A/MART-1 (Novocastra), β-actin (Santa Cruz), β5i/LMP7, β1i/LMP2, β2i/MECL-1 (laboratory stock), TAP1 (Rockland) and TAP2 (NBL). Detection was carried out by enhanced chemiluminescence. Densitometric analysis was performed using ImageJ NIG software.

Flow cytometry analysis. HLA-A*0201 surface expression as well as intracellular Melan-A/MART-1 antigen expression was determined by flow cytometry using a FITC-conjugated mAb BB7.2 for HLA-*0201 and a Melan-A/MART-1 antibody (NovoCastra) followed by staining with FITC-conjugated anti-mouse antibody (BD Biosciences) for Melan-A/MART-1. Cells were analyzed on a Becton Dickinson FACSCalibur with Cell Quest software (BD Biosciences).

CTL assay. After removing unbound peptides by three washing steps with PBS, Melan-A/MART-1 epitope presentation was determined in a TNF-α release assay. CTL-mediated lysis of resistant melanoma cell clone was investigated by incubating melanoma cells with 5 μM of the synthetic Melan-A/MART-1_{26-35} ELAGIGILTV peptide for 2 h, followed by a standard ^{51}Cr release assay, as previously described[54].

Cycloheximide (CHX) chase. HeLa cells were exposed to either non-targeting (control) or p97/VCP siRNA for 24 h prior to a subsequent transfection with an expression plasmid encoding the Melan-A/MART-1 full-length protein. After 24 h of transfection, 50 μg/ml of CHX was added to all samples (0 h chase). Cells were collected after 1, 2, 4 and 8 h and Western blot analysis was performed for each time point using antibodies specific for p97/VCP, Melan-A/MART-1 and GAPDH (loading control).

References

1. Rosenberg, S. A. Progress in human tumour immunology and immunotherapy. *Nature* **411,** 380–384 (2001).
2. Coulie, P. G., Van den Eynde, B. J., van der Bruggen, P. & Boon, T. Tumour antigens recognized by T lymphocytes: at the core of cancer immunotherapy. *Nat. Rev. Cancer* **14,** 135–146 (2014).
3. Schumacher, T. N. & Schreiber, R. D. Neoantigens in cancer immunotherapy. *Science* **348,** 69–74 (2015).
4. Sensi, M. & Anichini, A. Unique tumor antigens: evidence for immune control of genome integrity and immunogenic targets for T cell-mediated patient-specific immunotherapy. *Clin. Cancer Res.* **12,** 5023–5032 (2006).
5. Kloetzel, P. M. Antigen processing by the proteasome. *Nat. Rev. Mol. Cell Biol.* **2,** 179–187 (2001).
6. Ebstein, F., Kloetzel, P. M., Kruger, E. & Seifert, U. Emerging roles of immunoproteasomes beyond MHC class I antigen processing. *Cell. Mol. Life Sci.* **69,** 2543–2558 (2012).
7. Blum, J. S., Wearsch, P. A. & Cresswell, P. Pathways of antigen processing. *Ann. Rev. Immunol.* **31,** 443–473 (2013).
8. Strehl, B. *et al.* Interferon-gamma, the functional plasticity of the ubiquitin-proteasome system, and MHC class I antigen processing. *Immunol. Rev.* **207,** 19–30 (2005).
9. Vigneron, N. & Van den Eynde, B. J. Proteasome subtypes and regulators in the processing of antigenic peptides presented by class I molecules of the major histocompatibility complex. *Biomolecules* **4,** 994–1025 (2014).
10. Tanaka, K. Role of proteasomes modified by interferon-gamma in antigen processing. *J. Leukoc. Biol.* **56,** 571–575 (1994).
11. Bernasconi, R. & Molinari, M. ERAD and ERAD tuning: disposal of cargo and of ERAD regulators from the mammalian ER. *Curr. Opin. Cell Biol.* **23,** 176–183 (2011).
12. Meusser, B., Hirsch, C., Jarosch, E. & Sommer, T. ERAD: the long road to destruction. *Nat. Cell Biol.* **7,** 766–772 (2005).
13. Brodsky, J. L. & Wojcikiewicz, R. J. Substrate-specific mediators of ER associated degradation (ERAD). *Curr. Opin. Cell Biol.* **21,** 516–521 (2009).
14. Schulze, A. *et al.* The ubiquitin-domain protein HERP forms a complex with components of the endoplasmic reticulum associated degradation pathway. *J. Mol. Biol.* **354,** 1021–1027 (2005).
15. Iida, Y. *et al.* SEL1L protein critically determines the stability of the HRD1-SEL1L endoplasmic reticulum-associated degradation (ERAD) complex to optimize the degradation kinetics of ERAD substrates. *J. Biol. Chem.* **286,** 16929–16939 (2011).
16. Ye, Y., Meyer, H. H. & Rapoport, T. A. Function of the p97-Ufd1-Npl4 complex in retrotranslocation from the ER to the cytosol: dual recognition of nonubiquitinated polypeptide segments and polyubiquitin chains. *J. Cell Biol.* **162,** 71–84 (2003).
17. Ye, Y., Shibata, Y., Yun, C., Ron, D. & Rapoport, T. A. A membrane protein complex mediates retro-translocation from the ER lumen into the cytosol. *Nature* **429,** 841–847 (2004).
18. Seliger, B., Cabrera, T., Garrido, F. & Ferrone, S. HLA class I antigen abnormalities and immune escape by malignant cells. *Semin. Cancer Biol.* **12,** 3–13 (2002).
19. Paschen, A. *et al.* The coincidence of chromosome 15 aberrations and beta2-microglobulin gene mutations is causative for the total loss of human leukocyte antigen class I expression in melanoma. *Clin. Cancer Res.* **12,** 3297–3305 (2006).
20. Sun, Y. *et al.* Expression of the proteasome activator PA28 rescues the presentation of a cytotoxic T lymphocyte epitope on melanoma cells. *Cancer Res.* **62,** 2875–2882 (2002).
21. Guillaume, B. *et al.* Analysis of the processing of seven human tumor antigens by intermediate proteasomes. *J. Immunol.* **189,** 3538–3547 (2012).
22. Seliger, B. *et al.* Down-regulation of the MHC class I antigen-processing machinery after oncogenic transformation of murine fibroblasts. *Eur. J. Immunol.* **28,** 122–133 (1998).
23. Seliger, B. Molecular mechanisms of MHC class I abnormalities and APM components in human tumors. *Cancer Immunol. Immunother.* **57,** 1719–1726 (2008).
24. Kawakami, Y. *et al.* Cloning of the gene coding for a shared human melanoma antigen recognized by autologous T cells infiltrating into tumor. *Proc. Natl. Acad. Sci. USA* **91,** 3515–3519 (1994).
25. Romero, P. *et al.* Cytolytic T lymphocyte recognition of the immunodominant HLA-A*0201-restricted Melan-A/MART-1 antigenic peptide in melanoma. *J. Immunol.* **159,** 2366–2374 (1997).
26. Restifo, N. P. *et al.* Identification of human cancers deficient in antigen processing. *J. Exp. Med.* **177,** 265–272 (1993).
27. Seliger, B., Wollscheid, U., Momburg, F., Blankenstein, T. & Huber, C. Characterization of the major histocompatibility complex class I deficiencies in B16 melanoma cells. *Cancer Res.* **61,** 1095–1099 (2001).
28. Vembar, S. S. & Brodsky, J. L. One step at a time: endoplasmic reticulum-associated degradation. *Nat. Rev. Mol. Cell Biol.* **9,** 944–957 (2008).
29. Ye, Y., Meyer, H. H. & Rapoport, T. A. The AAA ATPase Cdc48/p97 and its partners transport proteins from the ER into the cytosol. *Nature* **414,** 652–656 (2001).
30. Kawakami, Y. *et al.* Production of recombinant MART-1 proteins and specific antiMART-1 polyclonal and monoclonal antibodies: use in the characterization of the human melanoma antigen MART-1. *J. Immunol. Methods* **202,** 13–25 (1997).
31. Rosenberg, S. A. & Restifo, N. P. Adoptive cell transfer as personalized immunotherapy for human cancer. *Science* **348,** 62–68 (2015).
32. Blankenstein, T., Leisegang, M., Uckert, W. & Schreiber, H. Targeting cancer-specific mutations by T cell receptor gene therapy. *Curr. Opin. Immunol.* **33,** 112–119 (2015).
33. Seliger, B., Wollscheid, U., Momburg, F., Blankenstein, T. & Huber, C. Coordinate downregulation of multiple MHC class I antigen processing genes in chemical-induced murine tumor cell lines of distinct origin. *Tissue antigens* **56,** 327–336 (2000).
34. Delp, K., Momburg, F., Hilmes, C., Huber, C. & Seliger, B. Functional deficiencies of components of the MHC class I antigen pathway in human tumors of epithelial origin. *Bone Marrow Transplant.* **25** Suppl 2, S88–95 (2000).
35. Kamphausen, E. *et al.* Distinct molecular mechanisms leading to deficient expression of ER-resident aminopeptidases in melanoma. *Cancer Immunol. Immunother.* **59,** 1273–1284 (2010).
36. Seliger, B. Different regulation of MHC class I antigen processing components in human tumors. *J. Immunotoxicol.* **5,** 361–367 (2008).
37. Meissner, M. *et al.* Defects in the human leukocyte antigen class I antigen processing machinery in head and neck squamous cell carcinoma: association with clinical outcome. *Clin. Cancer Res.* **11,** 2552–2560 (2005).
38. Ballar, P., Pabuccuoglu, A. & Kose, F. A. Different p97/VCP complexes function in retrotranslocation step of mammalian ER-associated degradation (ERAD). *Int. J. Biochem. Cell Biol.* **43,** 613–621 (2011).
39. Huang, L., Kuhls, M. C. & Eisenlohr, L. C. Hydrophobicity as a driver of MHC class I antigen processing. *EMBO J.* **30,** 1634–1644 (2011).
40. Huang, L., Marvin, J. M., Tatsis, N. & Eisenlohr, L. C. Cutting Edge: Selective role of ubiquitin in MHC class I antigen presentation. *J. Immunol.* **186,** 1904–1908 (2011).
41. Marin, M. B. *et al.* Tyrosinase degradation is prevented when EDEM1 lacks the intrinsically disordered region. *Plos One* **7,** e42998 (2012).
42. Hoelen, H. *et al.* Proteasomal Degradation of Proinsulin Requires Derlin-2, HRD1 and p97. *Plos One* **10,** e0128206 (2015).
43. Imai, J., Hasegawa, H., Maruya, M., Koyasu, S. & Yahara, I. Exogenous antigens are processed through the endoplasmic reticulum-associated degradation (ERAD) in cross-presentation by dendritic cells. *Int. Immunol.* **17,** 45–53 (2005).
44. Ackerman, A. L., Giodini, A. & Cresswell, P. A role for the endoplasmic reticulum protein retrotranslocation machinery during crosspresentation by dendritic cells. *Immunity* **25,** 607–617 (2006).

45. Giodini, A. & Cresswell, P. Hsp90-mediated cytosolic refolding of exogenous proteins internalized by dendritic cells. *EMBO J.* **27,** 201–211 (2008).
46. Menager, J. *et al.* Cross-presentation of synthetic long peptides by human dendritic cells: a process dependent on ERAD component p97/VCP but Not sec61 and/or Derlin-1. *Plos One* **9,** e89897 (2014).
47. Godefroy, E. *et al.* alpha v beta3-dependent cross-presentation of matrix metalloproteinase-2 by melanoma cells gives rise to a new tumor antigen. *J. Exp. Med.* **202,** 61–72 (2005).
48. Renaud, V. *et al.* Folding of matrix metalloproteinase-2 prevents endogenous generation of MHC class-I restricted epitope. *Plos One* **5,** e11894 (2010).
49. Sucker, A. *et al.* Genetic evolution of T-cell resistance in the course of melanoma progression. *Clin. Cancer Res.* **20,** 6593–6604 (2014).
50. Ebstein, F. *et al.* Maturation of human dendritic cells is accompanied by functional remodelling of the ubiquitin-proteasome system. *Int. J. Biochem. Cell Biol.* **41,** 1205–1215 (2009).
51. Fonteneau, J. F. *et al.* Generation of high quantities of viral and tumor-specific human $CD4^+$ and $CD8^+$ T-cell clones using peptide pulsed mature dendritic cells. *J. Immunol. Methods* **258,** 111–126 (2001).
52. Ebstein, F., Lehmann, A. & Kloetzel, P. M. The FAT10- and ubiquitin-dependent degradation machineries exhibit common and distinct requirements for MHC class I antigen presentation. *Cell. Mol. Life Sci.* **69,** 2443–2454 (2012).
53. Keller, M. *et al.* The proteasome immunosubunits, PA28 and ER-aminopeptidase 1 protect melanoma cells from efficient MART-1 -specific T-cell recognition. *Eur. J. Immunol.* **45,** 3257–3268 (2015).
54. Seifert, U. *et al.* Hepatitis C virus mutation affects proteasomal epitope processing. *J. Clin. Invest.* **114,** 250–259 (2004).

Acknowledgements

The project was supported by the Deutsche Forschungsgemeinschaft, grant DFG KL421/11-2 to P.M.K./P.W., to U.S. (SFB-TR36, CRC854) and by grant 106861 of the Deutsche Krebshilfe to P.M.K., D.S., A.P. and U.S and by a Collaborative Research Grant of the Berlin Institute of Health (P.M.K.). We thank T. Rapoport (Department of Cell Biology, Harvard Medical School, Boston, MA) for the p97 plasmids and for the antibodies anti-VIMP and anti-Derlin-1 and R. Hartmann-Petersen (Department of Biology, University of Copenhagen, Copenhagen, Denmark) for antibody anti-p97/VCP.

Author Contributions

F.E, M.K and E.B. performed the experiments. A.P. and D.S. provided the melanoma cell lines. P.W. conceived the study. M.S. designed the experiments and interpreted the data. E.K. interpreted the microarray data. P.M.K. and U.S. conceived and supervised the study, designed the experiments and wrote the manuscript.

Additional Information

Supplementary information accompanies this paper at http://www.nature.com/srep

Competing financial interests: The authors declare no competing financial interests.

How to cite this article: Ebstein, F. *et al.* Exposure to Melan-A/MART-1_{26-35} tumor epitope specific $CD8^+$ T cells reveals immune escape by affecting the ubiquitin-proteasome system (UPS). *Sci. Rep.* **6**, 25208; doi: 10.1038/srep25208 (2016).

SCIENTIFIC REPORTS

OPEN

Proteasomes generate spliced epitopes by two different mechanisms and as efficiently as non-spliced epitopes

Received: 05 January 2016
Accepted: 15 March 2016
Published: 06 April 2016

F. Ebstein[1], K. Textoris-Taube[1], C. Keller[1], R. Golnik[1], N. Vigneron[2], B. J. Van den Eynde[2], B. Schuler-Thurner[3], D. Schadendorf[4], F. K. M. Lorenz[5], W. Uckert[5,6], S. Urban[1], A. Lehmann[1], N. Albrecht-Koepke[1], K. Janek[1], P. Henklein[1], A. Niewienda[1], P. M. Kloetzel[1] & M. Mishto[1]

Proteasome-catalyzed peptide splicing represents an additional catalytic activity of proteasomes contributing to the pool of MHC-class I-presented epitopes. We here biochemically and functionally characterized a new melanoma gp100 derived spliced epitope. We demonstrate that the gp100$^{mel}_{47-52/40-42}$ antigenic peptide is generated *in vitro* and *in cellulo* by a not yet described proteasomal condensation reaction. gp100$^{mel}_{47-52/40-42}$ generation is enhanced in the presence of the β5i/LMP7 proteasome-subunit and elicits a peptide-specific CD8$^+$ T cell response. Importantly, we demonstrate that different gp100^{mel}-derived spliced epitopes are generated and presented to CD8$^+$ T cells with efficacies comparable to non-spliced canonical tumor epitopes and that gp100^{mel}-derived spliced epitopes trigger activation of CD8$^+$ T cells found in peripheral blood of half of the melanoma patients tested. Our data suggest that both transpeptidation and condensation reactions contribute to the frequent generation of spliced epitopes also *in vivo* and that their immune relevance may be comparable to non-spliced epitopes.

CD8$^+$ T cell responses involve in most cases the proteasome-dependent processing of antigens and cell surface presentation of the resulting peptides by MHC-class I molecules to cytotoxic T lymphocytes (CTLs). The 20S standard proteasome (s-proteasome) with its active site β-subunits β1, β2 and β5, the immunoproteasome (i-proteasome) with the IFN-γ-induced catalytic β-subunits β1i/LMP2, β2i/MECL1 and β5i/LMP7 or intermediate proteasome types containing both standard and immuno-subunits[1,2] are the catalytic cores of 30S proteasomes, which are formed by the association of two 19S regulator complexes with the 20S core[3]. The 30S proteasome isoforms execute the regulated degradation of ubiquitin (Ub)-tagged proteins, thereby generating peptides presented by MHC-class I proteins[4,5]. Exchange of standard catalytic subunits for the corresponding IFN-γ-induced β-subunits leads to variations of proteasome catalytic pocket structure and of the peptide transport along the proteasome inner channel[6–8]. Such variations may result in quantitative differences in the proteasome cleavage products, which in turn can strongly affect cell surface presentation of MHC-class I-bound virus- or tumor-specific antigenic peptides and in consequence also the efficacy of a peptide-specific CD8$^+$ T cell response[9,10].

Canonical MHC-class I-bound peptides generated by proteasomes mirror the linear sequence of the parental protein[10]. In contrast, spliced peptides that are presented by MHC-class I molecules and generated by proteasome-catalyzed peptide splicing (PCPS) result from the ligation of two separate distant proteasomal cleavage products that are not contiguous in the parental protein. We previously provided experimental proofs

[1]Institut für Biochemie, Charité-Universitätsmedizin Berlin, Charitéplatz 1, D-10117 Berlin, Germany. [2]Ludwig Institute for Cancer Research, WELBIO (Walloon Excellence in Life Sciences and Biotechnology) and the de Duve Institute, Université catholique de Louvain, Place de l'Université 1, B-1200 Brussels, Belgium. [3]Department of Dermatology, Universitätsklinikum Erlangen, Ulmenweg 18, D-91052 Erlangen, Germany. [4]Klinik für Dermatologie, Venerologie und Allergologie, Universitätsklinikum Essen D - 45122 Essen, Germany & German Cancer Consortium (DKTK), Hufelandstraße 55, D-69120 Heidelberg, Germany. [5]Max-Delbrück-Center for Molecular Medicine, Robert-Rössle-Str. 10, D-13092 Berlin, Germany. [6]Institute of Biology, Humboldt University Berlin, Charitéplatz 1, D-10115 Berlin, Germany. Correspondence and requests for materials should be addressed to P.M.K. (email: p-m.kloetzel@charite.de) or M.M. (email: michele.mishto@charite.de.)

for the hypothesis that PCPS proceeds via a transpeptidation reaction[11–14]. PCPS involves the formation of an *O*-acyl-enzyme intermediate consisting of a N-terminal peptide fragment linked to the Thr1 residue of one of the β-subunit active sites. In the course of the transpeptidation reaction, this acyl-enzyme intermediate is subjected to a nucleophilic attack by the amino-terminus of another peptide fragment leading to the creation of a new peptide containing two non-contiguous fragments of a protein[11,12,15]. Theoretically, spliced peptides may also be produced without the formation of a semi-stable *O*-acyl-enzyme intermediate by a so-called condensation reaction. Condensation reactions forming *de novo* peptide bonds have been described for some proteases to occur *in vitro* under conditions disfavoring diffusion of peptides from the active sites[16,17]. However, whether such a condensation reaction can take place *in cellulo* in the barrel-shaped proteasome controlling peptide diffusion and whether this can contribute to epitope production has yet to be shown.

Five spliced epitopes, derived from the fibroblast growth factor 5 (FGF-$5_{172-176/217-220}$), melanocyte protein gp100^{mel} (gp100$^{mel}_{40-42/47-52}$; gp100$^{mel}_{195-202/192}$), the SP100 nuclear phosphoprotein (SP$100_{296-301/286-289}$) and tyrosinase ($Tyr_{368-373/336-340}$) have been identified so far using cancer patient-derived CTLs for epitope identification[11,12,18–20]. Interestingly, two of these spliced peptide-specific CD8$^+$ T cells have previously been shown to induce regression of tumors in a clinical setting[20,21] or the engraftment of acute myeloid leukemia cells in non-obese diabetic/SCID mice[11,22], indicating their potential immune relevance.

PCPS represents a genuine catalytic activity of proteasomes competing with the normal proteasomal hydrolysis event[14]. Initial estimations of epitope splicing efficacy were calculated to range between 0.0002% and 0.01% of the total proteasome-dependent epitope generation. Therefore, epitope production by PCPS was thought to be an extremely rare event[12,13,16]. However, performing *in vitro* experiments we showed that PCPS may be a relatively frequent process controlled by certain sequence requirements guaranteeing that PCPS is also a highly reproducible reaction[14]. In fact, *in vitro* experiments suggested that potential MHC-class I epitopes are relatively more frequent among spliced peptides than among the "canonical" non-spliced proteasome cleavage products[14,23]. The limited number of spliced tumor epitopes identified most likely resides in the fact that identification of immune-relevant spliced peptides has so far been limited by the serendipitous availability of patient-derived CTLs and the concomitant considerable experimental effort to identify the cognate epitopes.

To close this gap, we here report an algorithm-aided reverse immunology approach permitting the facilitated identification of spliced peptides from a given protein sequence thereby overcoming the need for patient-derived CTLs. By applying this method we here identified a new spliced peptide derived from melanocytic protein gp100^{mel}. This peptide can be generated *in vitro* and *in cellulo* by a condensation reaction. This epitope is presented by patient-derived melanoma cells and triggers activation of CD8$^+$ T cells found in the peripheral blood of melanoma patients. Importantly, we show that spliced epitopes are presented at the cell surface and trigger CTL responses with efficacies similar to non-spliced epitope underlining that PCPS may play an important role in anti-tumor immune responses.

Results

The gp100$^{mel}_{47-52/40-42}$ antigenic peptide is generated by a new proteasomal catalytic mechanism. For identification of new spliced peptides and/or epitopes we subjected the gp100^{mel}-derived synthetic polypeptide substrate gp100$^{mel}_{40-52}$ [RTKAWNRQLYPEW] to *in vitro* digestion by purified human 20S proteasomes. By applying SpliceMet[23] we identified three spliced peptides among the proteasomal processing products. These were the previously reported spliced antigenic peptide gp100$^{mel}_{40-42/47-52}$ [RTK][QLYPEW][12] and the novel gp100$^{mel}_{47-52/40-46}$ [QLYPEW][RTKAWNR] and gp$100_{47-52/40-42}$ [QLYPEW][RTK] peptides (Fig. 1A, Fig. S1). Interestingly, a theoretical IC_{50} value of 86.1 μM for HLA-A*03:01 and HLA-A*011 binding was predicted for gp100$^{mel}_{47-52/40-42}$ [QLYPEW][RTK] by *in silico* analysis[24]. Therefore, we decided to analyze the formation of this potential new spliced tumor epitope in more detail.

Monitoring the *in vitro* generation of the spliced peptides revealed that the spliced peptide gp100$^{mel}_{40-42/47-52}$ was produced approximately 6-fold more efficiently by erythrocytes s-proteasomes than the new spliced gp100$^{mel}_{47-52/40-42}$ peptide, being composed of the same peptide fragments but in reversed order (Fig. 1B). Interestingly, opposite to the generation kinetics of the individual splice-reactants [QLYPEW], [RTKAWNR] or [RTK] (Fig. 1C), spleen i-proteasomes generated the spliced peptides gp$100_{47-52/40-46}$ and gp$100_{47-52/40-42}$ more efficiently than erythrocytes s-proteasomes (Fig. 1D, Fig. S2).

Both the gp100$^{mel}_{47-52/40-42}$ and gp100$^{mel}_{47-52/40-46}$ peptides were the result of the linkage between the gp100 Trp_{52} and Arg_{40} residues of the gp100-derived substrate (Fig. 1E). However, the Trp_{52} residue of the N-terminal splice-reactant [QLYPEW] represents the C-terminal residue of the synthetic polypeptide substrate gp100$^{mel}_{40-52}$. This excluded the formation of an *O*-acyl-enzyme intermediate with the proteasomal active site Thr_1 as a result of peptide-bond hydrolysis as demanded for the established transpeptidation reactions[12,14]. We therefore hypothesized that spliced peptides could also be produced in a proteasome-catalyzed condensation reaction.

To test this hypothesis we co-incubated purified 20S proteasomes with the two splice-reactant peptides gp100$^{mel}_{40-42}$ [RTK] and gp100$^{mel}_{47-52}$ [QLYPEW]. The resulting spliced peptide products were then analyzed by mass spectrometry. In support of our hypothesis, 20S proteasomes catalyzed the formation of the gp100$^{mel}_{47-52/40-42}$ peptide *in vitro* when the two peptides were added individually (Fig. 1E, Fig. S3). In accordance with the results shown in Fig. 1D i-proteasomes derived from different cellular sources catalyzed the condensation reaction with higher efficiency than s-proteasomes (Fig. 1F).

In principle, all active sites of both proteasome isoforms are capable of catalyzing a transpeptidation reaction[14]. However, because condensation reactions require specific favorable conditions[16] we next asked whether any of the proteasome active sites were specifically involved in the condensation reaction. To do so, proteasome active site subunit specific inhibitors, whose active site specificity had been previously documented[25] were added to 20S proteasomes derived from T2 cells (s-proteasome) or LCLs (i-proteasome) together with the two splice-reactants [RTK] and [QLYPEW]. PR-893 (0.5 μM) was used to block the activity of the β5 subunits of 20S s-proteasomes

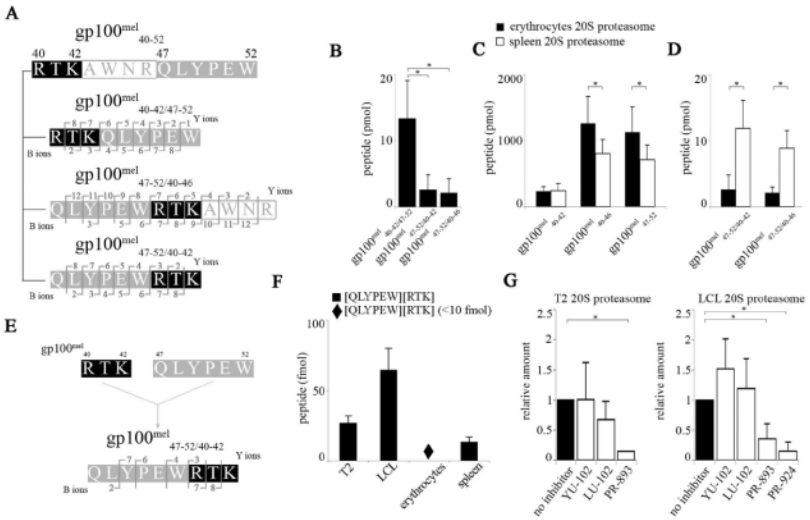

Figure 1. Involvement of proteasome standard- and immuno-subunits in *in vitro* spliced peptide generation. (**A**) B- and Y-ions of the spliced products gp100$^{mel}_{40–42/47–52}$ [RTK][QLYPEW], gp100$^{mel}_{47–52/40–42}$ [QLYPEW][RTK] and gp100$^{mel}_{47–52/40–46}$ [QLYPEW][RTKAWNR] as detected by MS/MS Orbitrap analysis (see also Fig. S1) and derived from gp100$^{mel}_{40–52}$ upon 20S proteasome-catalyzed digestion. (**B**) Erythrocyte 20S s-proteasomes generated larger amount of the spliced peptide gp100$^{mel}_{40–42/47–52}$ than of the gp100$^{mel}_{47–52/40–42}$ and gp100$^{mel}_{47–52/40–46}$ peptides. (**C,D**) Erythrocyte 20S s-proteasomes generated similar or larger amounts of the splice reactants gp100$^{mel}_{40–42}$ [RTK], gp100$^{mel}_{40–46}$ [RTKAWNR] and gp100$^{mel}_{47–52}$ [QLYPEW] (**C**) but less gp100$^{mel}_{47–52/40–42}$ and gp100$^{mel}_{47–52/40–46}$ spliced peptides than spleen 20S proteasomes (**D**). (**B–D**) The means of the amount measured after 3 hrs *in vitro* digestion and the SD between triplicates of two independent experiments are shown. Significant differences of the means are detected by student t test and marked by *. In particular, (**B**) gp100^{mel}: $_{40–42/47–52}$ *vs* $_{47–52/40–42}$, $p = 0.002$; $_{40–42/47–52}$ *vs* $_{47–52/40–46}$, $p < 0.001$; (**C**) gp100$^{mel}_{40–46}$ s- *vs* i-proteasome, $p = 0.036$; gp100$^{mel}_{47–52}$ s- *vs* i-proteasome, $p = 0.043$; (**D**) gp100$^{mel}_{47–52/40–42}$: s- *vs* i-proteasome $p < 0.001$; gp100$^{mel}_{47–52/40–46}$: s- *vs* i-proteasome $p < 0.001$. (**E**) B- and Y-ions of peptide gp100$^{mel}_{47–52/40–52}$ -detected by MALDI-TOF/TOF-MS (Fig. S3) – that was produced by hydrolysis-independent ligation of the splice-reactants [RTK] and [QLYPEW] by 20S proteasome. (**F**) The peptide gp100$^{mel}_{47–52/40–42}$ amount, generated by hydrolysis-independent ligation by i- and s-proteasomes is shown. Amounts below 10 fmol could be detected but not quantified and are symbolized with ♦. (**G**) Absolute amounts of gp100$^{mel}_{47–52/40–42}$ generated in the hydrolysis-independent assay by T2 and LCL 20S proteasomes in the presence of the inhibitors YU-102 (2 μM; β1/β1i-specific), LU-102 (2 μM; β2/β2i-specific), PR-893 (0.5 μM; β5-specific) and PR-924 (0.5 μM; β5i-specific). Significant differences due to the effect of the inhibitors are detected by paired student t test and marked by * (T2 proteasome, control *vs* PR-893, $p = 0.037$; LCL proteasome, control *vs* PR-893, $p = 0.050$; control *vs* PR-924, $p = 0.012$). (**F,G**) The mean (fmol measured in 9 μl reaction) and the SD of independent experiments ($n = 2–3$), each measured in two duplicates are shown.

and PR-924 (0.5 μM) to inhibit the activity of the β5i immuno-subunit[25]. Blockage of either the β5 active site as in T2 cell-derived 20S proteasome or the β5 and β5i active sites as present in LCL-derived proteasomes led to a strong reduction of the condensation reaction (Fig. 1G). In contrast, blocking the β1/β1i and β2/β2i active sites with YU-102 (2 μM) and LU-102 (2 μM) proteasome inhibitors[25], respectively, barely affected the production of the antigenic peptide, suggesting that the condensation reaction was mainly executed by the active sites of the β5 subunit isoforms (Fig. 1G).

Cellular condensation reaction results in the presentation of the gp100$^{mel}_{47–52/40–42}$ peptide. Although our *in vitro* experiments clearly demonstrated that proteasomes are able to generate spliced peptides in a condensation reaction, there still remained the possibility that the *in vitro* experiments as performed here may be artificially influenced by high enzyme and/or substrate concentrations. Therefore, to assess whether the gp100$^{mel}_{47–52/40–42}$ peptide is of any functional relevance and to study whether proteasomes could perform condensation reactions also *in cellulo* we established an immunological read-out system to monitor the generation and MHC class I presentation of gp100$^{mel}_{47–52/40–42}$ in HeLa cells. HLA-A binding affinity assays using HLA-A*03:01-transfected HeLa and T2 cells lines (Fig. 2A,B) as well as mature dendritic cells (data not shown) confirmed the predicted binding of the peptide to HLA-A*03:01 complex. We therefore generated a gp100$^{mel}_{47–52/40–42}$

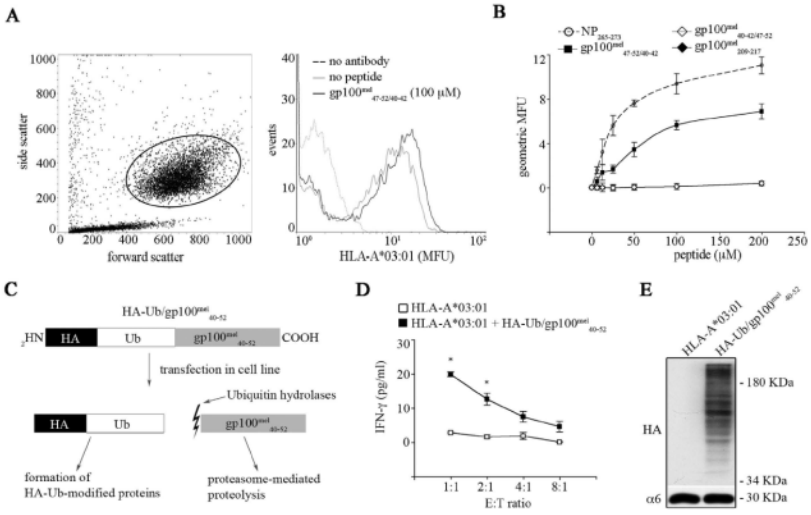

Figure 2. The spliced gp100$^{mel}_{47-52/40-42}$ peptide is generated from the gp100$^{mel}_{40-42}$ peptide by a condensation reaction *in cellulo*. (**A**,**B**) The spliced peptide gp100$^{mel}_{47-52/40-42}$ [QLYPEW][RTK] bound the HLA-A*03:01 complex on the cell surface of HeLa (**A**) and T2 (**B**) cell lines. In (**A**) the side / forward scatters charts are reported in the left panel. Cells included in the analysis are marked with a circle and their HLA-A*03:01 amount is shown in the right panel. (**B**) Shown is the binding affinity of the spliced peptide gp100$^{mel}_{47-52/40-42}$ compared to a known good HLA-A*03:01 – binder, *i.e.* [ILRGSVAHK] ($NP_{265-273}$)[35] and to the negative controls HLA-A*32:01-restricted gp100$^{mel}_{40-42/47-52}$ [RTK][QLYPEW] and HLA-A*02:01-restricted gp100$^{mel}_{209-217}$ [IMDQVPFSV] epitopes. Cells were transfected with HLA-A*03:01 protein encoding plasmids and pulsed with 100 µM (**A**) or different peptide concentrations (**B**). Binding affinity was measured by staining of HLA-A*03:01 and FACS analysis. Values are in mean fluorescence unit (MFU) and are means and SD of 2 replicates in a representative assay of 2–6 independent experiments. (**C**) Schematic representation of the HA-Ub/gp100$^{mel}_{40-52}$ fusion construct used in this study. The first amino acid of the gp100$^{mel}_{40-52}$ [RTKAWNRQLYPEW] sequence was directly fused in frame to the C-terminus of the Ub, which was N-terminally tagged with the YPYDVPDYA HA sequence. When expressed in cells, Ub hydrolases cleaved the fusion-polypeptide directly after the last amino acid (Gly_{76}) of Ub, liberating the gp100$^{mel}_{40-52}$ peptide from the first residue. (**D**) CTL response towards HeLa 33/2 cells transfected with HLA-A*03:01 individually or together with HA-Ub/gp100$^{mel}_{40-52}$ for 24 hrs. Their ability to present gp100$_{47-52/40-42}$ epitope was measured by using K631 1C CTL. After 16 hrs co-culture, the IFN-γ concentration in supernatants was determined by ELISA. Values are means and SD of 2 replicates in a representative assay of 6 independent experiments. Significant differences in the means of replicates are marked by * (student t-test; E:T ratio: 1:1, $p = 0.003$; 2:1, $p = 0.050$). (**E**) 10 µg of whole HeLa 33/2 cell extracts were resolved on a 15% SDS-PAGE for western blotting with anti-HA antibody to control the expression of the construct. The western blot is representative of 5 independent assays.

peptide-specific CTL clone from peripheral blood mononuclear cells (PBMCs) of a HLA-A*03:01$^+$ healthy donor (Fig. S4) allowing us to monitor the generation of this potential MHC class I-restricted epitope *in cellulo*.

To monitor the condensation reaction *in cellulo*, HeLa$^{HLA\text{-}A*03:01+}$ cells were transfected with a plasmid expressing a HA-Ub-gp100$^{mel}_{40-52}$ fusion protein (Hela$^{A*03:01+Ub/gp100mel}_{40-52}$). In the fusion protein the GG motif of the ubiquitin was directly linked to the first amino acid residue of the 13-mer gp100$_{40-52}$ peptide allowing the release of the unchanged full-length gp100$^{mel}_{40-52}$ peptide substrate after cleavage behind the GG motif by de-ubiquitinating enzymes (Fig. 2C). CTL assays using the gp100$^{mel}_{47-52/40-42}$ specific CD8$^+$ T cell clone demonstrated that proteasomes could indeed also perform a condensation reaction *in cellulo* (Fig. 2D,E), indicating that in addition to transpeptidation also condensation reactions may also contribute to the cellular pool of spliced epitopes.

The gp100$^{mel}_{47-52/40-42}$ peptide is a tumor epitope presented by melanoma cells. This data raised the question whether the proteasome-catalyzed generation of gp100$^{mel}_{47-52/40-42}$ was solely determined by the biochemical nature of the 13-mer gp100$^{mel}_{40-52}$ substrate and/or the specific assay conditions applied *in vitro* and/or *in cellulo*. To further validate our reverse immunology approach, we next investigated whether the gp100$^{mel}_{47-52/40-42}$ peptide was also naturally produced from full-length gp100^{mel} antigen by patient-derived melanoma cells. Of the five different patient-derived melanoma cell lines tested for gp100^{mel} protein and HLA-A*03:01 expression only Mel63a cells proved to be HLA-A*03:01$^+$/gp100^{mel+} (Fig. 3A,B). Immunoblotting revealed that

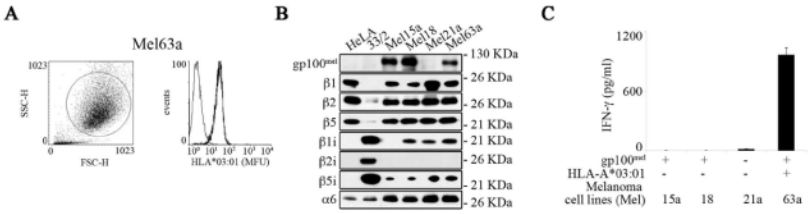

Figure 3. Melanoma Mel63a cells efficiently generate and present the gp100$^{mel}_{47-52/40-42}$ epitope. (**A**) Overlay histograms obtained by flow cytometry showing the cell surface expression of the HLA-A*03:01 molecule (thick line) compared to isotype control (thin line) of the Mel63a melanoma cell line. Shown is a representative staining of 2 independent experiments. (**B**) The four melanoma cell lines Mel15a, Mel18, Mel21a and Mel63a were analyzed by western blotting for their content of gp100^{mel}, the proteasome subunits β1, β2, β5, β1i, β2i, β5i and α6 (the latter as loading control). HeLa cells and HeLa 33/2 cells were used as controls for s- and i-proteasomes, respectively. (**C**) The four melanoma cell lines Mel15a (HLA-A*03:01$^-$/gp100$^+$); Mel18 (HLA-A*03:01$^-$/gp100^{mel+}), Mel21a (HLA-A*03:01$^-$/gp100^{mel-}) and Mel63a (HLA-A*03:01$^+$/gp100^{mel+}) were assessed for their ability to present the gp100$^{mel}_{47-52/40-42}$ epitope in a 16 hrs CTL assay to K631 1C CTL clone. Supernatants were collected and tested for their IFN-γ content by ELISA. Values are means and SD of 2 replicates in a representative assay of 2 independent experiments.

Mel63a cells mostly expressed intermediate-type proteasomes, expressing all standard and IFN-γ inducible proteasome subunits except the β2i subunit (Fig. 3B). Interestingly, the Mel63a cells elicited a strong IFN-γ release by the gp100$^{mel}_{47-52/40-42}$ specific T-cell clone, suggesting that the spliced peptide gp100$^{mel}_{47-52/40-42}$ can indeed be produced from the full-length gp100^{mel} protein (Fig. 3C). This proved that the spliced gp100$^{mel}_{47-52/40-42}$ peptide identified by applying SpliceMet in *in vitro* experiments represented a natural tumor epitope produced from the full-length gp100^{mel} membrane protein and was presented on the surface of gp100^{mel}/HLA-A*03:01$^+$ patient-derived melanoma cells.

The gp100$^{mel}_{47-52/40-42}$ epitope is generated by the ERAD pathway. To exclude the possibility that generation of the gp100$^{mel}_{47-52/40-42}$ peptide was restricted to a specific cell type and to study the contribution of individual proteasome subunits in the production of the peptide, HeLa cells were transfected with plasmids encoding the HLA-A*03:01 protein and a full-length gp100^{mel}-*myc*/His fusion protein. As shown in Fig. 4A, HeLa cells efficiently presented the gp100$^{mel}_{47-52/40-42}$ epitope in a proteasome-dependent manner providing evidence that epitope generation was not dependent on a specific cell type. The *in vitro* experiments had indicated a driving role for the two different β5 subunits in the generation of the gp100$^{mel}_{47-52/40-42}$ epitope (see Fig. 1F,G). To study the role of the β5-subunit isoforms in a cellular context, we monitored gp100$^{mel}_{47-52/40-42}$ epitope presentation in HeLa 33/2 cells, which constitutively express i-proteasomes, using a siRNA approach. The siRNA-induced silencing of β5i subunit expression resulted in its substitution by the standard β5 subunit within the 20S proteasome complex (Fig. 4B). This subunit substitution led to a remarkable reduction of gp100$^{mel}_{47-52/40-42}$ presentation underlining the importance of the β5i subunit for this splicing reaction (Fig. 4B). Corroborating this result, over-expression of the β5i subunit in HeLa cells and concomitant formation of β5i/ β1/β2 subunits containing intermediate type 20S proteasomes led to a strong increase in gp100$^{mel}_{47-52/40-42}$ presentation (Fig. 4C). Interestingly, the proteasome subunit composition found in Hela cells overexpressing β5i subunit was similar to that observed in Mel63a cells suggesting that the intermediate type proteasomes carrying β5i, β2 and β1 subunits are best equipped for the generation and presentation of this spliced epitope.

Because gp100^{mel} is a membrane protein we also asked whether generation of the gp100$^{mel}_{47-52/40-42}$ epitope from gp100^{mel} protein resulted from the ER-associated ubiquitin-dependent protein degradation pathway (ERAD). To test this, expression of the ubiquitin-receptor subunit Rpn10 residing in the 19S complex and of the ERAD component p97/VCP were silenced by siRNA. As shown in (Fig. 4D) silencing of either Rpn10 or p97/VCP expression significantly impaired the endogenous gp100$^{mel}_{47-52/40-42}$ epitope presentation providing evidence that PCPS takes place as part of normal ubiquitin-dependent protein degradation and can also involve the ERAD pathway.

PBMCs of melanoma patients harbor spliced epitope-specific T cells. Because the gp100$^{mel}_{47-52/40-42}$ epitope had been identified using an open unbiased algorithm-aided reverse immunology approach, the possibility still remained that its identification and generation may have been the result of the experimental set ups. Hence, it was important to validate whether the gp100$^{mel}_{47-52/40-42}$ peptide was also generated *in vivo* and that melanoma patients possessed CD8$^+$ T cells directed against this epitope.

For proof of principal, we therefore tested whether HLA-A*03:01$^+$ melanoma patients possessed CD8$^+$ T cells directed against the gp100$^{mel}_{47-52/40-42}$ peptide (Fig. 5A) and/or the HLA-A*03:01-restricted spliced peptide gp100$^{mel}_{195-202/192}$ [RSYVPLAH][R] (Fig. 5B), which was previously shown to trigger a T cell response in melanoma patients[18]. In total, PBMCs from 20 randomly chosen melanoma patients and 4 healthy controls were analyzed. Interestingly, 6/12 untreated patients and 2/8 vaccinated patients displayed T cells reactive against the gp100$^{mel}_{47-52/40-42}$ epitope (Fig. 5A). Only 1 out of 4 healthy controls had a measurable specific response toward

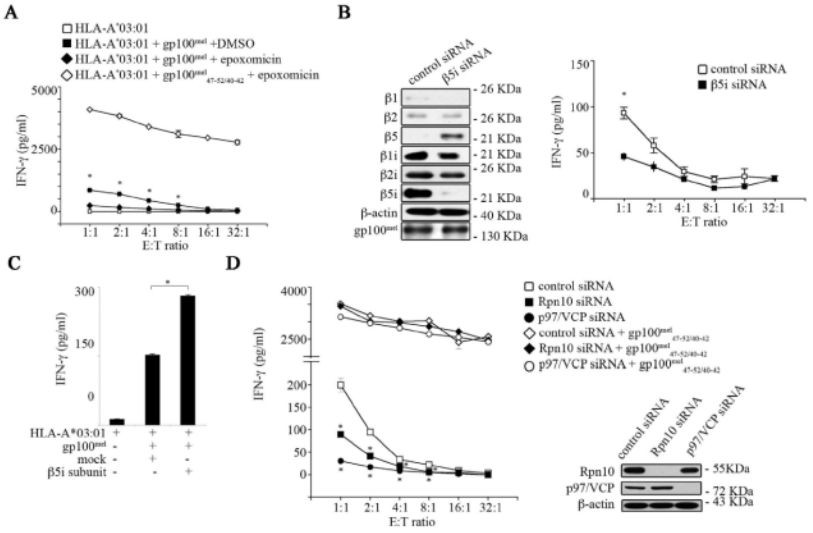

Figure 4. Ub-proteasome- and ERAD-dependent $gp100^{mel}_{47-52/40-42}$ epitope production is enhanced by β5i subunit. (**A**) HeLa cells were transfected with HLA-A*03:01 and $gp100^{mel}$, and were subjected to epoxomicin treatment (250 nM; 2 hrs) or DMSO (control) and compared to HeLa cells transfected with HLA-A*03:01 treated with epoxomicin (250 nM; 2 hrs) and pulsed with the synthetic peptide $gp100^{mel}_{47-52/40-42}$ (50 μM). Values are means and SD of 2 replicates in a representative assay of 2 independent experiments. Significant differences (between the samples with or without epoxomicin) in the means of replicates are marked by * (student t-test; E:T ratio: 1:1, $p = 0.002$; 2:1, $p = 0.001$; 4:1, $p < 0.001$; 8:1, $p < 0.001$). (**B**) HeLa 33/2 cells were exposed to β5i subunit or control siRNAs (30 nM for 24 hrs) and subsequently transfected with $gp100^{mel}$. Cell extracts were analyzed by western blotting (representative of 4 independent experiments). β5i subunit-depleted HeLa 33/2 cells were subjected to a 16 hr CTL assay. Values are means and SD of 2 replicates in a representative assay of 4 independent experiments. Significant differences in the means of replicates are marked by * (student t-test; $p = 0.047$). (**C**) HeLa cells were transfected with plasmids encoding HLA-A*03:01, $gp100^{mel}$ full-length protein, β5i subunit or the empty vector. The HeLa cell ability to process the $gp100^{mel}_{47-52/40-42}$ was assessed by CTL assay. Values are means and SD of 2 replicates in a representative assay of 4 independent experiments. Significant difference in the means of replicates is marked by * (student t-test; $p = 0.001$). (**D**) HeLa cells were exposed to 30 nM siRNA specific for the 19S Rpn10 subunit or p97/VCP (or control siRNA) prior to transfection with the HLA-A*03:01 and the full-length $gp100^{mel}$ protein plasmids and pulsed or not pulsed with the synthetic peptide $gp100^{mel}_{47-52/40-42}$ (30 μM). Values are means and SD of 2 replicates in a representative assay of 3 independent experiments. Significant differences in the means of replicates are marked by * (student t-test) for Rpn10 siRNA (E:T ratio: 1:1, $p = 0.038$; 2:1, $p = 0.029$; 4:1, $p = 0.047$; 8:1, $p = 0.002$) and for p97/VCP siRNA (E:T ratio: 1:1, $p = 0.016$; 2:1, $p = 0.020$; 4:1, $p = 0.024$; 8:1, $p = 0.001$). The knock-down efficiencies were monitored by determining the steady-state level of Rpn10 or p97/VCP proteins by western blotting.

the same spliced epitope (Fig. 5A), as further confirmed by FACS analysis (Fig. 5C). On the other hand, 5/6 untreated and 2/8 vaccinated melanoma patients contained T cells recognizing the $gp100^{mel}_{195-202/192}$ peptide (Fig. 5B). This data demonstrated that our algorithm-based reverse immunology approach is a potent strategy to identify new spliced epitopes. They also suggested that proteasome-catalyzed generation of spliced antigenic peptides is not an isolated singular event but is part of the physiological proteasome-dependent epitope generation process, which elicits specific $CD8^+$ T cell responses *in vivo* in melanoma patients.

Spliced and non-spliced epitopes are presented at the cell surface in comparable amount. Despite being an important issue in judging the immune relevance of spliced epitopes, there exists no study comparing the relative presentation efficacy of different spliced epitopes with each other or with non-spliced epitopes. The $gp100^{mel}$ antigen seemed be ideally suited for such an analysis because the spliced peptides $gp100^{mel}_{47-52/40-42}$ (HLA-A*03:01), $gp100^{mel}_{40-42/47-52}$ (HLA-A*32:01), $gp100^{mel}_{195-202/192}$ (HLA-A*03:01) and the non-spliced $gp100^{mel}_{209-217}$ (HLA-A*02:01) were all generated from the same protein. To extend the analysis to a second and $gp100^{mel}$-independent non-spliced epitope we also included the tumor-associated HLA-A*02:01-restricted epitope NY-ESO-$1_{157-165}$[26] into the comparison. However, to perform such comparison, different HLA-A peptide binding affinities, HLA expression levels as well as the different affinities of the $CD8^+$ T cells have to be taken into consideration.

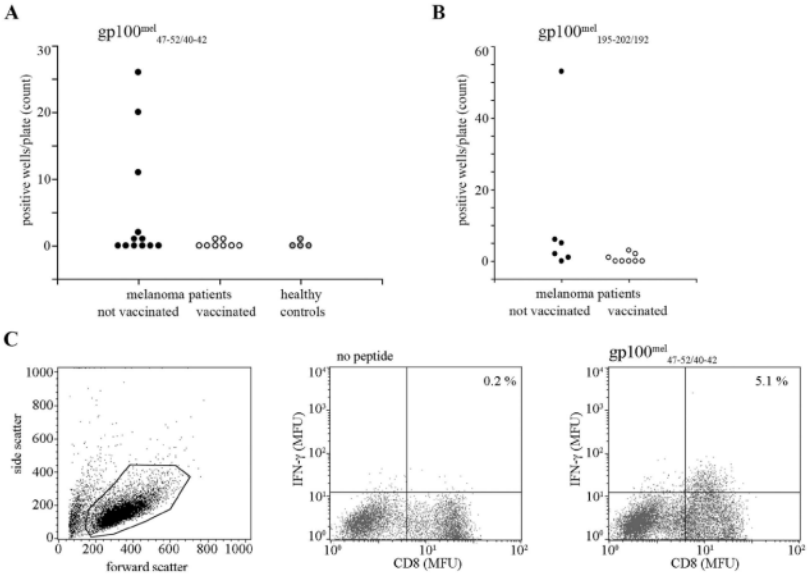

Figure 5. IFN-γ responses to the gp100$^{mel}_{47-52/40-42}$ and gp100$^{mel}_{195-202/192}$ spliced peptides in HLA-A*03:01^{+} healthy controls and melanoma patients. PBMCs from healthy controls and patients with melanoma vaccinated or not with dendritic cells pulsed with the gp100$^{mel}_{209-217}$ peptide were cultured in 96-well plates and stimulated with 30 μM gp100$^{mel}_{47-52/40-42}$ (**A**) or gp100$^{mel}_{195-202/192}$ (**B**) synthetic peptides. After 10 days of culture, the presence of CTLs specific for gp100$^{mel}_{47-52/40-42}$ and gp100$^{mel}_{195-202/192}$ epitopes in each well was assessed by re-stimulating the cells with the gp100$^{mel}_{47-52/40-42}$ or gp100$^{mel}_{195-202/192}$ peptide in a 16 hr assay in the presence of CD28/CD49d co-stimulatory molecules. A negative control without peptide was included in all experiments. After 16 hrs, supernatants were collected and tested for their IFN-γ content by ELISA. Shown is the number of wells per plate in which the IFN-γ secretion upon peptide stimulation was larger than 100 pg/ml and at least twice as large as that detected without peptide for each patient and/or control. (**C**) Validation of the ELISA outcome on the representative healthy control well showing the larger IFN-γ response by CD8^{+} T cells in presence of the target spliced epitope. CTLs were double stained for CD8 and intracellular IFN-γ by FACS analysis. The side/forward scatters chart is reported in the left panel. Cells included in the analysis are marked with a circle and are shown in the two right panels, where CTLs were co-cultivated for 16 hrs with antigen presenting cells pulsed or not pulsed with the 30 μM gp100$^{mel}_{47-52/40-42}$ synthetic peptide prior the FACS analysis.

Therefore we first performed titration experiments with HeLa cells expressing the target HLA-A molecules, pulsed with the antigenic peptides and co-cultivated them with the respective peptide-specific CD8^{+} T-cell clones (Fig. 6A–E upper panels). By measuring the resulting IFN-γ release, informative titration curves where obtained for all antigenic peptides (Fig. 6B–E) but the non-spliced gp100$^{mel}_{209-217}$ epitope (data not shown). Because gp100$^{mel}_{209-217}$ is known be a poor HLA-A*02:01 binder, we consequently performed the titration experiments with the previously described $_{M210}$gp100$^{mel}_{209-217}$ peptide, in which the anchor residue T_{210} of gp100^{mel} was exchanged with a Methionine for better HLA-A *02:01 binding. T cell assays were performed with transduced CD8^{+} T cells expressing the corresponding TCR. In this case satisfactory titration curves were obtained (Fig. 6A). We next transfected HeLa$^{HLA\text{-}A*03:01+}$ cells with plasmids encoding the $_{M210}$gp100^{mel} variant, or the NY-ESO-1 proteins together with the three HLA-A*32:01, -A*02:01 and -A*03:01molecules. The transfected cells were then tested for their ability to activate CD8^{+} T-cells specific for each of the peptides as outlined above (Fig. 6A–E lower panels).

We considered the measured IFN-γ release obtained with an 4:1 E:T ratio and determined the corresponding peptide concentrations on the basis of the titration experiments. We chose the 4:1 E:T ratio to obtain IFN-γ release values in the log-phase of the titration curves. By applying this method we obtained a semi-quantitative comparison of the amount of non-spliced *vs* spliced epitopes generated by proteasomes of HeLa cells and presented by MHC class I molecules and. As shown in Fig. 6F the amounts of the spliced gp100$^{mel}_{40-42/47-52}$ epitope and of the non-spliced epitope $_{M210}$gp100$^{mel}_{209-217}$ were comparable and the amounts of the spliced gp100$^{mel}_{40-42/47-52}$ epitope exceeded those of all other epitopes analyzed. In contrast, cell surface expression of the new spliced gp100$^{mel}_{47-52/40-42}$ epitope was significantly lower, which is in agreement with our observation that s-proteasomes produce only relatively low amounts of the gp100$^{mel}_{47-52/40-42}$ epitope. Interestingly, also the expression of the non-spliced NY-ESO-$1_{157-165}$ epitope was lower than that of the gp100$^{mel}_{40-42/47-52}$ and $_{T210M}$gp100$^{mel}_{209-217}$ epitopes and comparable with the

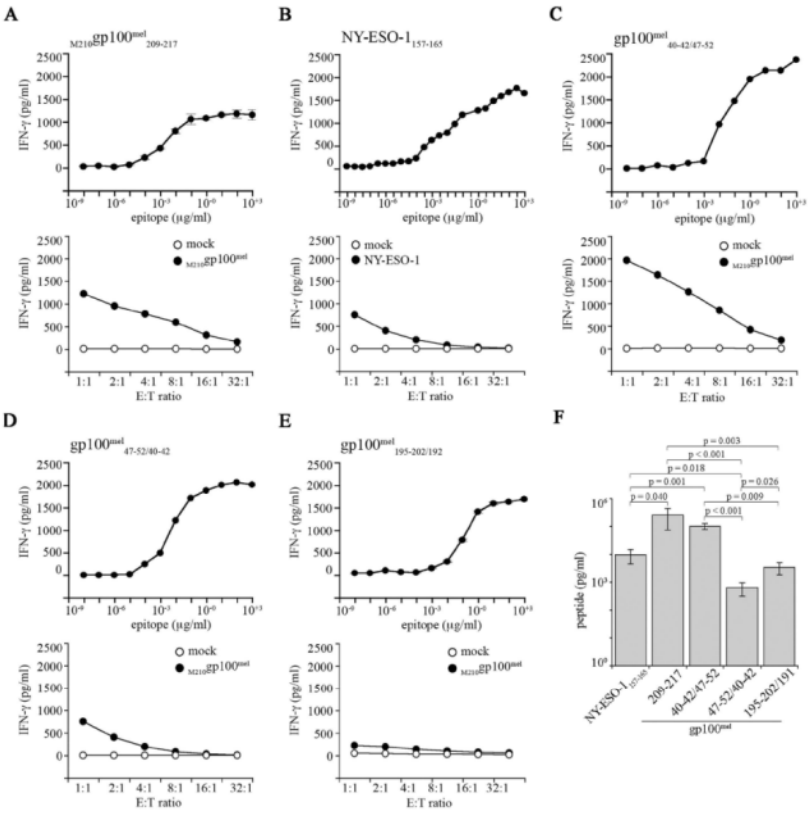

Figure 6. The processing efficacy of the gp100^{mel}–derived spliced epitopes is comparable to that of the non-spliced $_{M210}$gp100$^{mel}_{209–217}$ and NY-ESO-1$_{157–165}$ epitopes. (**A–E**) The IFN-γ-release by specific CD8$^+$ T cell clones exposed to HLA-A*03:01/-A*02:01/-A*32:01$^+$ HeLa cells (E:T = 1:1) pulsed with different concentrations of the synthetic peptides (upper panels) or HLA-A*03:01/-A*02:01/-A*32:01$^+$ HeLa cells transfected with the target antigen (lower panels) is shown for the epitopes $_{M210}$gp100$^{mel}_{209–217}$ (**A**), NY-ESO-1$_{157–165}$ (**B**), gp100$^{mel}_{40–42/47–52}$ (**C**), gp100$^{mel}_{47–52/40–42}$ (**D**) or gp100$^{mel}_{195–202/192}$ (**E**). The data are the mean and bars the SD of three replicates of a representative assay of independent experiments (n = 2–6). (**F**) We here report a marker of the amount of epitope presented on the cell surface of HLA-A*03:01/-A*02:01/-A*32:01$^+$ HeLa cells transfected with the target antigen. By titrations (upper panels in **A–E**) we calculated the amount of synthetic peptide pulsed on to HeLa cells, which triggered the release of IFN-γ amount corresponding to the IFN-γ released by the specific CD8$^+$ T cell clones exposed to HLA-A*03:01/-A*02:01/-A*32:01$^+$ HeLa cells transfected with the target antigen and cultivated in an E:T ratio = 4:1 (see lower panels in **A–E**). Values are the means and bars the SEM of independent experiments (n = 2–7; each experiment with three independent replicates). Significant differences in the means are marked and the corresponding by p values are reported (we applied the Mann-Whitney test with Bonferroni correction for multiple comparison). The IFN-γ-release in the medium was measured by ELISA after 16 hrs co-culture.

spliced gp100$^{mel}_{195–202/192}$ epitope, requiring C-terminal trimming. As a control, we compared the CD8$^+$ T-cell response towards gp100$^{mel}_{40–42/47–52}$ and gp100$^{mel}_{47–52/40–42}$ epitopes in HeLa cells expressing the wild-type gp100^{mel} and the mutated $_{T210M}$gp100^{mel} proteins in two independent experiments. No difference emerged confirming that the use of the $_{T210M}$gp100^{mel} variant did not affect the generation of the distant spliced epitopes (Fig. S5).

In summary, these experiments demonstrate that generation and presentation of spliced epitopes occurs with efficacies similar to what is observed for canonical non-spliced epitopes and do not represent exceptions with respect to their immune relevance.

Discussion

Generation of spliced epitopes is an additional proteasome-dependent activity, contributing to the pool of MHC-class I presented antigenic peptides. A number of features of the proteasome-dependent splicing events

indicate that peptide splicing is not an accidental side reaction of proteasome activity but rather an authentic post-translational modification. One important aspect of PCPS is the fidelity of the process because to trigger a $CD8^+$ T cell response a spliced peptide must be repeatedly generated from a given substrate protein. Thus, for a functional purpose of the resulting splicing products PCPS must be a finely tuned event[27]. However, a proteasome-catalyzed splicing event is difficult to detect because it requires the complementary information on gene sequence and processing events. Because of that, spliced epitopes have so far escaped wide spread identification using available databases in combination with mass spectrometric analyses. We here applied an algorithm aided reverse immunology approach, which *a priori* does not rely on available patient-derived $CD8^+$ T cells and therefore greatly facilitates the identification of new spliced epitopes.

As part of our analyses the spliced $gp100^{mel}_{47-52/40-42}$ peptide was identified as a new HLA-A*03:01-restricted tumor epitope expressed on patient-derived $gp100^{mel+}$ melanoma cells. Interestingly, the $gp100^{mel}_{47-52/40-42}$ peptide was generated *in vitro* from the same $gp100^{mel}_{40-52}$ 13-mer polypeptide substrate as the previously reported spliced $gp100^{mel}_{40-42/47-52}$ epitope[12] but with the same peptide fragments being arranged in reverse order. This disclosed that in addition to the well-established transpeptidation reaction[11,12,14] PCPS could also involve condensation reactions that *in vitro* are independent of prior proteasomal peptide-bond hydrolysis. Production of the spliced antigenic peptide in a condensation reaction could also be observed *in cellulo* when the 13-mer $gp100^{mel}_{40-52}$ polypeptide substrate was expressed in HeLa cells as part of an ubiquitin fusion protein. Condensation reactions performed by proteinases have only been reported to occur *in vitro* under defined diffusion-limiting conditions. The gated barrel-shaped catalytic cavity of the 20S proteasome hindering rapid diffusion of the generated peptide as well as the catalytic activity of Thr1 via the formation of an ester-bond intermediate may however explain why proteasomes are able to perform condensation reactions also in a cellular environment with relative efficacy. In fact, in case the peptide ligands are held in the right orientation in close proximity, this does not even require catalysis. It is however not possible to determine the extent to which condensations reactions participate *in cellulo* to the overall production of the $gp100^{mel}_{47-52/40-42}$ peptide from the full-length $gp100^{mel}$ protein.

Theoretically, only relatively few MHC-class I-peptide complexes have to be exposed at the cell surface to trigger an immune response[28] and T cells directed against spliced epitopes have been identified among a subset of tumor infiltrating lymphocytes[10]. Nevertheless, the notion that spliced epitopes represented a curiosity still prevailed and doubts remained whether PCPS was a sufficiently frequent event to play any significant role in MHC class I-restricted immune responses. Importantly, PCPS does not randomly produce an unlimited number of all theoretically possible spliced peptides[14,23]. Rather, PCPS seemed to be restricted by certain sequence characteristics of the substrate protein, guaranteeing a high reproducibility in the generation of spliced epitopes[14]. But similar to the well-characterized proteasome-generated non-spliced epitopes for which reliable rules are still missing, general sequence rules governing spliced epitope generation are so far unresolved.

An important issue with respect to their immune relevance and a still unresolved question was whether spliced epitope presentation is at all comparable with that of non-spliced conventional tumor epitopes. Therefore, in a semi-quantitative analysis we also compared for the first time the relative efficacy of endogenous presentation of three different $gp100^{mel}$ derived spliced epitopes with that of two non-spliced tumor epitopes. Relative cell surface presentation efficacy of the three $gp100^{mel}$ derived spliced epitopes analyzed here differed considerably among each other. In particular, cell surface expression of the spliced $gp100^{mel}_{40-42/47-52}$ epitope was significantly superior to the presentation of the newly identified $gp100^{mel}_{47-52/40-42}$ epitope, which is composed of the same splice-reactants but in reverse order. This difference may be explained in that the reverse order peptide-ligation by either transpeptidation or condensation is less efficient and/or that the generation of the $gp100^{mel}_{47-52/40-42}$ epitope is not favored by s-proteasomes. Importantly, our data show for the first time that the overall relative cell surface expression levels of the spliced epitopes is comparable to that of the non-spliced $gp100^{mel}_{209-217}$ and NY-ESO-$1_{157-165}$ epitopes. This suggests that with regard to their relative presentation efficacy proteasome-generated spliced epitopes exert features almost identical to those known for non-spliced epitopes and do not greatly differ from what is known for canonical epitopes.

Considering that the spliced $gp100^{mel}_{47-52/40-42}$ epitope was identified in an unbiased reverse immunology approach and the fact that the PBMCs from approximately 50% of randomly chosen untreated melanoma patients contained $CD8^+$ T cells that were stimulated by the $gp100^{mel}_{47-52/40-42}$ peptide suggested that generation of spliced epitopes is indeed a rather frequent event. Corroborating this result, five out of six untreated patient samples turned out to contain memory $CD8^+$ T cells responsive to the spliced HLA-A*03:01-restricted epitope $gp100^{mel}_{195-202/191}$ [RSYVPLAH][R] that had initially been identified through the analysis of tumor infiltrating lymphocytes[18]. That a fewer number of samples obtained from melanoma patients having undergone vaccination with dendritic cells were responsive to the spliced antigenic peptides might be owed to the fact that they contained a relatively larger percentage of T cells directed against the non-spliced peptides, which were used for vaccination. Although our assay conditions are not designed to prime naïve T-cells in that dendritic cells were in low number and not activated, we can not completely exclude that the immune response towards the spliced epitopes may in part be due to priming and the activation of naïve $CD8^+$ T cells during the *in vitro* assays

Supporting the conclusion that generation of MHC-class I ligands by PCPS was not a rare event, we also identified, by applying our SpliceMet-supported reverse immunology approach, a significant number of potential spliced epitopes derived from human $gp100^{mel}$ or *Listeria monocytogenes* LLO antigens and with high HLA-A and/or -B binding affinity, which warrant further immunological characterization (Table 1).

Our data also demonstrated that PCPS is intrinsically linked to ubiquitin-dependent proteasomal protein turnover and proteasomal hydrolysis events and that it was not a rare side reaction. Since peptide exhibiting features suitable for binding to MHC class I molecules seem to occur in among spliced peptides with a certain preference[14], the relative probabilities for generation of a spliced epitope or a non-spliced epitope from a given substrate are most likely not very different. Therefore, the pool of spliced antigenic peptides available for selection by the antigen presentation machinery may be significantly larger than previously estimated. In fact, as shown

Spliced peptide	Sequence	HLA-A and/or -B (IC50, nM)
substrate **gp100$^{mel}_{35-57}$ –VSRQLRTKAWNRQLYPEWTEAQR**		
gp100$^{mel}_{35-39/35-39}$	[VSRQL] [VSRQL]	B*27:05 (148)
gp100$^{mel}_{45-52/35-37}$	[NRQLYPEW][VSR]	A*31:01 (38)
gp100$^{mel}_{47-52/40-42}$	[QLYPEW][RTK]	A*03 (86)
gp100$^{mel}_{49-52/35-39}$	[YPEW][VSRQL]	B*07:02 (18)
substrate **gp100$^{mel}_{201-230}$ –AHSSSAFTITDQVPFSVSVSQLRALDGGNK**		
gp100$^{mel}_{201-207/201-207}$	[AHSSSAF][AHSSSAF]	A*24:03 (11), B*15:01 (120), B*15:03 (113)
gp100$^{mel}_{210-218/220-222}$	[TDQVPFSVS)][SQL]	B*07:02 (94), B35:01 (182), B39:01 (133)
substrate **LLO$_{291-317}$ –AYISSVAYGRQVYLKLSTNSHSTKVKA**		
LLO$_{291-293/295-302}$	[AYI][SVAYGRQV]	B*15:17 (31)
LLO$_{291-294/297-304}$	[AYIS][AYGRQVYL]	A*02:02 (199), A*02:11 (89), A*02:50 (115), B*15:17 (50).
LLO$_{291-298/291-292}$	[AYISSVAY][AY]	A*01:01 (121), A*29:02 (8), A*30:02 (20), A*68:01 (68), A*80:01 (38), B*15:01 (66), B*15:03 (100), B*35:01 (22)
LLO$_{291-298/291-293}$	[AYISSVAY][AYI]	A*30:01 (145), B*15:17 (52), B*58:01 (25)
LLO$_{299-304/291-293}$	[GRQVYL][AYI]	B*27:05 (99)

Table 1. Potential proteasome-catalyzed spliced antigenic peptides derived from human gp100$^{mel}_{35-57}$, gp100$^{mel}_{201-230}$ and LLO$_{291-317}$ substrates and identified by a reverse immunology approach. Proteasome-generated spliced epitopes were identified by applying SpliceMet[23] on the proteasome-mediated digestion of the synthetic substrates gp100$^{mel}_{35-57}$, gp100$^{mel}_{201-230}$ and *Listeria monocytogenes* LLO$_{291-317}$ as previously reported[14]. Afterwards, the spliced antigenic peptide list was analyzed for binding affinity to human MHC variants using the web-available ANN algorithm[24]. In agreement with our experience, only spliced epitopes with IC50 < 200 nM were considered as potential epitopes. We included in the list the N-terminal-extended precursors of the potential minimal epitopes. For each potential proteasome-catalyzed spliced epitope the human HLA variant and the predicted IC50 (nM) are disclosed.

here for the gp100^{mel} protein PCPS also seems to enlarge the HLA haplotype-restriction of antigenic peptides that can be produced from a single substrate protein thereby broadening the cellular immune response.

Materials and Methods

A detailed Material and Method section is disclosed in the Supplementary information.

Peptide synthesis and quantification. The sequence enumeration for the polypeptides gp100$_{40-52}$ [RTKAWNRQLYPEW], gp100$^{mel}_{209-217}$ [IMDQVPFSV], gp100$^{mel}_{195-202/92}$ [RSYVPLAH][R] are referred to the human protein gp100^{PMEL17}, for the peptide [SLLMWITQC] to the NY-ESO-1 human protein. All peptides were synthesized as described elsewhere[23]. LC-MS analyses were performed as previously described[14]. Database searching was performed using the SpliceMet's ProteaJ algorithm[23]. Quantification of proteasome-generated non-spliced and spliced peptides (Fig. 1, Fig. S2) was carried out by applying the QME method to LC-MS analyses as described elsewhere[14]. For semi-quantitative studies of the amount of the two spliced peptides [QLYPEW][RTK] and [RTK][QLYPEW] (Fig. 1F,G), the heavy peptides QLYPE^{+6}WRTK and RTK^{+6}QLYPEW were used as internal standards. The limit of quantification was set to 10 fmol upon preliminary experiments with synthetic peptide titration

***In vitro* processing of synthetic peptides.** The synthetic peptide gp100$^{mel}_{40-52}$ (40 μM) was digested by 3 μg 20S proteasomes in 100 μl TEAD buffer over time at 37 °C. In the *in vitro* hydrolysis-independent proteasome-mediated experiments (Fig. 1F,G) 5 μg 20S proteasomes were incubated in 100 μl TEAD buffer in presence of 100 μM peptides for 20 hours. For the experiments with the inhibitor PR-893, PR-924 (Onyx Pharmaceuticals, US), YU-102 and LU-102[25] the specific binding to the proteasome subunits was monitored.

20S proteasome purification. 20S proteasomes were purified from LCLs and T2 cell line as previously described[29]. 20S proteasome purified from human erythrocytes and spleen were purchased from BioMol.

Cell culture. Cells used in this study include LCLs, T2 cells, HeLa cells, HeLa 33/2 cells which were all previously described[9,30,31]. The melanoma cell lines Ma-Mel15a, Ma-Mel18, Ma-Mel21a and Ma-Mel63a were established from tumor metastasis and grown in RPMI 1640 with 10% FCS, 1% L-glutamine and 1% penicillin. The CTL clones K631 1C specific for the HLA-A*03:01-restricted gp100$^{mel}_{47-52/40-42}$ epitope and RG39 specific for the HLA*02:01-restricted NY-ESO-1$_{157-165}$ epitope were prepared according to the procedure of Fonteneau *et al.*[32]. The LG2-37.7.14 and M45-3B CD8$^+$ T cell clones specific for the HLA-A*32:01-restricted gp100$^{mel}_{40-42/47-52}$ and HLA-A*03:01-restricted gp100$^{mel}_{195-202/192}$ spliced peptides, respectively were described elsewhere[12,18]. The gp100^{mel}-specific TCR-transduced T cells were generated as previously described[33,34].

HLA-A03:01-peptide binding affinity. Binding affinity of synthetic peptides were computed with different peptide concentration in a standard binding affinity assay measured by flow cytometry as described elsewhere[29], using HeLa or T2 cells transfected with the HLA-A*03:01-expressing plasmid.

Plasmid and siRNA transfection. Expression vectors used in thy study include the pcDNA3.1 (HLA-A*02:01, HLA-A*32, β5i), pcDNA3.1/myc-HIS ($gp100^{mel}$, NY-ESO-1) and the pcDNA3.1(+)/Zeo (HLA-A*03:01, HA-Ub/$gp100^{mel}_{40-52}$) plasmids. Transfection of HeLa and 33/2 cells or T2 cells was performed using Lipofectamin2000 or Amaxa-Nucleofactor technology, respectively, according to the manufacturer's instructions. All siRNA (control, Rpn10 and p97/VCP) used in this study were purchased from Dharmacon and introduced into HeLa or 33/2 cells as previously described[31].

Antibodies and western blotting. Cell extracts were prepared as previously described[31]. Proteins were resolved by SDS-PAGE and blotted with β1i, β2i, β5i, β1, β2, β5, α6 proteasome subunits, Rpn10, HA, $gp100^{mel}$, p97/VCP and β-actin (as a loading control).

CTL assays and screening of $gp100_{47-52/40-42}$-specific $CD8^+$ T cells in HLA-A*03:01 healthy donors' and melanoma patients' PBMCs. Targets cells were serially diluted and co-cultured with a fixed amount of T cells, resulting in graded effector-to-target (E:T) ratio for 12 h prior to the measurement of IFN-γ release by ELISA. PBMCs from healthy donor or patients with melanoma were pulsed with 30 μM of the $gp100^{mel}_{47-52/40-42}$ synthetic peptide in RPMI medium supplemented with 8% human AB serum, 1% penicillin and IL-2 (50 U/ml). After 10 days of culture, their capacity to produce IFN-γ in response to the cognate peptide was measured by ELISA.

Statistical Analysis

Data were tested for normality distribution and homoscedasticity by Kolmogorov-Smirnov, Shapiro-Wilk and Levene tests. To identify significant difference between groups reported in Fig. 6, Kruskal-Wallis followed by Mann-Whitney tests with Bonferroni Post Hoc correction for multiple comparisons were applied. Otherwise, paired and unpaired Student t-tests were carried out. Descriptive statistics were carried out with SPSS (version 17) and R; a p-value $<= 0.05$ was considered statistically significant.

References

1. Dahlmann, B., Ruppert, T., Kuehn, L., Merforth, S. & Kloetzel, P. M. Different proteasome subtypes in a single tissue exhibit different enzymatic properties. *J Mol Biol* **303,** 643–653 (2000).
2. Guillaume, B. *et al.* Two abundant proteasome subtypes that uniquely process some antigens presented by HLA class I molecules. *Proc Natl Acad Sci USA* **107,** 18599–18604 (2010).
3. Groll, M. *et al.* Structure of 20S proteasome from yeast at 2.4 A resolution. *Nature* **386,** 463–471 (1997).
4. Navon, A. & Ciechanover, A. The 26 S proteasome: from basic mechanisms to drug targeting. *J Biol Chem* **284,** 33713–33718 (2009).
5. Kloetzel, P. M. Antigen processing by the proteasome. *Nat Rev Mol Cell Biol* **2,** 179–187 (2001).
6. Liepe, J. *et al.* Quantitative time-resolved analysis reveals intricate, differential regulation of standard- and immuno-proteasomes. *Elife* doi: 10.7554/eLife.07545 (2015).
7. Huber, E. M. *et al.* Immuno- and constitutive proteasome crystal structures reveal differences in substrate and inhibitor specificity. *Cell* **148,** 727–738 (2012).
8. Arciniega, M., Beck, P., Lange, O. F., Groll, M. & Huber, R. Differential global structural changes in the core particle of yeast and mouse proteasome induced by ligand binding. *Proc Natl Acad Sci USA* **111,** 9479–9484 (2014).
9. Mishto, M. *et al.* Proteasome isoforms exhibit only quantitative differences in cleavage and epitope generation. *Eur J Immunol* **44,** 3508–3521 (2014).
10. Vigneron, N. & Van den Eynde, B. J. Proteasome subtypes and the processing of tumor antigens: increasing antigenic diversity. *Curr Opin Immunol* **24,** 84–91 (2011).
11. Warren, E. H. *et al.* An antigen produced by splicing of noncontiguous peptides in the reverse order. *Science* **313,** 1444–1447 (2006).
12. Vigneron, N. *et al.* An antigenic peptide produced by peptide splicing in the proteasome. *Science* **304,** 587–590 (2004).
13. Dalet, A., Vigneron, N., Stroobant, V., Hanada, K. & Van den Eynde, B. J. Splicing of distant Peptide fragments occurs in the proteasome by transpeptidation and produces the spliced antigenic peptide derived from fibroblast growth factor-5. *J Immunol* **184,** 3016–3024 (2010).
14. Mishto, M. *et al.* Driving Forces of Proteasome-catalyzed Peptide Splicing in Yeast and Humans. *Mol Cell Proteomics* **11,** 1008–1023 (2012).
15. Borissenko, L. & Groll, M. Diversity of proteasomal missions: fine tuning of the immune response. *Biol Chem* **388,** 947–955 (2007).
16. Berkers, C. R., de Jong, A., Ovaa, H. & Rodenko, B. Transpeptidation and reverse proteolysis and their consequences for immunity. *Int J Biochem Cell Biol* **41,** 66–71 (2009).
17. Somalinga, B. R. & Roy, R. P. Volume exclusion effect as a driving force for reverse proteolysis. Implications for polypeptide assemblage in a macromolecular crowded milieu. *J Biol Chem* **277,** 43253–43261 (2002).
18. Michaux, A. *et al.* A Spliced Antigenic Peptide Comprising a Single Spliced Amino Acid is Produced in the Proteasome by Reverse Splicing of a Longer Peptide Fragment followed by Trimming. *J Immunol* **192,** 1962–1971 (2014).
19. Hanada, K., Yewdell, J. W. & Yang, J. C. Immune recognition of a human renal cancer antigen through post-translational protein splicing. *Nature* **427,** 252–256 (2004).
20. Dalet, A. *et al.* An antigenic peptide produced by reverse splicing and double asparagine deamidation. *Proc Natl Acad Sci USA* **108,** 323–331 (2011).
21. Robbins, P. F. *et al.* Recognition of tyrosinase by tumor-infiltrating lymphocytes from a patient responding to immunotherapy. *Cancer Res* **54,** 3124–3126 (1994).
22. Bonnet, D., Warren, E. H., Greenberg, P. D., Dick, J. E. & Riddell, S. R. CD8(+) minor histocompatibility antigen-specific cytotoxic T lymphocyte clones eliminate human acute myeloid leukemia stem cells. *Proc Natl Acad Sci USA* **96,** 8639–8644 (1999).
23. Liepe, J. *et al.* The 20S Proteasome Splicing Activity Discovered by SpliceMet. *Plos Computational Biology* **6,** e1000830 (2010).
24. Peters, B. & Sette, A. Integrating epitope data into the emerging web of biomedical knowledge resources. *Nat Rev Immunol* **7,** 485–490 (2007).
25. Bellavista, E. *et al.* Immunoproteasome in cancer and neuropathologies: a new therapeutic target? *Curr Pharm Des* **19,** 702–718 (2013).

26. Jager, E. *et al.* Induction of primary NY-ESO-1 immunity: CD8+ T lymphocyte and antibody responses in peptide-vaccinated patients with NY-ESO-1+ cancers. *Proc Natl Acad Sci USA* **97,** 12198–12203 (2000).
27. Saska, I. & Craik, D. J. Protease-catalysed protein splicing: a new post-translational modification? *Trends Biochem Sci* **33,** 363–368 (2008).
28. Cresswell, P. Antigen processing and presentation. *Immunol Rev* **207,** 5–7 (2005).
29. Mishto, M. *et al.* Immunoproteasome LMP2 60HH variant alters MBP epitope generation and reduces the risk to develop multiple sclerosis in Italian female population. *Plos One* **5,** e9287 (2010).
30. Mishto, M. *et al.* A structural model of 20S immunoproteasomes: effect of LMP2 codon 60 polymorphism on expression, activity, intracellular localisation and insight into the regulatory mechanisms. *Biol Chem* **387,** 417–429 (2006).
31. Ebstein, F., Lehmann, A. & Kloetzel, P. M. The FAT10- and ubiquitin-dependent degradation machineries exhibit common and distinct requirements for MHC class I antigen presentation. *Cell Mol Life Sci* **69,** 2443–2454 (2012).
32. Fonteneau, J. F. *et al.* Generation of high quantities of viral and tumor-specific human CD4+ and CD8+ T-cell clones using peptide pulsed mature dendritic cells. *J Immunol Methods* **258,** 111–126 (2001).
33. Sommermeyer, D. *et al.* Designer T cells by T cell receptor replacement. *Eur J Immunol* **36,** 3052–3059 (2006).
34. Morgan, R. A. *et al.* High efficiency TCR gene transfer into primary human lymphocytes affords avid recognition of melanoma tumor antigen glycoprotein 100 and does not alter the recognition of autologous melanoma antigens. *J Immunol* **171,** 3287–3295 (2003).
35. Grant, E. *et al.* Nucleoprotein of influenza A virus is a major target of immunodominant CD8+ T-cell responses. *Immunol Cell Biol* **91,** 184–194 (2013).

Acknowledgements

Work described here was supported by a Collaborative Research Grant of the Berlin Institute of Health (P.M.K. & W.U.), the Einstein-Stiftung Berlin (P.M.K.) and the Berlin Krebsgesellschaft (P.M.K.). N.V. is supported by Belgian Program of Interuniversity Poles of Attraction initiated by the Belgian State (Prime Minster´s Office, Science Policy Programming). We thank K. Hummel and E. Bellavista for excellent technical assistance, P. Kunert and B. Brecht-Jachan for the peptide synthesis, T. Ruppert (ZMBH) for Orbitrap support, H.S. Overkleeft, S. Stefanović, K.B. Kim, P. Coulie and Onyx Pharmaceuticals-Amgen subsidiary for providing biotechnological tools to carry out the experiments.

Author Contributions

F.E. and M.M. designed the project, performed experiments, analyzed data and contributed to write the manuscript; P.M.K. designed the project, analyzed data and contributed to write the manuscript; K.T.-T., C.K. and V.N. performed experiments and analyzed data; F.K.M.L., S.U., N.A.-K., P.H., A.N., A.L. and R.G. performed the experiments; K.J. analyzed the data; B.J.V.d.E. and W.U. contributed to write the manuscript; B.S.-T. and D.S. provided clinical samples.

Additional Information

Supplementary information accompanies this paper at http://www.nature.com/srep

Competing financial interests: The authors declare no competing financial interests.

How to cite this article: Ebstein, F. *et al.* Proteasomes generate spliced epitopes by two different mechanisms and as efficiently as non-spliced epitopes. *Sci. Rep.* **6**, 24032; doi: 10.1038/srep24032 (2016).

4.5. Identification of the Rpn10 proteasome subunit as a universal receptor of the MHC class I antigen presentation pathway (this chapter is based on the work of Golnik and coworkers (Golnik et al., 2016))

The degradation of intracellular proteins via the UPS ensures the supply of most of the MHC class I-restricted peptides. Up to now, it remains unclear whether this process is regulated by ubiquitin linkages, length and attachment sites of antigens. In an attempt to better understand the relationship between antigen ubiquitination and MHC class I presentation, we manipulated the ubiquitination profile of the NY-ESO-1 cancer/testis antigen by removing its unique lysine residue at position 124 (K124). Surprisingly, we show that a lysine-free form of NY-ESO-1 (NY-ESO-1^{K0}) was incapable of undergoing K48-linked ubiquitination. Nonetheless, the loss of K48 ubiquitin linkages did not substantially influence the presentation of the HLA-A*0201-restricted NY-ESO-$1_{157\text{-}165}$ antigenic peptide. Indeed, the NY-ESO-$1_{157\text{-}165}$ CTL responses initiated by either wild-type NY-ESO-1 or NY-ESO-1^{K0} were comparable and mainly driven by the β_2 catalytic proteasome subunit. Of note, despite exhibiting distinct ubiquitination patterns, both of these antigen forms were entirely dependent on the Rpn10 proteasome subunit for the generation of the NY-ESO-$1_{157\text{-}165}$ epitope. Our work therefore identifies Rpn10 as a major antigen receptor of the MHC class I processing pathway, and further suggests that such recognition of antigens occurs independently of their ubiquitination profile.

THE JOURNAL OF BIOLOGICAL CHEMISTRY VOL. 291, NO. 16, pp. 8805–8815, April 15, 2016

Major Histocompatibility Complex (MHC) Class I Processing of the NY-ESO-1 Antigen Is Regulated by Rpn10 and Rpn13 Proteins and Immunoproteasomes following Non-lysine Ubiquitination*

Received for publication, November 20, 2015, and in revised form, February 19, 2016 Published, JBC Papers in Press, February 22, 2016, DOI 10.1074/jbc.M115.705178

Richard Golnik, Andrea Lehmann, Peter-Michael Kloetzel, and Frédéric Ebstein[1]

From the Institute for Biochemistry, Charité-Universitätsmedizin Berlin, Charité Platz 1/Virchowweg 6, 10117 Berlin, Germany

The supply of MHC class I-restricted peptides is primarily ensured by the degradation of intracellular proteins via the ubiquitin-proteasome system. Depending on the target and the enzymes involved, ubiquitination is a process that may dramatically vary in terms of linkages, length, and attachment sites. Here we identified the unique lysine residue at position 124 of the NY-ESO-1 cancer/testis antigen as the acceptor site for the formation of canonical Lys-48-linkages. Interestingly, a lysine-less form of NY-ESO-1 was as efficient as its wild-type counterpart in supplying the HLA-A*0201-restricted NY-ESO-$1_{157–165}$ antigenic peptide. In fact, we show that the regulation of NY-ESO-1 processing by the ubiquitin receptors Rpn10 and Rpn13 as a well as by the standard and immunoproteasome is governed by non-canonical ubiquitination on non-lysine sites. In summary, our data underscore the significance of atypical ubiquitination in the modulation of MHC class I antigen processing.

Most of the MHC class I-restricted antigenic peptides are generated through the degradation of intracellular proteins by proteasomes (1, 2). Proteasomes are multicatalytic assemblies that are primarily found as 20S and/or 26S complexes in the cytoplasm and nuclei of all eukaryotic cells. The 20S particle is defined as the latent and free form of proteasomes and consists of two copies of seven different α and seven different β subunits with two α rings surrounding two β rings (3, 4). The 26S complex is made up of one 20S catalytic core that is bound to each end by one 19S regulatory complex (5). The peptidase activity of both 20S and 26S complexes is ensured by the incorporation of the β5, β1, and β2 catalytic subunits. Upon exposure to IFN-α/β and/or IFN-γ, three additional non-essential catalytic β subunits (β5i, β1i, and β2i) are up-regulated and incorporated in place of the β5, β1, and β2 subunits during *de novo* assembly, ensuring a shift from the standard proteasome configuration to an immunoproteasome (IP),[2] which has been shown to be more effective at the removal of damaged proteins (6–8). Under physiological conditions, the majority of proteasomes exist in the form of 26S complexes, which is the configuration responsible for ATP- and ubiquitin (Ub)-dependent degradation (9).

In this pathway, substrates destined to be broken down must undergo a so-called ubiquitination process (sometimes also referred as to ubiquitylation) that relies on a three-step enzymatic cascade involving E1, E2, and E3 enzymes that allows the covalent transfer of cellular Ub to target proteins. Ubiquitination primarily occurs via isopeptide bonds to lysine residues of target proteins (10). Meanwhile, a number of protein substrates have been shown to be conjugated on threonine, serine, and cysteine residues as well as at the N terminus (11–13). The Ub molecule itself possesses seven lysine residues (Lys-6, Lys-11, Lys-27, Lys-29, Lys-33, Lys-48, and Lys-63) as well as an NH_2-terminal methionine (referred as to M1), each of which serves as a potential acceptor site for the formation of poly-Ub chains (14). This allows the assembly of at least eight types of poly-Ub chains with distinct topologies and outcomes for the modified protein. Importantly, ubiquitination is thought to operate at least at two distinct levels *in vivo*. It may be initiated on fully translated mature proteins or during protein synthesis. The latter is part of a quality control process that allows the rapid ubiquitination and subsequent proteasome-mediated degradation of newly synthetized proteins that have accumulated errors and/or damage during translation (*i.e.* defective ribosomal products or DRiPs) (15, 16). Both mature proteins and DRiPs have been shown to be sources for MHC class I antigen presentation (17, 18).

Depending on the number and/or nature of acceptor sites, mature proteins or DRiPs may therefore be subjected to a considerable variety of ubiquitination combinations. Whether these ubiquitination sites and/or linkage types directly influence MHC class I antigen presentation is unknown. Here we set out to address this issue by analyzing the ubiquitination profile of the NY-ESO-1 cancer/testis antigen, which presents the unique advantage of containing only one lysine residue at position 124. In this work, we show that the mature NY-ESO-1 form devoid of Lys-124 (NY-ESO-1^{K0}) greatly differs from its wild-type counterpart in terms of attachment sites and linkages. However, despite those differences, the presentation of the HLA-A*0201-restricted NY-ESO-$1_{157–165}$ peptide emerging from NY-ESO-

* This work was supported by grants from the Berlin Institute of Health (CRG Project) (to P. M. K.) and from the Einstein Foundation Berlin (to P. M. K.). The authors declare that they have no conflicts of interest with the contents of this article.

[1] To whom correspondence should be addressed: Charité-Universitätsmedizin Berlin, Institut für Biochemie, Charité Platz 1/Virchowweg 6, 10117 Berlin, Germany. Tel.: 49-30-450-528-394; Fax: 49-30-450-528-921; E-mail: frederic.ebstein@charite.de.

[2] The abbreviations used are: IP, immunoproteasome; Ub, ubiquitin; DRiP, defective ribosomal product; CTL: cytotoxic T lymphocyte; TEV, tobacco etch virus; NY-ESO-1, New York esophageal squamous cell carcinoma 1.

1^{K0} was not altered. Our data suggest that atypical linkages and/or sites actively participate in the regulation of MHC class I antigen processing.

Experimental Procedures

Reagents—The proteasome inhibitors MG-132 and epoxomicin were purchased from Calbiochem. *N*-ethylmaleimide and cycloheximide were obtained from Sigma. The PR-893-specific inhibitor for the β5 standard subunit was provided by Onyx Pharmaceuticals, Inc. (an Amgen subsidiary, South San Francisco, CA) and the YU-102 β1/LMP2-specific inhibitor was a gift from Dr. Kyung-Bo Kim (Department of Pharmaceutical Sciences, University of Kentucky, Lexington, KY).

Antibodies—The mouse monoclonal antibodies against NY-ESO-1 (clone E978), LMP7 (clone A-12), c-*myc* (clone 9E10), Rpn13 (clone Q31), cathepsin D (sc-6486), and β-actin (clone C4) were obtained from Santa Cruz Biotechnology, Inc. Antibodies directed against ubiquitin (clone FK2), β1 (clone MCP421), β2 (clone MCP165), Rpn10 (clone S5a-18), and α6 (clone MCP20) were purchased from Enzo Life Sciences. The goat anti-MECL1 polyclonal antibody (PA5-19146) was obtained from Thermo Scientific. Rabbit anti-β5 (ab3330) and anti-LMP2 (ab3328) antibodies were purchased from Abcam. Other antibodies used in this work included HA.11 (clone 16B12, Covance), GFP (clone JL-8, TaKaRa, Clontech), LC3B (2775, Cell Signaling Technology), and ubiquitin (Dako). The secondary goat anti-rabbit or anti-mouse antibodies conjugated with peroxidase were obtained from Calbiochem and used at a 1:5000 dilution.

Cells and Culture Conditions—HeLa cells were cultivated in Iscove's medium supplemented with 10% FCS, 1% L-glutamine, and 1% penicillin/streptomycin (all purchased from Biochrom AG). The 33/2 cell line is a derivative of HeLa cells and has been described previously (19). The CTL clone RG39 specific for the HLA-A*0201-restricted NY-ESO-$1_{157-165}$ peptide was prepared as described previously (19).

Plasmid Construction and Transfection—The cDNA for CTAG1b encoding the full-length NY-ESO-1 protein was amplified by RT-PCR from RNA of HT1080 cells and cloned into pcDNA3.1/*myc*-HIS version B (Invitrogen) to construct a C-terminally *myc*-HIS-tagged NY-ESO-1. A single amino acid substitution (Lys-3→Arg-3) of the EQKLISEEDL *myc* tag sequence was introduced by site-directed mutagenesis using primer pairs containing the appropriate base changes to generate a pcDNA3.1/NY-ESO-1/*myc**-HIS with a modified EQRLISEEDL *myc** tag devoid of lysine residues. The pcDNA3.1/NY-ESO-1/*myc**-HIS was used again as a template for site-directed mutagenesis to substitute the unique lysine residue of NY-ESO-1 at position 124 into an arginine (K124R) and to generate a pcDNA3.1/NY-ESO-1^{K124R}/*myc**-HIS construct (referred as to NY-ESO-1^{K0} in this paper). For N-terminal tagging of NY-ESO-1 and NY-ESO-1^{K0}, oligonucleotides encoding a short 9-mer V5 sequence (IPNPLLGLD) fused to a tobacco etch virus (TEV) protease-sensitive site (ENLYFQG) were constructed, annealed, and inserted in-frame into the pcDNA3.1/NY-ESO-1/*myc**-HIS and pcDNA3.1/NY-ESO-1^{K0}/*myc**-HIS plasmids to generate V5-TEV-NY-ESO-1-*myc**/HIS and V5-TEV-NY-ESO-1^{K0}-*myc**/HIS constructs. Both of these constructs were further used as templates for site-directed mutagenesis to substitute the NY-ESO-1 methionine initiation codon at position 20 into a valine one and to generate the V5-TEV-NY-ESO-1^{M20V}-*myc**/HIS, V5-TEV-NY-ESO-$1^{M20V/K0}$-*myc**/HIS variants. The HA-Ub-GFP construct has been described previously (19). Multiple lysine mutations of HA-Ub-GFP were generated by site-directed mutagenesis to generate HA-$Ub^{K6\text{-only}}$-GFP, HA-$Ub^{K11\text{-only}}$-GFP, HA-$Ub^{K27\text{-only}}$-GFP, HA-$Ub^{K29\text{-only}}$-GFP, HA-$Ub^{K33\text{-only}}$-GFP, HA-$Ub^{K48\text{-only}}$-GFP, and HA-$Ub^{K63\text{-only}}$-GFP. Mammalian cells were transfected using Lipofectamine 2000 (Invitrogen) according to the instructions of the manufacturer.

NY-ESO-1 Pulldown—Subconfluent HeLa or 33/2 cells grown in 10-cm tissue culture dishes were subjected to a first transfection with the wild-type HA-Ub-GFP plasmid or one of the HA-Ub-GFP mutant constructs for 24 h prior to another subsequent transfection with either NY-ESO-1 or NY-ESO-1^{K0}. Sixteen hours after the second transfection, cells were incubated with 10 μM MG-132 for 6 h before collection. Cells expressing an NY-ESO-1 antigen form or not (as negative control) were washed twice with PBS and lysed in lysis buffer containing 50 mM Tris HCl (pH 8.0), 150 mM NaCl, 1% Triton X-100, as well as 10 μM MG-132 and 50 mM *N*-ethylmaleimide. Whole cell extracts were incubated for 30 min at 4 °C and subsequently centrifuged at 10,000 rpm for 10 min at 4 °C. Supernatants were then collected and used immediately for the pulldown of *myc*-tagged NY-ESO-1 proteins using magnetic beads conjugated with μMACS anti-*myc* antibodies (Miltenyi Biotec). Briefly, 5 mg of protein lysate was supplemented with 50 μl of μMACS anti-*myc* beads for 30 min at 4 °C. Subsequently, labeled cell lysates were applied to MACS columns in a separator (Miltenyi Biotec) and washed five times with a first buffer containing 50 mM NaCl, 1% Nonidet P-40, 0.5% sodium deoxycholate, and 0.1% SDS. In some experiments, the NaCl concentration in this wash buffer was increased up to 3 M. The second wash was carried out using a buffer consisting of 20 mM Tris HCl (pH 7.5). After the last washing step, proteins were eluted in 85 μl of elution buffer (50 mM Tris HCl (pH 6.8), 50 mM DTT, 1 mM EDTA, 0.005% bromphenol blue, and 10% glycerol). The precipitates were finally subjected to SDS-PAGE, followed by Western blotting using specific antibodies.

TEV Protease On-bead Digestion Assay—HeLa cells were transfected with HA-Ub-GFP together with V5-TEV-NY-ESO-1^{M20V}-*myc**/HIS, V5-TEV-NY-ESO-$1^{M20V/K0}$-*myc**/HIS, or MART-1-*myc*/HIS (as a control). One day after transfection, cells were exposed to a 6-h treatment with 10 μM MG-132 prior to a NY-ESO-1 pulldown as described above. Digestion of V5-TEV-NY-ESO-1^{M20V}-*myc**/HIS and V5-TEV-NY-ESO-$1^{M20V/K0}$-*myc**/HIS was carried out while the proteins were still bound to μMACS anti-*myc* beads by adding 20 units of TEV protease for 150 min at 22 °C. Subsequently, the beads were washed several times, as described above, and the eluted material was further assessed by Western blotting.

siRNA Transfection—ON-TARGET-plus SMARTpool siRNA duplexes (Dharmacon) against Rpn10 (PSMD4, L-011365-00-0005), Rpn13 (ADMR1, L-01234-00-0005), LMP7 (PSMB8,

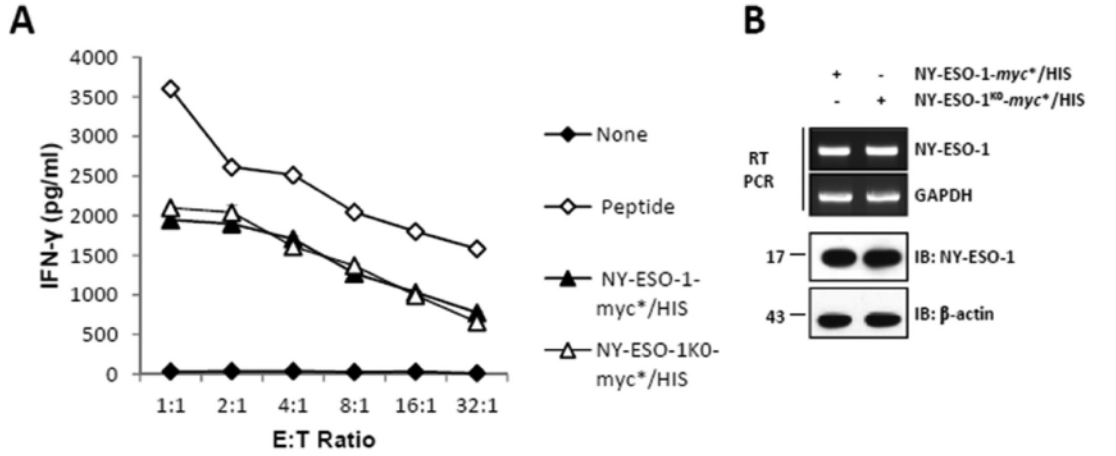

FIGURE 1. **The unique lysine residue of NY-ESO-1 at position 124 is not essential for NY-ESO-1$_{157-165}$ presentation.** *A*, HeLa cells were subjected to 24-h transfection with HLA-A*0201 together with either NY-ESO-1 or NY-ESO-1^{KO}. The NY-ESO-1$_{157-165}$ CTL response was assessed using the CTL clone RG39 specific for NY-ESO-1$_{157-165}$ at various effector:target ratios as indicated. Internal controls in this experiment consisted of HLA-A*0201-expressing HeLa cells or cells loaded with 10 μM of the 9-mer SLLMWITQV synthetic peptide. After 16 h of co-culture, supernatants were tested for their IFN-γ content by ELISA. The results are expressed as mean ± S.D. of duplicate values. Shown is one representative experiment of three. *B*, NY-ESO-1 expression was analyzed by RT-PCR (*top panel*) and Western blotting (*bottom panel*) as indicated. *IB*, immunoblot.

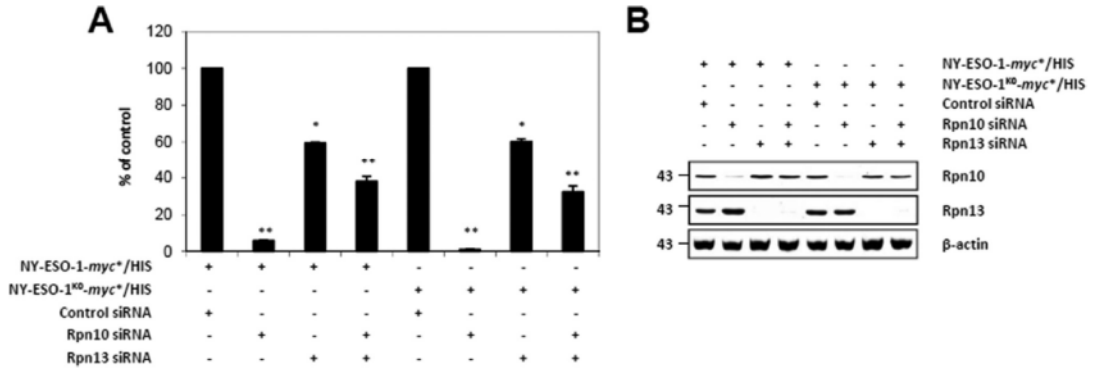

FIGURE 2. **The Rpn10 and/or Rpn13 dependences do not vary between NY-ESO-1 and NY-ESO-1^{KO} for presentation of the NY-ESO-1$_{157-165}$ antigenic peptide.** *A*, HeLa cells were exposed to control siRNA or siRNA specific against Rpn10 and/or Rpn13 for 3 days prior to subsequent transfection with either NY-ESO-1 or NY-ESO-1^{KO}, as indicated. The NY-ESO-1$_{157-165}$ CTL response arising from NY-ESO-1 or NY-ESO-1^{KO} in cells exposed to Rpn10 and/or Rpn13 siRNA was assessed by culturing these cells in the presence of the RG39 CTL clone at a ratio of 1:1. After 16 h of co-culture, supernatants were tested for their IFN-γ content by ELISA. Data are expressed as the percentage relative to cells exposed to control siRNA. Shown is one representative experiment of three. *, $p < 0.05$; **, $p < 0.01$ *versus* control siRNA (Student's *t* test). *B*, the knockdown efficiency of Rpn10 and/or Rpn13 in these cells was evaluated by monitoring the steady-state levels of both of these proteins by Western blotting with antibodies specific for Rpn10 and Rpn13.

L-006022-00-0005), and LMP2 (PSMB9, L-006023-00-0005) were used at 50 nM final concentration. Approximately 2×10^5 cells were seeded into one well of a 6-well tissue culture plate the day before siRNA transfection. All transfections were done using X-tremeGENE siRNA reagent (Roche). The siRNA efficiency in this work was validated by monitoring the siRNA-induced knockdown by Western blotting.

RNA Isolation, Reverse Transcription, and PCR Analysis—Total RNA was isolated using the kit from Roche according to the instructions of the manufacturer. RT-PCR was then performed using 1 μg of total RNA with a primer specific for NY-ESO-1 and GAPDH (loading control).

Antigen Presentation Assays—HeLa cells were transiently transfected with HLA-A*0201 together with either NY-ESO-1 or NY-ESO-1^{KO} and used as targets for their potential to activate the production of IFN-γ by the CTL clone RG39 recognizing the NY-ESO-1$_{157-165}$ peptide. Following a 24-h transfection, target cells were serially diluted and then co-cultured with a fixed amount of T cells, resulting in graded effector:target ratio in a final volume of 100 μl on 96-well plates. After 16-h incubation, the supernatants were collected, and the IFN-γ content was determined using a commercially available human ELISA kit (BD Biosciences) according to the instructions of the manufacturer. The data in the figures refer to the mean of two replicates. The standard deviation was below 5% of the mean.

Statistics—Student's *t* test (one-tailed) was used for data analysis when appropriate.

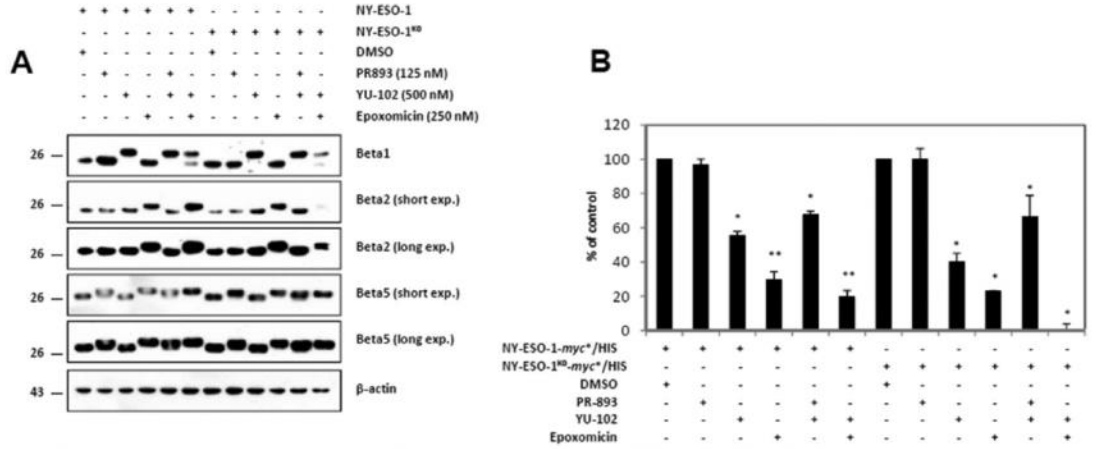

FIGURE 3. **The generation of the NY-ESO-$1_{157-165}$ peptide from NY-ESO-1 or NY-ESO-1^{KO} is mainly driven by the β2 catalytic proteasomal subunit.** *A*, HeLa cells expressing HLA-A*0201 together with either NY-ESO-1 or NY-ESO-1^{KO} were treated for 2 h with PR-893 (125 nM), YU-102 (500 nM), and epoxomicin (250 nM) individually or in combination, as indicated. Covalent binding of the inhibitors to any of the three standard subunits in cells expressing HLA-A*0201/NY-ESO-1 or HLA-A*0201/NY-ESO-1^{KO} was monitored by Western blotting using antibodies specific for β1, β2, β5, and β-actin (loading control). *DMSO*, dimethyl sulfoxide. *B*, the effects of the PR-893, YU-102, and/or epoxomicin on the NY-ESO-$1_{157-165}$ CTL responses emerging from NY-ESO-1 or NY-ESO-1^{KO} were examined in a 16-h CTL assay using RG39 CTL. IFN-γ was measured by ELISA. The results are expressed as percentage relative to cells exposed to dimethyl sulfoxide. Shown is one representative experiment of three. *, $p < 0.05$; **, $p < 0.01$ *versus* dimethyl sulfoxide (Student's *t* test).

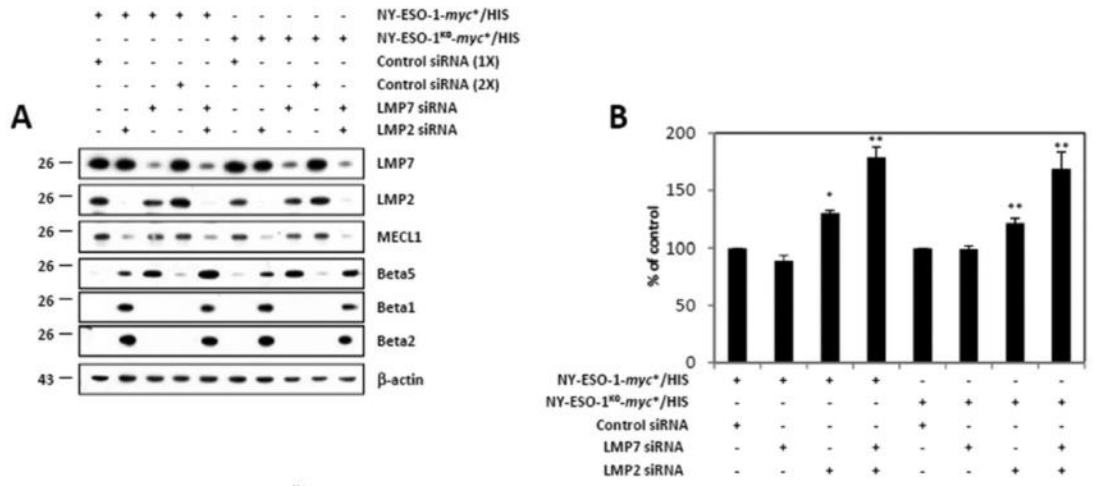

FIGURE 4. **Both NY-ESO-1 and NY-ESO-1^{KO} are more effective at producing the NY-ESO-$1_{157-165}$ antigenic peptide in cells lacking the IP-inducible subunits.** *A*, 33/2 cells were exposed to control (once or twice), LMP7, and/or LMP2 siRNA for 2 days before being subjected to a subsequent transfection with NY-ESO-1 or NY-ESO-1^{KO}. Cell extracts were analyzed by Western blotting using antibodies specific for LMP7, LMP2, MECL1, β5, β1, β2, and β-actin (loading control). *B*, 33/2 cells with a knockdown of LMP7 and/or LMP2 and expressing either NY-ESO-1 or NY-ESO-1^{KO} were evaluated for their capacity to present the NY-ESO-$1_{157-165}$ peptide by exposing them to our CTL clone RG39 for 16 h at a effector:target ratio of 8:1. IFN-γ was measured by ELISA. The data are expressed as percentage relative to cells exposed to control siRNA. Shown is one representative experiment of three. *, $p < 0.05$; **, $p < 0.001$ *versus* control siRNA (Student's *t* test).

Results

The Removal of the Unique Lysine Residue of the NY-ESO-1 Antigen Does Not Affect the Presentation of the NY-ESO-$1_{157-165}$ Antigenic Peptide—To determine whether the unique lysine residue of NY-ESO-1 is an essential target for ubiquitination, allowing degradation and subsequent MHC class I antigen presentation, we generated a lysine-free form of NY-ESO-1 (*i.e.* NY-ESO-1^{KO}) by introducing a single Lys-to-Arg change into a C-terminal *myc**/HIS-tagged version of NY-ESO-1 protein at position 124. As shown in Fig. 1*A*, NY-ESO-1 and NY-ESO-1^{KO} yielded comparable NY-ESO-$1_{157-165}$ CTL responses when expressed in HeLa cells, as evidenced by similar IFN-γ levels produced by our RG39 clone. Likewise, the Lys-to-Arg mutation had no substantial effect on the transcription and/or steady-state expression level of NY-ESO-1 and/or NY-ESO-1^{KO}, as determined by RT-PCR and Western blotting, respectively (Fig. 1*B*). Together, these data demonstrate that Lys-124, as the unique canonical ubiquitination site of the NY-ESO-1

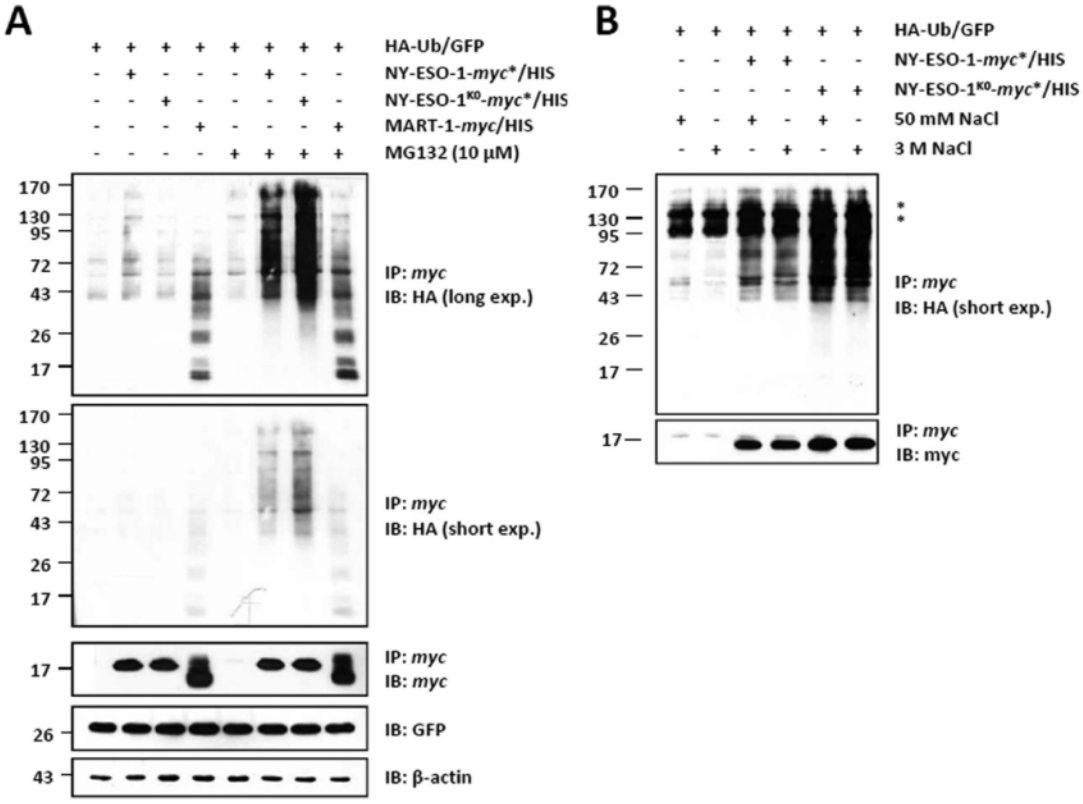

FIGURE 5. **The unique lysine residue of NY-ESO-1 at position 124 is not required for NY-ESO-1 ubiquitination.** *A*, whole cell extracts were prepared from HeLa cells co-expressing HA-Ub-GFP together with NY-ESO-1, NY-ESO-1^{KO}, or the MART-1 melanoma antigen (as a control) in the presence or absence of a 6-h treatment with 10 μM MG-132. *In vivo* ubiquitination of NY-ESO-1 or NY-ESO-1^{KO} was visualized by pulling down NY-ESO-1 with anti-*myc* beads, followed by Western blotting using antibodies specific for HA and NY-ESO-1 (which served as a loading control for the pulldown). Cell extracts were subjected to Western blotting analysis using antibodies specific for HA, *myc*, GFP, and β-actin (loading control) as indicated. *IP*, immunoprecipitation; *IB*, immunoblot. *B*, *in vivo* ubiquitination of NY-ESO-1 or NY-ESO-1^{KO} was visualized by precipitating NY-ESO-1 with anti-*myc* beads prior to five stringent washes with either 50 mM or 3 M NaCl as indicated. After a final wash with 20 mM Tris, the anti-*myc*-bound material was eluted, and the precipitates were analyzed by Western blotting using antibodies specific for HA and *myc*. The *asterisks* represent nonspecific bands. Shown is one representative experiment of two.

antigen, is not essential for the presentation of NY-ESO-1$_{157-165}$ peptide.

NY-ESO-1$_{157-165}$ Presentation Relies on Rpn10 and, to a Lesser Extent, on Rpn13—We next determined whether our two NY-ESO-1 antigen sources differ in their capacity to bind the Ub receptors Rpn10 (20, 21) and/or Rpn13 (22). Consistent with its role as the major Ub receptor, Rpn10 knockdown led to a nearly complete inhibition of NY-ESO-1$_{157-165}$ presentation regardless of the NY-ESO-1 form used (Fig. 2*A*). Interestingly, a much lower inhibition of the NY-ESO-1$_{157-165}$ CTL response was observed in cells with an individual knockdown of Rpn13 or a combined knockdown of Rpn10 and Rpn13 for both NY-ESO-1 and NY-ESO-1^{KO}. The observation that Rpn10/Rpn13 double knockdown was less efficient than the Rpn10 single one in impeding the NY-ESO-1$_{157-165}$ CTL response can likely be attributed to the fact that cells exposed to both Rpn10 and Rpn13 siRNA achieved a less effective down-regulation of Rpn10 compared with cells exposed to Rpn10 siRNA alone (Fig. 2*B*). The exact similarity in the levels of NY-ESO-1$_{157-165}$ CTL response between NY-ESO-1 and NY-ESO-1^{KO} following depletion of Rpn10 and/or Rpn13 suggests that both of these antigens are equally well recognized by 26 proteasomes.

NY-ESO-1 Critically Requires Proteasomal β2 Catalytic Activity for Generation of the NY-ESO-1$_{157-165}$ Antigenic Peptide—To unveil a possible relationship between ubiquitination and proteasomal processing, we next profiled the contribution of the three catalytic activities of the β5, β1, and β2 standard subunits to the generation of the NY-ESO-1$_{157-165}$ peptide. To this end, HeLa cells were engineered to express either NY-ESO-1 or NY-ESO-1^{KO} before being treated with the PR-893, YU-102, and/or epoxomicin inhibitors. PR-893 is the human homolog of the PR-825 inhibitor specific for the β5 subunit, whereas YU-102 is an inhibitor known for its capacity to block β1-activity without affecting β5 and β2 activities (23). Epoxomicin is an irreversible proteasome inhibitor that blocks β5 at low concentrations and both β5 and β2 when incubated with cells at higher concentrations (24). The specificity of these inhibitors in our cell system was controlled by monitoring their

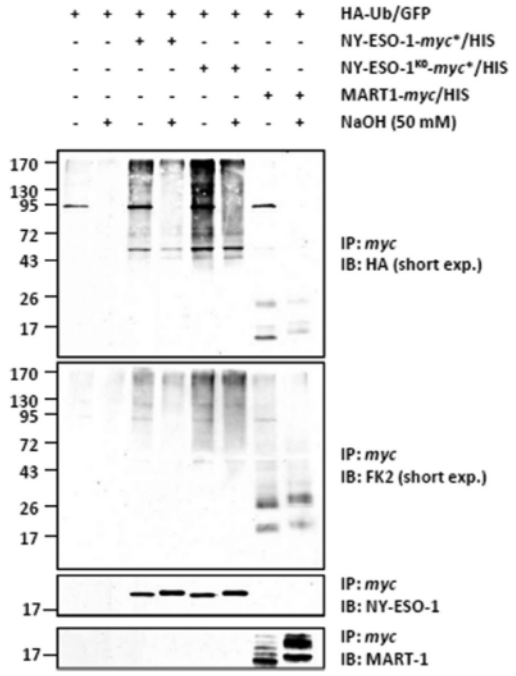

FIGURE 6. **Ubiquitination of the NY-ESO-1 and NY-ESO-1^{KO} tumor antigens occurs on serine and/or threonine residues in HeLa cells.** HeLa cells expressing HA-Ub-GFP in combination with NY-ESO-1, NY-ESO-1^{KO}, or the MART-1 melanoma antigen (as a control) were subjected to protein extraction. NY-ESO-1 and/or NY-ESO-1^{KO} were pulled down by anti-*myc* beads, and the precipitates were treated with 50 mM NaOH for 25 min at 32 °C or left untreated, as indicated. The negative control for the immunoprecipitation (*IP*) in this experiment consisted in HeLa cells only transfected with the HA-Ub-GFP construct (*first* and *second lanes*). The effect of the alkaline treatment on the ubiquitination of NY-ESO-1, NY-ESO-1^{KO}, and MART-1 was assessed by Western blotting using antibodies specific for HA, ubiquitin, and NY-ESO-1 (loading control). *IB*, immunoblot.

potential binding to any of the β_1, β_2, and β_5 subunits by Western blotting. As expected, β5 and β1 shifted up in the presence of PR-893 and YU-102, respectively, confirming subunit inhibition specificity in this assay (Fig. 3*A*). Exposure of the cells to 250 nM epoxomicin resulted in an evident upward shift of the β5 and β2 bands.

Treatment of cells with epoxomicin together with YU-102 resulted in the covalent modification of all three subunits (Fig. 3*A*) and was accompanied by a significant drop in NY-ESO-$1_{157-165}$ presentation regardless of the NY-ESO-1 antigen form used (Fig. 3*B*). These data unambiguously indicate that the generation of the NY-ESO-$1_{157-165}$ peptide is proteasome-dependent. Unexpectedly, PR-893 alone failed to substantially influence the NY-ESO-$1_{157-165}$ CTL response emerging from NY-ESO-1 or NY-ESO-1^{KO}. By contrast, a substantial reduction in NY-ESO-$1_{157-165}$ presentation could be observed following exposure of the cells to the YU-102 inhibitor. Of note, PR-893 showed no substantial additive effect on the YU-102-induced down-regulation of the NY-ESO-$1_{157-165}$ presentation, confirming that the activity of the β5 subunits was dispensable in this process. Because epoxomicin, which blocks both β5 and β2, dramatically affects presentation and given that β5 was not required, we reasoned that generation of NY-ESO-$1_{157-165}$ is mainly driven by the β2 subunit.

The NY-ESO-$1_{157-165}$ CTL Response Is Affected by IP—We next compared the abilities of NY-ESO-1 and NY-ESO-1^{KO} to generate the NY-ESO-$1_{157-165}$ peptide in the presence of immunoproteasomes. To this end, 33/2 cells that stably expressed LMP7, LMP2, and MECL1 (19) were treated with siRNA directed against each of the inducible subunit prior to a 24-h transfection with plasmids encoding either NY-ESO-1 or NY-ESO-1^{KO}. As expected the down-regulation of LMP7 was accompanied by a parallel rise of its β5 standard counterpart subunit (Fig. 4*A*). Similarly, the suppression of LMP2 and MECL1 by LMP2 siRNA resulted in an increased expression of both of the β1 and β2 standard subunits. As shown in Fig. 4*B*, the NY-ESO-$1_{157-165}$ CTL response was not affected by LMP7 depletion in cells expressing either NY-ESO-1 or NY-ESO-1^{KO}. However, the NY-ESO-$1_{157-165}$ presentation was improved in 33/2 cells expressing either NY-ESO-1 or NY-ESO-1^{KO} following exposure to LMP2 siRNA. Likewise, 33/2 cells with an LMP7/LMP2 double knockdown and expressing either NY-ESO-1 or NY-ESO-1^{KO} exhibited a typical standard proteasome composition that was by far much more efficient than the IP of 33/2 cells exposed to control siRNA in generating the NY-ESO-$1_{157-165}$ antigenic peptide (Fig. 4*B*). These data show that standard proteasomes process the NY-ESO-$1_{157-165}$ peptide better than IPs.

Lys-124 Removal Affects the Ubiquitination Profile of the NY-ESO-1 Mature Protein—To determine whether the K124R mutation affects NY-ESO-1 ubiquitination, HeLa cells were transiently transfected with a C-terminal *myc**/HIS-tagged version of NY-ESO-1 or NY-ESO-1^{KO} or the MART-1 melanoma antigen (as a control) in combination with an HA-tagged Ub-GFP (HA-Ub-GFP) construct. As shown in Fig. 5*A*, significant amounts of slowly migrating forms of NY-ESO-1 were detected with both NY-ESO-1 and NY-ESO-1^{KO} precipitates using the HA antibody. Importantly, such HA-protein conjugates were only detectable in the presence of MG-132, indicating that they serve as a target signal for proteasome-mediated degradation. Noteworthy, apart from the fact that the NY-ESO-1 pulldown was conducted utilizing ionic detergent-based buffers, the exposure of the NY-ESO-1 bead-bound immune complexes to very high salt concentrations failed to alter the HA smears of NY-ESO-1 and NY-ESO-1^{KO} (Fig. 5*B*). This indicates that the binding of HA-Ub to NY-ESO-1 or NY-ESO-1^{KO} is indeed of a covalent nature. Surprisingly, the conjugation of NY-ESO-1^{KO} to the HA-Ub construct was even superior to that observed with NY-ESO-1. Because a C terminus-mediated sample enrichment exclusively provides full-length (*i.e.* fully translated) products, these data suggest that Lys-124 removal increases ubiquitination arising from the mature NY-ESO-1 protein.

NY-ESO-1 and NY-ESO-1^{KO} Use Different Acceptor Sites for Ubiquitination—Having demonstrated that Lys-124 of NY-ESO-1 is not critical for either ubiquitination and/or presentation of the NY-ESO-$1_{157-165}$ peptide, we next sought to identify other sites responsible for NY-ESO-1 ubiquitination. To determine whether NY-ESO-1 undergoes ubiquitination via Ser and/or Thr residues, HeLa cells were first engineered to

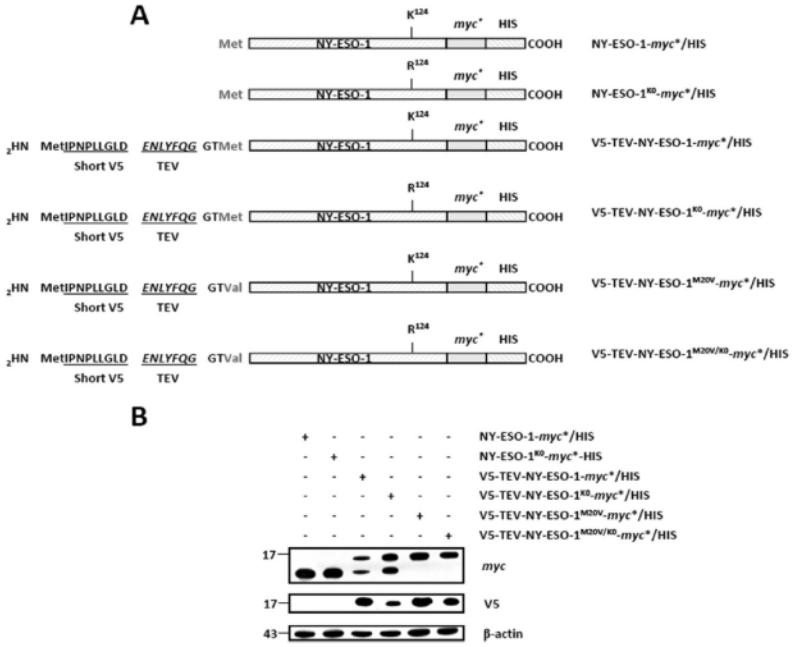

FIGURE 7. **The expression of an N-terminal V5-tagged version of NY-ESO-1 and/or NY-ESO-1^{KO} requires the removal of the original NY-ESO-1 start codon.** *A*, sequences of the NY-ESO-1 constructs used in this study. All NY-ESO-1 constructs were C-terminally tagged with a double *myc**/HIS epitope. In some experiments, NY-ESO-1-*myc**/HIS and NY-ESO-1^{KO}-*myc**/HIS were N-terminally tagged with a short 9-mer V5 epitope (IPNPLLGLD) directly upstream of a TEV protease-sensitive site (ENLYFQG). Both V5-TEV-NY-ESO-1-*myc**/HIS and V5-TEV-NY-ESO-1^{KO}-*myc**/HIS were finally subjected to M20V site-directed mutagenesis to remove the NY-ESO-1 original methionine initiator codon. *B*, HeLa cells were transfected with each of the six NY-ESO-1 variant for 24 h prior to protein extraction. Whole cell extracts were resolved on 15% SDS-PAGE and subsequently analyzed by Western blotting using anti-*myc*, anti-V5, and anti-β-actin (loading control) antibodies as indicated. The M20V in both of V5-TEV-NY-ESO-1-*myc**/HIS and V5-TEV-NY-ESO-1^{KO}-*myc**/HIS prevents the expression of N-terminally untagged NY-ESO-1-*myc**/HIS and NY-ESO-1-*myc**/HIS, respectively.

express HA-Ub-GFP in combination with NY-ESO-1, NY-ESO-1^{KO}, or MART-1 (as a control) prior to a 6-h treatment with 10 μM MG-132. Following NY-ESO-1 pulldown, the precipitates were left untreated or treated with 50 mM NaOH for 25 min at 32 °C. Fig. 6 shows that the ubiquitination of NY-ESO-1 and NY-ESO-1^{KO} was reduced following alkaline treatment. Importantly, peptide bonds were not hydrolyzed under these conditions, as evidenced by the levels of eluted NY-ESO-1, which remained unchanged following sodium hydroxide treatment. This indicates that both NY-ESO-1 and NY-ESO-1^{KO} are modified on Ser and/or Thr residues in these cells. Noteworthy, the use of the anti-Ub antibody (FK2) revealed the presence of Lys-29, Lys-48, and/or Lys-63 linkages on NY-ESO-1^{KO} that were resistant to NaOH treatment (Fig. 6).

NY-ESO-1 and NY-ESO-1^{KO} Do Not Use Their Respective N Termini for Ubiquitination—We next asked whether the N terminus of the NY-ESO-1 tumor antigen may act as a site for ubiquitination. To address this question, we introduced a short V5 (IPNPLLGLD) epitope at the N terminus of both of the NY-ESO-1-*myc**/HIS and NY-ESO-1^{KO}-*myc**/HIS constructs, which was immediately followed by a TEV protease recognition site (ENLYFQG) (Fig. 7*A*). To avoid the expression of untagged NY-ESO-1 proteins deprived of the N-terminal V5 epitope, the original NY-ESO-1 methionine initiator codon at position 20 of both of the V5-TEV-NY-ESO-1-*myc**/HIS and V5-TEV-NY-ESO-1^{KO}-*myc**/HIS constructs was changed into a valine (M20V), as depicted in Fig. 7, *A* and *B*. If the ubiquitination of NY-ESO-1 and/or NY-ESO-1^{KO} indeed partially relies on their N termini, it should be affected upon treatment with the TEV protease (Fig. 8*A*). Remarkably, on-bead digestion of the cell lysates with TEV protease resulted in loss of the V5 epitope as well as in a decrease in size of the eluted NY-ESO-1 proteins, as determined by Western blotting (Fig. 8*B*). This unambiguously indicates that the N-terminal V5 tag was efficiently cleaved off and stripped away from both of the NY-ESO-1 full-length proteins. Interestingly, despite being devoid of their respective N termini, both NY-ESO-1 and NY-ESO-1^{KO} exhibited an HA staining that was comparable with that observed with the untreated NY-ESO-1 proteins (Fig. 8*B*). These data demonstrate that the free N terminus of either NY-ESO-1 or NY-ESO-1^{KO} is not essentially involved in the ubiquitination process under these conditions.

Removal of Lys-124 of NY-ESO-1 Results in the Loss of Lys-48-linked Ub Chains—We next set out to identify the linkages of the poly-Ub chains assembled on both NY-ESO-1 and NY-ESO-1^{KO}. To this end, both of these proteins were expressed together with HA-tagged Lys-6-only, Lys-11-only, Lys-27-only, Lys-29-only, Lys-33-only, Lys-48-only, and Lys-63-only Ub constructs in which all lysine residues were altered to arginine except for lysines 6, 11, 27, 29, 33, 48, and 63, respectively. Internal controls in this experiment consisted of the use of a wild-type HA-Ub construct and an HA-tagged K0 Ub

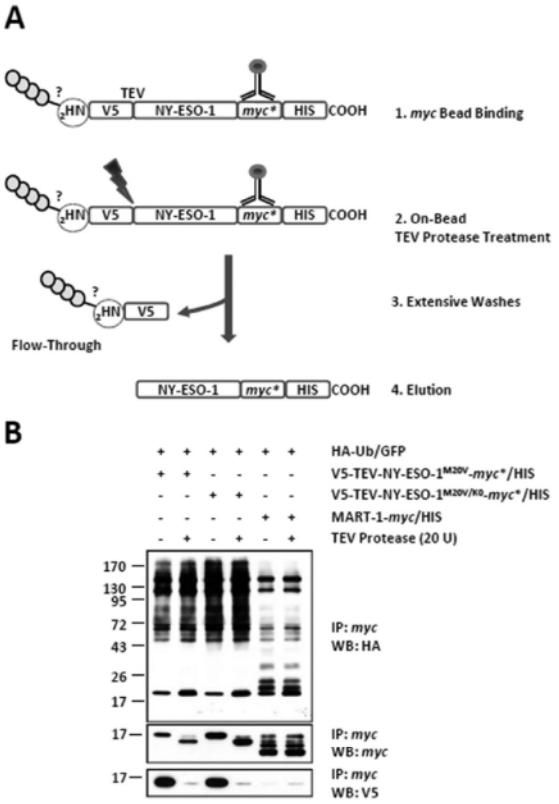

FIGURE 8. **The N-terminal $-NH_2$ group of either NY-ESO-1 or NY-ESO-1^{Ko} is not a site of conjugation.** *A*, HeLa cells expressing HA-Ub-GFP in combination with V5-TEV-NY-ESO-1^{M20V}-*myc**/HIS or V5-TEV-NY-ESO-$1^{M20V/Ko}$-*myc**/HIS were subjected to protein extraction and incubated with μMACS anti-*myc* beads that were subsequently left untreated or treated with 20 U TEV protease for 150 min at 22 °C as indicated. Extensive washing of the μMACS anti-*myc* bead-bound material resulted in the elimination of the N terminus and its potential anchored Ub chains in the flow-through fraction. After five washes, the material bound to the μMACS anti-*myc* beads was eluted. *B*, the effect of the removal of the V5 N terminus on the ubiquitination of NY-ESO-1 and NY-ESO-1^{Ko} was assessed by Western blotting (*WB*) using antibodies specific for HA, ubiquitin, V5, and *myc* (loading control). The negative control for the immunoprecipitation (*IP*) in this experiment consisted of HeLa cells transfected with the HA-Ub-GFP construct in combination with an expression vector encoding the MART-1 melanoma antigen (*fifth* and *sixth lanes*). Shown is one representative experiment of three.

mutant (HA-Ub^{Ko}) devoid of all of its lysine residues. NY-ESO-1 poly-ubiquitination was supported by wild-type, Lys-11-only, Lys-27-only, Lys-29-only, Lys-33-only, Lys-48-only, and Lys-63-only Ub chains but not by the Lys-6-only mutant (Fig. 9*A*). NY-ESO-1^{Ko} showed a ladder of anti-HA reactivity when cells were engineered to express wild-type Ub as well as Lys-11-only, Lys-27-only, Lys-29-only, Lys-33-only, or Lys-63-only Ub mutants, suggesting efficient poly-ubiquitination of NY-ESO-1^{Ko} by these Ub species (Fig. 9*B*). Strikingly, co-expression of NY-ESO-1^{Ko} with either Lys-6-only or Lys-48-only mutants did not result in the formation of HA-modified protein conjugates, indicating that both of these mutants were not used for conjugation and that such linkages were therefore dispensable for poly-Ub chain formation. Besides the loss of Lys-48 chains, our densitometric analysis demonstrated an increased formation of Lys-11, Lys-29 and Lys-33 linkages following the Lys-to-Arg mutation, whereas the levels of Lys-27 and Lys-63 linkages remained unchanged.

Discussion

In this paper, we identified Lys-124 of the NY-ESO-1 cancer/testis antigen as the major site for the formation of canonical Lys-48-linked poly-Ub chains (Fig. 8, *A* and *B*). Unexpectedly, abrogation of this site did not prevent the formation of NY-ESO-1 Ub-conjugates or the presentation of the NY-ESO-$1_{157-165}$ antigenic peptide (Figs. 1*A* and 5). This suggests that the MHC class I processing of the NY-ESO-1 antigen is driven by non-lysine residues and non-canonical poly-Ub chains. Consistently, our investigations show that NY-ESO-1 uses the hydroxyl groups of its Ser and/or Thr residues to form ester bonds with Ub, which eventually results in the formation of atypical chains containing Lys-11, Lys-27, Lys-29, Lys-33, and Lys-63 linkages (Figs. 6 and 9, *A* and *B*). Noteworthy is that such NY-ESO-1 Ub species were detected in the presence of MG-132, confirming their potency as signals for targeting NY-ESO-1 to proteasome-mediated degradation. The notion that proteasomes do not necessarily recognize canonical linkages is in agreement with previous studies showing that atypical poly-Ub may actively participate in the regulation of protein breakdown (25–27). Importantly, our analysis of the NY-ESO-1 ubiquitination profile was carried out following enrichment of the full-length protein using a C-terminal epitope tagging strategy. Such an experimental design does not preclude the pull-down of incompletely synthetized NY-ESO-1 polypeptides, including those resulting from premature translation termination, which are believed to represent a form of DRiPs (15–17). This point is of great importance because DRiPs have been shown to largely contribute to the supply of the pool of antigenic peptides (15, 16). One should, however, emphasize that the HLA-A*0201-restricted NY-ESO-$1_{157-165}$ epitope lies very close to the extreme C terminus of the 180-amino acid-long NY-ESO-1 mature protein. It is therefore highly unlikely that NY-ESO-$1_{157-165}$ presentation arises from ubiquitination of incomplete NY-ESO-1 polypeptides during protein biosynthesis. Nonetheless, this does not necessarily exclude DRiPs as the relevant antigen source for presentation of the NY-ESO-$1_{157-165}$ peptide. It is indeed conceivable that the 9-mer peptide is generated from co-translation ubiquitination of full-length misfolded NY-ESO-1 proteins. The observation that the Lys-124 removal is accompanied by increased ubiquitination, whereas the steady-state level of the mature protein does not change, strongly suggests the generation of NY-ESO-1 DRiPs in the form of improperly folded full-length proteins (Fig. 5).

Remarkably, the NY-ESO-$1_{157-165}$ CTL response was entirely dependent on Rpn10 (Fig. 2*A*). These findings show that the recognition of Ub-modified proteins by Rpn10 and Rpn13 is not restricted to those bearing Lys-48-linked poly-Ub chains. These data also suggest that Rpn10 is a unique receptor for the recognition and subsequent degradation of both NY-ESO-1 and NY-ESO-1^{Ko}. However, this assumption is somehow in conflict with the observation that the NY-ESO-$1_{157-165}$ presentation was also affected in cells with an individual knock-

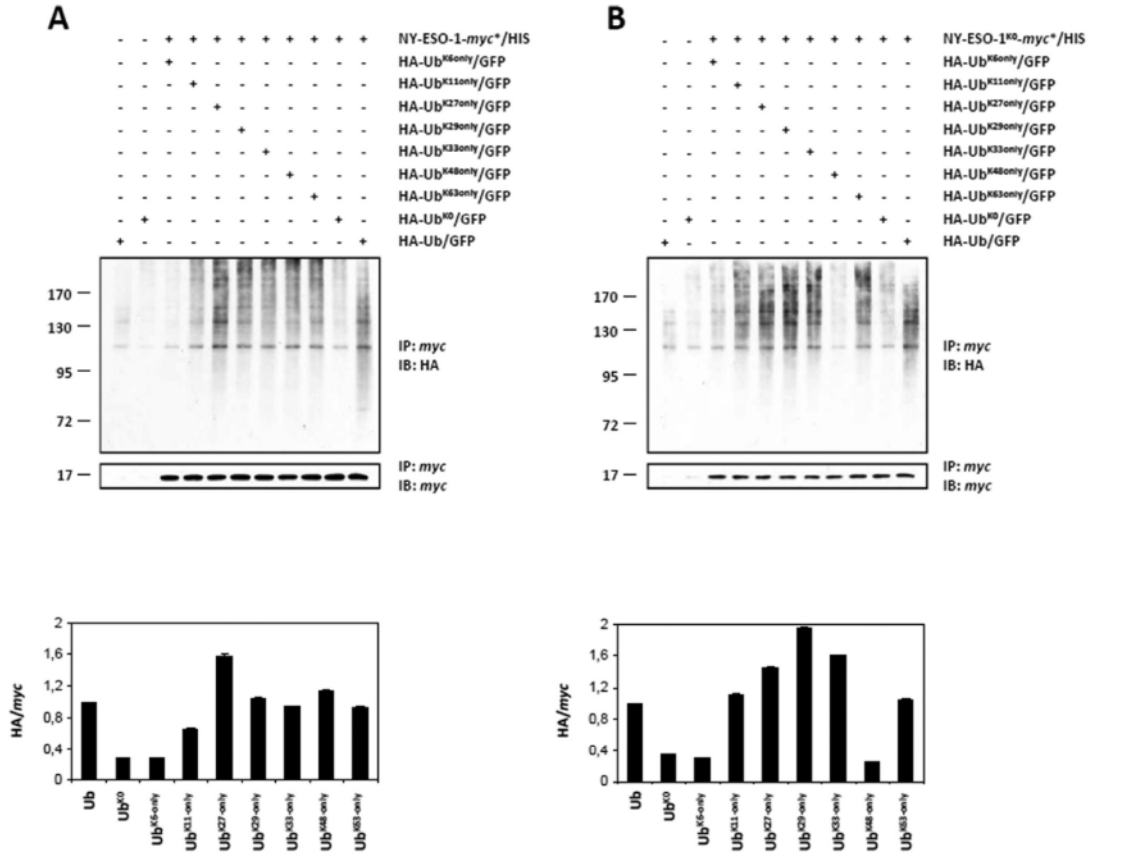

FIGURE 9. **NY-ESO-1 and NY-ESO-1^{K0} distinguish themselves in terms of poly-Ub chains.** *A* and *B*, ubiquitination of NY-ESO-1 (*A*) and NY-ESO-1^{K0} (*B*) was examined following overexpression of a HA-tagged wild-type Ub, a Lys-0 HA-tagged Ub (HA-Ub^{K0}) devoid of all its seven lysine residues, as well as HA-tagged Lys-6-only, Lys-11-only, Lys-27-only, Lys-29-only, Lys-33-only, Lys-48-only, or Lys-63-only Ub mutants in which all lysine residues were altered to arginine except for lysines 6, 11, 27, 29, 33, 48, and 63, respectively, and as indicated. Ubiquitination of NY-ESO-1 and/or NY-ESO-1^{K0} was visualized by pulling down NY-ESO-1 with anti-*myc* beads, followed by Western blotting using antibodies specific for HA and NY-ESO-1 (loading control). Pulldowns with cells overexpressing HA-Ub or HA-Ub^{K0} (*first* and *second lanes*) but lacking NY-ESO-1 (*A*) or NY-ESO-1^{K0} (*B*) demonstrate the specificity of the assay. A densitometric analysis of ubiquitinated NY-ESO-1 and NY-ESO-1^{K0} normalized to pulled-down NY-ESO-1 and NY-ESO-1^{K0} is plotted (mean ± S.D., $n = 2$). For both of the ubiquitinated species of NY-ESO-1 and NY-ESO-1^{K0}, the mean of the signals obtained with the wild-type HA-Ub-GFP construct was set at 1. *IP*, immunoprecipitation; *IB*, immunoblot.

down of Rpn13, albeit to a much lesser extent (~50%). One possible explanation for these apparent discrepancies might be that Rpn13 requires the presence of Rpn10 in 26S complexes to exert its function as Ub receptor. As such, any individual down-regulation of Rpn10 would inactivate Rpn13 and result in a nearly complete loss of capacity for 26S complexes to cope with ubiquitinated proteins. In agreement with previous reports, our findings point to a structure-function relationship between Rpn10 and Rpn13 that regulates the access of Ub-modified proteins to 26S proteasome complexes (28).

There is disagreement in the field with respect to the involvement of 26S complexes in the generation of the NY-ESO-$1_{157-165}$ 9-mer antigenic peptide. Indeed, early reports argued that the NY-ESO-$1_{157-165}$ presentation was insensitive to proteasome inhibitors (29), suggesting that the NY-ESO-1 protein may be degraded by an alternative route. However, it was later shown that dendritic cells were capable of stabilizing NY-ESO-1 when treated with the *N*-acetyl-L-leucyl-L-leucyl-L-norleucinal (LLnL) proteasome inhibitor (30). In our hands, the NY-ESO-$1_{157-165}$ presentation arising from either NY-ESO-1 or NY-ESO-1^{K0} in HeLa cells fully relied on proteasomal activity (Fig. 3*B*). Surprisingly, the generation of the NY-ESO-$1_{157-165}$ antigenic peptide was not affected when the β5 catalytic subunit was inhibited, suggesting that the β5 activity in this situation was either dispensable or could be compensated for by the other β1 and/or β2 catalytic subunits. Of note, epoxomicin, which blocks both β5 and β2, was accompanied by a significant decrease in NY-ESO-$1_{157-165}$ CTL response. Given that β5 is not important, we deduced from this experiment that the major driving force for the generation of the NY-ESO-$1_{157-165}$ peptide is the β2 catalytic subunit.

The role of the inducible subunits in this process was addressed by using the 33/2 cell line. The siRNA-mediated down-regulation of LMP7 had no substantial influence on the

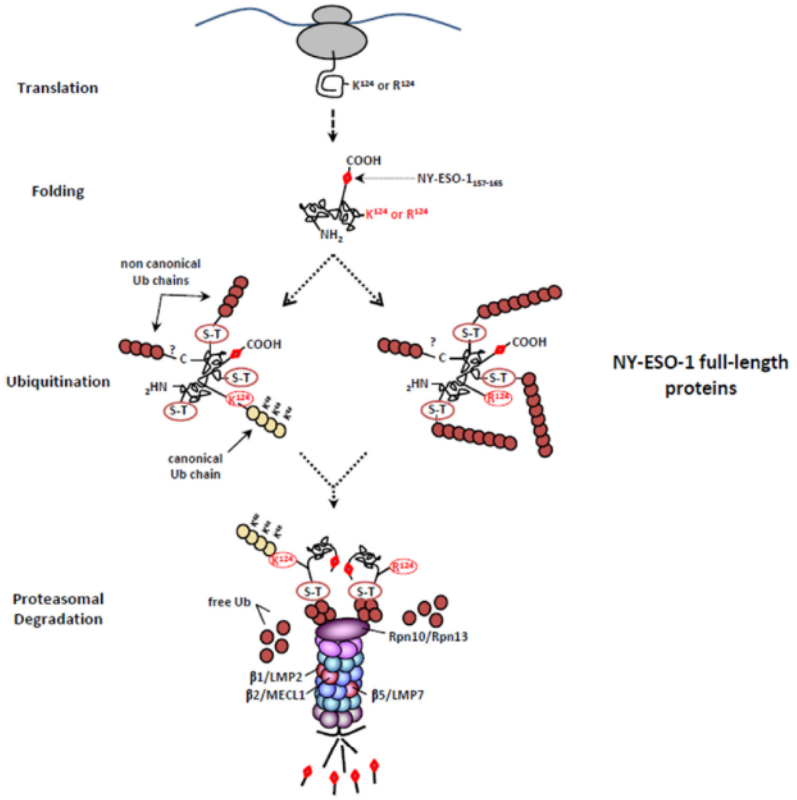

FIGURE 10. **The processing of NY-ESO-1 relies on atypical ubiquitination occurring on non-lysine sites.** The presence of the NY-ESO-$1_{157-165}$ antigenic peptide at the C terminus of the 180-amino acid-long NY-ESO-1 full-length protein required the protein to be fully synthetized before ubiquitination. Following translation, the full-length NY-ESO-1 protein was subjected to both typical and atypical ubiquitination on Lys-124 and on non-canonical sites (Ser-Thr), respectively. The removal of Lys-124 abrogated the formation of Lys-48-linked poly-Ub chains, which was also accompanied by increased generation of atypical chains. Despite these qualitative and quantities differences, both the wild-type and lysine-less forms of NY-ESO-1 converged on the same regulatory proteasome-mediated MHC class I processing pathway involving the Rpn10 and Rpn13 19S subunits as well as the trypsin-like activity of the β2 standard subunit. This eventually leads to similar production of antigenic peptides, which are equally presented on HLA-A*0201 molecules.

generation of the NY-ESO-$1_{157-165}$ antigenic peptide, reinforcing the notion that the β5/LMP7 chymotryptic-like activity is not relevant in this process. Combined down-regulation of LMP7 and LMP2 resulted in a substantial increase in the production of the NY-ESO-$1_{157-165}$ peptide (Fig. 4*B*). Our data therefore identify NY-ESO-$1_{157-165}$ as a new member the growing family of peptides such as MART-1_{26-35} (31) and gp$100_{209-217}$ (32) whose presentation has been reported to be impaired by IPs. Importantly, the preferential processing of NY-ESO-$1_{157-165}$ by standard proteasomes occurred independently of the type of ubiquitination harbored by NY-ESO-1.

Overall, using NY-ESO-1 as a model substrate, we show that neither lysine residues nor canonical Lys-48 linkages represent a prerequisite for MHC class I antigen processing and presentation. As illustrated in Fig. 10, although the lysine-less and wild-type forms of NY-ESO-1 exhibit ubiquitination patterns that are quantitatively and qualitatively different, they both enter the same proteasome-dependent MHC class I pathway, which is regulated by Rpn10, Rpn13, and the standard β2 subunit. Together, these data point to a critical contribution of atypical ubiquitination on non-lysine residues in MHC class I antigen processing that may be much more important than previously assumed.

Author Contributions—R. G. and A. L. performed the research and analyzed the data. P. M. K. designed the research and analyzed the data. F. E. designed the research, analyzed the data, and wrote the manuscript.

Acknowledgments—We thank Ellen Hilgenberg (Deutsches Rheuma-Forschungszentrum Berlin) for help with the irradiation of peripheral blood mononuclear cells and EBV-transformed B cells.

References

1. Sijts, E. J., and Kloetzel, P. M. (2011) The role of the proteasome in the generation of MHC class I ligands and immune responses. *Cell. Mol. Life Sci.* **68,** 1491–1502
2. Rock, K. L., York, I. A., Saric, T., and Goldberg, A. L. (2002) Protein degradation and the generation of MHC class I-presented peptides. *Adv. Immunol.* **80,** 1–70
3. Murata, S., Yashiroda, H., and Tanaka, K. (2009) Molecular mechanisms

of proteasome assembly. *Nat. Rev. Mol. Cell Biol.* **10,** 104–115
4. Ciechanover, A., and Stanhill, A. (2014) The complexity of recognition of ubiquitinated substrates by the 26S proteasome. *Biochim. Biophys. Acta* **1843,** 86–96
5. DeMartino, G. N., and Slaughter, C. A. (1999) The proteasome, a novel protease regulated by multiple mechanisms. *J. Biol. Chem.* **274,** 22123–22126
6. Seifert, U., Bialy, L. P., Ebstein, F., Bech-Otschir, D., Voigt, A., Schröter, F., Prozorovski, T., Lange, N., Steffen, J., Rieger, M., Kuckelkorn, U., Aktas, O., Kloetzel, P. M., and Krüger, E. (2010) Immunoproteasomes preserve protein homeostasis upon interferon-induced oxidative stress. *Cell* **142,** 613–624
7. Strehl, B., Seifert, U., Krüger, E., Heink, S., Kuckelkorn, U., and Kloetzel, P. M. (2005) Interferon-γ, the functional plasticity of the ubiquitin-proteasome system, and MHC class I antigen processing. *Immunol. Rev.* **207,** 19–30
8. Shin, E. C., Seifert, U., Kato, T., Rice, C. M., Feinstone, S. M., Kloetzel, P. M., and Rehermann, B. (2006) Virus-induced type I IFN stimulates generation of immunoproteasomes at the site of infection. *J. Clin. Invest.* **116,** 3006–3014
9. Livnat-Levanon, N., Kevei, É., Kleifeld, O., Krutauz, D., Segref, A., Rinaldi, T., Erpapazoglou, Z., Cohen, M., Reis, N., Hoppe, T., and Glickman, M. H. (2014) Reversible 26S proteasome disassembly upon mitochondrial stress. *Cell Rep.* **7,** 1371–1380
10. Breitschopf, K., Bengal, E., Ziv, T., Admon, A., and Ciechanover, A. (1998) A novel site for ubiquitination: the N-terminal residue, and not internal lysines of MyoD, is essential for conjugation and degradation of the protein. *EMBO J.* **17,** 5964–5973
11. McDowell, G. S., Kucerova, R., and Philpott, A. (2010) Non-canonical ubiquitylation of the proneural protein Ngn2 occurs in both *Xenopus* embryos and mammalian cells. *Biochem. Biophys. Res. Commun.* **400,** 655–660
12. Tait, S. W., de Vries, E., Maas, C., Keller, A. M., D'Santos, C. S., and Borst, J. (2007) Apoptosis induction by Bid requires unconventional ubiquitination and degradation of its N-terminal fragment. *J. Cell Biol.* **179,** 1453–1466
13. Vosper, J. M., McDowell, G. S., Hindley, C. J., Fiore-Heriche, C. S., Kucerova, R., Horan, I., and Philpott, A. (2009) Ubiquitylation on canonical and non-canonical sites targets the transcription factor neurogenin for ubiquitin-mediated proteolysis. *J. Biol. Chem.* **284,** 15458–15468
14. Komander, D., and Rape, M. (2012) The ubiquitin code. *Annu. Rev. Biochem.* **81,** 203–229
15. Yewdell, J. W., and Nicchitta, C. V. (2006) The DRiP hypothesis decennial: support, controversy, refinement and extension. *Trends Immunol.* **27,** 368–373
16. Dolan, B. P., Bennink, J. R., and Yewdell, J. W. (2011) Translating DRiPs: progress in understanding viral and cellular sources of MHC class I peptide ligands. *Cell. Mol. Life Sci.* **68,** 1481–1489
17. Rock, K. L., Farfán-Arribas, D. J., Colbert, J. D., and Goldberg, A. L. (2014) Re-examining class-I presentation and the DRiP hypothesis. *Trends Immunol.* **35,** 144–152
18. Schubert, U., Antón, L. C., Gibbs, J., Norbury, C. C., Yewdell, J. W., and Bennink, J. R. (2000) Rapid degradation of a large fraction of newly synthesized proteins by proteasomes. *Nature* **404,** 770–774
19. Ebstein, F., Lehmann, A., and Kloetzel, P. M. (2012) The FAT10- and ubiquitin-dependent degradation machineries exhibit common and distinct requirements for MHC class I antigen presentation. *Cell. Mol. Life Sci.* **69,** 2443–2454
20. Deveraux, Q., van Nocker, S., Mahaffey, D., Vierstra, R., and Rechsteiner, M. (1995) Inhibition of ubiquitin-mediated proteolysis by the *Arabidopsis* 26S protease subunit S5a. *J. Biol. Chem.* **270,** 29660–29663
21. van Nocker, S., Deveraux, Q., Rechsteiner, M., and Vierstra, R. D. (1996) *Arabidopsis* MBP1 gene encodes a conserved ubiquitin recognition component of the 26S proteasome. *Proc. Natl. Acad. Sci. U.S.A.* **93,** 856–860
22. Husnjak, K., Elsasser, S., Zhang, N., Chen, X., Randles, L., Shi, Y., Hofmann, K., Walters, K. J., Finley, D., and Dikic, I. (2008) Proteasome subunit Rpn13 is a novel ubiquitin receptor. *Nature* **453,** 481–488
23. Myung, J., Kim, K. B., Lindsten, K., Dantuma, N. P., and Crews, C. M. (2001) Lack of proteasome active site allostery as revealed by subunit-specific inhibitors. *Mol. Cell* **7,** 411–420
24. Kisselev, A. F., Callard, A., and Goldberg, A. L. (2006) Importance of the different proteolytic sites of the proteasome and the efficacy of inhibitors varies with the protein substrate. *J. Biol. Chem.* **281,** 8582–8590
25. Dammer, E. B., Na, C. H., Xu, P., Seyfried, N. T., Duong, D. M., Cheng, D., Gearing, M., Rees, H., Lah, J. J., Levey, A. I., Rush, J., and Peng, J. (2011) Polyubiquitin linkage profiles in three models of proteolytic stress suggest the etiology of Alzheimer disease. *J. Biol. Chem.* **286,** 10457–10465
26. Bedford, L., Layfield, R., Mayer, R. J., Peng, J., and Xu, P. (2011) Diverse polyubiquitin chains accumulate following 26S proteasomal dysfunction in mammalian neurons. *Neurosci. Lett.* **491,** 44–47
27. Xu, P., Duong, D. M., Seyfried, N. T., Cheng, D., Xie, Y., Robert, J., Rush, J., Hochstrasser, M., Finley, D., and Peng, J. (2009) Quantitative proteomics reveals the function of unconventional ubiquitin chains in proteasomal degradation. *Cell* **137,** 133–145
28. Besche, H. C., Sha, Z., Kukushkin, N. V., Peth, A., Hock, E. M., Kim, W., Gygi, S., Gutierrez, J. A., Liao, H., Dick, L., and Goldberg, A. L. (2014) Autoubiquitination of the 26S proteasome on Rpn13 regulates breakdown of ubiquitin conjugates. *EMBO J.* **33,** 1159–1176
29. Chen, J. L., Dunbar, P. R., Gileadi, U., Jäger, E., Gnjatic, S., Nagata, Y., Stockert, E., Panicali, D. L., Chen, Y. T., Knuth, A., Old, L. J., and Cerundolo, V. (2000) Identification of NY-ESO-1 peptide analogues capable of improved stimulation of tumor-reactive CTL. *J. Immunol.* **165,** 948–955
30. Batchu, R. B., Moreno, A. M., Szmania, S. M., Bennett, G., Spagnoli, G. C., Ponnazhagan, S., Barlogie, B., Tricot, G., and van Rhee, F. (2005) Protein transduction of dendritic cells for NY-ESO-1-based immunotherapy of myeloma. *Cancer Res.* **65,** 10041–10049
31. Morel, S., Lévy, F., Burlet-Schiltz, O., Brasseur, F., Probst-Kepper, M., Peitrequin, A. L., Monsarrat, B., Van Velthoven, R., Cerottini, J. C., Boon, T., Gairin, J. E., and Van den Eynde, B. J. (2000) Processing of some antigens by the standard proteasome but not by the immunoproteasome results in poor presentation by dendritic cells. *Immunity* **12,** 107–117
32. Chapiro, J., Claverol, S., Piette, F., Ma, W., Stroobant, V., Guillaume, B., Gairin, J. E., Morel, S., Burlet-Schiltz, O., Monsarrat, B., Boon, T., and Van den Eynde, B. J. (2006) Destructive cleavage of antigenic peptides either by the immunoproteasome or by the standard proteasome results in differential antigen presentation. *J. Immunol.* **176,** 1053–1061

5. Comprehensive discussion and outlook

The dissection and full characterization of the MHC class I antigen processing pathway is crucial for understanding the events that trigger the initiation of a CTL immune response and for the design of potential drug targets in tumor immunology and/or autoimmunity.

5.1. Identification of the FAT10/NUB1(L) axis as a novel route for MHC class I antigen presentation

Because the priming of naïve T cells is strictly dependent on antigen presentation by DC (Inaba et al., 1990), our initial aim in this work was to determine regulation of the UPS in DC in response to various maturation-inducing strategies including pro-inflammatory cytokines, LPS, Poly-IC and CD40L treatments. Although a number of genes showed down-regulation, we found an overall increase in expression affecting the majority of UPS sequences, regardless of the maturation regimen employed. Amongst commonly up-regulated genes was found the 18-kDa ubiquitin-like modifier FAT10, which is believed to provide a ubiquitin-independent pathway for proteasome degradation (Hipp et al., 2005; Schmidtke et al., 2006). The elevated amount of FAT10 transcripts in maturing DC was followed by a parallel rise of FAT10-modified proteins which were only visualized in the presence of the proteasome inhibitor MG132, thereby confirming the role of FAT10 as degradation signal (Hipp et al., 2004). Here, we also provide compelling evidence that FAT10 modification of the HCMV-derived antigen pp65 results in its increased intracellular degradation with improved presentation of the HLA-A2-restricted $pp65_{495\text{-}509}$ antigenic peptide. Importantly, FAT10 was as efficient as ubiquitin in its capacity to enhance the $pp65_{495\text{-}509}$ CD8+ T cell-response. To our knowledge, this the first report stating that antigens have the potential to be modified by addition of either ubiquitin or FAT10, thereby providing two alternative pathways for antigen processing and subsequent MHC class I presentation. It is tempting to speculate that, besides the ubiquitin-conjugation pathway, the less-defined FAT10-conjugation pathway also participates to eliciting a functional CD8+ T cell response *in vivo.* Herein, the existence of this new route may allow presentation of antigenic peptides that would not be generated in adequate amounts by the classical ubiquitin-conjugation pathway, thus increasing the diversity of epitopes displayed by the immune system. Nevertheless, the contribution of each pathway to antigen presentation may difficult to assess. The fact that FAT10 is normally not express under physiological conditions suggests

that the FAT10-conjugation pathway is only a complementary one which is used by the cell when the conventional ubiquitin pathway is overloaded. This notion is further supported by the lack of substantial phenotypic and functional impairment in FAT10 knockout mice (Canaan et al., 2006).

Both NUB1L and its natural splicing variant NUB1 (with a deletion of 14 amino acids) have been reported to shuttle FAT10-modified proteins to 26S proteasome complexes (Hipp et al., 2005; Hipp et al., 2004). Our experimental data confirm the capacity of both of these proteins to promote proteasome-mediated degradation of FAT10-protein conjugates, as shown by the drop of the steady-state expression level of FAT10-pp65 in the presence of NUB1 or NUB1L. This notion is also in line with the fact that both NUB1 and NUB1L contain a UBL domain that allows interactions with the Rpn10 proteasome subunit (Kamitani et al., 2001) thereby facilitating the targeting of FAT10-pp65 to proteasome-mediated degradation. More importantly, the increased degradation rate of FAT10-pp65 following over-expression of either NUB1 or NUB1L resulted in substantial improvement of $pp65_{495\text{-}503}$ presentation. Nevertheless and in contrast to previous findings (Hipp et al., 2005), our data suggest that NUB1 exhibits a preference for FAT10 binding over ubiquitin binding, as evidenced by the failure of NUB1 to accelerate the degradation of the ubiquitin-pp65 fusion protein. It is conceivable that the specificity of NUB1 and NUB1L for ubiquitin and/or FAT10 is determined by their intrinsic number of ubiquitin-associated domains (UBA). Hence, NUB1L with 3 UBA domains has access to both of the FAT10 and ubiquitin pathways, while NUB1 with only 2 UBA domains can only enter the FAT10 pathway (Fig. 6). This in turn, would imply that FAT10 binds to UBA domains with a higher affinity than its ubiquitin counterpart.

Although the ability of ubiquitin fusion proteins to improve MHC class I-restricted antigen presentation is well established (Townsend et al., 1988), there is less agreement as to their ability to facilitate antigen cross-presentation. Indeed, controversy still exists with respect to the optimal form of antigenic source for effective cross-priming. It was earlier suggested that cross-presentation favors unstable antigens or defective ribosomal products (DriPs) (Fu et al., 1998; Janda et al., 2004).

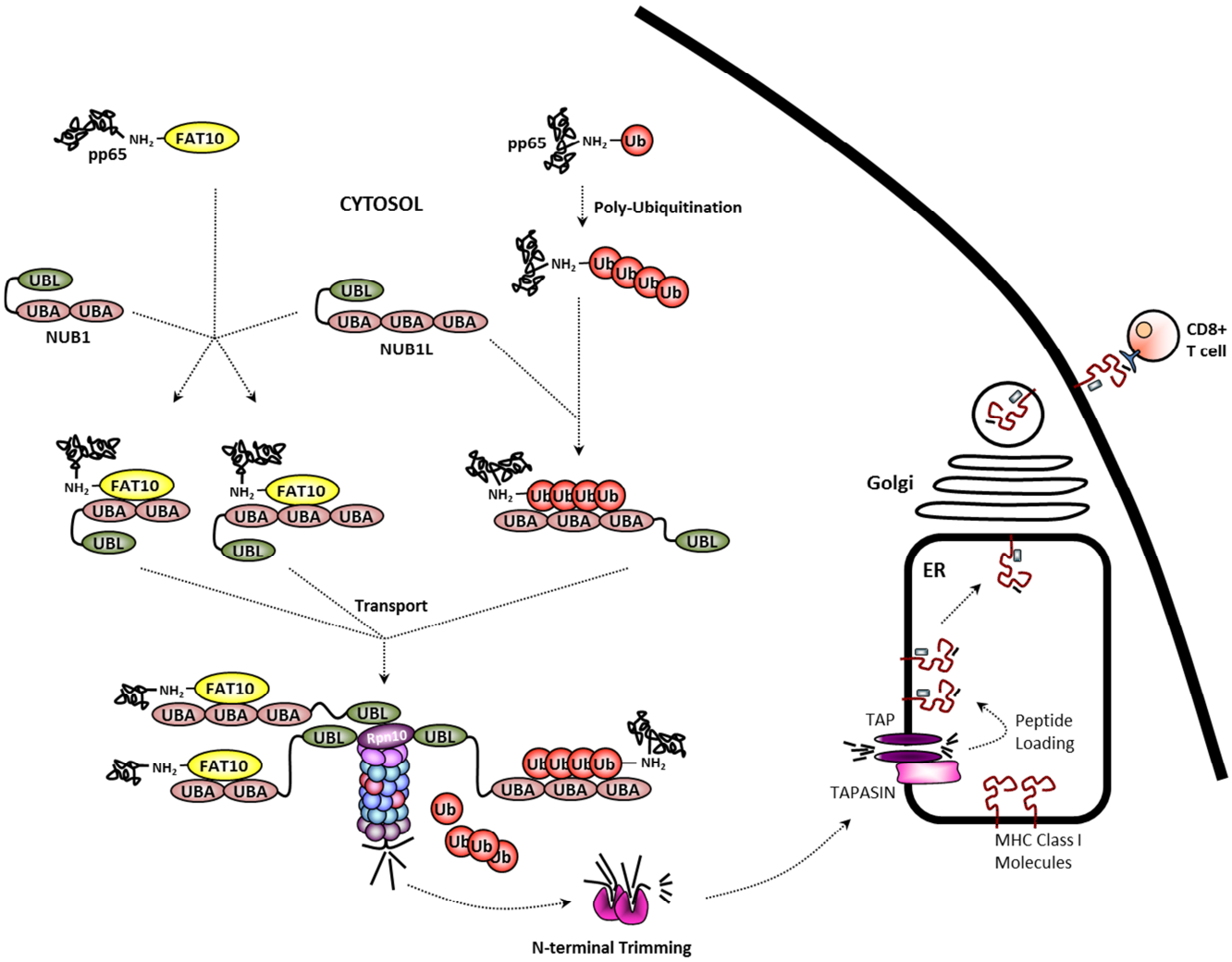

Figure 6: Both ubiquitin- and FAT10-modified proteins are good antigen sources for MHC class I presentation. FAT10- and ubiquitin-modified proteins are recognized by the UBA domains of NUB1 and/or NUB1L which then transport them to the 26S proteasome thanks to their UBL domain which interacts with Rpn10. While NUB1 is restricted to the FAT10 pathway, NUB1L recognizes both FAT10- and ubiquitin-modified antigens.

However, it was later shown that mature proteins were more effective than DriPs as antigen sources for cross-priming (Basta et al., 2005). In our hands, feeding DC with either ubiquitin or FAT10 fusion proteins was more effective than exposing DC with untagged pp65 at activating CTL, suggesting that short-lived proteins serve as good antigen sources for DC-based cross-priming. Nevertheless, the mechanisms by which ubiquitin and FAT10 promote

cross-presentation of their fused antigen remain elusive. One can speculate that cross-presentation is improved thanks to the increased available concentrations of pre-processed peptides resulting from the accelerated antigen degradation rate in donor cells, as previously suggested (Norbury et al., 2004). On the other hand, the mechanisms by which ubiquitin and FAT10 promote cross-presentation may occur through chaperoning the antigen into DC. Of note, differences could be detected between Ub-pp65 and FAT10-pp65 processing in kinetic assays with the extent of enhancement of cross-presentation by FAT10-pp65 being lower than that observed with Ub-pp65 in the very early phases of co-culture. These findings could reflect differences in antigen uptake with ubiquitin-modified substrates being faster internalized than FAT10-protein conjugates. Besides, we show that NUB1 is the major isoform up-regulated in mature DC. Surprisingly, knocking NUB1 down by specific siRNA was accompanied by a slight but significant decrease of the pp65 cross-presentation levels by DC. Such impairment was not restricted to DC loaded with FAT10-pp65 but was also observed to a similar extent with DC loaded with either untagged pp65 or Ub-pp65. Importantly, because we have shown that NUB1 can only enhance MHC class I presentation of FAT10 substrates, the sensibility of pp65 and Ub-pp65 to NUB1 down-regulation suggests that both of these antigen sources undergo FAT10 modification within DC prior to proteasomal degradation for cross-presentation. However, the precise contribution of the FAT10-dependent degradation machinery to the cross-presentation process remains to be determined. The inhibitory effect of the knockdown of NUB1 on cross-presentation was only partial (~20%), suggesting that poly-ubiquitination may occur in parallel, which would in turn allow multiple routes for proteasome-mediated degradation.

5.2. The ERAD p97/VCP is a ubiquitin-binding protein functioning at the interface of direct and cross-presentation

In an attempt to determine the cross-presentation requirements upstream proteasomal degradation, we next monitored the fate of a selected a 25-mer SLP of the Melan-A/MART-1 melanoma-associated antigen bearing an anchor optimized analog of the immunodominant $CD8^+$ epitope (epitope of Melan-A/$MART1_{26–35}$ A27L on HLA-A2) (Chauvin et al., 2012; Vignard et al., 2005) in DC. Our data show that SLP_{16-40} is taken up by DC into

early endosomes before gaining access to both cytoplasm and lysosomes whereby only the cytosolic part of the internalized antigen leads to successful cross-presentation.

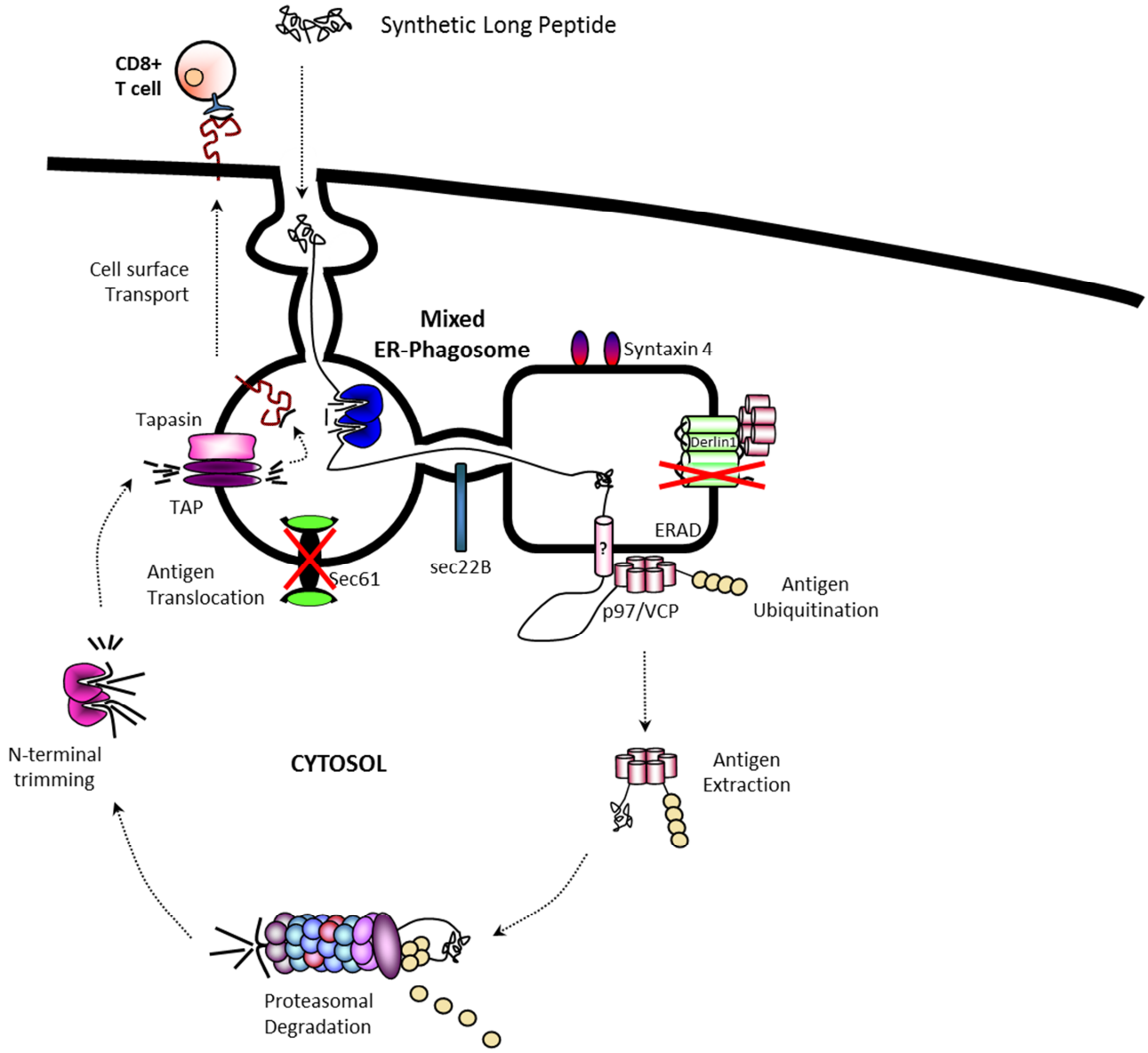

Figure 7: MHC class I cross-presentation of SLP uses a proteasomal pathway. The transfer of internalized SLP from ER-endosome mixed compartments into the cytosol for degradation by 26S proteasome complexes is mediated by a so-far unidentified channel. This process is not dependent on sec61 and/or Derlin-1 but fully relies on the p97/VCP ERAD protein suggesting the involvement of a retro-translocation channel.

In the cytoplasm, SLP_{16-40} is processed by proteasome and the generated Melan-A/MART-1_{26-35} peptide is then reimported by TAP into endosome-ER mixed compartment for loading onto MHC class I molecules. The mechanisms by which internalized antigens in DC

are transferred from endosomes to the cytosol for cross-presentation remain ill-defined. There is growing evidence that the ERAD pathway might play a role in this process (Ackerman et al., 2006; Giodini et al., 2009; Imai et al., 2005b). The ERAD pathway normally ensures the removal of misfolded secretory and/or membrane proteins from the ER back to the cytoplasm for subsequent destruction by the 26S proteasome (an event also referred to as "retro-translocation"). Herein, the proteins used a yet unidentified channel before being extracted from the ER membrane by the p97/VCP AAA-ATPase (Needham and Brodsky, 2013). Our data confirm a potential role for ERAD in the transfer of the SLP_{16-40} from endosome-ER mixed organelles into the cytosol, as evidenced by the drop of the SLP_{16-40} cross-presentation detected in DC with a knockdown of p97/VCP. Noteworthy, the down-regulation of sec61 had virtually no effect on the ability of DC to cross-present the SLP_{16-40}, confirming that the access of such antigens to the cytosol is mediated by retro-translocation and not by translocation (Fig. 7). The identity of this retro-translocation channel for cross-presentation remains, however, an open question. Although retro-translocation in mammalian cells has been shown to be blocked by antibodies directed to Derlin-1 (Wahlman et al., 2007), our data show that such ERAD component had no substantial impact on the SLP_{16-40} presentation. Future investigations will attempt to evaluate the cross-presenting capacities of DC with a knockdown of the ubiquitin E3 ligase HRD1 which has been recently put forward as a retro-translocation channel in yeast (Baldridge and Rapoport, 2016).

Strikingly, a critical role for p97/VCP was also observed in direct presentation of the Melan-A/MART-1_{26-35} epitope in melanoma cells. Indeed, we identified the down-regulation of p97/VCP as a major escape mechanism in melanoma cells leading to resistance to cytolysis mediated by Melan-A/MART-1_{26-35} specific CTL. This notion was confirmed by experiments showing that re-expression of p97/VCP in CTL-resistant melanoma cell clones could re-establish the Melan-A/MART-1_{26-35} epitope presentation to normal levels and their sensitivity to apoptosis by CTL specific for Melan-A/MART-1_{26-35}. Importantly, the p97/VCP-dependency for MHC class I antigen processing was not restricted to Melan-A/MART-1_{26-35} peptide but could be also observed for the $gp100_{47-52/40-42}$ antigenic spliced peptide which also arises from a membrane-spanning antigen. The potential involvement of p97/VCP in MHC class I antigen direct presentation seems therefore to depend on antigen localization.

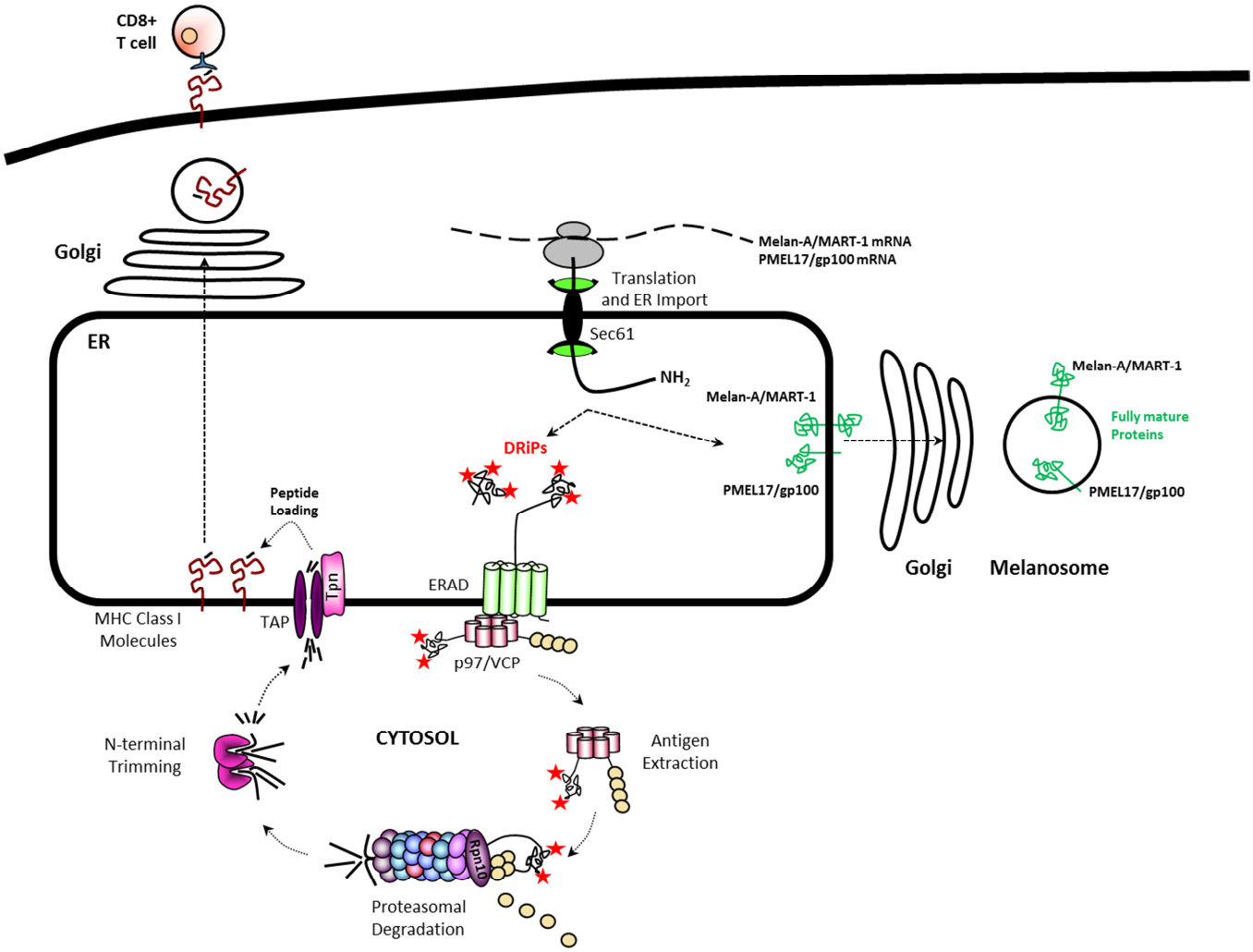

Figure 8: MHC class I direct presentation of the Melan-A/MART-1 and PMEL17/gp100 antigens depends on the p97/VCP ERAD protein. Newly synthetized Melan-A/MART-1 and PMEL17/gp100 proteins enter the ER via the sec61 translocation channel before being subsequently transported into melanosomes using the Golgi apparatus. Damaged and/or missfolded proteins (DRiPs) in the ER are exported back into the cytosol for degradation by 26S proteasomes. This retro-translocation process is mediated by the ERAD pathway and in particular p97/VCP. The observation that the presentation of Melan-A/MART-1_{26-35} and PMEL17/$gp100_{47-52/40-42}$ are fully dependent on p97/VCP indicates that DRiPs are the major antigen source for MHC class I presentation.

From our data, the p97/VCP protein seems to be implicated in the cross-presentation of exogenous antigens and in the direct presentation of endogenous proteins. The observation that p97/VCP allows the processing of both soluble (SLP) and membrane-spanning proteins (endogenous Melan-A/MART-1 and gp100), suggests the existence of two

different mechanisms. During cross-presentation, it is argued that p97/VCP removes endocytosed antigens from phagocytic vesicles to allow proteasome-mediated presentation. Because p97/VCP, as part of the ERAD pathway, only recognizes ubiquitin-modified proteins, this implies that antigens that have been taken up by DC undergo a ubiquitination process. However, there is so far little evidence that cross-presented antigens are subjected to ubiquitination (Burgdorf et al., 2008; Imai et al., 2005a), thereby raising the possibility that p97/VCP might have roles beyond a "simple" ERAD function for cross-presentation. This assumption would be in agreement with previous works showing that p97/VCP is involved in other cellular processes including endocytosis (Meyer et al., 2012). Future work will attempt to address the role of p97/VCP independently of antigen translocation.

The role of p97/VCP in the endogenous presentation of the Melan-A/MART-1_{26-35} and $gp100_{47-52/40-42}$ antigenic peptides is easier to understand since both of these epitopes arise from membrane-spanning proteins which, as such, traffic through the ER before maturation (Fig. 8). Herein, such antigens are legitimately subjected to ERAD-mediated degradation when defective. This point is of great importance and indicates that ERAD substrates represent a major source for antigen presentation and supports the notion that the contribution of mature long-lived proteins to MHC class I antigen presentation is negligible. This is fully in agreement with the DRiPs hypothesis proposed by Yewdell and colleagues stating that defective proteins failing to achieve a stable conformation are better peptide suppliers than the native and functional ones (Yewdell et al., 1996; Yewdell and Nicchitta, 2006). This is also in line with a previous study showing that Melan-A/MART-1_{26-35} presentation depends on transcription, and as such, on the continuous supply of DRiPs (Labarriere et al., 1997).

5.3. Rpn10 is a major and universal receptor of ubiquitin-modified antigens for MHC class I presentation

Our data indicate that the supply of the $pp65_{495-503}$ antigenic peptide arising from the pp65 full-length protein modified with either FAT10 or ubiquitin is impaired in cells treated with siRNA specific for the ubiquitin receptor Rpn10, which is also a subunit of the 19S proteasome regulatory particle (Deveraux et al., 1995). This suggests that Rpn10 may serve

as a receptor for both ubiquitin and FAT10. The notion that FAT10 shares with ubiquitin the same ubiquitin receptor is in agreement with a later study showing that FAT10 is capable of binding to the VWA domain of Rpn10 (Rani et al., 2012). Apart from the $pp65_{495-503}$ epitope, both of the $gp100_{47-52/40-42}$ and NY-ESO-$1_{157-165}$ antigenic peptides were fully Rpn10-dependent, reinforcing the view that Rpn10 is a unique receptor for ubiquitin-modified proteins in MHC class I antigen presentation. This assumption appears to be in conflict with the observation that the NY-ESO-$1_{157-165}$ presentation was also affected in cells depleted with Rpn13, the other ubiquitin receptor of the 19S proteasome regulatory particle (Husnjak et al., 2008). However, the Rpn13 down-regulation affected the NY-ESO-$1_{157-165}$ CTL response to a much lesser extent than that observed with the Rpn10 down-regulation. In addition, Rpn13 could not rescue MHC class I antigen presentation of the NY-ESO-$1_{157-165}$ peptide in cells depleted with Rpn10, although the expression of Rpn13 was not affected by the Rpn10 knockdown. These data point to a structure-function relationship between Rpn10 and Rpn13 in which Rpn13 requires the presence of Rpn10 to fulfill its function as a ubiquitin receptor. Such interplay is in agreement with a previous study reporting inter-dependence between these two subunits (Besche et al., 2014).

Importantly, we identified K124 of the NY-ESO-1 tumor antigen as the major acceptor site for K48-linked poly-ubiquitin chains. Surprisingly, the removal of K124 did not affect the Rpn10 dependency for the supply of the HLA-A*0201-restricted NY-ESO-$1_{157-165}$ epitope. This suggests that the recognition of ubiquitin-modified proteins by Rpn10 is not necessarily restricted to K48-linked poly-ubiquitin chains, as previously assumed (Chau et al., 1989; Thrower et al., 2000). Our experiments show that NY-ESO-1 undergoes a ubiquitination process that involves other ubiquitin linkages including those occurring through K11, K27, K29, K33 and K63. From a quantitative point of view, the chain type that remains constant following the removal of K124 is represented by the K27 linkages. Based on this and given that the degradation rate does not vary between the two NY-ESO-1 forms; it is conceivable that such K27 ubiquitin chains may constitute the biologically relevant signal for degradation and subsequent presentation of the NY-ESO-$1_{157-165}$ peptide. This assumption would be in agreement with a previous work showing that K27-linked poly-ubiquitin chains are capable of targeting their modified substrate for proteasome-mediated breakdown (Ashida et al., 2010). Besides, it is also seductively easy to imagine that the loss of such K48-linkages might be compensated by the gain of other linkages which, in turn, can fulfil the function of

initiating proteasome-dependent degradation. Interestingly, our data show an increased formation of K11, K29 and K33 ubiquitin chains following the K-to-R mutation at position 124. Because these chains have been reported to participate in protein breakdown (Bedford et al., 2011; Dammer et al., 2011; Xu et al., 2009), it is conceivable that NY-ESO-1^{K0} overcomes its incapacity to assemble K48-linked poly-ubiquitin chains by increasing the formation of K11-, K29- and K33-linked poly-ubiquitin on various sites until a point is reached at which the protein is efficiently targeted for degradation. In any case, the complete loss of MHC class I antigen presentation in Rpn10-silenced cells implies that the recognition of poly-ubiquitination antigens is a prerequisite for the supply of MHC class I-restricted peptides. Apart from Rpn10 and Rpn13, the proteasome subunit DSS1 has been recently identified as a third ubiquitin receptor of the 19S regulatory particle (Paraskevopoulos et al., 2014) and its contribution to MHC class I antigen processing remains to be fully addressed.

Collectively, the data presented in this work provide new insights into the MHC class I antigen direct and cross-presentation pathways. We show that, like ubiquitin, the FAT10 ubiquitin-like modifier is an efficient signal targeting proteins to MHC class I direct presentation and identify the Rpn10 proteasome subunit as the major receptor for FAT10- and ubiquitin-modified antigens. Besides, we provide evidence that the MHC class I antigen processing machinery includes the ERAD pathway whose function essentially relies on extracting antigens from ER and/or ER-like vesicles for direct and cross-presentation, respectively. Future work will need to accurately characterize the nature of such ERAD complexes in both DC and non-professional antigen-presenting cells.

6. Literature

Ackerman, A.L., Giodini, A., and Cresswell, P. (2006). A role for the endoplasmic reticulum protein retrotranslocation machinery during crosspresentation by dendritic cells. Immunity *25*, 607-617.

Ackerman, A.L., Kyritsis, C., Tampe, R., and Cresswell, P. (2003). Early phagosomes in dendritic cells form a cellular compartment sufficient for cross presentation of exogenous antigens. Proc Natl Acad Sci U S A *100*, 12889-12894.

Aichem, A., Pelzer, C., Lukasiak, S., Kalveram, B., Sheppard, P.W., Rani, N., Schmidtke, G., and Groettrup, M. (2010). USE1 is a bispecific conjugating enzyme for ubiquitin and FAT10, which FAT10ylates itself in cis. Nature communications *1*, 13.

Arnold, D., Faath, S., Rammensee, H., and Schild, H. (1995). Cross-priming of minor histocompatibility antigen-specific cytotoxic T cells upon immunization with the heat shock protein gp96. J Exp Med *182*, 885-889.

Ashida, H., Kim, M., Schmidt-Supprian, M., Ma, A., Ogawa, M., and Sasakawa, C. (2010). A bacterial E3 ubiquitin ligase IpaH9.8 targets NEMO/IKKgamma to dampen the host NF-kappaB-mediated inflammatory response. Nature cell biology *12*, 66-73; sup pp 61-69.

Baldridge, R.D., and Rapoport, T.A. (2016). Autoubiquitination of the Hrd1 Ligase Triggers Protein Retrotranslocation in ERAD. Cell *166*, 394-407.

Basler, M., Kirk, C.J., and Groettrup, M. (2013). The immunoproteasome in antigen processing and other immunological functions. Current opinion in immunology *25*, 74-80.

Basler, M., Youhnovski, N., Van Den Broek, M., Przybylski, M., and Groettrup, M. (2004). Immunoproteasomes down-regulate presentation of a subdominant T cell epitope from lymphocytic choriomeningitis virus. J Immunol *173*, 3925-3934.

Basta, S., Stoessel, R., Basler, M., van den Broek, M., and Groettrup, M. (2005). Cross-presentation of the long-lived lymphocytic choriomeningitis virus nucleoprotein does not require neosynthesis and is enhanced via heat shock proteins. J Immunol *175*, 796-805.

Baumeister, W., Walz, J., Zuhl, F., and Seemuller, E. (1998). The proteasome: paradigm of a self-compartmentalizing protease. Cell *92*, 367-380.

Bedford, L., Layfield, R., Mayer, R.J., Peng, J., and Xu, P. (2011). Diverse polyubiquitin chains accumulate following 26S proteasomal dysfunction in mammalian neurones. Neuroscience letters *491*, 44-47.

Beninga, J., Rock, K.L., and Goldberg, A.L. (1998). Interferon-gamma can stimulate post-proteasomal trimming of the N terminus of an antigenic peptide by inducing leucine aminopeptidase. The Journal of biological chemistry *273*, 18734-18742.

Besche, H.C., Sha, Z., Kukushkin, N.V., Peth, A., Hock, E.M., Kim, W., Gygi, S., Gutierrez, J.A., Liao, H., Dick, L*., et al.* (2014). Autoubiquitination of the 26S proteasome on Rpn13 regulates breakdown of ubiquitin conjugates. The EMBO journal *33*, 1159-1176.

Bialas, J., Groettrup, M., and Aichem, A. (2015). Conjugation of the ubiquitin activating enzyme UBE1 with the ubiquitin-like modifier FAT10 targets it for proteasomal degradation. PloS one *10*, e0120329.

Boname, J.M., Thomas, M., Stagg, H.R., Xu, P., Peng, J., and Lehner, P.J. (2010). Efficient internalization of MHC I requires lysine-11 and lysine-63 mixed linkage polyubiquitin chains. Traffic *11*, 210-220.

Breitschopf, K., Bengal, E., Ziv, T., Admon, A., and Ciechanover, A. (1998). A novel site for ubiquitination: the N-terminal residue, and not internal lysines of MyoD, is essential for conjugation and degradation of the protein. The EMBO journal *17*, 5964-5973.

Brosch, S., Tenzer, S., Akkad, N., Lorenz, B., Schild, H., and von Stebut, E. (2012). Priming of Leishmania-reactive CD8+ T cells in vivo does not require LMP7-containing immunoproteasomes. The Journal of investigative dermatology *132*, 1302-1305.

Buchsbaum, S., Bercovich, B., Ziv, T., and Ciechanover, A. (2012). Modification of the inflammatory mediator LRRFIP2 by the ubiquitin-like protein FAT10 inhibits its activity during cellular response to LPS. Biochemical and biophysical research communications *428*, 11-16.
Burgdorf, S., Kautz, A., Bohnert, V., Knolle, P.A., and Kurts, C. (2007). Distinct pathways of antigen uptake and intracellular routing in CD4 and CD8 T cell activation. Science *316*, 612-616.
Burgdorf, S., Scholz, C., Kautz, A., Tampe, R., and Kurts, C. (2008). Spatial and mechanistic separation of cross-presentation and endogenous antigen presentation. Nature immunology *9*, 558-566.
Canaan, A., Yu, X., Booth, C.J., Lian, J., Lazar, I., Gamfi, S.L., Castille, K., Kohya, N., Nakayama, Y., Liu, Y.C.*, et al.* (2006). FAT10/diubiquitin-like protein-deficient mice exhibit minimal phenotypic differences. Mol Cell Biol *26*, 5180-5189.
Cebrian, I., Visentin, G., Blanchard, N., Jouve, M., Bobard, A., Moita, C., Enninga, J., Moita, L.F., Amigorena, S., and Savina, A. (2011). Sec22b regulates phagosomal maturation and antigen crosspresentation by dendritic cells. Cell *147*, 1355-1368.
Chapiro, J., Claverol, S., Piette, F., Ma, W., Stroobant, V., Guillaume, B., Gairin, J.E., Morel, S., Burlet-Schiltz, O., Monsarrat, B.*, et al.* (2006). Destructive cleavage of antigenic peptides either by the immunoproteasome or by the standard proteasome results in differential antigen presentation. Journal of immunology *176*, 1053-1061.
Chau, V., Tobias, J.W., Bachmair, A., Marriott, D., Ecker, D.J., Gonda, D.K., and Varshavsky, A. (1989). A multiubiquitin chain is confined to specific lysine in a targeted short-lived protein. Science *243*, 1576-1583.
Chauvin, J.M., Larrieu, P., Sarrabayrouse, G., Prevost-Blondel, A., Lengagne, R., Desfrancois, J., Labarriere, N., and Jotereau, F. (2012). HLA anchor optimization of the melan-A-HLA-A2 epitope within a long peptide is required for efficient cross-priming of human tumor-reactive T cells. Journal of immunology *188*, 2102-2110.
Chiu, Y.H., Sun, Q., and Chen, Z.J. (2007). E1-L2 activates both ubiquitin and FAT10. Mol Cell *27*, 1014-1023.
Chou, B., Hiromatsu, K., Hisaeda, H., Duan, X., Imai, T., Murata, S., Tanaka, K., and Himeno, K. (2010). Genetic immunization based on the ubiquitin-fusion degradation pathway against Trypanosoma cruzi. Biochemical and biophysical research communications *392*, 277-282.
Chou, B., Hisaeda, H., Shen, J., Duan, X., Imai, T., Tu, L., Murata, S., Tanaka, K., and Himeno, K. (2008). Critical contribution of immunoproteasomes in the induction of protective immunity against Trypanosoma cruzi in mice vaccinated with a plasmid encoding a CTL epitope fused to green fluorescence protein. Microbes and infection / Institut Pasteur *10*, 241-250.
Ciechanover, A., Elias, S., Heller, H., Ferber, S., and Hershko, A. (1980). Characterization of the heat-stable polypeptide of the ATP-dependent proteolytic system from reticulocytes. The Journal of biological chemistry *255*, 7525-7528.
Ciechanover, A., Hod, Y., and Hershko, A. (1978). A heat-stable polypeptide component of an ATP-dependent proteolytic system from reticulocytes. Biochemical and biophysical research communications *81*, 1100-1105.
Coux, O., Tanaka, K., and Goldberg, A.L. (1996). Structure and functions of the 20S and 26S proteasomes. Annu Rev Biochem *65*, 801-847.
Cox, J.H., Galardy, P., Bennink, J.R., and Yewdell, J.W. (1995). Presentation of endogenous and exogenous antigens is not affected by inactivation of E1 ubiquitin-activating enzyme in temperature-sensitive cell lines. Journal of immunology *154*, 511-519.
Cresswell, P., Bangia, N., Dick, T., and Diedrich, G. (1999). The nature of the MHC class I peptide loading complex. Immunol Rev *172*, 21-28.
Dammer, E.B., Na, C.H., Xu, P., Seyfried, N.T., Duong, D.M., Cheng, D., Gearing, M., Rees, H., Lah, J.J., Levey, A.I.*, et al.* (2011). Polyubiquitin linkage profiles in three models of proteolytic stress suggest the etiology of Alzheimer disease. The Journal of biological chemistry *286*, 10457-10465.
Dannull, J., Lesher, D.T., Holzknecht, R., Qi, W., Hanna, G., Seigler, H., Tyler, D.S., and Pruitt, S.K. (2007). Immunoproteasome down-modulation enhances the ability of dendritic cells to stimulate antitumor immunity. Blood *110*, 4341-4350.

de Graaf, N., van Helden, M.J., Textoris-Taube, K., Chiba, T., Topham, D.J., Kloetzel, P.M., Zaiss, D.M., and Sijts, A.J. (2011). PA28 and the proteasome immunosubunits play a central and independent role in the production of MHC class I-binding peptides in vivo. European journal of immunology *41*, 926-935.
Deveraux, Q., van Nocker, S., Mahaffey, D., Vierstra, R., and Rechsteiner, M. (1995). Inhibition of ubiquitin-mediated proteolysis by the Arabidopsis 26 S protease subunit S5a. The Journal of biological chemistry *270*, 29660-29663.
Dolan, B.P., Bennink, J.R., and Yewdell, J.W. (2011). Translating DRiPs: progress in understanding viral and cellular sources of MHC class I peptide ligands. Cellular and molecular life sciences : CMLS *68*, 1481-1489.
Ebstein, F., Keller, M., Paschen, A., Walden, P., Seeger, M., Burger, E., Kruger, E., Schadendorf, D., Kloetzel, P.M., and Seifert, U. (2016a). Exposure to Melan-A/MART-126-35 tumor epitope specific CD8(+)T cells reveals immune escape by affecting the ubiquitin-proteasome system (UPS). Scientific reports *6*, 25208.
Ebstein, F., Kloetzel, P.M., Kruger, E., and Seifert, U. (2012a). Emerging roles of immunoproteasomes beyond MHC class I antigen processing. Cellular and molecular life sciences : CMLS *69*, 2543-2558.
Ebstein, F., Lange, N., Urban, S., Seifert, U., Kruger, E., and Kloetzel, P.M. (2009). Maturation of human dendritic cells is accompanied by functional remodelling of the ubiquitin-proteasome system. The international journal of biochemistry & cell biology *41*, 1205-1215.
Ebstein, F., Lehmann, A., and Kloetzel, P.M. (2012b). The FAT10- and ubiquitin-dependent degradation machineries exhibit common and distinct requirements for MHC class I antigen presentation. Cellular and molecular life sciences : CMLS *69*, 2443-2454.
Ebstein, F., Textoris-Taube, K., Keller, C., Golnik, R., Vigneron, N., Van den Eynde, B.J., Schuler-Thurner, B., Schadendorf, D., Lorenz, F.K., Uckert, W.*, et al.* (2016b). Proteasomes generate spliced epitopes by two different mechanisms and as efficiently as non-spliced epitopes. Scientific reports *6*, 24032.
Ebstein, F., Voigt, A., Lange, N., Warnatsch, A., Schroter, F., Prozorovski, T., Kuckelkorn, U., Aktas, O., Seifert, U., Kloetzel, P.M.*, et al.* (2013). Immunoproteasomes are important for proteostasis in immune responses. Cell *152*, 935-937.
Emmerich, C.H., Ordureau, A., Strickson, S., Arthur, J.S., Pedrioli, P.G., Komander, D., and Cohen, P. (2013). Activation of the canonical IKK complex by K63/M1-linked hybrid ubiquitin chains. Proceedings of the National Academy of Sciences of the United States of America *110*, 15247-15252.
Fonteneau, J.F., Kavanagh, D.G., Lirvall, M., Sanders, C., Cover, T.L., Bhardwaj, N., and Larsson, M. (2003). Characterization of the MHC class I cross-presentation pathway for cell-associated antigens by human dendritic cells. Blood *102*, 4448-4455.
Frausto, R.F., Crocker, S.J., Eam, B., Whitmire, J.K., and Whitton, J.L. (2007). Myelin oligodendrocyte glycoprotein peptide-induced experimental allergic encephalomyelitis and T cell responses are unaffected by immunoproteasome deficiency. Journal of neuroimmunology *192*, 124-133.
Fu, T.M., Guan, L., Friedman, A., Ulmer, J.B., Liu, M.A., and Donnelly, J.J. (1998). Induction of MHC class I-restricted CTL response by DNA immunization with ubiquitin-influenza virus nucleoprotein fusion antigens. Vaccine *16*, 1711-1717.
Geisler, S., Holmstrom, K.M., Skujat, D., Fiesel, F.C., Rothfuss, O.C., Kahle, P.J., and Springer, W. (2010). PINK1/Parkin-mediated mitophagy is dependent on VDAC1 and p62/SQSTM1. Nature cell biology *12*, 119-131.
Gil-Torregrosa, B.C., Raul Castano, A., and Del Val, M. (1998). Major histocompatibility complex class I viral antigen processing in the secretory pathway defined by the trans-Golgi network protease furin. The Journal of experimental medicine *188*, 1105-1116.
Giodini, A., Rahner, C., and Cresswell, P. (2009). Receptor-mediated phagocytosis elicits cross-presentation in nonprofessional antigen-presenting cells. Proceedings of the National Academy of Sciences of the United States of America *106*, 3324-3329.
Golnik, R., Lehmann, A., Kloetzel, P.M., and Ebstein, F. (2016). Major Histocompatibility Complex (MHC) Class I Processing of the NY-ESO-1 Antigen Is Regulated by Rpn10 and Rpn13 Proteins and

Immunoproteasomes following Non-lysine Ubiquitination. The Journal of biological chemistry *291*, 8805-8815.
Goto, E., Yamanaka, Y., Ishikawa, A., Aoki-Kawasumi, M., Mito-Yoshida, M., Ohmura-Hoshino, M., Matsuki, Y., Kajikawa, M., Hirano, H., and Ishido, S. (2010). Contribution of lysine 11-linked ubiquitination to MIR2-mediated major histocompatibility complex class I internalization. The Journal of biological chemistry *285*, 35311-35319.
Grant, E.P., Michalek, M.T., Goldberg, A.L., and Rock, K.L. (1995). Rate of antigen degradation by the ubiquitin-proteasome pathway influences MHC class I presentation. Journal of immunology *155*, 3750-3758.
Guermonprez, P., Saveanu, L., Kleijmeer, M., Davoust, J., Van Endert, P., and Amigorena, S. (2003). ER-phagosome fusion defines an MHC class I cross-presentation compartment in dendritic cells. Nature *425*, 397-402.
Guillaume, B., Chapiro, J., Stroobant, V., Colau, D., Van Holle, B., Parvizi, G., Bousquet-Dubouch, M.P., Theate, I., Parmentier, N., and Van den Eynde, B.J. (2010). Two abundant proteasome subtypes that uniquely process some antigens presented by HLA class I molecules. Proceedings of the National Academy of Sciences of the United States of America *107*, 18599-18604.
Guillaume, B., Stroobant, V., Bousquet-Dubouch, M.P., Colau, D., Chapiro, J., Parmentier, N., Dalet, A., and Van den Eynde, B.J. (2012). Analysis of the processing of seven human tumor antigens by intermediate proteasomes. Journal of immunology *189*, 3538-3547.
Haglund, K., Sigismund, S., Polo, S., Szymkiewicz, I., Di Fiore, P.P., and Dikic, I. (2003). Multiple monoubiquitination of RTKs is sufficient for their endocytosis and degradation. Nature cell biology *5*, 461-466.
Hershko, A., Ciechanover, A., and Rose, I.A. (1979). Resolution of the ATP-dependent proteolytic system from reticulocytes: a component that interacts with ATP. Proceedings of the National Academy of Sciences of the United States of America *76*, 3107-3110.
Hipp, M.S., Kalveram, B., Raasi, S., Groettrup, M., and Schmidtke, G. (2005). FAT10, a ubiquitin-independent signal for proteasomal degradation. Mol Cell Biol *25*, 3483-3491.
Hipp, M.S., Raasi, S., Groettrup, M., and Schmidtke, G. (2004). NEDD8 ultimate buster-1L interacts with the ubiquitin-like protein FAT10 and accelerates its degradation. J Biol Chem *279*, 16503-16510.
Houde, M., Bertholet, S., Gagnon, E., Brunet, S., Goyette, G., Laplante, A., Princiotta, M.F., Thibault, P., Sacks, D., and Desjardins, M. (2003). Phagosomes are competent organelles for antigen cross-presentation. Nature *425*, 402-406.
Huang, F., Zeng, X., Kim, W., Balasubramani, M., Fortian, A., Gygi, S.P., Yates, N.A., and Sorkin, A. (2013). Lysine 63-linked polyubiquitination is required for EGF receptor degradation. Proceedings of the National Academy of Sciences of the United States of America *110*, 15722-15727.
Huang, L., Marvin, J.M., Tatsis, N., and Eisenlohr, L.C. (2011). Cutting Edge: Selective role of ubiquitin in MHC class I antigen presentation. Journal of immunology *186*, 1904-1908.
Hurley, J.H., Lee, S., and Prag, G. (2006). Ubiquitin-binding domains. The Biochemical journal *399*, 361-372.
Husnjak, K., Elsasser, S., Zhang, N., Chen, X., Randles, L., Shi, Y., Hofmann, K., Walters, K.J., Finley, D., and Dikic, I. (2008). Proteasome subunit Rpn13 is a novel ubiquitin receptor. Nature *453*, 481-488.
Hutchinson, S., Sims, S., O'Hara, G., Silk, J., Gileadi, U., Cerundolo, V., and Klenerman, P. (2011). A dominant role for the immunoproteasome in CD8+ T cell responses to murine cytomegalovirus. PloS one *6*, e14646.
Ikeda, F., and Dikic, I. (2008). Atypical ubiquitin chains: new molecular signals. 'Protein Modifications: Beyond the Usual Suspects' review series. EMBO reports *9*, 536-542.
Imai, J., Hasegawa, H., Maruya, M., Koyasu, S., and Yahara, I. (2005a). Exogenous antigens are processed through the endoplasmic reticulum-associated degradation (ERAD) in cross-presentation by dendritic cells. International immunology *17*, 45-53.
Imai, J., Hasegawa, H., Maruya, M., Koyasu, S., and Yahara, I. (2005b). Exogenous antigens are processed through the endoplasmic reticulum-associated degradation (ERAD) in cross-presentation by dendritic cells. Int Immunol *17*, 45-53.

Inaba, K., Metlay, J.P., Crowley, M.T., Witmer-Pack, M., and Steinman, R.M. (1990). Dendritic cells as antigen presenting cells in vivo. International reviews of immunology *6*, 197-206.
Ishii, K., Hisaeda, H., Duan, X., Imai, T., Sakai, T., Fehling, H.J., Murata, S., Chiba, T., Tanaka, K., Hamano, S.*, et al.* (2006). The involvement of immunoproteasomes in induction of MHC class I-restricted immunity targeting Toxoplasma SAG1. Microbes and infection / Institut Pasteur *8*, 1045-1053.
Janda, J., Schoneberger, P., Skoberne, M., Messerle, M., Russmann, H., and Geginat, G. (2004). Cross-presentation of Listeria-derived CD8 T cell epitopes requires unstable bacterial translation products. J Immunol *173*, 5644-5651.
Ji, F., Jin, X., Jiao, C.H., Xu, Q.W., Wang, Z.W., and Chen, Y.L. (2009). FAT10 level in human gastric cancer and its relation with mutant p53 level, lymph node metastasis and TNM staging. World J Gastroenterol *15*, 2228-2233.
Kamitani, T., Kito, K., Fukuda-Kamitani, T., and Yeh, E.T. (2001). Targeting of NEDD8 and its conjugates for proteasomal degradation by NUB1. The Journal of biological chemistry *276*, 46655-46660.
Kim, H.T., Kim, K.P., Lledias, F., Kisselev, A.F., Scaglione, K.M., Skowyra, D., Gygi, S.P., and Goldberg, A.L. (2007). Certain pairs of ubiquitin-conjugating enzymes (E2s) and ubiquitin-protein ligases (E3s) synthesize nondegradable forked ubiquitin chains containing all possible isopeptide linkages. The Journal of biological chemistry *282*, 17375-17386.
Kim, W., Bennett, E.J., Huttlin, E.L., Guo, A., Li, J., Possemato, A., Sowa, M.E., Rad, R., Rush, J., Comb, M.J.*, et al.* (2011). Systematic and quantitative assessment of the ubiquitin-modified proteome. Molecular cell *44*, 325-340.
Kincaid, E.Z., Che, J.W., York, I., Escobar, H., Reyes-Vargas, E., Delgado, J.C., Welsh, R.M., Karow, M.L., Murphy, A.J., Valenzuela, D.M.*, et al.* (2012). Mice completely lacking immunoproteasomes show major changes in antigen presentation. Nature immunology *13*, 129-135.
Kirkin, V., Lamark, T., Johansen, T., and Dikic, I. (2009). NBR1 cooperates with p62 in selective autophagy of ubiquitinated targets. Autophagy *5*, 732-733.
Klare, N., Seeger, M., Janek, K., Jungblut, P.R., and Dahlmann, B. (2007). Intermediate-type 20 S proteasomes in HeLa cells: "asymmetric" subunit composition, diversity and adaptation. Journal of molecular biology *373*, 1-10.
Kloetzel, P.M., and Ossendorp, F. (2004). Proteasome and peptidase function in MHC-class-I-mediated antigen presentation. Curr Opin Immunol *16*, 76-81.
Knobeloch, K.P., Utermohlen, O., Kisser, A., Prinz, M., and Horak, I. (2005). Reexamination of the role of ubiquitin-like modifier ISG15 in the phenotype of UBP43-deficient mice. Mol Cell Biol *25*, 11030-11034.
Komander, D., and Rape, M. (2012). The ubiquitin code. Annual review of biochemistry *81*, 203-229.
Kovacsovics-Bankowski, M., and Rock, K.L. (1995). A phagosome-to-cytosol pathway for exogenous antigens presented on MHC class I molecules. Science *267*, 243-246.
Kravtsova-Ivantsiv, Y., and Ciechanover, A. (2012). Non-canonical ubiquitin-based signals for proteasomal degradation. Journal of cell science *125*, 539-548.
Kruger, E., and Kloetzel, P.M. (2012). Immunoproteasomes at the interface of innate and adaptive immune responses: two faces of one enzyme. Current opinion in immunology *24*, 77-83.
Labarriere, N., Diez, E., Pandolfino, M.C., Viret, C., Guilloux, Y., Le Guiner, S., Fonteneau, J.F., Dreno, B., and Jotereau, F. (1997). Optimal T cell activation by melanoma cells depends on a minimal level of antigen transcription. Journal of immunology *158*, 1238-1245.
Lam, Y.A., Lawson, T.G., Velayutham, M., Zweier, J.L., and Pickart, C.M. (2002). A proteasomal ATPase subunit recognizes the polyubiquitin degradation signal. Nature *416*, 763-767.
Lazaro, S., Gamarra, D., and Del Val, M. (2015). Proteolytic enzymes involved in MHC class I antigen processing: A guerrilla army that partners with the proteasome. Molecular immunology *68*, 72-76.
Lee, C.G., Ren, J., Cheong, I.S., Ban, K.H., Ooi, L.L., Yong Tan, S., Kan, A., Nuchprayoon, I., Jin, R., Lee, K.H.*, et al.* (2003). Expression of the FAT10 gene is highly upregulated in hepatocellular carcinoma and other gastrointestinal and gynecological cancers. Oncogene *22*, 2592-2603.

Lenschow, D.J., Lai, C., Frias-Staheli, N., Giannakopoulos, N.V., Lutz, A., Wolff, T., Osiak, A., Levine, B., Schmidt, R.E., Garcia-Sastre, A*., et al.* (2007). IFN-stimulated gene 15 functions as a critical antiviral molecule against influenza, herpes, and Sindbis viruses. Proc Natl Acad Sci U S A *104*, 1371-1376.
Li, M., Davey, G.M., Sutherland, R.M., Kurts, C., Lew, A.M., Hirst, C., Carbone, F.R., and Heath, W.R. (2001). Cell-associated ovalbumin is cross-presented much more efficiently than soluble ovalbumin in vivo. J Immunol *166*, 6099-6103.
Liu, G., Zheng, W., and Chen, X. (2007). Molecular cloning of proteasome activator PA28-beta subunit of large yellow croaker (Pseudosciana crocea) and its coordinated up-regulation with MHC class I alpha-chain and beta 2-microglobulin in poly I:C-treated fish. Molecular immunology *44*, 1190-1197.
Livnat-Levanon, N., Kevei, E., Kleifeld, O., Krutauz, D., Segref, A., Rinaldi, T., Erpapazoglou, Z., Cohen, M., Reis, N., Hoppe, T*., et al.* (2014). Reversible 26S Proteasome Disassembly upon Mitochondrial Stress. Cell reports *7*, 1371-1380.
McDowell, G.S., Kucerova, R., and Philpott, A. (2010). Non-canonical ubiquitylation of the proneural protein Ngn2 occurs in both Xenopus embryos and mammalian cells. Biochemical and biophysical research communications *400*, 655-660.
Medina, F., Ramos, M., Iborra, S., de Leon, P., Rodriguez-Castro, M., and Del Val, M. (2009). Furin-processed antigens targeted to the secretory route elicit functional TAP1-/-CD8+ T lymphocytes in vivo. Journal of immunology *183*, 4639-4647.
Menager, J., Ebstein, F., Oger, R., Hulin, P., Nedellec, S., Duverger, E., Lehmann, A., Kloetzel, P.M., Jotereau, F., and Guilloux, Y. (2014). Cross-presentation of synthetic long peptides by human dendritic cells: a process dependent on ERAD component p97/VCP but Not sec61 and/or Derlin-1. PloS one *9*, e89897.
Meusser, B., Hirsch, C., Jarosch, E., and Sommer, T. (2005). ERAD: the long road to destruction. Nat Cell Biol *7*, 766-772.
Meyer, H., Bug, M., and Bremer, S. (2012). Emerging functions of the VCP/p97 AAA-ATPase in the ubiquitin system. Nature cell biology *14*, 117-123.
Meyer, H.J., and Rape, M. (2014). Enhanced protein degradation by branched ubiquitin chains. Cell *157*, 910-921.
Michalek, M.T., Grant, E.P., Gramm, C., Goldberg, A.L., and Rock, K.L. (1993). A role for the ubiquitin-dependent proteolytic pathway in MHC class I-restricted antigen presentation. Nature *363*, 552-554.
Michalek, M.T., Grant, E.P., and Rock, K.L. (1996). Chemical denaturation and modification of ovalbumin alters its dependence on ubiquitin conjugation for class I antigen presentation. Journal of immunology *157*, 617-624.
Morel, S., Levy, F., Burlet-Schiltz, O., Brasseur, F., Probst-Kepper, M., Peitrequin, A.L., Monsarrat, B., Van Velthoven, R., Cerottini, J.C., Boon, T*., et al.* (2000). Processing of some antigens by the standard proteasome but not by the immunoproteasome results in poor presentation by dendritic cells. Immunity *12*, 107-117.
Morris, J.R., and Solomon, E. (2004). BRCA1 : BARD1 induces the formation of conjugated ubiquitin structures, dependent on K6 of ubiquitin, in cells during DNA replication and repair. Human molecular genetics *13*, 807-817.
Needham, P.G., and Brodsky, J.L. (2013). How early studies on secreted and membrane protein quality control gave rise to the ER associated degradation (ERAD) pathway: The early history of ERAD. Biochim Biophys Acta.
Norbury, C.C., Basta, S., Donohue, K.B., Tscharke, D.C., Princiotta, M.F., Berglund, P., Gibbs, J., Bennink, J.R., and Yewdell, J.W. (2004). CD8+ T cell cross-priming via transfer of proteasome substrates. Science *304*, 1318-1321.
Norbury, C.C., Hewlett, L.J., Prescott, A.R., Shastri, N., and Watts, C. (1995). Class I MHC presentation of exogenous soluble antigen via macropinocytosis in bone marrow macrophages. Immunity *3*, 783-791.
Nussbaum, A.K., Rodriguez-Carreno, M.P., Benning, N., Botten, J., and Whitton, J.L. (2005). Immunoproteasome-deficient mice mount largely normal CD8+ T cell responses to lymphocytic choriomeningitis virus infection and DNA vaccination. J Immunol *175*, 1153-1160.

Ortmann, B., Copeman, J., Lehner, P.J., Sadasivan, B., Herberg, J.A., Grandea, A.G., Riddell, S.R., Tampe, R., Spies, T., Trowsdale, J.*, et al.* (1997). A critical role for tapasin in the assembly and function of multimeric MHC class I-TAP complexes. Science *277*, 1306-1309.
Osiak, A., Utermohlen, O., Niendorf, S., Horak, I., and Knobeloch, K.P. (2005). ISG15, an interferon-stimulated ubiquitin-like protein, is not essential for STAT1 signaling and responses against vesicular stomatitis and lymphocytic choriomeningitis virus. Mol Cell Biol *25*, 6338-6345.
Paraskevopoulos, K., Kriegenburg, F., Tatham, M.H., Rosner, H.I., Medina, B., Larsen, I.B., Brandstrup, R., Hardwick, K.G., Hay, R.T., Kragelund, B.B.*, et al.* (2014). Dss1 is a 26S proteasome ubiquitin receptor. Molecular cell *56*, 453-461.
Park, M.J., Kim, E.K., Han, J.Y., Cho, H.W., Sohn, H.J., Kim, S.Y., and Kim, T.G. (2010). Fusion of the Human Cytomegalovirus pp65 antigen with both ubiquitin and ornithine decarboxylase additively enhances antigen presentation to CD8(+) T cells in human dendritic cells. Human gene therapy *21*, 957-967.
Passmore, L.A., and Barford, D. (2004). Getting into position: the catalytic mechanisms of protein ubiquitylation. The Biochemical journal *379*, 513-525.
Peaper, D.R., Wearsch, P.A., and Cresswell, P. (2005). Tapasin and ERp57 form a stable disulfide-linked dimer within the MHC class I peptide-loading complex. The EMBO journal *24*, 3613-3623.
Peng, J., Schwartz, D., Elias, J.E., Thoreen, C.C., Cheng, D., Marsischky, G., Roelofs, J., Finley, D., and Gygi, S.P. (2003). A proteomics approach to understanding protein ubiquitination. Nature biotechnology *21*, 921-926.
Pickart, C.M., and Eddins, M.J. (2004). Ubiquitin: structures, functions, mechanisms. Biochimica et biophysica acta *1695*, 55-72.
Puttaparthi, K., Van Kaer, L., and Elliott, J.L. (2007). Assessing the role of immuno-proteasomes in a mouse model of familial ALS. Experimental neurology *206*, 53-58.
Raasi, S., Schmidtke, G., and Groettrup, M. (2001). The ubiquitin-like protein FAT10 forms covalent conjugates and induces apoptosis. J Biol Chem *276*, 35334-35343.
Rahnefeld, A., Klingel, K., Schuermann, A., Diny, N.L., Althof, N., Lindner, A., Bleienheuft, P., Savvatis, K., Respondek, D., Opitz, E.*, et al.* (2014). Ubiquitin-like protein ISG15 (interferon-stimulated gene of 15 kDa) in host defense against heart failure in a mouse model of virus-induced cardiomyopathy. Circulation *130*, 1589-1600.
Rajapurohitam, V., Bedard, N., and Wing, S.S. (2002). Control of ubiquitination of proteins in rat tissues by ubiquitin conjugating enzymes and isopeptidases. American journal of physiology Endocrinology and metabolism *282*, E739-745.
Rani, N., Aichem, A., Schmidtke, G., Kreft, S.G., and Groettrup, M. (2012). FAT10 and NUB1L bind to the VWA domain of Rpn10 and Rpn1 to enable proteasome-mediated proteolysis. Nature communications *3*, 749.
Rechsteiner, M., and Hill, C.P. (2005). Mobilizing the proteolytic machine: cell biological roles of proteasome activators and inhibitors. Trends in cell biology *15*, 27-33.
Rock, K.L., Farfan-Arribas, D.J., Colbert, J.D., and Goldberg, A.L. (2014). Re-examining class-I presentation and the DRiP hypothesis. Trends in immunology *35*, 144-152.
Rock, K.L., and Shen, L. (2005). Cross-presentation: underlying mechanisms and role in immune surveillance. Immunol Rev *207*, 166-183.
Sadasivan, B., Lehner, P.J., Ortmann, B., Spies, T., and Cresswell, P. (1996). Roles for calreticulin and a novel glycoprotein, tapasin, in the interaction of MHC class I molecules with TAP. Immunity *5*, 103-114.
Saveanu, L., Carroll, O., Lindo, V., Del Val, M., Lopez, D., Lepelletier, Y., Greer, F., Schomburg, L., Fruci, D., Niedermann, G.*, et al.* (2005). Concerted peptide trimming by human ERAP1 and ERAP2 aminopeptidase complexes in the endoplasmic reticulum. Nature immunology *6*, 689-697.
Saveanu, L., Carroll, O., Weimershaus, M., Guermonprez, P., Firat, E., Lindo, V., Greer, F., Davoust, J., Kratzer, R., Keller, S.R.*, et al.* (2009). IRAP identifies an endosomal compartment required for MHC class I cross-presentation. Science *325*, 213-217.

Schmidtke, G., Kalveram, B., Weber, E., Bochtler, P., Lukasiak, S., Hipp, M.S., and Groettrup, M. (2006). The UBA domains of NUB1L are required for binding but not for accelerated degradation of the ubiquitin-like modifier FAT10. J Biol Chem *281*, 20045-20054.
Schubert, U., Anton, L.C., Gibbs, J., Norbury, C.C., Yewdell, J.W., and Bennink, J.R. (2000). Rapid degradation of a large fraction of newly synthesized proteins by proteasomes. Nature *404*, 770-774.
Schulman, B.A., and Harper, J.W. (2009). Ubiquitin-like protein activation by E1 enzymes: the apex for downstream signalling pathways. Nature reviews Molecular cell biology *10*, 319-331.
Seifert, U., Bialy, L.P., Ebstein, F., Bech-Otschir, D., Voigt, A., Schroter, F., Prozorovski, T., Lange, N., Steffen, J., Rieger, M.*, et al.* (2010). Immunoproteasomes preserve protein homeostasis upon interferon-induced oxidative stress. Cell *142*, 613-624.
Shen, L., Sigal, L.J., Boes, M., and Rock, K.L. (2004). Important role of cathepsin S in generating peptides for TAP-independent MHC class I crosspresentation in vivo. Immunity *21*, 155-165.
Shen, X.Z., Billet, S., Lin, C., Okwan-Duodu, D., Chen, X., Lukacher, A.E., and Bernstein, K.E. (2011). The carboxypeptidase ACE shapes the MHC class I peptide repertoire. Nature immunology *12*, 1078-1085.
Sijts, A.J., Standera, S., Toes, R.E., Ruppert, T., Beekman, N.J., van Veelen, P.A., Ossendorp, F.A., Melief, C.J., and Kloetzel, P.M. (2000). MHC class I antigen processing of an adenovirus CTL epitope is linked to the levels of immunoproteasomes in infected cells. J Immunol *164*, 4500-4506.
Stoltze, L., Schirle, M., Schwarz, G., Schroter, C., Thompson, M.W., Hersh, L.B., Kalbacher, H., Stevanovic, S., Rammensee, H.G., and Schild, H. (2000). Two new proteases in the MHC class I processing pathway. Nature immunology *1*, 413-418.
Strehl, B., Seifert, U., Kruger, E., Heink, S., Kuckelkorn, U., and Kloetzel, P.M. (2005). Interferon-gamma, the functional plasticity of the ubiquitin-proteasome system, and MHC class I antigen processing. Immunological reviews *207*, 19-30.
Tait, S.W., de Vries, E., Maas, C., Keller, A.M., D'Santos, C.S., and Borst, J. (2007). Apoptosis induction by Bid requires unconventional ubiquitination and degradation of its N-terminal fragment. The Journal of cell biology *179*, 1453-1466.
Tanaka, K. (1994). Role of proteasomes modified by interferon-gamma in antigen processing. Journal of leukocyte biology *56*, 571-575.
Tanaka, K., and Tsurumi, C. (1997). The 26S proteasome: subunits and functions. Mol Biol Rep *24*, 3-11.
Thrower, J.S., Hoffman, L., Rechsteiner, M., and Pickart, C.M. (2000). Recognition of the polyubiquitin proteolytic signal. The EMBO journal *19*, 94-102.
Tiwari, N., Garbi, N., Reinheckel, T., Moldenhauer, G., Hammerling, G.J., and Momburg, F. (2007). A transporter associated with antigen-processing independent vacuolar pathway for the MHC class I-mediated presentation of endogenous transmembrane proteins. Journal of immunology *178*, 7932-7942.
Tokunaga, F., and Iwai, K. (2012). LUBAC, a novel ubiquitin ligase for linear ubiquitination, is crucial for inflammation and immune responses. Microbes and infection / Institut Pasteur *14*, 563-572.
Townsend, A., Bastin, J., Gould, K., Brownlee, G., Andrew, M., Coupar, B., Boyle, D., Chan, S., and Smith, G. (1988). Defective presentation to class I-restricted cytotoxic T lymphocytes in vaccinia-infected cells is overcome by enhanced degradation of antigen. The Journal of experimental medicine *168*, 1211-1224.
Tu, L., Moriya, C., Imai, T., Ishida, H., Tetsutani, K., Duan, X., Murata, S., Tanaka, K., Shimokawa, C., Hisaeda, H.*, et al.* (2009). Critical role for the immunoproteasome subunit LMP7 in the resistance of mice to Toxoplasma gondii infection. European journal of immunology *39*, 3385-3394.
Urban, S., Textoris-Taube, K., Reimann, B., Janek, K., Dannenberg, T., Ebstein, F., Seifert, C., Zhao, F., Kessler, J.H., Halenius, A.*, et al.* (2012). The efficiency of human cytomegalovirus pp65(495-503) CD8+ T cell epitope generation is determined by the balanced activities of cytosolic and endoplasmic reticulum-resident peptidases. Journal of immunology *189*, 529-538.

Van Kaer, L., Ashton-Rickardt, P.G., Eichelberger, M., Gaczynska, M., Nagashima, K., Rock, K.L., Goldberg, A.L., Doherty, P.C., and Tonegawa, S. (1994). Altered peptidase and viral-specific T cell response in LMP2 mutant mice. Immunity *1*, 533-541.
Vignard, V., Lemercier, B., Lim, A., Pandolfino, M.C., Guilloux, Y., Khammari, A., Rabu, C., Echasserieau, K., Lang, F., Gougeon, M.L*., et al.* (2005). Adoptive transfer of tumor-reactive Melan-A-specific CTL clones in melanoma patients is followed by increased frequencies of additional Melan-A-specific T cells. Journal of immunology *175*, 4797-4805.
Vigneron, N., and Van den Eynde, B.J. (2012). Proteasome subtypes and the processing of tumor antigens: increasing antigenic diversity. Current opinion in immunology *24*, 84-91.
Vosper, J.M., McDowell, G.S., Hindley, C.J., Fiore-Heriche, C.S., Kucerova, R., Horan, I., and Philpott, A. (2009). Ubiquitylation on canonical and non-canonical sites targets the transcription factor neurogenin for ubiquitin-mediated proteolysis. The Journal of biological chemistry *284*, 15458-15468.
Wagner, S.A., Beli, P., Weinert, B.T., Nielsen, M.L., Cox, J., Mann, M., and Choudhary, C. (2011). A proteome-wide, quantitative survey of in vivo ubiquitylation sites reveals widespread regulatory roles. Molecular & cellular proteomics : MCP *10*, M111 013284.
Wahlman, J., DeMartino, G.N., Skach, W.R., Bulleid, N.J., Brodsky, J.L., and Johnson, A.E. (2007). Real-time fluorescence detection of ERAD substrate retrotranslocation in a mammalian in vitro system. Cell *129*, 943-955.
Weimershaus, M., Maschalidi, S., Sepulveda, F., Manoury, B., van Endert, P., and Saveanu, L. (2012). Conventional dendritic cells require IRAP-Rab14 endosomes for efficient cross-presentation. Journal of immunology *188*, 1840-1846.
Wickliffe, K.E., Williamson, A., Meyer, H.J., Kelly, A., and Rape, M. (2011). K11-linked ubiquitin chains as novel regulators of cell division. Trends in cell biology *21*, 656-663.
Wilkinson, K.D., Urban, M.K., and Haas, A.L. (1980). Ubiquitin is the ATP-dependent proteolysis factor I of rabbit reticulocytes. The Journal of biological chemistry *255*, 7529-7532.
Wong, J.J., Pung, Y.F., Sze, N.S., and Chin, K.C. (2006). HERC5 is an IFN-induced HECT-type E3 protein ligase that mediates type I IFN-induced ISGylation of protein targets. Proceedings of the National Academy of Sciences of the United States of America *103*, 10735-10740.
Xu, P., Duong, D.M., Seyfried, N.T., Cheng, D., Xie, Y., Robert, J., Rush, J., Hochstrasser, M., Finley, D., and Peng, J. (2009). Quantitative proteomics reveals the function of unconventional ubiquitin chains in proteasomal degradation. Cell *137*, 133-145.
Ye, Y., Shibata, Y., Kikkert, M., van Voorden, S., Wiertz, E., and Rapoport, T.A. (2005). Recruitment of the p97 ATPase and ubiquitin ligases to the site of retrotranslocation at the endoplasmic reticulum membrane. Proceedings of the National Academy of Sciences of the United States of America *102*, 14132-14138.
Yellen-Shaw, A.J., and Eisenlohr, L.C. (1997). Regulation of class I-restricted epitope processing by local or distal flanking sequence. Journal of immunology *158*, 1727-1733.
Yewdell, J.W., Anton, L.C., and Bennink, J.R. (1996). Defective ribosomal products (DRiPs): a major source of antigenic peptides for MHC class I molecules? Journal of immunology *157*, 1823-1826.
Yewdell, J.W., and Nicchitta, C.V. (2006). The DRiP hypothesis decennial: support, controversy, refinement and extension. Trends in immunology *27*, 368-373.
York, I.A., Mo, A.X., Lemerise, K., Zeng, W., Shen, Y., Abraham, C.R., Saric, T., Goldberg, A.L., and Rock, K.L. (2003). The cytosolic endopeptidase, thimet oligopeptidase, destroys antigenic peptides and limits the extent of MHC class I antigen presentation. Immunity *18*, 429-440.
Yuan, W., and Krug, R.M. (2001). Influenza B virus NS1 protein inhibits conjugation of the interferon (IFN)-induced ubiquitin-like ISG15 protein. Embo J *20*, 362-371.
Yuan, W.C., Lee, Y.R., Lin, S.Y., Chang, L.Y., Tan, Y.P., Hung, C.C., Kuo, J.C., Liu, C.H., Lin, M.Y., Xu, M*., et al.* (2014). K33-Linked Polyubiquitination of Coronin 7 by Cul3-KLHL20 Ubiquitin E3 Ligase Regulates Protein Trafficking. Molecular cell *54*, 586-600.
Zaiss, D.M., Bekker, C.P., Grone, A., Lie, B.A., and Sijts, A.J. (2011). Proteasome immunosubunits protect against the development of CD8 T cell-mediated autoimmune diseases. J Immunol *187*, 2302-2309.

Zehner, M., Marschall, A.L., Bos, E., Schloetel, J.G., Kreer, C., Fehrenschild, D., Limmer, A., Ossendorp, F., Lang, T., Koster, A.J.*, et al.* (2015). The translocon protein Sec61 mediates antigen transport from endosomes in the cytosol for cross-presentation to CD8(+) T cells. Immunity *42*, 850-863.
Zhang, Z., Clawson, A., and Rechsteiner, M. (1998). The proteasome activator 11 S regulator or PA28. Contribution By both alpha and beta subunits to proteasome activation. J Biol Chem *273*, 30660-30668.
Zhao, C., Denison, C., Huibregtse, J.M., Gygi, S., and Krug, R.M. (2005). Human ISG15 conjugation targets both IFN-induced and constitutively expressed proteins functioning in diverse cellular pathways. Proc Natl Acad Sci U S A *102*, 10200-10205.
Zou, L., Zhou, J., Zhang, J., Li, J., Liu, N., Chai, L., Li, N., Liu, T., Li, L., Xie, Z.*, et al.* (2009). The GTPase Rab3b/3c-positive recycling vesicles are involved in cross-presentation in dendritic cells. Proceedings of the National Academy of Sciences of the United States of America *106*, 15801-15806.

7. Abbreviations

ACE	Angiotensin-Converting Enzyme
AP-B	Aminopeptidase B
ATP	Adenosine Triphosphate
β2m	β2-microglobulin
BAG6	BCL2-Associated Athanogene 6
BH	Bleomycin Hydrolase
CHIP	Carboxy terminus of Hsc70-Interacting Protein
CTL	Cytotoxic T Lymphocyte
DC	Dendritic Cell
DRiPs	Defective Ribosomal Products
EBV	Epstein Barr Virus
ER	Endoplasmic Reticulum
ERAD	Endoplasmic Reticulum-associated Degradation
ERAP	Endoplasmic Reticulum Aminopeptidase
FAT10	HLA-F adjacent Transcript 10
HPV	Human Papilloma Virus
Hsc70	Heat Shock Cognate 70 kDa
HSV	Herpes Simplex Virus
IFN	Interferon
IL	Interleukin
I-Proteasome	Immunoproteasome
ISG15	Interferon-Stimulated Gene 145
LAP	Leucine Aminopeptidase
LCMV	Lymphocytic Choriomeningitis Virus
LMP	Low Molecular weight Protein
LPS	Lipopolysaccharide
Melan-A/MART-1	Melanoma Antigen Recognized by T Cells
MECL1	Multicatalytic Endopeptidase Complex subunit 1
MHC	Major Histocompatibility Complex
NUB1	NEDD8 Ultimate Buster 1

NUB1L	NEDD8 Ultimate Buster 1 Long
NY-ESO-1	New York Esophageal antigen 1
p97/VCP	p97/Valosin containing Protein
PA28	Proteasome Activator 28
PGE2	Prostaglandin E2
PLC	Peptide Loading Complex
Poly-IC	Polyinosinic Polycytidylic Acid
POP	prolyl-oligopeptidase
PSA	puromycin-sensitive aminopeptidase
SLP	Standard Long Peptide
SNARE	Soluble N-ethylmaleimide-sensitive factor attachment receptor
S-Proteasome	Standard Proteasome
TAP	Transporter with Antigen Processing
TNF	Tumor Necrosis Factor
TOP	thimet oligopeptidase
TPP2	tripeptidyl-peptidase 2
Tsn	Tapasin
UPS	Ubiquitin-Proteasome System
VIMP	VCP-Interacting Membrane Protein
VSV	Vesicular Stomatitis Virus

8. Danksagung

Mein aufrichtiger Dank gilt selbstverständlich dem Herrn Prof. Dr. Peter Kloetzel dafür, dass er mich in seine Arbeitsgruppe aufnahm. Für die Bereitstellung des Themas, die exzellenten Arbeitsbedingungen, die Diskussionsbereitschaft und seine ständige Unterstützung bin ich ihm sehr dankbar. Ohne ihn hätte ich mich keineswegs für die Biochemie entschieden.

Ich möchte unserer Institutsdirektorin Frau Prof. Dr. Britta Eickholt für die Ermöglichung der Fortsetzung dieser Arbeit und meiner Beteiligung an der Lehre des Instituts für Biochemie meinen ausdrücklichen Dank aussprechen.

Herzlichen Dank an Prof. Dr. Ulrike Seifert und Prof. Dr. Elke Krüger für ihre Unterstützung, ihre wertvollen Ratschläge und ihre ständige Hilfsbereitschaft bei allen Fragen des wissenschaftlichen Lebens.

Ich danke im besonderen Maße Dr. Ulrike Kuckelkorn und PD Dr. Michael Seeger für die Konstruktiven Diskussionen der Methodik und des experimentellen Vorgehens.

Ein ganz besonderer Dank geht an Andrea Lehmann für Ihre Leistung und Motivation. Sie hat wesentlich zum gelingen dieser Arbeit beigetragen, indem sie unzählige Überstunden auf sich genommen hat.

Ein großes Dankeschön an Herrn Prof. Dr. Burkhart Dahlmann für die vielen Fachgespräche und Anregungen.

Ebenfalls möchte ich Dr. Michele Mishto und Dr. Karin Schmidt für ihre Hilfsbereitschaft und ihre aktive Beteiligung an der Interpretation meiner Versuchsergebnisse bedanken.

Bei meinen Doktoranden Richard Golnik und Nadine Andresen möchte ich mich ausdrücklich bedanken. Ihr Engagement, ihre Leistung und Produktivität haben zur Erstellung dieser Arbeit signifikant beigetragen.

Allen derzeitigen und ehemaligen Mitarbeitern des Instituts für Biochemie der Charité Universitätsmedizin Berlin mochte ich für die gute und angenehme wissenschaftliche Atmosphäre bedanken. Insbesondere möchte ich mich bei Isa, Sabrina, Alex, Christin, Anja, und Agathe für ihre Kollegialität bedanken.

Und nicht zuletzt möchte ich der deutschen Forschungsgemeinschaft für ihre finanzielle Unterstützung herzlich bedanken.

9. Erklärung

§ 4 Abs. 3 (k) der HabOMed der Charité

Hiermit erkläre ich, dass

- weder früher noch gleichzeitig ein Habilitationsverfahren durchgeführt oder angemeldet wurde,
- die vorgelegte Habilitationsschrift ohne fremde Hilfe verfasst, die beschriebenen Ergebnisse selbst gewonnen sowie die verwendeten Hilfsmittel, die Zusammenarbeit mit anderen Wissenschaftlern/Wissenschaftlerinnen und mit technischen Hilfskräften sowie die verwendete Literatur vollständig in der Habilitationsschrift angegeben wurden,
- mir die geltende Habilitationsordnung bekannt ist.

Ich erkläre ferner, dass mir die Satzung der Charité – Universitätsmedizin Berlin zur Sicherung Guter Wissenschaftlicher Praxis bekannt ist und ich mich zur Einhaltung dieser Satzung verpflichte.

…… ……..

Datum Unterschrift